

EXTRACELLULAR RECOMBINANT HUMAN GROWTH HORMONE
PRODUCTION BY *Pichia pastoris*

A THESIS SUBMITTED TO
THE GRADUATE SCHOOL OF NATURAL AND APPLIED SCIENCES
OF
MIDDLE EAST TECHNICAL UNIVERSITY

BY

MEHMET ALİ ORMAN

IN PARTIAL FULFILLMENT OF THE REQUIREMENTS
FOR
THE DEGREE OF MASTER OF SCIENCE
IN
CHEMICAL ENGINEERING

AUGUST 2007

Approval of the Graduate School of Natural and Applied Sciences

Prof. Dr. Canan Özgen
Director

I certify that this thesis satisfies all the requirements as a thesis for the degree of Master of Science.

Prof. Dr. Nurcan Baç
Head of Department

This is to certify that we have read this thesis and that in our opinion it is fully adequate, in scope and quality, as a thesis and for the degree of Master of Science.

Prof. Dr. H. Tunçer Özdemir
Co-Supervisor

Prof. Dr. Pınar Çalık
Supervisor

Examining Committee Members

Prof. Dr. Timur Doğu (METU, CHE)

Prof. Dr. Pınar Çalık (METU, CHE)

Prof. Dr. Tunçer H. Özdamar (Ankara Uni., CHE)

Prof. Dr. Ufuk Bakır (METU, CHE)

Assoc. Prof. A. Elif Erson (METU, BIO)

I hereby declare that all information in this document has been obtained and presented in accordance with academic rules and ethical conduct. I also declare that, as required by these rules and conduct, I have fully cited and referenced all material and results that are not original to this work.

Name, Last name: Mehmet Ali Orman

Signature :

ABSTRACT

EXTRACELLULAR RECOMBINANT HUMAN GROWTH HORMONE PRODUCTION BY *Pichia pastoris*

Orman, Mehmet Ali

M.S., Department of Chemical Engineering

Supervisor: Prof. Dr. Pınar Çalık

Co-Supervisor: Prof. Dr. Tunçer H. Özdamar

August 2007, 168 pages

In this study, the effects of bioprocess operation parameters on recombinant human growth hormone (rhGH) production by *P. pastoris* were systematically investigated. In this frame, first, for the extracellular expression and purification of human growth hormone by recombinant *P. pastoris* the cDNA of hGH, fused with a polyhistidine tag and also fused with a target site for the Factor Xa protease in which cleavage produces a mature N- and C-termini of rhGH, was cloned into pPICZaA plasmid and the constructed system within the plasmid, *pPICZaA::hGH*, was integrated to AOX1 locus of *P. pastoris* and expressed under alcohol oxidase promoter which is induced by methanol. With *dot-blot* analysis, the appropriate two strains producing human growth hormone at high levels and having different methanol utilization phenotype (Mut⁺ and Mut^S) were chosen among the other transformants. Then, the effects of methanol concentrations on the expression of rhGH and cell growth were analyzed and both of the phenotypes were compared in defined and complex media in laboratory scale air filtered shake bioreactors. The highest rhGH concentration for Mut⁺ and Mut^S, was found as 0.052 kg m⁻³ and 0.16 kg m⁻³, respectively, at 2 %(v/v) methanol concentration in complex medium. When methanol was used as the sole carbon source in defined medium, Mut^S

phenotype had very low specific growth rate on methanol due to the intrinsic characteristics of it, therefore detectable rhGH was not observed, on the other hand, optimum rhGH concentration produced by Mut⁺ strain was found as 0.032 kg m⁻³ at 3% (v/v) methanol concentration in defined medium. In mixed system (glycerol/methanol) which is also defined, when the optimum glycerol concentration, 30 kg m⁻³, was used, Mut^s produced the highest rhGH, 0.110 kg m⁻³, at 1% (v/v) methanol concentration and any increase in methanol concentration resulted in lower rhGH production, on the other hand, Mut⁺ strain produced 0.060 kg m⁻³ rhGH at 4% (v/v) methanol concentration, which indicated that higher rhGH production capacity of Mut⁺ strain was obtained at high methanol concentrations.

Using the designed defined medium for Mut⁺ phenotype where methanol was used as the sole carbon source with an optimum concentration of 3% (v/v), the effects of oxygen transfer on rhGH production, by-product formation, and cell growth, oxygen transfer and fermentation characteristics were investigated by using pilot scale bioreactor. Oxygen transfer effects on rhGH production were investigated at $Q_{O_2}/V_R=0.5$ vvm; $N=250, 500, 625, 750$ min⁻¹ conditions. The variations in rhGH, cell, amino acid and organic acid concentrations with the cell cultivation time, specific cell growth rate, the oxygen uptake rate, the liquid phase coefficient by using the dynamic method, maintenance coefficient for oxygen and yield coefficients were determined. The highest rhGH concentration was obtained at 0.5 vvm, 500 min⁻¹ condition as 0.023 kg m⁻³ with 5.37 kg m⁻³ cell density.

Key words: Human growth hormone, *Pichia pastoris*, AOX1, medium design, oxygen transfer.

ÖZ

Pichia pastoris İLE HÜCREĐİŐİ REKOMBİNANT İNSAN BÜYÜME HORMONU ÜRETİMİ

Orman, Mehmet Ali

Yüksek Lisans, Kimya Mühendisliđi

Tez Yöneticisi: Prof. Dr. Pınar Çalık

Ortak Tez Yöneticisi: Prof. Dr. Tunçer H. Özdamar

Ađustos 2007, 168 sayfa

Bu çalıŐmada, biyoproses iŐletim parametrelerinin *Pichia pastoris* ile insan büyüme hormonu üretimi üzerine etkisi sistematik olarak incelenmiştir. Bu kapsamda, rekombinant insan büyüme hormonunun (rhGH) hücre dıŐı salgılanması ve üretim ortamından saflaŐtırılması için metabolik mühendislik tasarımı yapılmıştır. İnsan büyüme hormonun kromatografik yöntemlerle ayrılmasını sađlayan 6xhistidin dizinini ve saflaŐtırılmıŐ hormonun bu amino asitlerden ayrılmasını sađlayan Faktör Xa proteaz enziminin tanıdıđı amino asit dizinini kodlayan DNA *hGH* hormonun genine PCR yöntemi ile entegre edilmiŐ; ve oluŐturulan *pPICZaA::hGH*, *P. pastoris* kromozomunun AOX1 (alkol oksidaz 1 enzim geni) bölgesine entegre edilerek, metanol tarafından tetiklenen AOX1 promoteri kontrolünde hGH sentezlenmiştir. *Dot-blot* analiz yöntemi ile klonlanmış olan mikroorganizmalar arasından en uygun farklı iki fenotip, Mut⁺ ve Mut^s, seçilmiştir. Mut⁺ ve Mut^s ile methanol deriŐiminin rhGH üretimine tanımlı ve kompleks ortamlarda etkisi incelenmiştir. Kompleks ortamda (BMMY ortam), hacimce %2(h/h) metanol deriŐiminde optimum rhGH saptanmıştır. Bu koŐullarda, Mut⁺ fenotip 0.052 kg m⁻³, Mut^s ise 0.16 kg m⁻³ rhGH üretmiştir.

Tanımlı ortamda, sadece metanol karbon kaynağı olarak kullanıldığında, Mut^s fenotipi metanolu tam olarak kullanamadığından yeterli hücre derişimine ulaşamamış ve rhGH üretimi gerçekleşmemiştir. Mut⁺ fenotipi metanolu etkin olarak kullanabildiğinden, hücre çoğalmış ve %3(h/h)'lük metanol derişimde 0.032 kg m⁻³ rhGH üretebilmiştir. Gliserol ve methanol birlikte kullanıldığında, bu iki fenotip için en çok rhGH üretimi farklı metanol derişimlerinde bulunmuştur. Optimum gliserol derişimde, 30 kg m⁻³, Mut^s %1(h/h) metanol içeren ortamda 0.110 kg m⁻³, Mut⁺ %4 (h/h) metanol içeren ortamda 0.060 kg m⁻³ rhGH üretebilmiştir.

Tasarlanan üretim ortamı kullanılarak (%3 (h/h) metanol içeren tanımlı ortam) biyoreaktör işletim parametrelerinden oksijen aktarımı; fermantasyon ve oksijen aktarım karakteristikleri pilot ölçek biyoreaktörde incelenmiştir. İnsan büyüme hormonu üretiminde oksijen aktarımının etkileri, hava giriş hızı $Q_0/V_R=0.5$ vvm; karıştırma hızları $N=250, 500, 625, 750$ dk⁻¹ ve koşullarında incelenmiştir. İnsan büyüme hormonunun, hücre, amino asit, organik asit konsantrasyonlarının kalma süresi ile değışimi; dinamik yöntem kullanılarak, biyoprosesin büyüme evresi süresince , oksijen tüketim hızı ve sıvı faz kütle aktarım katsayısı; verim ve yaşam katsayıları belirlenmiştir. İncelenen koşullar arasında en yüksek hGH derişimi 0.023 kg m⁻³ olarak 5.37 kg m⁻³ hücre konsantrasyonunda $Q_0/V_R=0.5$ vvm ve $N=500$ dk⁻¹ koşullarında elde edilmiştir.

Anahtar kelimeler: İnsan büyüme hormonu, *Pichia Pastoris*, AOX1, ortam tasarımı, oksijen aktarım.

To my family

ACKNOWLEDGEMENTS

I wish to express my sincere gratitude to my supervisor Prof. Dr. Pinar alık and my co-supervisor Prof. Dr. H. Tuner zdamar for their continuous support, guidance and help, in all the possible way, throughout this study.

I would like to express my special thanks to Eda elik and Dr. Halloran for carrying out MALDI-TOF mass spectrometry analysis.

I am grateful to my friends in our research group in Industrial Biotechnology Laboratory, Vahideh Anghardi, Nuriye Korkmaz, Hande Levent, Iřık Haykır, Arda Byksungur, Hande Kaya, Ayřegl Ersayın Yařınok, and my other friends, mer Ensari and Davut Yıldız for their support, great friendship, advice and encouragement throughout my graduate program.

Financial Support provided by TUBITAK and METU-Research Fund are gratefully acknowledged.

Above all, I would like to thank to my family for loving, supporting and encouraging me all through my life.

TABLE OF CONTENTS

ABSTRACT	iv
ÖZ	vi
DEDICATION	viii
ACKNOWLEDGEMENTS.....	ix
TABLE OF CONTENTS.....	x
LIST OF TABLES.....	xiii
LIST OF FIGURES.....	xvi
NOMENCLATURE	xxi
CHAPTER	
1. INTRODUCTION	1
2. LITERATURE SURVEY	5
2.1 Proteins	5
2.1.1 Hormones.....	6
2.1.2 Human Growth Hormone.....	6
2.2 Genetic Engineering Techniques: Methodology.....	14
2.3 Bioprocess Parameters in Recombinant Protein Production.....	17
2.3.1 Choosing Microorganism	18
2.3.1.1 <i>Pichia pastoris</i>	18
2.3.2 Medium Design	26
2.3.3 Bioreactor Operation Parameters	29
2.3.4 Computation of Bioprocess Characteristics	30
3. MATERIALS AND METHODS.....	39
3.1 Chemicals	39
3.2 The Microorganisms and Plasmids.....	39
3.3 The Solid Medium	39

3.4 The Precultivation Medium	41
3.5 The Production Medium	42
3.6 Analysis	43
3.6.1 Cell Concentration	43
3.6.2 Methanol, Glycerol and Organic Acid Concentrations	43
3.6.3 Amino Acid Concentrations	44
3.6.4 Protein Analysis	45
3.7 Genetic Engineering Techniques	52
3.7.1 Materials.....	52
3.7.1.1 Enzymes, Kits, and Molecular Size Markers	52
3.7.1.2 Buffers and Solutions	53
3.7.2 Determination of DNA Concentration.....	53
3.7.3 PCR Amplification of DNA Targets	53
3.7.4 Purification of PCR Products	55
3.7.5 Restriction Digestion Reaction.....	55
3.7.6 Ligation Reaction	56
3.7.7 DNA Sequencing	57
3.7.8 Transformation of Plasmid DNA by CaCl ₂ Method to <i>Escherichia Coli</i> .57	
3.7.9 Isolation of Plasmid DNA	58
3.7.10 Purification of Plasmid DNA.....	59
3.7.11 Transfection of <i>P. pastoris</i>	59
3.7.12 Isolation of Genomic DNA from <i>Yeast</i>	60
3.7.13 DNA Extraction from Agarose Gel	61
4. RESULTS AND DISCUSSION.....	62
4.1 Development of Recombinant <i>P. pastoris</i> carrying hGH gene	62
4.1.1 Primer Design for Generation of <i>hGH</i> Gene	64
4.1.2 Amplification of hGH Gene by Polymerase Chain Reaction (PCR)	65
4.1.3 Restriction Enzyme Digestion and Ligation	67
4.1.4 Transformation of <i>E. coli</i> cells with pPICZaA:: <i>hGH</i> and Selection of the True Transformants	70
4.1.5 Transfection of <i>P. pastoris</i> cells with pPICZaA:: <i>hGH</i> plasmid.....	72
4.2 Expression of Human Growth Hormone in Recombinant <i>P. pastoris</i> in Laboratory Scale Air Filtered Shake Bioreactors.....	76
4.2.1 Microorganism Selection.....	76
4.2.2 Effects of Carbon Sources on rhGH Production and Cell Growth for both <i>P. pastoris-hGH-Mut^s</i> and <i>P. pastoris-hGH-Mut⁺</i>	79

4.2.2.1 Effects of Methanol Concentrations in Complex Medium.....	79
4.2.2.2 Effects of Methanol Concentrations in Defined Medium	85
4.2.2.3 Effects of Mixed Batch System (Glycerol/Methanol).....	90
4.3 Expression of Human Growth Hormone in Recombinant <i>P. pastoris</i> in Pilot Scale Bioreactor.....	104
4.3.1 Oxygen Transfer Effects in Batch Fermentation System	106
4.3.1.1 Dissolved Oxygen Profiles	106
4.3.1.2 Cell Growth Profiles.....	107
4.3.1.3 Methanol Concentration Profiles	109
4.3.1.4 rhGH Concentration Profiles	110
4.3.1.5 Formaldehyde, Organic and Amino Acid Concentration Profiles	113
4.3.1.6 Oxygen Transfer Characteristics.....	117
4.3.1.7 Specific Growth Rate, Yield and Maintenance Coefficients	124
4.3.2 Effects of Cell Density in Impulse Feeding Fermentation.....	130
4.4 Purification of rhGH Produced by <i>Pichia Pastoris</i>	137
5. CONCLUSION.....	142
REFERENCES	148
APPENDICES	
A. Preparations of Buffers and Solutions Used in Experiment	157
B. Preparation of SDS-Polyacrylamide Gel and Staining	161
C. Thermodynamic Properties of Designed Primers Together with Dimer and Self-Complimentary Formation Affinities.....	163
D. Sequence of pPICZaA :: <i>hGH</i> plasmid	165
E. SDS-Page Analysis Showing The Cultivation Media at Different Time When Mixed Carbon Sources (Glycerol/Methanol) were Used.....	167
F. SDS-Page Analysis of Bioreactors at Different Time	168

LIST OF TABLES

TABLE

1.1 List of some fermentation products and some market values in year 2000	2
2.1 Published studies about the production of recombinant human growth hormone: Microorganisms, promoters, signal peptides and results, etc.	10
2.2 Published studies about the production of recombinant human growth hormone; Bioreactor operation parameters.	12
2.3 Recognition sites and cleavage points of restriction enzymes	16
2.4 Advantages and disadvantages of <i>P. pastoris</i>	19
2.5 Definition of yield coefficients.	33
3.1 Strains and plasmids used in this study.....	40
3.2 The composition of the solid medium (LSLB) for <i>E. coli</i> strains.	40
3.3 The composition of the solid medium (YPD) for <i>P. pastoris</i> strains.....	40
3.4 The final concentration of antibiotics in the media	41
3.5 The composition of the precultivation medium of <i>P. pastoris</i> strain (BMGY).....	41
3.6 The composition of the complex production medium of <i>P. pastoris</i> strain (BMMY)	42
3.7 The composition of the defined production medium of <i>P. pastoris</i>	43
3.8 Conditions for HPLC system for methanol, glycerol and organic acid analysis	44
3.9 Conditions for HPLC system for amino acid analysis	45

3.10 Procedure for silver staining	49
3.11 PCR process parameters	54
3.12 Component of reaction mixture of PCR.	55
3.13 Components of reaction mixture of restriction digestion with <i>EcoRI</i> and <i>Xba1</i> RE's	55
3.14 Components of reaction mixture of restriction digestion with <i>PstI</i> RE.	56
3.15 Ligation reaction component.....	56
4.1 Primers designed for amplification of desired gene fragments.....	64
4.2 PCR process parameters and components of reaction mixture of PCR for amplification of <i>hGH</i> gene	67
4.3 Components of reaction mixture of restriction digestion of <i>hGH</i> gene and pPICZaA vector with <i>EcoRI</i> RE and <i>Xba1</i> RE	68
4.4 pPICZaA:: <i>hGH</i> ligation reaction conditions	69
4.5 Primers and expected PCR products length	71
4.6 Recombinant hGH concentrations, final cell concentrations and overall yield coefficients of <i>P.pastoris-hGH-Mut⁺</i> strain.....	85
4.7 Recombinant hGH concentrations, final cell concentrations and overall yield coefficients of <i>P.pastoris-hGH-Mut^s</i> strain	85
4.8 Recombinant hGH concentrations, final cell concentrations and overall yield coefficients of <i>P.pastoris-hGH-Mut⁺</i> strain.....	90
4.9 Recombinant hGH concentrations and final cell concentrations of <i>P.pastoris-hGH- Mut⁺</i> and <i>P.pastoris-hGH-Mut^s</i> strain	96
4.10 Recombinant hGH concentrations and final cell concentrations of <i>P.pastoris-hGH- Mut⁺</i> and <i>P.pastoris-hGH-Mut^s</i> strain	103
4.11 Recombinant hGH concentrations, final cell concentrations and overall yield coefficients of bioreactors.....	112

4.12 The variations in organic acid concentrations with cultivation time and oxygen transfer conditions.....	114
4.13 The variations in amino acid concentrations with cultivation time and oxygen transfer conditions.....	115
4.14 The variations in oxygen transfer parameters with oxygen transfer conditions	118
4.15 The variations in specific growth rate and yield coefficients	125
4.16 The variations in Leudeking-Piret constants and maintenance coefficients.....	129
4.17 The variations in organic acid concentrations with cultivation time	136
4.18 The variations in amino acid concentrations with cultivation time	136

LIST OF FIGURES

FIGURE

2.1	Nucleotide sequence of human growth hormone.....	7
2.2	Amino acid sequence of hGH	7
2.3	Tertiary structure of hGH.	8
2.4	Methanol metabolism in <i>P. Pastoris</i>	20
2.5	Metabolic pathways of glycerol in <i>Pichia pastoris</i>	21
2.6	pPICZaA vector	24
4.1	Flowchart of the research plan, for the development of the <i>r-P. pastoris</i> producing extracellular hGH.	63
4.2	Schematic illustrations of polymerase chain reactions with primers designed	66
4.3	(a)Agarose gel electrophoresis image of pUC19:: <i>hGH</i> plasmid, and (b) Agarose gel electrophoresis image of <i>hGH</i> gene	68
4.4	Agarose gel electrophoresis image of pPICZaA vector after restriction digestion.....	69
4.5	Scheme for the construction of the expression system for hGH production in <i>P.pastoris</i> strain	70
4.6	Agarose gel electrophoresis image of r-pPICZaA vectors isolated from <i>E. coli</i> transformants.....	71
4.7	Agarose gel electrophoresis image of PCR products of pPICZaA:: <i>hGH</i> plasmid.....	72
4.8	Schematic representation of pPICZaA:: <i>hGH</i> integration into <i>P. pastoris</i> genome	74

4.9 Agarose gel electrophoresis image of PCR products of <i>hGH</i> gene insert from genomic DNA <i>P. pastoris</i> transformants.....	75
4.10 Dot-blot analysis.....	77
4.11 Cell growth (solid line) and methanol utilization (dashed line) diagrams for <i>P. pastoris-hGH-Mut^s</i> (□) and <i>P. pastoris-hGH-Mut⁺</i> (Δ)	78
4.12 Effects of methanol concentrations on cell growth of <i>P. pastoris-hGH-Mut⁺</i> strain in complex medium	80
4.13 Effects of methanol concentrations on cell growth of <i>P. pastoris-hGH-Mut^s</i> strain in complex medium.....	81
4.14 Methanol utilization diagram of <i>P. pastoris-hGH-Mut⁺</i> strain in complex medium.....	81
4.15 Methanol utilization diagram of <i>P. pastoris-hGH-Mut^s</i> strain in complex medium.....	82
4.16 SDS-page image of rhGH produced by <i>P. pastoris-hGH-Mut⁺</i> (a) and <i>P. pastoris-hGH-Mut^s</i> (b)	83
4.17 Effects of methanol concentrations on cell growth of <i>P. pastoris-hGH-Mut⁺</i> strain in defined medium	86
4.18 Effects of methanol concentrations on cell growth of <i>P. pastoris-hGH-Mut^s</i> strain in defined medium	87
4.19 Methanol utilization diagram of <i>P. pastoris-hGH-Mut⁺</i> strain in defined medium	87
4.20 Methanol utilization diagram of <i>P. pastoris-hGH-Mut^s</i> strain in defined medium	88
4.21 SDS-page image of rhGH produced by <i>P. pastoris-hGH-Mut⁺</i>	89
4.22 Effects of glycerol concentrations on cell growth of <i>P. pastoris-hGH-Mut⁺</i> strain in defined mixed-batch medium containing methanol at an initial concentration; 3% v/v (solid lines) or without methanol (dashed lines).....	92

4.23 Effects of glycerol concentrations on cell growth of <i>P. pastoris-hGH-Mut^s</i> strain in defined mixed-batch medium containing methanol at constant concentration; 3% v/v (solid lines) or without methanol (dashed lines).....	93
4.24 Glycerol utilization diagram of <i>P. pastoris-hGH-Mut⁺</i> strain in defined mixed-batch medium	93
4.25 Glycerol utilization diagram of <i>P. pastoris-hGH-Mut^s</i> strain in defined mixed-batch medium	94
4.26 Methanol utilization diagram of <i>P. pastoris-hGH-Mut⁺</i> strain in defined mixed-batch medium	94
4.27 Methanol utilization diagram of <i>P. pastoris-hGH-Mut^s</i> strain in defined mixed-batch medium	95
4.28 SDS-page image of rhGH produced by <i>P. pastoris-hGH-Mut^s</i> (a) and <i>P. pastoris-hGH-Mut⁺</i> (b).....	96
4.29 Effects of methanol concentrations on cell growth of <i>P. pastoris-hGH-Mut⁺</i> strain in defined mixed-batch medium containing glycerol at an initial concentration; 30 kg m ⁻³ (solid lines).....	98
4.30 Effects of methanol concentrations on cell growth of <i>P. pastoris-hGH-Mut^s</i> strain in defined mixed-batch medium containing glycerol at an initial concentration; 30 kg m ⁻³ (solid lines)Dot-blot analysis	98
4.31 Glycerol utilization diagram of <i>P. pastoris-hGH-Mut⁺</i> strain in defined mixed-batch medium	99
4.32 Glycerol utilization diagram of <i>P. pastoris-hGH-Mut^s</i> strain in defined mixed-batch medium	99
4.33 Methanol utilization diagram of <i>P. pastoris-hGH-Mut⁺</i> strain in defined mixed-batch medium	100
4.34 Methanol utilization diagram of <i>P. pastoris-hGH-Mut^s</i> strain in defined mixed-batch medium	100

4.35 SDS-page image of rhGH produced by <i>P. pastoris-hGH-Mut^s</i> (a) and <i>P. pastoris-hGH-Mut⁺</i> (b).....	102
4.36 The variations in the dissolved oxygen concentration with the cultivation time, agitation and air inlet rates applied	107
4.37 The variations in cell concentration with the cultivation time, agitation and air inlet rates applied	108
4.38 The variations in methanol concentration with the cultivation time, agitation and air inlet rates applied	109
4.39 The variations in rhGH concentration with the cultivation time, agitation and air inlet rates applied	111
4.40 The variations in formaldehyde concentration with the cultivation time, agitation and air inlet rates applied	116
4.41 The trend of K_La profiles with cell concentration and stirring rate	119
4.42 The variation of OUR with cell concentration and stirring.....	122
4.43 The variation of OTR with cell concentration and stirring rate	123
4.44 The variation of Da numbers with cell concentration and stirring rate	123
4.45 The variation of η with cell concentration and stirring rate	124
4.46 The variations in the specific growth rates with the cultivation time, and agitation rate.....	126
4.47 The variations in the oxygen uptake rates with the cultivation time, and agitation rate.....	127
4.48 The variations in the specific substrate consumption rate with the cultivation time	127
4.49 The variations in the specific production formation rate with the cultivation time, and agitation rate	128
4.50 The variations in the dissolved oxygen, methanol and cell concentration with the cultivation time	130

4.51 The variations in rhGH concentration of impulse feeding fermentation with the cultivation time.....	132
4.52 The variations in formaldehyde concentration of impulse feeding fermentation with the cultivation time	133
4.53 SDS-page and Western blot of rhGH, produced by <i>P. pastoris</i> and purified.....	140
4.54 MALDI-TOF MS analysis.	141
A.1 First forward primer	163
A.2 Second forward primer	163
A.3 Reverse primer	164
A.4 SDS-page analysis showing the cultivation media at different time when mixed carbon sources (glycerol/methanol) were used.....	167
A.5 SDS page analysis of bioreactors at different time	168

NOMENCLATURE

C_{DO}	Dissolved oxygen concentration, mol m ⁻³ ; kg m ⁻³
C_O^*	Oxygen saturation concentration, mol m ⁻³ ; kg m ⁻³
C_{form}	Formaldehyde concentration, kg m ⁻³
C_{Gly}	Glycerol concentration, kg m ⁻³
C_{hGH}	Human growth hormone concentration, kg m ⁻³
C_{MeOH}	Methanol concentration, kg m ⁻³
C_P	Product concentration, kg m ⁻³
C_S	Concentration of the substrate, mM; kg m ⁻³
C_X	Cell concentration, kg dry cell m ⁻³
Da	Damköhler number (=OD / OTR _{max} ; Maximum possible oxygen utilization rate per maximum mass transfer rate)
E	Enhancement factor (=K _L a / K _L a ₀); mass transfer coefficient with chemical reaction per physical mass transfer coefficient
K_{La_0}	Physical overall liquid phase mass transfer coefficient; s ⁻¹
K_{La}	Overall liquid phase mass transfer coefficient; s ⁻¹
N	Agitation rate, min ⁻¹
m_0	Rate of oxygen consumption for maintenance, kg oxygen kg ⁻¹ dry cell weight h ⁻¹
m_S	Maintenance coefficients for substrate, kg substrate kg ⁻¹ dry cell weight h ⁻¹
pH_0	Initial pH
Q_0	Volumetric air feed rate, m ³ min ⁻¹
q_0	Specific oxygen uptake rate, kg kg ⁻¹ DW h ⁻¹
q_s	Specific substrate consumption rate, kg kg ⁻¹ DW h ⁻¹
r_0	Oxygen uptake rate, mol m ⁻³ s ⁻¹ ; kg m ⁻³ h ⁻¹
r_X	Rate of cell growth, kg m ⁻³ h ⁻¹
T	Bioreaction medium temperature, °C

t	Bioreactor cultivation time, h
V_R	Volume of the bioreaction medium, m ³
$Y_{X/S}$	Yield of cell on substrate, kg kg ⁻¹
$Y_{X/O}$	Yield of cell on oxygen, kg kg ⁻¹
$Y_{S/O}$	Yield of substrate on oxygen, kg kg ⁻¹
$Y_{P/X}$	Yield of product on cell, kg kg ⁻¹
$Y_{P/S}$	Yield of product on substrate, kg kg ⁻¹
$Y_{P/O}$	Yield of product on oxygen, kg kg ⁻¹

Greek Letters

α, β	Leudeking-Piret constants
η	Effectiveness factor (=OUR/OD; the oxygen uptake rate per maximum possible oxygen utilization rate)
μ	Specific cell growth rate, h ⁻¹
μ_{\max}	Maximum specific cell growth rate, h ⁻¹
λ	Wavelength, nm

Abbreviations

DO	Dissolved oxygen
hGH	Human growth hormone
Mut ⁺	Wild type methanol utilization phenotype
Mut ^s	Methanol utilization slow phenotype
Mut ⁻	Methanol utilization minus phenotype
OD	Oxygen demand (= $\mu_{\max} C_X / Y_{X/O}$; mol m ⁻³ s ⁻¹)
OUR	Oxygen uptake rate, mol m ⁻³ s ⁻¹
OTR	Oxygen transfer rate, mol m ⁻³ s ⁻¹
OTR _{max}	Maximum possible mass transfer rate (= $K_L a C_{O^*}$; mol m ⁻³ s ⁻¹)
rhGH	Recombinant human growth hormone

CHAPTER 1

INTRODUCTION

During the 20th century, especially the last few decades, the advances in biological sciences and increasing interaction of these sciences with engineering disciplines have resulted in an increase in research areas about the production of bio-molecules which are very important for human beings. Due to the increasing demand for the medical, agricultural and food products used for improving the human health and environment, disciplines such as biotechnology, based on the biological and engineering sciences, began to develop new methods in order to optimize the production of these industrial products. In this frame, with the help of methodology of recombinant DNA technology which is newly progressive branch, it is now possible to produce bio-molecules which are produced by human metabolism but not other organisms by cloning targeted gene, which is responsible for the production of the desired bio-molecules, into the different organism' genome. These genetically altered organisms and enhanced fermentation processes are always applied to biotechnological research areas in order to produce a broad spectrum of products (Table 1.1) (Nielsen et al., 2003).

Recombinant versions of most of the hormones, crucial chemicals regulating the metabolic activities of a human body, have been already produced in the Biotechnology industry and have considerable market values as seen on Table 1.1. Human growth hormone (hGH) is also one of the industrial proteins produced for pharmaceutical applications. Human growth hormone, a non-glycosylated protein known as somatotrophic hormone, is extracted from human pituitary glands and regulates the growth. Recombinant version of hGH, having a molar mass of 22 kDa and 191 amino acid residues, has been used to treat hypopituitary dwarfism, injuries, bone fractures, bleeding ulcers, and burns, furthermore it appears to be considerably benefit to girls with Turner's syndrome, children with chronic renal failure and adults

with growth hormone deficiency or human immunodeficiency virus (HIV) syndrome (Baulieu et al., 1990; Binkley, 1994, Trevino et al., 2000).

Table 1.1 List of some fermentation products and some market values in year 2000 (Nielsen et al., 2003).

Product	Typical organism	Market value
Erythropoietin	Chinese Hamster Ovary cells	3.6 billion US\$
Penicillins	<i>Penicillium chrysogenum</i>	4 billion US\$
Insulin	<i>Saccharomyces cerevisia</i>	3 billion US\$
Human growth hormone	<i>Escherichia coli</i>	1 billion US\$
Interferons	<i>Escherichia coli</i>	2 billion US\$
Ethanol	<i>Saccharomyces cerevisia</i>	12 billion US\$
Lactic acid	<i>Zymomonas mobilis</i>	200 million US\$
Citric acid	<i>Rhizopus oryzae</i>	1.5 billion US\$
Glutamate	<i>Aspergillus niger</i>	1 billion US\$
Lysine	<i>C. glutamicum</i>	500 million US\$
Phenylalanine	<i>C. glutamicum</i>	200 million US\$
Single cell protein	Methylotrophic bacteria	-
Taxol	Plant cells	1 billion US\$
Detergent enzymes	<i>Bacilli, Aspergilli</i>	600 million US\$
Starch industry	<i>Bacilli, Aspergilli</i>	200 million US\$
Xanthan gum	<i>Xanthomonas campestris</i>	400 million US\$

Until 1985, hGH was extracted from the human pituitary glands of the limited cadavers. With the increase in the number of the Creutzfeldt-Jacob Disease, demand for the hGH rised, which resulted in development in the production of the recombinant hGH by using the biotechnological approaches. Goeddel et al. (1979) was the first group producing recombinant hGH. In this study, the hybrid hGH gene, whose initial part, first 23 codes, was chemically synthesized and the remain part, from 24th to 191st code, was produced by the reverse transcriptase from RNA taken from human pituitary, was expressed in *E. coli* under the control of *lac*. Since *E. coli* is a well known microorganism and can be handled easily, most of the studies have been reported from *E. coli* by applying different promoters, signal peptides for extracellular protein

production and bioprocess operation parameters (Ikehara et al., 1984; Gray et al., 1985; Kato et al., 1987; Shin et al., 1998b; Tabandeh et al., 2004). Hsiung et al., (1988) have been able to efficiently produce hGH using *E. coli* cells harboring two vectors, the hGH secretion vector *pOmpA-hGH2* including *pOmpA* signal peptide sequence and *pJL3* vector including bacteriocin release protein gene. With the use of IPTG as inducer for the production of recombinant protein, they were able to produce 69.6 mg hGH L⁻¹.

There are other microorganisms that have been used for the production of the recombinant hGH. Choosing microorganism for the production of hGH is very important. Microorganism should require an inexpensive and easy to prepare medium and should grow rapidly and enable to produce high amounts of the product. Due to its ability to secrete protein to the extracellular medium and high product capacity and its convenience, bacillus species is also used for the recombinant hGH production (Nakayama et al., 1988; Franchi et al., 1991; Kajino et al., 1997; Şentürk, 2006). Nakayama et al. (1988) compared two *B. subtilis* strains containing different plasmids, one of which includes neutral protease terminator gene with *hGH* gene and the other has only *hGH* gene; and the plasmid containing neutral protease terminator gene produced hGH more than ten fold and in the semi-batch fermentation broth 40 mg hGH L⁻¹ was obtained.

The other strong candidate for the production of the recombinant proteins is *P. pastoris*. Although *P. pastoris* is a eukaryotic microorganism, which can be easily handled, needs simple media and has a high protein production capacity due to the availability of strong alcohol oxidize 1 promoter which initialize the synthesis of the first enzyme in methanol utilization pathway. Furthermore *P. pastoris* has the capability of performing many eukaryotic posttranslational modifications, such as glycosylation, disulfide bond formation and proteolytic processing. In literature, there are no profound studies about purification of hGH, optimization of medium and investigation of bioprocess operation parameters of *P. pastoris* cells producing rhGH. Nevertheless, Trevino et al. (2000) was the first group who intended to produce and secrete mature and biologically active rhGH from *P. pastoris* by manipulating and inserting the hGH cDNA into the genome of this methylotrophic yeast. They produced up to 11 mg rhGH L⁻¹ in shake tubes having 3 ml of culture medium, while they obtained about 49 mg rhGH L⁻¹

with high cell density cultures using a defined fed-batch fermentation medium within a 2-l bioreactor. Eurwilaichitr et al. (2002) investigated whether glutamic acid and alanine spacer (glu-ala) was necessary for the removal of MFa-1signal sequence fused to the hGH produced from *P. pastoris* by constructing three different vectors including no glu-ala, one glu-ala and two glu-ala repeats, respectively. They also investigated the optimal conditions producing high level of extracellular rhGH. As a result, they found that removal of glu-ala repeats from the hGH were not efficient and they were not necessary for the removal of MFa-1signal sequence. They also obtained the highest hGH concentration as 190 mg L⁻¹ at 3% (v/v) methanol concentration after 3 day induction in complex medium.

In this study, first, a strategy for the extracellular expression by recombinant *P. pastoris* and purification of human growth hormone was applied by using molecular genetic techniques. The cDNA of hGH fused with a polyhistidine tag for rapid purification using immobilized metal affinity chromatography (IMAC) purification, and also fused with a target site for the Factor Xa protease, in which cleavage produces a mature form of rhGH, having N- and C- termini, was synthesized using primer extension and PCR amplification approaches. The constructed system within the plasmid, *pPICZaA::hGH*, was integrated to AOX1 locus of *P. pastoris* and expressed under alcohol oxidase promoter. Thereafter, the effects of carbon sources, glycerol and methanol, on rhGH production were investigated in laboratory scale air filtered shake bioreactors and using the designed defined medium finally effects of oxygen transfer on rhGH production, by-product formation, and cell growth, oxygen transfer and fermentation characteristics were investigated by using pilot scale bioreactor.

CHAPTER 2

LITERATURE SURVEY

For the production of rhGH by using a recombinant microorganism with the desired properties, principles of two main fields should be taken into consideration. These are the principles of genetic engineering used for cloning the hGH gene to a convenient plasmid and the principles of bioprocess engineering which include choosing the microorganism, medium design and investigating bioreactor operation conditions. In this context, this chapter reviews the literature on the product, hGH; genetic engineering techniques and bioprocess operation parameters.

2.1 PROTEINS

Proteins are large organic molecules composed of amino acids joined together by peptide bonds between the carboxyl and amino groups. The sequence of amino acids in a protein is defined by a gene and encoded in the genetic code. Most proteins fold into unique 3-dimensional structures. The shape into which a protein naturally folds is known as its native state. There are four distinct types of a protein's structure: 1) *Primary structure*: the amino acid sequence, 2) *Secondary structure*: regularly repeating structures stabilized by hydrogen bonds, 3) *Tertiary structure*: the 3-dimensional structure of a single protein molecule stabilized by nonlocal interactions, that is, hydrophobic interactions, salt bridges, hydrogen bonds, disulfide bonds, and even post-translational modifications, 4) *Quaternary structure*: the shape or structure that results from the interaction of more than one protein molecule (Lehninger, 1979).

Proteins have many functions. They can be used as enzymatic catalysts, transport molecules and storage molecules; they are needed for mechanical support and movement. Moreover, they can serve as hormones

which control growth and cell differentiation and immune protection (Lehninger, 1979).

2.1.1 Hormones

A hormone is a chemical messenger from a cell or a group of cells and serves as a signal to the target cells. Hormone affects the body very widely (Baulieu et al., 1990; Binkley, 1994):

- stimulation or inhibition of growth,
- induction or suppression of apoptosis (programmed cell death),
- activation or inhibition of the immune system,
- regulation of the metabolism and preparation for a new activity or phase of life.

2.1.1.1 Human Growth Hormone (hGH)

Growth hormone is secreted by the somatotrope cells of the pituitary gland and regulates the growth. Peptides released by the cells in the hypothalamus controls the excretion of the hGH. Growth hormone releasing factor (GHRF) produced by the arcuate nucleus which is an aggregation of neurons in the mediobasal hypothalamus and ghrelin produced by the cells lining the stomach promote GH secretion, on the other hand, somatostatin from the periventricular nucleus inhibits it. The amount of the hGH in the blood also regulates the secretion process, i.e. it has a feed back regulation system. In addition to the regulatory systems listed above, there are also some other physiological stimulators such as sleep, protein dietary, exercise, hypoglycemia, estradiol, and physiological inhibitors like dietary carbohydrate and glucocorticoids (Baulieu et al., 1990; Binkley, 1994).

a) Biological and Genetic Structure of hGH:

The hGH genes are located in the q22-24 region of the chromosome 17 of human beings and they are closely related to hCS genes known as placental lactogen genes. The nucleotide sequence of hGH is shown on figure 2.1 (Goeddel et al. 1979; Goeddel and Heyneker 1982). There are two isoforms of hGH; one of them has a weight of 22 kDa and the other one has a weight of

20 kDa. The human growth hormone which has a molecular weight of 22 kDa is found in pituitary glands much more than the other, almost 90% of total hGH in pituitary glands. Functions of the isoform molecular weight of which is 20 kDa are not known. For the normal development of skeletal and other tissues, the isoform which has a molecular weight of 22 kDa is needed (Baulieu et al., 1990; Binkley, 1994).

```

ttc cca act ata cca cta tct cgt cta ttc gat aac gct atg ctt cgt gct
cat cgt ctt cat cag ctg gcc ttt gac acc tac cag gag ttt gaa gaa gcc
tat atc cca aag gaa cag aag tat tca ttc ctg cag aac ccc cag acc tcc
ctc tgt ttc tca gag tct att ccg aca ccc tcc aac agg gag gaa aca caa
cag aaa tcc aac cta gag ctg ctc cgc atc tcc ctg ctg ctc atc cag tgg
tgg ctg gag ccc gtg cag ttc ctc agg agt gtc ttc gcc aac agc cta gtg
tac ggc gcc tct gac agc aac gtc tat gac ctc cta aag gac cta gag gaa
ggc atc caa acg ctg atg ggg agg ctg gaa gat ggc agc ccc cgg act ggg
cag atc ttc aag cag acc tac agc aag ttc gac aca aac tca cac aac gat
gac gca cta ctc aag aac tac ggg ctg ctc tac tgc ttc agg aag gac atg
gac aag gtc gag aca ttc ctg cgc atc gtg cag tgc cgc tct gtg gag ggc
agc tgt ggc ttc tag ctg ccc ggg tgg cat ccc tgt gac ccc tcc cca gtg
cct ctc ctg gcc

```

Figure 2.1 Nucleotide sequence of human growth hormone (Baulieu et al., 1990; Binkley, 1994).

The hGH that is required in order to perform the body functions has 191 amino acids and has a molecular weight of 22 kDa, approximately. The protein includes four helices for the necessary interaction with the hGH receptors. The four cysteine biomolecules which are found on 35th, 165th, 182nd, and 189th positions of the hGH chain result in two disulfide bonds which enable to form tertiary structure or active form of protein. The secondary structure of hGH which has only one chain is in the form of alpha-helix and the isoelectric point of the protein, pI is 4.9 (Binkley,1994). The amino acid sequence and structure of human growth hormone are shown on figure 2.2 and figure 2.3 (<http://www.ncbi.nlm.nih.gov>).

```

mfptiplsrl fdnamlrahr lhqlafdtyq efeeayipke qkysflqnpq
tslcfesesip tpsnreetqq ksnlellris llliqswlep vqflrsvfan
slvygasdsn vydllkdlee giqtlmgrle dgsprtggqif kqtyskfdtn
shnddallkn ygllycfrkd mdkvetflri vqcrsvegsc gf

```

Figure 2.2 Amino acid sequence of hGH (<http://www.ncbi.nlm.nih.gov>).



Figure 2.3 Tertiary structure of hGH (<http://www.ncbi.nlm.nih.gov>).

b) Physiological Effects and Functions of hGH

The main function of the human growth hormone is that it stimulates the growth, and division of the cells of tissues. Growing is a complex process which is related with the metabolic activities and nourishment of organism and it also needs different hormones working in a coordinate. Human growth hormone has two effecting mechanisms on tissues; direct and indirect effects. Its direct effects occur by binding to receptors of its target cells. Its indirect effects occur by the insulin like growth factor- 1 (IGF-1) which is secreted by liver and some other tissues as a response to hGH. Therefore, hGH plays important role indirectly in the growing of muscles by stimulating the proliferation of muscle, bone and cartilage cells.

Human growth hormone affects protein metabolism by postponing the catabolism of amino acid and increasing the production of protein and lipid metabolism by stimulating oxidation of triglyceride which increases the usage of fat and also carbohydrate metabolism because it is an anti-insulin.

Secretion of hGH in an excess amount can result in adenoma causing headaches, impair vision and deficiency of other pituitary hormones. Prolonged hGH excess in older people thickens the bones of the jaw, fingers and toes, named as acromegaly, associated with pressure on nerves, muscle weakness, etc. Moreover, excess secretion during the childhood causes excessive growth referred pituitary gigantism less secretion results in hypopituitary dwarfism, children with short stature.

Human growth hormone makes it possible to treat not only children with short stature but other disorders as a therapeutic usage. In adults with hGH deficiency, it has a important effect on body composition, and improves physical activity and cardiac function. It is also used in the treatment of injuries, bone fractures, bleeding ulcers, burns, and some problems related with dermatology and nourishment. In addition to these treatments, hGH is thought to be of considerable benefit to girls with Turner's syndrome, children with chronic renal failure and adults with growth hormone deficiency or human immunodeficiency virus (HIV) syndrome (Baulieu et al., 1990; Binkley, 1994; Şentürk, 2006, Trevino et al., 2000).

c) Studies about the rhGH production in literature

Up to 1985, hGH has been extracted from the human pituitary glands of the limited cadavers. Goedel et al. (1979) was the first group producing rhGH using *Escherichia coli*. Most of the studies since then have been reported from different microorganisms by using different promoters, signal peptides for the extracellular protein secretion and bioprocess operation parameters. Table 2.1 and Table 2.2 summarize the studies about the production of rhGH in literature.

E. coli and *B. subtilis* genomes have been fully mapped, and in addition as they require inexpensive medium and can be easily handled, *E. coli* and *B. subtilis* cells are commonly used for the production of rhGH (Table 2.1 and Table 2.2)

Table 2.1 Published studies about the production of recombinant human growth hormone: Microorganisms, promoters, signal peptides and results, etc.

Microorganism	Plasmid (s)	Promoter	Signal peptide	Medium	Type of product	Analysis of hGH conc.	Results	Source
<i>E. coli</i> 294	<i>pGHG107</i>	<i>lac</i>	-	-	Intracellular	RIA	2.4 µl/ml hGH was obtained.	Goeddel et al., 1979
<i>E. coli</i> HB101	<i>pGH-1</i> <i>pGH-L8</i> <i>pGH-L9</i> <i>pGH-L9</i> <i>pGH-L11</i> <i>pGH-L13</i>	<i>trp</i>	-	-	Intracellular	RIA	The highest hGH production was obtained as 168.7 µl/ml by using <i>pGH-L9</i> plasmid.	Ikehara et al., 1984
<i>E. coli</i> 294	<i>pPreHGH207-2</i> <i>pAPH-1</i>	<i>trp</i> <i>phoA</i>	<i>pre-hGH</i> <i>pho-hGH</i>	Complex	Periplasmic	RIA	450 ng/ml/A ₅₅₀ with <i>pPreHGH207-2</i> plasmid, 230 ng/ml/A ₅₅₀ hGH with <i>pAPH-1</i> plasmid were produced.	Gray et al., 1985
<i>E. coli</i> K-12 RV308	<i>pOmpA-hGH1</i> <i>pOmpA-hGH2</i>	<i>lpp-lac</i>	<i>ompA</i>	Complex	Periplasmic Intracellular	RIA ELISA	10-15 µg hGH/ A ₆₀₀ was produced and 72 % total hGH was secreted into periplasm. .	Becker and Hsiung, 1986; Hsiung et al., 1986;
<i>E. coli</i> HB101	<i>p8hGH1</i> <i>pPS-hGH11</i>	<i>Ex-K</i> <i>Ex</i>	<i>Bacillus penicillinase</i>	Complex	Extracellular Intracellular Periplasmic	RIA	When <i>p8hGH1</i> plasmid was used, permeability of cell membrane was increased. %55 (11.2mg/l) of total protein was obtained extracellularly, %42 was produced periplasmic, %3 was secreted intracellularly.	Kato et al., 1987
<i>E. coli</i> BL21	<i>pT2GH</i>	<i>lacUV5</i>	-	Complex	Intracellular	Western blot SDS-PAGE	9 g hGH/l was obtained intracellularly and it was seen that 80% of hGH was not soluble in cytoplasm.	Shin et al., 1998b
<i>E. coli</i> A6-5	<i>pET21-hgh</i> <i>pGPI-2</i>	T7 <i>AP₂</i>	-	Defined Complex	Intracellular	ELISA	Glycerol and glucose were used as carbon sources and 2 ve 2.7 g hGH/l were obtained, respectively.	Tabandeh et al., 2004.

Cont'd of Table 2.1.

<i>B. subtilis</i> MTS00	<i>phGH324</i> <i>phGH526</i>	Promoter of <i>B. amyloliquef</i> <i>aciens'</i> <i>natural</i> <i>protease</i> <i>gene</i>	Pre-signal of <i>B. amyloliquef</i> <i>aciens'</i> <i>natural</i> <i>protease</i> <i>gene</i>	Complex	Extracellular	EIA	40 mg hGH/l was secreted extracellularly by using <i>phGH526</i> plasmid.	Makayama et al., 1988
<i>B. subtilis</i> SMS118	<i>pSM214</i> <i>pSM215</i> <i>pSM274</i> <i>pSM250</i>	-	<i>pSM212</i>	Complex	Intracellular	Western blot	It was seen that long peptide sequences which were added to 5' end of hGH for the purification decreased the solubility of hGH. Since short peptide sequences changed the pI of protein, they simplified the purification.	Franchi et al., 1991
<i>B. brevis</i> HPD31 <i>B. brevis</i> 31-OK	<i>pNU211hGH</i> <i>pNU211L4hGH</i> <i>pNU211R2L4hGH</i> <i>pNU211L15hGH</i>	<i>pNU211hGH</i>	<i>MWP</i> <i>L4</i> <i>R2L4</i> <i>L15</i>	Complex	Extracellular	ELISA	The production of hGH was increased 12 fold (148 mg/ml) when <i>MWP</i> signal peptide was used instead of <i>R2L4</i> signal peptide. hGH production was further increased by optimizing production medium and operation conditions.	Kajino et al., 1997
<i>B. subtilis</i> 1A751 <i>B. subtilis</i> 1A179	<i>pre(subC)::hGH::pUC19</i> <i>pre(subC)::hGH::pMK4</i>	Promoter of <i>SAP gene</i>	Pre signal sequence of <i>SAP gen</i> (subC)	Defined	Extracellular	Capillary electrophoresis	The maximum hGH production was obtained as 70 mg/l at $Q_{10}/V_{10}=0.5$ vvm, $N=800$ min ⁻¹ conditions.	Şentürk, 2006
<i>P. pastoris</i> GS115	<i>pPIC9hGH22K</i>	<i>AOX1</i>	<i>S. cerevisiae</i> α -factor	Defined	Extracellular	Western-blot	O_2 -limited induction of recombinant yeast strains in shake tubes with 3 ml of culture medium produced up to 11 mg rhGH l ⁻¹ , while high cell density cultures using a 2-l bioreactor produced about 49 mg rhGH l ⁻¹ .	Trevino et al., 2000
<i>P. Pastoris</i> KM71	<i>phGH1</i> <i>phGH2</i>	-	<i>S. cerevisiae</i> α -factor	Complex	Extracellular	SDS-PAGE	The highest hGH production was obtained as 190 mg/l at 3% (v/v) methanol concentration after 3 day induction.	Eurwilaichtr et al., 2002

Table 2.2 Published studies about the production of recombinant human growth hormone; Bioreactor operation parameters.

Microorganism	Bioreactor operation parameters							Feeding regime	Prod. Medium/ Carbon source	Type of hGH production	Results			Source	
	Bioreactor operation type	T °C	pH	V _R dm ³	N min ⁻¹	Q _o /V wvm	DO %				Analysis of hGH	C _{hGH} g/l	C _{DC} g/l		C _A g/l
<i>E.coli</i> MC1061	Batch	30	7.2	-	? 500	1	? 20	-	Complex/ glucose	Cytoplasmic	ELISA	0.4	30	10	Jensen and Carlsen, 1990
	Cemostat	30	7.2	1.3	? 500	1	? 20	0.12				30	1.6		
	Fed-batch	30	7.2	-	? 500	1	? 20	1.0				40	2-3		
	Fed-batch	30	7.2	-	? 500	1	? 20	2.0				40	0		
<i>E.coli</i> BL21(DE3)	Fed-batch	37	6.75	-	-	-	40	Cont./ dynamic	Complex/ glucose	Cytoplasmic	SDS-PAGE/ Western blott	15 ^o	70	0	Shin et al., 1998a.
	Fed-batch	37	6.75	-	-	-	40	pH-stat	Complex/ glucose	Cytoplasmic	SDS-PAGE/ Western blott	9 ^o	90	0	Shin et al., 1998b
<i>E.coli</i> W3110	Lab. scale Fed-batch	30	7.0	9	1000	1.4	-	Cont.	Complex/ glucose	Cytoplasmic	HPLC	64.6	90	0	Bylund et al., 2000
	Fed-batch	30	7.0	-	1000	1.4	-	Cont.				75.8	80	20	
	Pilot-scale Fed-batch	30	7.0	3000	205	1.4	-	Cont.				41.7	95	30	
	Cell production Fed-batch: hGH production	34	7.0	4	? 1000	1	20	Cont.				-	75	0.5	
<i>E.coli</i> A6-5	Fed-batch	34	7.0	6	? 1000	1	20	Cont.	Defined/ Glucose	Cytoplasmic	HPLC	37au	-	0.7	
	Fed-batch	30	7.0	-	400-900	1	? 40	pH-stat	Defined/ Glucose	Cytoplasmic	ELISA	-	25	-	Tabandeh et al., 2004
	Fed-batch	30	7.0	-	400-900	1	? 40	Cont. ; dynamic	Complex/ glucose	Cytoplasmic	ELISA	2	60	2	
Fed-batch	30	7.0	-	400-900	1	? 40	Cont. ; dynamic	Complex/ glucose	Cytoplasmic	ELISA	2.7	100	1		

Contd of Table 2.2.

Microorganism	Bioreactor operation parameters							Feeding regime pH	Prod. Medium / Carbon source	Results					
	Bioreactor operation type	T °C	pH	V _R dm ³	N Min ⁻¹	Q/V vvm	DO %			Type of hGH production	Analysis of hGH	C _{HGH} g/l	C _{hC} g/l	Source	
<i>B.subtilis</i> MT500	Batch	30	6-7	1	-	-	0-70	Defined/ Glucose	Extracellular	Western Blott	0.006	-	Nakayama et al., 1988		
	Fed-batch	30	6.5-7	4	-	-	0-10				0.04			0.35	
<i>B.subtilis</i> 1A751	Batch	37	7.25	0.55	500	0.5	-	-	Defined/ Glucose	Extracellular	Capillary Electroph.	0.036	1.3	Şentürk 2006	
					700	0.5						0.054			1.75
					800	0.5						0.07			1.9
					800	0.7						0.06			2.1
<i>P. pastoris</i> GS115	Fed-batch (Methanol)	30	5.8	1	700	-	>20	Cont. (Methanol)	Defined/ Glycerol and methanol	Extracellular	Western blott	0.049	73 (dry weight)	Trevino et al., 2000	

Although, *P. pastoris* is one of the strong candidates which have been used for the production of the recombinant proteins, in literature there are only two studies about the rhGH production from this microorganism. Trevino et al. (2000) was the first group who intended to produce and secrete mature and biologically active rhGH from *P. pastoris* by manipulating and inserting the hGH cDNA into the genome of this methylotrophic yeast. They produced up to 11 mg rhGH L⁻¹ in shake tubes having 3 ml of defined culture medium, while they obtained about 49 mg rhGH l⁻¹ with high cell density cultures using a 2-l bioreactor. Eurwilaichitr et al. (2002) investigated whether glutamic acid and alanine spacer was necessary for the removal of MFa-1signal sequence fused to the hGH produced from *P. pastoris* by constructing three different vectors including no glu-ala, one glu-ala and two glu-ala repeats, respectively. They also investigated the optimal conditions producing high level of secreted rhGH. They synthesized hGH cDNA, for construction of vector, by using codons preferred by *Escherichia coli*, except for the first 20 amino acids, which were changed to that preferred by *Saccharomyces cerevisiae* and *Pichia pastoris*. As a result, they found that removal of glu-ala repeats from the hGH were not efficient and they were not necessary for the removal of MFa-1signal sequence. They also obtained the highest hGH concentration as 190 mg/l at 3% (v/v) methanol concentration after 3 day induction in complex medium.

2.2 GENETIC ENGINEERING TECHNIQUES: METHODOLOGY

The techniques of genetic engineering, alternatively known as recombinant DNA technology, brought about a revolution in biotechnology science. The fact that recombinant proteins have come into prominence has led to the development of genetic engineering techniques. Amplifying the specific DNA regions by Polymerase Chain Reaction (PCR) method, determination of DNA concentration, restriction digestion and ligation reaction are some basic principles used in recombinant DNA technology. The procedure or steps of this technique are explained below:

- The gene amplified with PCR and convenient plasmid are cut with suitable restriction enzymes, which is necessary for the combining of plasmid and the gene.

- After digestion, two fragments (gene and plasmid) are ligated and recombinant plasmid including the gene is transformed into the microorganisms.
- The microorganisms are plated on a medium containing an antibiotic. Since plasmid has the antibiotic resistant gene, only the microorganisms that containing the plasmid can grow, therefore cloned microorganisms can be easily selected.
- It is also controlled again with other biological methods whether the selected microorganism have plasmid or not.

In order to apply this procedure the gene of interest should be amplified by using PCR, polymerase chain reaction. It is a technique for amplifying DNA sequences in vitro by separating the DNA into two strands and incubating it with oligonucleotide primers and DNA polymerase. It can amplify a specific sequence of DNA by as many as one billion times and is important in biotechnology, forensics, medicine, and genetic research. Three major steps are involved in a PCR device. These three steps are repeated for 30 or 40 cycles. The cycles are done on an automated cycler, which rapidly heats and cools the test tubes containing the reaction mixture. Each step -- denaturation (the double-stranded DNA melts at greater than 90 °C and opens into single-stranded DNA), annealing (joining primers and single stranded DNA), and extension (replication of DNA by polymerase at 72 °C) -- takes place at a different temperature. The annealing temperature is a key variable in determining the specificity of a PCR so temperatures and times used vary depending on the sequences to be amplified. The heat-stable enzyme commonly used is derived from a thermophilic Gram-negative eubacterium, *Thermus aquaticus* (Glazer, 1995). One of these early isolates Taq DNA polymerase and its derivatives have a 5' to 3' polymerization depended exonuclease activity. For nucleotide incorporation, the enzyme works best at 75-80°C, depending on the target sequence; its polymerase activity is reduced by a factor of 2 at 60°C and by a factor of 10 at 37°C (Sambrook and Russell, 2001).

Choosing plasmid where the gene of interest is cloned is the other important step in recombinant DNA technology. Plasmids are autonomously replicating, extrachromosomal circular DNA molecules, distinct from the normal bacterial genome and nonessential for cell survival under nonselective

conditions (Clug et al., 2006). Some plasmids are capable of integrating into the host genome. A number of artificially constructed plasmids are used as cloning vectors. Plasmids most commonly used in recombinant DNA technology have three common regions essential for DNA cloning: a replication origin; a marker that permits selection, usually a drug resistance gene; and a region in which exogenous DNA fragments can be inserted (Lodish et. al., 2003). Plasmids are classified with regard to their functions. The classes that have been well studied are *F-plasmids* which are capable of conjugation, *R-plasmids* containing genes that can build a resistance against antibiotics and poisons, *Col-plasmids* containing genes that code for proteins having the ability to kill other bacteria and *recombinant plasmids* (Klug et al., 2006).

In order to produce recombinant plasmids, first the gene of interest and plasmid are digested with desired restriction enzymes. These enzymes serve the bacteria in which they occur as protection from foreign DNA. The enzymes cut foreign DNA from outside the helix, but do not digest the host DNA due to characteristic methylation patterns on the DNA (Scragg, 1988). There are several types of restriction enzymes; the most useful for cloning, the Type II restriction enzymes recognize specific sequences, usually 4-8 bp in length, and cut DNA molecules within these sequences (Kirk and Othmer, 1994). The restriction enzymes used in this study and their recognition sequences are listed in Table 2.3.

Table 2.3 Recognition sites and cleavage points of restriction enzymes

Enzyme	Target site
<i>EcoRI</i>	5'-G [^] AATTC-3'
<i>SacI</i>	5'-GAGCT [^] C-3'
<i>XbaI</i>	5'-T [^] CTAGA-3'

The DNA fragment of interest cut by a restriction enzyme leads to single stranded tails, sticky ends, which have a tendency to anneal with the complementary strand present in the ligation reaction mixture. The addition of vector DNA cut open by the same restriction enzyme results in the annealing of the foreign DNA to the complementary ends of the cut vector. The phosphodiester bonds missing between the attached strands are covalently

bond by DNA ligase. This enzyme catalyzes the condensation of 3'-hydroxyl group with a 5'-phosphate group to add the missing links. The ligation reaction is the rate limiting step in genetic engineering techniques since this reaction requires the cohesive ends of foreign DNA and open plasmid DNA to attach in correct orientation and anneal while preventing the relegation of opened vector DNA.

After ligation, the mixture containing recombinant vector including the gene of interest is then transfer into the recipient or host cell. In most cases this is done by transformation (Schuler and Kargı, 2002). There are four different methods for direct introduction by transformation: 1) *Natural transformation* where foreign DNA is taken up by the bacteria and fused to the chromosomal DNA of the organism, 2) *Artificial transformation* where the cells are converted to competent state to make ready for DNA transformation by CaCl₂ solution at 0°C, 3) *Protoplast transformation* in which enzymes are used to hydrolyze the rigid cell wall to convert the cell into protoplast bounded by the cytoplasmic membrane and 4) *Electroporation* where short electrical pulses of very high voltage is applied to create transient holes in the membrane (Glazer, 1995).

2.3 BIOPROCESS PARAMETERS IN RECOMBINANT PROTEIN PRODUCTION

Any operation involving the transformation of some raw material (biological or non-biological) into some product by means of microorganisms, animal or plant cell cultures, or by materials derived from them (e.g. enzymes, organelles), may be termed as a "bioprocess" (Moses and Cape, 1991). From the economical point of view, the aim is to optimize the system, i.e. to maximize the yield and productivity of industrial products. In this scope, bioprocess parameters which are choosing microorganism, medium composition, bioreactor operation parameters such as temperature, pH, oxygen transfer rate should be investigated comprehensively.

2.3.1 Choosing Microorganism

In bioprocesses, the selection of host microorganism for production of industrial proteins is often critical for the success of the process. Potential hosts should give sufficient yields, be able to secrete large amounts of protein, be suitable for industrial fermentations, produce a large cell mass per volume quickly and on cheap media, be considered safe based on historical experience or evaluation by regulatory authorities, and should not produce harmful substances or any other undesirable products (Kirk and Othmer, 1994). The most common microorganisms used as foreign gene expression systems are *E. coli* and *B. subtilis*, but they are less capable of performing many eukaryote-specific post translational protein modifications (Daly and Hearn, 2005). Although these microorganisms produce eukaryotic foreign proteins at high levels, the absence of eukaryotic post translational modification systems result in proteins that are often insoluble and inactive (Cregg, 1999), therefore researchers have recently turned to eukaryotic cells such as *P. pastoris*, a yeast, for the production of eukaryotic proteins.

2.3.1.1 *Pichia pastoris*

One of the important microorganisms that can be used for the secretion of recombinant hGH is *P. pastoris*. It is methylotrophic yeast that can use methanol as its sole carbon source. The media and the protocols for the *P. pastoris* growth medium were firstly described by the Phillips Petroleum Company during 1970s. Since then, *P. pastoris* began to be used for the biotechnological goals, and it has been genetically engineered in order to produce recombinant proteins. Nearly 400 proteins, including human growth hormone, have been reported (Cereghino et al., 2000; Cereghino et al., 2002).

P. pastoris is a mesophilic microorganism from the yeast species. Yeasts are unicellular fungi which usually appear as oval cells 1-5 μm wide by 5-30 μm long, they have typical eukaryotic cell structure and generally have a thick polysaccharide cell wall, and they are facultative anaerobes. *Pichia pastoris* reproduce asexually, i.e., it is a homothallic ascomycetous yeast and remains haploid unless forced to mate (Cregg, 1999).

P. pastoris species has advantages of eukaryotic cells. The detailed advantages/disadvantages of *P. pastoris* are shown on table 2.4 (Cregg, 1999; Daly and Hearn, 2005; Macauley-Patrick et al., 2005).

Table 2.4 Advantages and disadvantages of *P. pastoris*

<p>Advantages:</p> <ul style="list-style-type: none"> • High yield • High productivity • Chemically defined media-simple, inexpensive formulation • Product processing like mammalian cells • Stable production strains • Low purification cost • High levels of expression of intracellular and secreted proteins • Eukaryotic post-translational modifications • No endotoxin problem • Non-pathogenic • Broad pH range: 3- 7 • Ability of utilizing methanol • Strong promoter (AOX1) 	<p>Disadvantages:</p> <ul style="list-style-type: none"> • Potential of proteolysis, non-native glycosylation, hyper glycosylation, • Long time for cell cultivation • Monitoring methanol during a process is very difficult in order to induce AOX1 promoter. • Since methanol is a petrochemical substance, it may be unsuitable for use in the food industry and also storing of this in industrial scale is undesirable because it is a fire hazard.
--	--

a) Metabolism of *P. pastoris*:

Studies show that some essential enzymes required for the methanol metabolism are found at high levels only when the cells are grown on methanol (Cereghino et al., 2000). The enzyme alcohol oxidase (AOX) catalyzes the first step in the methanol utilization pathway, converts the methanol to formaldehyde and hydrogen peroxide (figure 2.4). Some portion of formaldehyde leaves peroxisome and is further oxidized to formate and

carbon dioxide, which is a source of energy. The remaining formaldehyde reacts with xylulose 5-monophosphate in order to form glyceraldehyde 3-phosphate and dihydroxyacetone which leave the peroxisome and enter a cytoplasmic pathway for the reproduction of xylulose 5-monophosphate and other cell materials (Charoenrat et al., 2005).

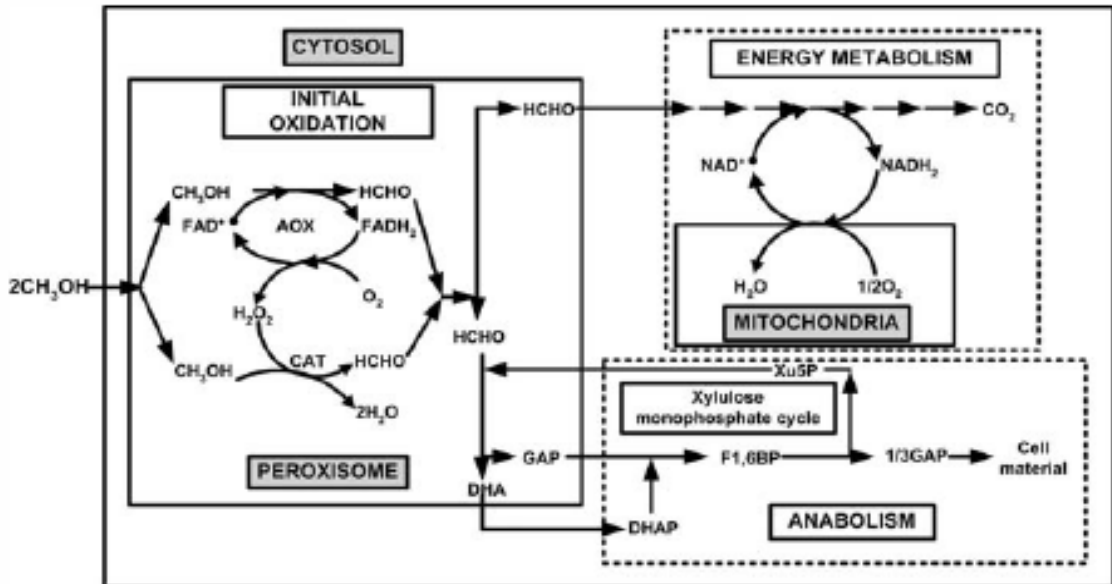


Figure 2.4 Methanol metabolism in *P. pastoris*; AOX alcohol oxidase; CAT catalase, GAP glyceraldehyde-3-phosphate; DHA dihydroxyacetone; DHAP dihydroxyacetone phosphate; F1,6BP fructose-1,6-bisphosphate; Xu5P xylulose-5-phosphate (Charoenrat et al., 2005).

In general, two phases, growth phase and production phase have been seen in *P. pastoris*. Glycerol usually used as a carbon source at growing phase. Glycerol utilization pathway is also shown in figure 2.5.

According to methanol utilization pathway, there are actually three phenotypes of *Pichia pastoris*. Mut^+ , wild type methanol utilization phenotype, can grow on methanol rapidly. Generally when higher methanol concentration is used, the Mut^+ expression is higher. Mut^s , methanol utilization slow phenotype, grows on methanol slowly due to the disruption of alcohol oxidase 1 gene, therefore this strains relies on weaker AOX2 enzyme. If the folding is rate limited, the slower growth and protein production of Mut^s on methanol is particularly preferable. Mut^- , methanol utilization minus phenotype, can not

grow on methanol because both AOX1 and AOX2 genes are deleted. The last two phenotypes are, in some cases, preferable since less methanol is used. There are reports about the expression of recombinant proteins at high levels when non-AOX repressing carbon sources, such as sorbitol, mannitol, trehalose, are used with small amounts of methanol for induction (Daly and Hearn, 2005).

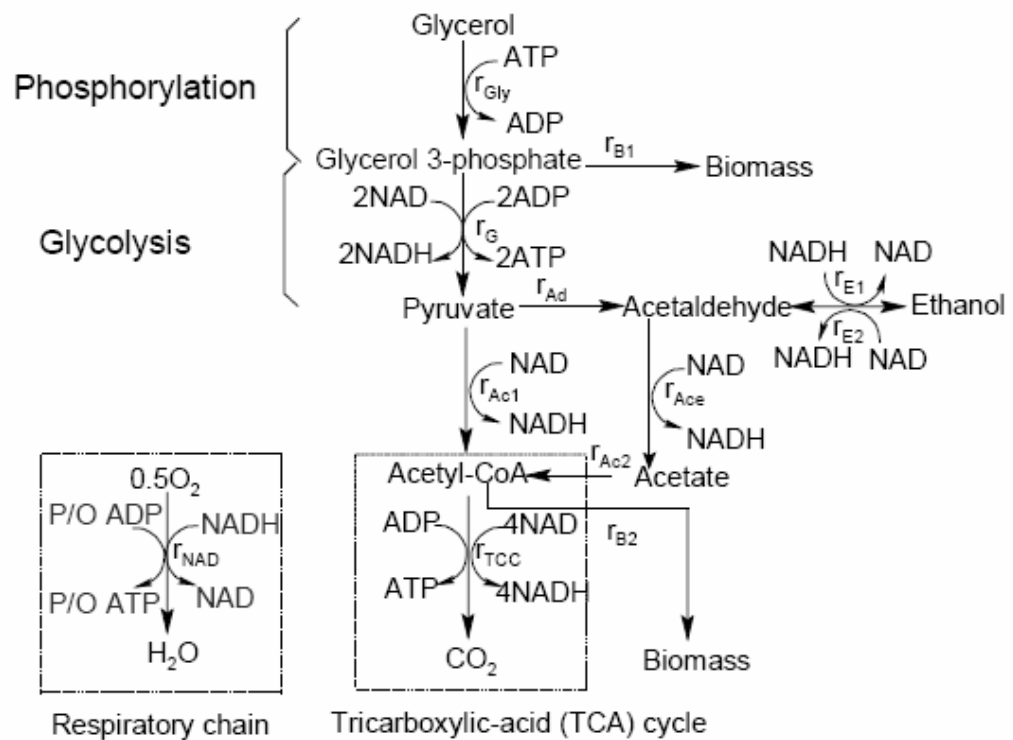


Figure 2.5 Metabolic pathways of glycerol in *Pichia pastoris* (Rena et al., 2006).

b) *P. pastoris* Expression System:

The most important reason why *P. pastoris* is one of the most attractive microorganisms for the production of the recombinant protein is that it has strong system regulating the promoter of the alcohol oxidase 1 (AOX1) which induced by methanol (Cereghino et al., 2002). Actually, there are two kinds of alcohol oxidase enzymes required for the methanol metabolism, AOX1, and AOX2 which is weaker. The AOX1 promoter is so strong that in the cells on

methanol fermenter cultures, AOX levels can be substantially induced, constituting almost or greater than 30% of soluble protein but it is undetectable in cells cultured on carbon sources such as glucose, glycerol or ethanol (Cereghino and Cregg, 2000).

The AOX1 gene was first isolated from cDNA library constructed with RNA derived from methanol grown *P. pastoris* cells by Ellis et al. (1985). After isolation of AOX1, further investigations outlined probable regulatory system that control AOX1 transcription which appeared to be under the control of both a general carbon catabolite repression/depression mechanism and a carbon source specific induction mechanism (Tschopp et al., 1987; Cregg et al., 1993).

To have a high capacity, being able to produce AOX protein greater than 30% of soluble protein expressed, indicates that the metabolic regulation system, from the evolutionary point of view, works in such a way that it can able to produce extra resources such as precursors, energy and other proteins which are involved in the production of AOX protein. It is also investigated that increasing the number of copies of the expression cassette generally has the effects of increasing the amount of protein expressed. Sunga and Cregg (2004) reported that when the number of copies of *lacZ* gene was increased to 22, it was seen a 17- fold increase in the activity of β -gal relative the activity observed when a single copy of gene was present. When compared with the other microorganisms such as *B. subtilis* and *E. coli*, increased copies of the gene of interest might not affect the expression of the gene after a certain copies because of due to lack of resources during the transcription and translation. The study of Wang et al. (2004) showed that increasing the number of copy after 4-5 copies of gene of interest are present in *B. licheniformis* did not affect the expression of protein.

Although AOX1 promoter has been used most widely and successfully for the production of foreign proteins, in some cases this promoter may not be suitable. Since methanol is used for the induction of this tightly regulated promoter, it may be unsuitable for use in the production of certain food products and additives. Furthermore, methanol is a fire hazard, thus storing the large quantities required for large scale fermentation process is undesirable (Cereghino and Cregg, 2000). Therefore, there are some other

alternative promoters such as GAP (glyceraldehydes 3-phosphate dehydrognase gene promoter) expressed on glucose, AOX2 induced by methanol, FLD1 (glutathione-dependent formaldehyde dehydrogenase gene promoter) induced by either methanol or methyl amine and ICL1 which is a isocitrate lyase gene promoter, which have been investigated and could successfully express desired recombinant protein at high levels (Macauley-Patrick et al., 2005).

In order to produce a foreign protein, there should be used some plasmid or integration vectors which insert the desired gene to the chromosome. An integration vector requires combination of strong promoters, ribosome binding sites, termination sequences, affinity tag or solubilization sequences and multi enzyme restriction site. The other most important thing for the selection of the integration vector is that it should be such that a double cross-over recombinant event can occur during the process of integration of foreign gene to the chromosome, which is expected to be more stable than the one integrated by a single crossover event (Middleton and Hofmeister, 2004). The first vectors generated for the *P. pastoris* are *pHIL-D2* and *pPIC9*, contained the functional histidine dehydrogenase gene (*HIS4*) that can be used as a selectable marker (Daly and Hearn, 2005). Since large sizes of *pHIL-D2* and *pPIC9* vectors (9.0-9.3 kb) resulting in transformants which are genetically less stable and difficulties in selecting multi-copy integrants when these vector are used, alternate vectors, such as *pPICZaA* used in this study, having smaller size (3.0-3.3 kb) and *Sh ble* (zeocin resistan gene) for multi selection have been designed (figure 2.6).

c) Post-Translational Modifications and Secretion of Proteins:

One of the major advantages of *P. pastoris* when compared with the bacteria is that it has the potential of performing many eukaryotic post translational modifications such as (Cereghino 2000):

- Processing of signal peptides,
- Folding
- Addition of lipid that is required
- O- and N-linked glycosylation

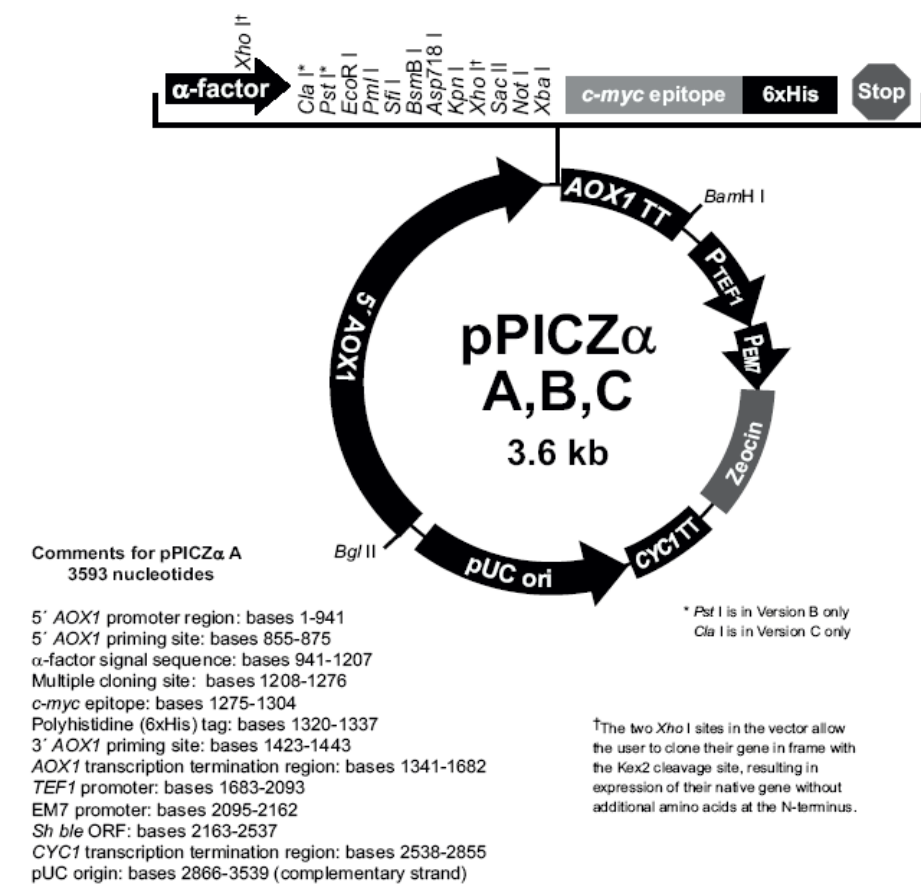


Figure 2.6 pPICZαA vector (Invitrogen, catalog V195-20).

For the production of extracellular protein, a specific signal peptide should be used in order to direct the proteins into secretory pathway. Alpha-factor prepro-signal from *S. cerevisia* and phosphatase (*PHO1*) signal are some of the signal peptides that are commonly used (Macauley-Patrick et al., 2005). Unfortunately, there are no any criteria for the selection of the optimum secretion signal peptides for the recombinant protein that is wanted to be secreted to the medium, because of difficulties in making correlations between the characteristics of signal peptides and mature protein and intracellular conditions. Therefore, in order to see the effects of the any signal peptide, experimental studies are required. Another alternative for convenient signal peptide may be the use of the recombinant protein's native signal which may result in successful expression system (Daly and Hearn, 2005).

Many proteins, especially those which are naturally secreted, contain pre- pro region that are required for correct folding (Bryan, 2002). In *P. pastoris*, the signal sequences of prepro-proteins mediate translocation into the endoplasmic reticulum and are removed by signal peptidase during this translocation. The folding of proteins usually begins with the formation of secondary structures and rapid generation of disulfide bonds in the endoplasmic reticulum. Then, the pro-proteins are transported to golgi complex where the pro-region is removed by dibasic endo-peptidase, kex2 which is a serine protease, a member of the pro-hormone convertase family and recognizes basic pairs of amino acid residues such as Lys-Arg or Arg-Arg. From the golgi, the recombinant proteins are packed into the secretory vesicles and then sent to the surface of the cell (Daly and Hearn, 2005).

The other post-translational modification that *P. pastoris* is capable of doing is the glycosylation. There are two types of glycosylation that *P. pastoris* can perform, O- and N- linked glycosylation. It generates the glycosylated products generally having much shorter glycosyl chains than those expressed in *S. cerevisia*.

Pichia, like other yeasts and fungi, add O-oligosaccharides to the hydroxyl groups of serine and threonine of the protein that is secreted. Although the protein produced by the native host contains glycosyl chains in its native form, *Pichia* may not add glycosyl chains or vice versa.

N- linked glycosylation is one of the undesired thing for the production of the therapeutic protein such as hormones because of its immunogenicity effects in human beings. In all eukaryotes, N -linked glycosylation leads to the formation of an oligosaccharide unit $\text{Man}_8\text{GlcNAc}_2$ located on asparagines in the recognition sequence Asn-X-Ser/Thr (X is any amino acid), and begins on the cytoplasmic side of endoplasmic reticulum (Cereghino et al., 2002; Macauley-Patrick et al., 2005). The oligosaccharide unit is further increased in Golgi by the mannosyltransferases. In humans, on the other hand, this side is mainly like $\text{Man}_{5-6}\text{GlcNAc}_2$.

Humanizing the glycosylation patterns of recombinant proteins which is used as pharmaceuticals is essential in order to get rid of the glycosylation or reduce the glycosyl chains. This may include changing the culture conditions,

by either using mutant strains which are lack of some genes producing enzymes essential for the glycosylation, or using enzymes removing the glycosyl chains such as peptide-N-glycosidase F , endoglycosidase H or adding some chemicals such as tunicamycin which is a competitive inhibitor of UDP-GlcNAc dolichol P-GlcNAc transferase, an enzyme in glycosylation machinery (Daly an Hearn, 2005). Due to absent of the recognition sequences for O- and N- linked glycosylation in hGH, there is no need any additional processes to get rid of the glycosylation or reduce the glycosyl chains. Trevino et al. (2000) and Eurwilaichitr et al. (2002) were able to produce mature rhGH without glycosyl chains by applying recombinant *P. pastoris*.

2.3.2 Medium Design

All living cells require certain nutrients for their growth and development. These nutrients must contain the chemical elements which constitute the cellular materials and structures, as well as those elements which are required for membrane transport, enzyme activity, and for the generation of the energy required for biosynthetic processes (Scragg, 1988). Nutrients required by cells can be classified in two categories (Shuler and Kargi, 2002); 1) *Macronutrients*, compounds needed in the concentrations larger than 10^{-4} M, for example carbon, nitrogen, oxygen, hydrogen, sulfur, phosphorus, magnesium and potassium; 2) *Micronutrients*, compounds needed in the concentrations of less than 10^{-4} M for example, trace elements such as Mo^{2+} , Zn^{2+} , Cu^{2+} , Mn^{2+} , Fe^{2+} , Ca^{2+} , Na^{2+} , vitamins, etc. There are two major types of growth media, defined medium containing specific amounts of pure chemical compounds with known chemical compositions and complex media containing natural compounds whose chemical composition is not exactly known. Complex medium often results in higher cell and protein yields due to its rich ingredients; on the other hand, defined medium allows better control over the fermentation and leads to easier and cheaper recovery and purification of a product (Shuler and Kargi, 2002).

Optimized feeding regime is necessary for the production of recombinant proteins at high levels; therefore, trace salt solution, the amount of nitrogen sources, carbon sources affecting the amount of recombinant protein retained within the cells as well as biomass are some important nutritional parameters which should be taken into consideration. The method that is generally applied

for the production of foreign protein from *P. pastoris*, is that the strains are grown initially in a defined medium containing glycerol as a sole carbon source which inhibits the expression of the protein desired, then glycerol is fed to the culture at a growth limiting rate during the transition phase which has a positive effect on AOX1 promoter and finally, methanol or mixture of glycerol and methanol is fed to the culture to induce expression (Cereghino et al., 2002). The proportion of methanol and glycerol fed to the fermentation broth is important, because different carbon sources specify the metabolism resulting in different by-products which may inhibit the expression of the desired protein, for example *P. pastoris* produces small amount of ethanol as a by-product during the glycerol fed-batch phase and mixed-feed induction phase of high cell density fermentations, regardless of the phenotypes of organisms, which represses AOX1 promoter (İnan et al., 2001). Optimization and controlling of methanol is also important because of excess amount of it can be toxic, on the other hand low levels of it may not be enough to initiate transcription (Macauley-Patrick et al., 2005).

Addition of adequate ammonium ions, vitamins and trace elements shows that it increases the yield of recombinant proteins (Boze et al. 2001 and Xie et al. 2003). Other nitrogen sources such as yeast extract, casamino acids, L-arginine and EDTA are also used to increase the production level because these amino acid rich supplements, which are alternative and competing substrates for proteases and repress protease induction caused by nitrogen limitation, reduce product degradation (Macauley-Patrick et al., 2005; Daly and Hearn, 2005)

Carbon sources play important roles over the recombinant protein production and cell growth. Most commonly used carbon sources are methanol, glycerol, sorbitol, glucose, mannitol, trehalose, etc (Brierley et al., 1990; Sreekrishna et al., 1997; Thorpe et al., 1999; Inan and Meagher, 2001). Methanol is used not only as an inducer for the expression of recombinant protein, but also as a sole carbon source. Above certain concentrations, growth is substrate-inhibited by methanol (Zhang et al., 2000); therefore a fed-batch protocol is generally used. In literature no detailed studies about defined-batch cultivation have been performed.

The highest specific production rates of Mut⁺ strain are found with the methanol concentration that maximizes the growth rate (Zhang et al., 2000) or at a concentration as high as 30 kg m⁻³ (Katakura et al., 1998). Although the highest specific production rates require higher methanol concentration, generally the maximum product concentrations are reached at considerably lower concentrations in fed-batch system. Furthermore, methanol concentration influences the extent to which C-terminal amino acids are cleaved from the product (Zhou and Zhang, 2002).

Due to its important process parameter, keeping the methanol concentration constant is one of the problems especially for fed-batch system. By using on-line methanol sensors, by dissolved oxygen level or by constant feeding rate, it can be controlled. Any excess methanol concentration is actually undesired thing due to the rapid accumulation of formaldehyde and hydrogen peroxide inside cells, both of which are the oxidized products of methanol by alcohol oxidase enzyme and are toxic to the cell (Zhang et al., 2000).

The use of multi-carbon substrate in addition to methanol is the other approach to increase cell density and process productivity, as well as to reduce the induction time. This strategy has been mostly employed for fermentations using Mut^s strains because of their genetically reduced capacity to assimilate methanol which results in long induction times above 100 h (Ramon et al., 2007).

Brierley et al. (1990) was the first group attempting fed-batch strategy using mixed substrates; glycerol/methanol. Although glycerol is one of the good substrate ensuring cell growth, its concentration plays important role because glycerol excess represses the AOX1 promoter, which results in lower productivity. Thorpe et al. (1999) compared methanol/glycerol and methanol/sorbitol mixed-feed strategies and they found that cell yields are lower on sorbitol although higher specific product formation rates are obtained. Inan and Meagher (2001) compared different carbon sources; alanine, sorbitol, mannitol, trehalose, in terms of their ability to support growth and expression of β -Gal for *P. pastoris* Mut⁻ strain in shake flasks. They confirmed that Mut⁻ strain growing in media containing these carbon sources with methanol (0.5%) as an inducing agent expressed as much or higher

amount of β -Gal as compared to the Mut⁺ grown in methanol containing media.

2.3.3 Bioreactor Operation Parameters

Oxygen transfer, pH, and temperature, which are the major bioreactor operation parameters, show diverse effects on product formation in aerobic fermentation processes by influencing metabolic pathways and changing metabolic fluxes (Çalık et al., 1999). Therefore these parameters should be taken into consideration and examine profoundly because they affect the yields and protein production.

Temperature, one of the important parameters, is desired to keep constant at optimum value throughout the fermentation process. Its influence on individual cell processes can be very different and quite complex (Nielsen et al. 2003). In general, high temperature results in denaturation of protein, which needs extra energy to repair the mechanism, on the other hand, low temperature decreases the reaction rate and transport processes, etc.

Lower cultivation temperature usually influences the yield of recombinant protein produced by *Pichia pastoris* due to the poor stability of recombinant protein at high temperature and release of more proteases from dead cells as a result of long induction phase and folding problems at higher temperature (Macauley-Patrick et al., 2005). The effects of decreased temperatures have been reported in most studies. For example, expression of human μ -opioid receptor fusion protein was higher at 15-20 °C when compared with the expression levels at 25°C and 30°C (Sarramegna et al., 2002). The yield of herring antifreeze proteins and cell viability were also increased by lowering the temperature (Li et al., 2001).

Hydrogen ion concentrations (pH) affect the activity of enzymes, transport mechanisms and other extracellular and intracellular events, thus the microbial growth rate. Different organisms have different pH optima, however, for many bacteria, pH optima ranges from 3.0 to 8.0 (Shuler and Kargı, 2002). *Pichia pastoris* can tolerate a broad pH range between 3.0 and 7.0 which actually does not affect the cell growth significantly. Studies show that different pH values were found to be optimal (Brierley et al., 1994; Clare

et al., 1991) since recombinant proteins can be stable at different pH and proteolysis of recombinant protein can be decreased by adjusting the pH values.

One of the reasons for the popularity of the *P. pastoris* expression system is that physiologically it prefers a respiratory rather than a fermentative mode of growth (Cereghino et al., 2002). It is an obligately anaerobic organism when it grows on methanol since it requires oxygen throughout the methanol metabolism and thus it can not produce inhibiting products such as ethanol and acetic acid. The oxygen transfer rate can be increased by running the process with oxygen limitation, which usually results in rate of methanol consumption and higher cell productivity (Jahic et al., 2006). Therefore, there are studies where oxygen limitation fed batch processes were used (Trentmann et al., 2004; Trinh et al., 2003; Narendar et al., 2006). Charoenrat et al, 2005 were compared oxygen limited fed batch (OLFB) process with methanol limited fed batch (MLFB) process for the production of Thai Rosewood β -glucosidase and they found 35% higher oxygen uptake rate, higher productivity and specific activity in OLFB when compared with MLFB.

Oxygen shows diverse effect on product formation in aerobic fermentation processes by influencing metabolic pathways and changing metabolic fluxes (Çalık et al., 1998; Çalık et al., 1999; Çalık et al., 2000). Requirement of the oxygen by the cells in fermentation medium is actually affected by the nature of the microorganism, i.e. characteristics of metabolic pathway of that microorganism, and carbon sources and other nutrition used. In order to understand the biochemical reactions occurring in the cells and their selectivity, which are important for product yield, the effects of oxygen transfer should be investigated with all details.

2.3.4 Computation of Bioprocess Characteristics

a) Cell growth, yield factors and maintenance coefficients:

Microbial growth can be considered as an increase in the number of individuals in the population as a result of both replication and change in cell size due to the chemical reactions occur inside the cell (Nielsen and Villadsen,

1994; Scragg, 1988). When cells are inoculated in batch cultivation, a characteristic sequence of events termed in the growth cycle takes place. In *lag phase*, physicochemical equilibration between the organism and the environment following inoculation occurs with very little growth. Growth starts to occur in *acceleration phase* and it achieves its maximum rate in *growth phase*. In *stationary phase* no net growth is observed since nutrients are depleted and cell deaths begin (Atkinson and Mavituna, 1991; Shuler and Kargı, 2002).

The rate of microbial growth is characterized by the specific growth rate, μ , which is defined as,

$$\mu = \frac{1}{C_x} \cdot \frac{dC_x}{dt} \quad (2.1)$$

where C_x is the cell mass concentration (kg m^{-3}), t is time (h), and μ is the specific growth rate (h^{-1}). The rate of cell growth, r_x , is described by the following equation (Shuler and Kargı, 1992):

$$r_x = \frac{dC_x}{dt} = \mu C_x \quad (2.2)$$

Similarly the substrate consumption rate, $-r_s$, and product formation rate, r_p , can be expressed as follows:

$$r_p = \frac{dC_p}{dt} \quad (2.3)$$

$$-r_s = \frac{dC_s}{dt} \quad (2.4)$$

Microbial growth, product formation and substrate utilization rates are usually express in the form of specific rates:

$$q_p = \frac{1}{C_x} \frac{dC_p}{dt} \quad (2.5)$$

$$q_s = \frac{1}{C_X} \frac{dC_S}{dt} \quad (2.6)$$

The biomass and product yields, $Y_{X/S}$ and $Y_{P/S}$, respectively, are other important parameters which demonstrate the efficiency of conversion of the substrate into biomass and product. They are defined as the mass of biomass or product formed per unit mass of substrate consumed:

$$Y_{X/S} = \frac{dC_X}{dC_S} = \frac{dC_X/dt}{dC_S/dt} = \frac{r_X}{r_S} \quad (2.7)$$

$$Y_{P/S} = \frac{dC_P}{-dC_S} = \frac{dC_P/dt}{-dC_S/dt} = \frac{r_P}{r_S} \quad (2.8)$$

For measuring the biomass and product yields, a general method can be defined as shown on equations 2.7 and 2.8:

$$\bar{Y}_{X/S} = \frac{\Delta C_X}{\Delta C_S} \quad (2.9)$$

$$\bar{Y}_{P/S} = \frac{\Delta C_P}{\Delta C_S} \quad (2.10)$$

where, C_X , C_P and C_S are mass of cell, product and substrate, respectively, involved in metabolism. These are the overall yield coefficients that is the total biomass or product formed compared with the total substrate consumed over the whole growth cycle.

A list of frequently used yield coefficients is given in Table 2.5.

It is important to realize that the yield coefficients are not constant throughout the growth phase since they change with growth rate due to the requirement of maintenance energy (m) that represents the energy expenditures to repair damaged cellular components, to transfer some nutrients and products in and out of the cell, for motility, and to adjust the osmolarity of the cells' interior volume (Scragg, 1988).

Table 2.5 Definition of yield coefficients.

Symbol	Definition	Unit
$Y_{X/S}$	Mass of cells produced per unit mass of substrate consumed	kg cell kg ⁻¹ substrate
$Y_{X/O}$	Mass of cells produced per unit mass of oxygen consumed	kg cell kg ⁻¹ oxygen
$Y_{S/O}$	Mass of substrate produced per unit mass of oxygen consumed	kg substrate kg ⁻¹ oxygen
$Y_{P/X}$	Mass of product formed per unit mass of cell produced	kg product kg ⁻¹ cell
$Y_{P/S}$	Mass of product formed per unit mass of substrate consumed	kg product kg ⁻¹ substrate
$Y_{P/O}$	Mass of product formed per unit mass of oxygen consumed	kg product kg ⁻¹ oxygen

The maintenance coefficient for oxygen, m_o , represents the amount of oxygen for maintenance. In an aerobic process, oxygen is mainly consumed for three purposes: cell growth, product and by-product formations, and maintenance. The oxygen consumption rate for cell growth can be defined as:

$$-r_{O1} = \frac{dC_x / dt}{Y_{X/O}} \quad (2.11)$$

Oxygen consumption for by-product formation is defined as:

$$-r_{O2} = \frac{dC_{BP} / dt}{Y_{BP/O}} \quad (2.12)$$

Oxygen consumption for maintenance is defined as:

$$-r_{O3} = m_o C_x \quad (2.13)$$

The total oxygen consumption rate is as follows:

$$-r_o = (-r_{o1}) + (-r_{o2}) + (-r_{o3}) \quad (2.14)$$

Equations (2.11)-(2.13) are substituted into (2.14) to obtain,

$$-\frac{dC_o}{dt} = -r_o = \left(\frac{1}{Y_{X/o}}\right) \frac{dC_x}{dt} + \left(\frac{1}{Y_{BP/o}}\right) \frac{dC_{BP}}{dt} + m_o C_x \quad (2.15)$$

Also,

$$q_{BP} = \frac{1}{C_x} \frac{dC_{BP}}{dt} \quad (2.16)$$

and

$$\mu = \frac{1}{C_x} \frac{dC_x}{dt} \quad (2.17)$$

Substituting (2.16) and (2.17) into (2.15),

$$-r_o = \left(\frac{1}{Y_{X/o}}\right)(\mu C_x) + \left(\frac{1}{Y_{BP/o}}\right)(q_{BP} C_x) + m_o C_x \quad (2.18)$$

Dividing (2.18) by C_x

$$\frac{-r_o}{C_x} = \frac{\mu}{Y_{X/o}} + \frac{q_{BP}}{Y_{BP/o}} + m_o \quad (2.19)$$

q_{BP} can be defined as follows, where α is the term for growth associated organic acid formation and β is the term for non-growth associated organic acid formation:

$$\frac{dC_{BP}}{dt} = \alpha \frac{dCx}{dt} + \beta Cx \quad (2.20)$$

Dividing (2.20) to Cx,

$$q_{BP} = \frac{1}{Cx} \frac{dC_{BP}}{dt} = \alpha \mu + \beta \quad (2.21)$$

Substituting (2.21) into (2.19),

$$\frac{-r_o}{Cx} = \frac{\mu}{Y_{X/O}} + \frac{\alpha \mu + \beta}{Y_{BP/O}} + m_o \quad (2.22)$$

Dividing (2.22) by μ ,

$$\frac{-r_o}{\mu Cx} = \frac{1}{Y_{X/O}} + \frac{\alpha + (\beta/\mu)}{Y_{BP/O}} + \frac{m_o}{\mu} \quad (2.23)$$

Rearranging (2.23),

$$\frac{-r_o}{\mu Cx} = \left(\frac{\alpha}{Y_{BP/O}} + \frac{1}{Y_{X/O}} \right) + \left(\frac{1}{\mu} \right) \left(m_o + \frac{\beta}{Y_{BP/O}} \right) \quad (2.24)$$

and,

$$\frac{1}{Y_{X/O}} = \left(\frac{\alpha}{Y_{BP/O}} + \frac{1}{Y_{X/O}} \right) + \left(\frac{1}{\mu} \right) \left(m_o + \frac{\beta}{Y_{BP/O}} \right) \quad (2.25)$$

From the slope of the plot of $\frac{1}{Y_{X/O}}$ versus $\frac{1}{\mu}$, $\left(m_o + \frac{\beta}{Y_{BP/O}} \right)$ (g oxygen g⁻¹ dry cell weight h⁻¹) and from the intercept, $\left(\frac{\alpha}{Y_{BP/O}} + \frac{1}{Y_{X/O}} \right)$ could

be determined, where Y represents the apparent and $\bar{Y}_{x/o}$ represents the true yield (Calik et al., 2006)

When by-product formation is neglected, equation (2.15) becomes:

$$-\frac{dC_o}{dt} = -r_o = \left(\frac{1}{\bar{Y}_{x/o}}\right) \frac{dCx}{dt} + m_o Cx \quad (2.26)$$

If the above equation is reorganized:

$$\frac{-r_o}{dCx/dt} = \frac{1}{\bar{Y}_{x/o}} = \frac{1}{\bar{Y}_{x/o}} + \frac{m_o}{\mu} \quad (2.27)$$

is obtained (Calik et al., 2004). From the slope of $\frac{1}{\bar{Y}_{x/o}}$ versus $\frac{1}{\mu}$, oxygen consumption for maintenance is obtained.

By using the same approach, i.e. material balance for substrate, the maintenance coefficient of substrate, m_s , can be also determined.

b) Oxygen transfer characteristics:

The transfer of oxygen from the fermentation medium to microorganism takes place in several steps which are explained in details by Scragg, (1988) and Bailey and Ollis (1986). When cells are dispersed in the liquid, and the bulk fermentation broth is well mixed, the major resistance to oxygen transfer is the liquid film surrounding the gas bubbles; therefore the rate of oxygen transfer from gas to liquid is rate limiting step.

An expression for oxygen transfer rate (OTR) from gas to liquid is given by the following equation:

$$OTR = k_L a (C_o^* - C_o) \quad (2.28)$$

where, k_L is the oxygen transfer coefficient, a is the gas-liquid interfacial area, $k_L a$ is the volumetric oxygen transfer coefficient, C_o^* is saturated dissolved oxygen concentration, C_o is the actual dissolved oxygen

concentration in the broth. Since solubility of oxygen in aqueous solutions is very low, the liquid phase mass transfer resistance dominates, and the overall liquid phase mass transfer coefficient, $K_L a$, is approximately equal to liquid phase mass transfer coefficient, $k_L a$ (Shuler and Kargi, 2002).

The oxygen uptake rate can be defined as:

$$\text{OUR} = -r_o = q_o C_x \quad (2.29)$$

where q_o is the specific rate of oxygen consumption and C_x is the cell concentration (Shuler and Kargi, 2002).

Mass transfer characteristics of a fermentation process are required in order to understand fermentation process and characteristics of the microorganism. Numerous methods have been developed for the experimental determination of $K_L a$ values. Dynamic method is widely used for the determination of the value of $K_L a$ experimentally, and it can be applied during the fermentation process. This method based on a material balance on the oxygen in the liquid phase (Scragg, 1988 and Rainer, 1990):

$$\frac{dC_o}{dt} = K_L a(C_o^* - C_o) - q_o C_x \quad (2.30)$$

In dynamic method, the broth is first de-oxygenated by stopping the air flow. During this period, dissolved oxygen concentration, C_{o0} , drops, and since there is no oxygen transfer in this region, oxygen uptake rate, $-r_o$, can be determined by using equation (2.30) which reduces to:

$$\frac{dC_o}{dt} = -r_o \quad (2.31)$$

Air inlet is then turned back on, and the increase in C_o is monitored as a function of time. In this period, the equation (2.30) is valid. Combining equations (2.30) and (2.31) and rearranging,

$$C_o = -\frac{1}{K_L a} \left(\frac{dC_o}{dt} - r_o \right) + C_o^* \quad (2.32)$$

From the slope of a plot of C_o versus $(dC_o/dt - r_o)$, K_La can be determined.

The Dynamic Method can also be applied to conditions under which there is no reaction, i.e., $r_o=0$ (Nielsen and Villadsen, 1994) in order to determine the physical mass transfer coefficient, K_La_o , from the slope of a plot of C_o versus dC_o/dt .

In order to compare the relative rates of maximum oxygen transfer and biochemical reactions and find the rate limiting step of the bioprocess, the maximum possible oxygen utilization rate (OD=oxygen demand) which is defined as (Çalık et al., 2004),

$$OD = \frac{\mu_{\max} Cx}{Y_{X/O}}$$

(2.33)

and the maximum possible mass transfer rate is defined as,

$$OTR_{\max} = k_L a C_{DO}^* \quad (2.34)$$

should be determined throughout the bioprocess.

In order to express the oxygen limitation in an aerobic process, the effectiveness factor, η (oxygen uptake rate per maximum possible oxygen utilization rate) and Damköhler number, Da (maximum possible oxygen utilization rate per maximum mass transfer rate) are defined according to the equations given below (Çalık et al., 2000):

$$\eta = \frac{OUR}{OD} \quad (2.35)$$

$$Da = \frac{OD}{OTR_{\max}} \quad (2.36)$$

CHAPTER 3

MATERIALS AND METHODS

3.1 Chemicals

All chemicals were analytical grade, and obtained from Sigma Ltd., Difco Laboratories, Fluka Ltd. and Merck Ltd.

3.2 The Microorganism and Plasmids

Escherichia coli TOP10 strain containing pPICZαA plasmid and *E.coli* JM109 strain used for construction and amplification of pPICZαA::hGH plasmid and *Pichia pastoris* used for the expression of hGH were obtained from Invitrogen (Carlsbad, CA) (Table 3.1).

The recombinant microorganisms are stored in the microbanks (PRO-LAB), by inoculating young colonial growth into cryopreservative fluid present in the vial. After providing the adsorption of microorganisms into the porous beads, excess cryopreservative was aspirated and inoculated cryovial stored at -55°C.

3.3 The Solid Medium

The recombinant *E. coli* JM109 and TOP10-pPICZαA strains stored on LSLB (Table 3.2) at 4°C or stored on microbanks at 55°C, were inoculated onto the freshly prepared agar slants under sterile conditions, and were incubated at 37°C overnight. Recombinant *Pichia pastoris* strains were also stored on YPD agar slants (Table 3.3) and stored at -55°C but were incubated at 30°C for 48-72 hours. According to the antibiotic resistance ability of the microorganisms, antibiotic was added to the agars after steam sterilization at

121°C for 20 minutes properly. Amounts of the antibiotics added to the medium are stated in Table 3.4.

Table 3.1 Strains and plasmids used in this study.

Genus	Species	Strain	Genotype/plasmid	Source
<i>Escherichia</i>	<i>coli</i>	JM109	Wild type	Yanish-Peron et. al (1985)
<i>Escherichia</i>	<i>coli</i>	TOP10-pPICZaA	pPICZaA	Invitrogen (USA)
<i>Escherichia</i>	<i>coli</i>	pPICZaA::hGH	pPICZaA::hGH	This study
<i>Pichia</i>	<i>pastoris</i>	X-33	wild type	Invitrogen (USA)
<i>Pichia</i>	<i>pastoris</i>	hGH-Mut ⁺	pPICZaA::hGH::Mut ⁺	This study
<i>Pichia</i>	<i>pastoris</i>	hGH-Mut ^s	pPICZaA::hGH::Mut ^s	This study

Table 3.2 The composition of the solid medium (LSLB) for *E.coli* strains.

Compound	Concentration, kg m ⁻³
Yeast extract	5.0
Soytryptone	10.0
NaCl	5.0
Agar	15.0
pH	7.0

Table 3.3 The composition of the solid medium (YPD) for *P. pastoris* strains.

Compound	Concentration, kg m ⁻³
Yeast extract	10.0
Peptone	20.0
Glucose	20.0
Agar	20.0
pH	7.0

Table 3.4 The final concentration of antibiotics in the media.

Antibiotic	Concentration, kg m ⁻³
Zeocin for <i>E.coli</i>	0.025
Zeocin for <i>P. pastoris</i>	0.100
Chloramphenicol for <i>P.pastoris</i>	0.035

3.4 The Precultivation Medium

The recombinant *P. pastoris* strain, grown in the solid medium, was inoculated into precultivation medium and incubated at 30°C and N=225 min⁻¹ for 24 h in agitation and heating rate controlled orbital shakers (B.Braun, Certomat BS-1) using air-filtered Erlenmeyer flasks 150 ml in size that had working volume capacities of 10 ml. The composition of precultivation medium was given in Table 3.5. The selective antibiotics, zeocin or chloramphenicol, were added to the precultivation medium in amounts stated in Table 3.4 after sterilization.

Table 3.5 The composition of the precultivation medium of *P. pastoris* strain (BMGY).

Compound	Concentration, kg m ⁻³
Yeast extract	10.0
Peptone	20.0
Potassium phosphate buffer pH 6.0	0.1 M
YNB	13.4
Biotin	4×10 ⁻⁵
Glycerol	10.0

3.5 The Production Medium

The recombinant *P. pastoris* strain inoculated in precultivation medium was grown for 24 h. The cells were harvested by centrifugation at 4000 rpm, 10 min⁻¹ at room temperature and resuspended in BMMY production medium or defined medium (Tables 3.6 and 3.7). Defined medium composition was taken from the study of Jungo et al., (2006) with some modifications (ammonium sulfate was used instead of ammonium chloride). The selective antibiotics, zeocin or chloramphenicol, were added to the production medium in amounts stated in Table 3.4. All of the medium components except trace salts sterilized with filter were autoclaved at 121°C for 20 min.

The laboratory scale experiments for microbial growth and medium design were executed in air filtered, baffled Erlenmeyer flasks 250 ml in size that had working volume capacities of 50 ml and the recombinant cells incubated at 30°C and N=225 min⁻¹ for 24 h by using these flasks. The pilot scale batch bioreactor with a 3.0 dm³ volume (B.Braun Biostat Q4), having a working volume of 1.0 dm³, and consisting of temperature, pH, foam and stirring rate controls, was used for the investigation of oxygen transfer effects.

Table 3.6 The composition of the complex production medium of *P. pastoris* strain (BMMY)

Compound	Concentration, kg m ⁻³
Yeast extract	10.0
Peptone	20.0
Potassium phosphate buffer pH 6.0	0.1 M
YNB	13.4
Biotin	4×10 ⁻⁵
Methanol	10.0

Table 3.7 The composition of the defined production medium of *P. pastoris*

Compound	Amount (kg m ⁻³)
Glycerol / methanol	40 / 20
Ammonium sulfate	18.84
KH ₂ PO ₄	5.62
Magnesium sulfate	1.18
Calcium sulfate	0.83
CuSO ₄ · 5 H ₂ O	0.008
Potassium iodide	0.0012
MnSO ₄ · H ₂ O	0.028
Sodium molybdate	0.0052
Boric acid	0.008
Cobalt chloride	0.008
Zinc sulfate	0.044
FeCl ₃ · 6 H ₂ O	0.075
Biotin	0.00174

3.6 Analysis

Throughout the bioprocesses, samples were taken at characteristic cultivation times. After determining the cell concentration, the medium was centrifuged at 4000 min⁻¹ for 10 min at 4°C to precipitate the cells. In recombinant *P. pastoris* strains, supernatant was used for protein analysis and to determine methanol and glycerol concentrations, organic and amino acid concentrations.

3.6.1 Cell Concentration

Cell concentrations based on dry weights were measured with a UV-Vis spectrophotometer (Thermo Spectronic, Helios α).

3.6.2 Methanol, Glycerol and Organic Acid Concentrations:

Methanol, glycerol and organic acid concentrations were measured with HPLC (Waters, Alliance 2695). The method is based on reversed phase HPLC, in which their concentrations were calculated from the chromatogram, based on the chromatogram of the standard solutions. Samples were filtered with 45

μm filters (ACRODISC CR PTFE) and loaded to the analysis system. Mobile phase containing 3.12% (w/v) NaH_2PO_4 and $0.62 \times 10^{-3}\%$ (v/v) H_3PO_4 was used for the organic acid analysis (İleri and Çalık 2006) and only filtered dH_2O is used as the mobile phase for methanol and glycerol analysis. Needle and seal wash were conducted with dH_2O and 20% (v/v) acetonitrile solution, respectively. The analysis was performed under the conditions specified below:

Table 3.8 Conditions for HPLC system for methanol, glycerol and organic acid analysis

Column	Capital Optimal ODS, 5 μm
Column dimensions	4.6 x250 mm
System	:Reversed phase chromatography
Mobile phase flow rate	:0.8 ml/min for organic acid analysis :0.7 ml/min for methanol and glycerol analysis
Column temperature	:25 °C
Detector and wavelength	:Waters 2487 Dual absorbance detector, 210 nm for organic acid analysis : Refractive index detector for methanol and glycerol analysis.
Injection volume	:10 μl
Analysis period	:15 min

3.6.3 Amino Acids Concentrations

Amino acid concentrations were measured with an amino acid analysis system (Waters, HPLC), using the Pico Tag method (Cohen, 1983). The method is based on reversed phase HPLC, using a pre-column derivation technique with a gradient program developed for amino acids. The amino acid concentrations were calculated from the chromatogram, based on the chromatogram of the standard amino acids solution. Samples were filtered with 45 μm filters (ACRODISC CR PTFE) and loaded to the analysis system with a mobile phase of 6.0% (v/v) acetonitrile, 1.79% (w/v) NaAc from solvent A and 66.6% (v/v) acetonitrile from solvent B. The analysis was performed under the conditions specified below:

Table 3.9 Conditions for HPLC system for amino acid analysis

Column	:Amino acid analysis column (Nova-Pak C18, Millipore)
Column dimensions	:3.9 mm x 30 cm
System	:Reversed phase chromatography
Mobile phase flow rate	:1 ml/min
Column temperature	:38 °C
Detector and wavelength	:UV/VIS, 254 nm
Injection volume	:4 µl
Analysis period	:20 min

3.6.4 Protein analysis:

a) Bradford assay:

Total protein concentration was determined spectrophotometrically using Bradford assay (Bradford, 1976). 20 µl of sample was mixed with 1 ml of Bradford reagent (BioRad), incubated at room temperature for 5 min and the absorbance was read at 595 nm. The calibration curve was obtained using BSA in the concentration range of 0-2 mg/ml.

b) Determination of hGH concentration:

Human growth hormone concentrations were determined according to relative intensity and size of the bands on SDS-page by using a software program. As a standard, pure rhGH with histidine tag obtained by BD talon resin purification system (clontech, CA) was used and its concentration was determined by Bradford assay. The intensity and size of this standard's band with known concentration on SDS-page was used in order to determine concentrations of rhGH from cultivation media by comparing the bands on the gel.

c) Ultrafiltration:

The production medium was concentrated and desalted by ultrafiltration using 400 ml stirred cells (Amicon) and 10 kDa cut-off regenerated cellulose ultrafiltration membranes (Millipore). The process was carried in cold room (2-8°C) using N₂ gas pressure of maximum 55 psi (3.8 bar), until at least 10 fold concentration of the medium was obtained.

d) Purification of His-Tag by BD TALON Resin:

Since hGH was fused with a polyhistidine tag, the protein was purified with immobilized metal affinity chromatography. The solutions used for BD Talon purifications are given in Appendix A and detailed protocol is explained below:

1. Thoroughly resuspend the BD TALON Resin.
2. Immediately transfer the required amount of resin suspension to a sterile tube that will accommodate 10–20 times the resin bed volume.
3. Centrifuge at 700 rpm for 2 min to pellet the resin.
4. Remove and discard the supernatant.
5. Add 10 bed volumes of 1X Equilibration/Wash Buffer and mix briefly to pre-equilibrate the resin.
6. Recentrifuge at 700 rpm for 2 min to pellet the resin. Discard the supernatant.
7. Repeat Steps 5 and 6.
8. Add the clarified sample from Section VI.A, B or C to the resin.
9. Gently agitate at room temperature for 20 min on a platform shaker to allow the polyhistidine-tagged protein to bind the resin.
10. Centrifuge at 700 rpm for 5 min.
11. Carefully remove as much supernatant as possible without disturbing the resin pellet.
12. Wash the resin by adding 10–20 bed volumes of 1X Equilibration/Wash Buffer. Gently agitate the suspension at room temperature for 10 min on a platform shaker to promote thorough washing.
13. Centrifuge at 700 rpm for 5 min.
14. Remove and discard the supernatant.
15. Repeat Steps 12–14.

16. Add one bed volume of the 1X Equilibration/Wash Buffer to the resin, and resuspend by vortexing.
17. Transfer the resin to a 2-ml gravity-flow column with an end-cap in place, and allow the resin to settle out of suspension.
18. Remove the end-cap, and allow the buffer to drain until it reaches the top of the resin bed, making sure no air bubbles are trapped in the resin bed.
19. Wash column once with 5 bed volumes of 1X Equilibration/Wash Buffer.
20. [Optional]: If necessary, repeat Step 19 under more stringent conditions using 5–10 mM imidazole in 1X Equilibration/Wash Buffer.
21. Elute the polyhistidine-tagged protein by adding 5 bed volumes of Elution Buffer to the column. Collect the eluate in 500- μ l fractions.

e) Factor Xa Digestion of rhGH:

After purification of the polyhistidine tagged recombinant protein, the 6xHis Tag was digested using the Factor Xa protease recognition sequence cloned in the 5' end of the hGH sequence in order to obtain native protein. However, since Factor Xa protease is sensitive to imidazole used in elution of His-Tag purification, the sample was first desalted using ultrafiltration spin columns with 10 kDa cut-off (Sartorius). 10 μ g protein sample was digested using 1 U of Factor Xa protease (Qiagen) at 25°C for 16 h. The protease was removed using Xa removal resin provided with the enzyme, according to manufacturer's instructions. The native protein was further purified from the cleaved 6xHis peptides and the undigested 6xHis-tagged protein using the cobalt-based metal affinity resins as described previously.

f) SDS Page :

Proteins secreted were analyzed with SDS-PAGE according to the method described by Laemmli, et. al. (1970), with some modifications. Gels were stained with silver staining method or coomassie brilliant blue after electrophoretic run was completed using the procedure of Blum *et al.* (1987). All chemicals and solutions are explained in Appendix B.

Pouring SDS-polyacrlamide Gels:

1. Clean the glasses with ethanol. And assemble the glass plates according to the manufacturer's instructions. To check whether the glasses are properly sealed, pour distilled water between glasses. If water level does not decrease, glasses are properly sealed. Then, pour out the water and let the glasses to dry.
2. In an Erlenmeyer flask, prepare appropriate volume of solutions containing the desired concentration of monomer solution for 12% separating gel, using the values given in AppendixB. Mix the solutions in order shown. Polymerization will begin as soon as the NNN'N'-Tetramethylethylenediamine (TEMED) and 10% (w/v) ammonium persulfate (APS) have been added.
3. Swirl the mixture rapidly and immediately pour the solution into the gap between the glass plates. Leave sufficient space for the stacking gel. Add some water to overlay the monomer solution and leave the gel in a vertical position until polymerization is completed.
4. After 30 min, pour off the water and dry the area above the separating gel with filter paper before pouring the stacking gel. Place a comb in the gel sandwich and tilt it so that the teeth are at a slight ($\sim 10^\circ$) angle. This will prevent air from being trapped under the comb teeth while the monomer solutions are poured. Allow the gel to polymerize 30-45 minutes.

Preparation of Samples and Running the Gel:

1. While stacking gel is polymerizing, prepare samples by diluting at least 1:1 with sample buffer and heated at 95°C for 5 minutes.
2. After polymerization is complete (30 min), mount the gel in electrophoresis apparatus and fill the reservoir with running buffer.
3. Load up 20 μ l of each sample into the wells and start running with 30 mA. After the dye front has moved into the separating gel increase the applied current. The usual run time is approximately 45 minutes. This electrophoresis cell is for rapid separation and is not recommended for runs over 60 minutes long.

Staining SDS-Polyacrylamide Gels with Coomassie Brilliant Blue:

1. After running is completed, immerse the gel in 5 volumes of staining solution and place on a slowly rotating platform for 4h at room temperature.
2. Remove the stain and save it for future use. Destain the gel by soaking it in the methanol:acetic acid solution without the dye on a slowly rotating platform for 4-8h, changing the destaining solution 3-4 times. After destaining store the gel in dH₂O.

Staining SDS-Polyacrylamide Gels with Silver Salts:

The gels were silver stained using the procedure of Blum *et al.* (1987).

Table 3.10 Procedure for silver staining

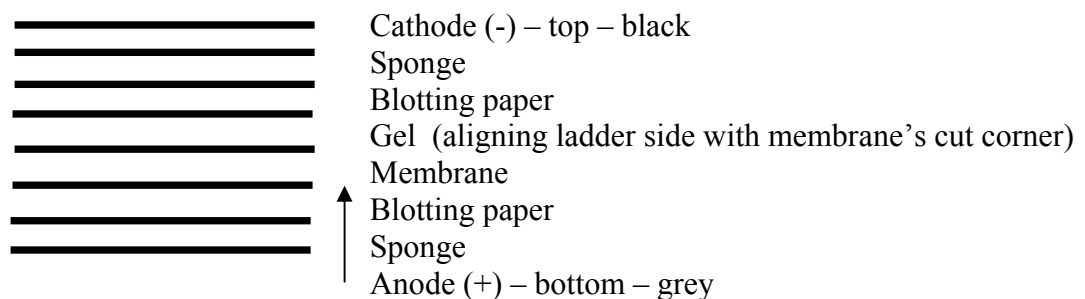
	STEP	SOLUTION	TIME OF TREATMENT	COMMENTS
1	Fixing	Fixer	≥ 1 hr	Overnight incubation is all right
2	Washing	50% Ethanol	3 x 20 min	Should be fresh
3	Pre-treatment	Pretreatment Solution	1 min	Should be fresh
4	Rinse	Distilled water	3 x 20 sec	Time should be exact
5	Impregnate	Silver Nitrate Solution	20 min	
6	Rinse	Distilled water	2 x 20 sec	Time should be exact
7	Developing	Developing Solution	~ 5 min	After a few minutes add some distilled water to proceed the reaction slowly. Time should be determined by observation of color development
8	Wash	Distilled water	2 x 2 min	
9	Stop	Stop Solution	≥ 10 min	The gels can be kept in this solution overnight

g) Western Blotting:

Western Blotting was performed to distinguish hGH by using its specific antibody. After the samples were run on SDS-PAGE gel, the gel was sandwiched between membrane, blotting paper, sponges and the blotting cassette. Blotting was performed electrophoretically, in the cold room for 3h at 50 V. The blotted membrane was then treated with TBS-T-Milk, primary antibody and secondary antibody. Detailed protocol is explained below:

Blotting:

- 1) Cut off stacking gel and nick top left-hand corner of resolving gel for orientation.
- 2) Transfer gel, while still attached to glass plate, into glass tray filled with at least 3 cm of 1x transfer buffer and peel off gently with a wet spatula, and keep for 15-20 min at RT to remove salts and SDS.
- 3) Cut membrane and 2 blotting papers to size, and cut one corner
- 4) Pre-wet PVDF or other hydrophobic membranes with methanol and transfer to the tray to equilibrate in transfer buffer for at least 10 min before blotting.
- 5) Put 2 sponges and 2 blotting papers into the tray to wet.
- 6) Open the cassette by releasing both latch tabs along the edge opposite the hinges. Place the opened cassette into the tray filled with transfer buffer and assemble the transfer stack so that the molecules will migrate toward the membrane. Make sure there are no bubbles in btw the gel and the membrane.



- 7) Close the cassette and press lightly to lock the tabs.
- 8) The cassette must be oriented so that the hinges face up so the black side of each cassette faces the black cathode panel.
- 9) Throw a magnetic stirrer inside. Inspect the buffer level, should be btw min-max lines.

10) Close the lid, turn on the stirrer and run the gel in cold room, at 50 V for 3 h, regardless of the number of gels.

Blocking, Antibody Incubation and Detection :

- 1) Remove the membrane from cassette, put in a box, protein side facing up. Wash the membrane 2-3 times with TBS-T. Tween prevents non-specific binding of the Ab and optimizes the hybridization conditions.
- 2) Immerse the membrane in TBS-T-Milk for 1 hr, RT, shaking.
- 3) Wash 3 times (shaking 15 min, 5min, 5 min with fresh changes) with large volumes of TBS-T, at RT.
- 4) Transfer the membrane to a lid of 96-well microtiter plate or similar low volume container.
- 5) Dilute the primary antibody in TBS-T as 1:200 (monoclonal anti-human hGH antibody, R&D Systems, Minneapolis, MN)
- 6) Incubate the membrane in the diluted primary antibody for o/n at 4 °C, on shaker platform.
- 7) Transfer the membrane into gel box and wash as in step 3.
- 8) Dilute the secondary antibody in TBS-T as 1:10 000 (antimouse IgG horseradish peroxidase-linked whole antibody, Amersham Biosciences, Uppsala, Sweden)
(Dilution factor should be determined empirically for each Ab as 1:1 000 - 1:10 000; more dilution will improve the linearity and increase the sensitivity).
- 9) Transfer the membrane back to the small container and incubate the membrane in the diluted secondary antibody for 1 hr at RT, on shaker platform.
- 10) Transfer the membrane into gel box and wash 3 times (10 min/wash) with fresh changes of large volumes of TBS-T buffer, at RT.
- 11) Visualize the bands by using the Substrate -Chromogen Kit (S10 HRP, BioMeda, ABD).

h) MALDI-TOF Mass Spectrometry Analysis :

The molecular weights of the rhGH and the factor Xa digested rhGH were determined by the use of a MALDI-LR (Waters-Micromass, UK) instrument. Spectra were generated using a pulsed nitrogen gas laser (337 nm) in positive linear mode, with a low mass gate of 1000 Da. The accelerating voltage was

15 kV. 3 μ l of 10 mg/ml sinapinic acid matrix dissolved in 50% acetonitrile and 0.1% TFA solution, was mixed with 1 μ l of approximately 10 pmol/ μ l sample and 1 μ l of this mixture was spotted on target plate and air dried ("dried droplet" technique; Karas and Hillenkamp, 1988). Cytochrome c and somatotropin hormone (standard hGH) were used as external molecular weight standards. Spectra were generated from the sum of 100-200 laser pulses and mass determinations were made by finding the peak centroid of a smoothed signal (by Savitzky-Golay algorithm) after background subtraction

i) N-terminal hGH sequencing:

For N-terminal sequencing of rhGH, rhGH was first purified with Talon resin from cultivation medium and treated with Factor Xa enzyme. Then, it was electroporesed as described above and transferred onto a polyvinylidene difluoride membranes (Millipore, USA). After stained with Coomassie blue, the rhGH band was excised, and automated Edman degradation was performed by PROCISE 494 gas-phase/liquid-pulse sequencer (Applied Biosystems, Foster City, CA).

3.7 Genetic Engineering Techniques

3.7.1 Materials

3.7.1.1 Enzymes, Kits, and Molecular Size Markers

Taq DNA polymerase, *Pfu* DNA polymerase, Ribonuclease A (DNase and protease free), T4 DNA ligase, dNTP mixture, and restriction enzymes (EcoRI and XbaI) and their buffers were purchased from MBI Fermentas.

QIAGEN Plasmid Purification Kit, QIAquick PCR purification Kit and QIAexpress Ni-NTA Spin Columns were obtained from QIAGEN Inc. Gene Elution Kit was purchased from GeneMark Molecular Biology Tools.

Lambda DNA/HindIII Marker and 6X Loading Dye were from MBI Fermentas.

3.7.1.2 Buffers and Solutions

All buffers and stock solutions listed in Appendix A were prepared with distilled water (dH₂O). The sterilization of solutions was performed either by autoclaving at 121°C for 20 min or by filter sterilization through 0.20 µm filters (Sartorius).

3.7.2 Determination of DNA Concentration

The concentration of DNA fragments after restriction digestion, PCR amplification or concentration of isolated plasmids after digestion or purification; or DNA molecules treated with any manipulation were analyzed by gel electrophoresis with 0.8-1.7% (w/v) agarose gels according to the weight of the DNA fragment and 1XTBE buffer (for DNA fragments bigger than 1500 bp 0.8% (w/v) agarose gels were used). DNA samples of 10-20µl, mixed with 1/5 volume of 6X loading dye (MBI Fermentas) were applied to the gel which was supplemented by ethidium bromide (Sigma-10 mg/ml) with a final concentration of 0.8µL/ml. At the end of the electrophoresis, bands were visualized with a UV transilluminator and gel photographs were taken using gel imaging and documentation system (UVP Bioluminescence System, and Hamamatsu Digital CCD Camera).

The molecular weights and the concentrations of the DNA fragments analyzed were determined by referring to Labworks image acquisition and analysis software (UVP Bioluminescence System)

3.7.3 PCR Amplification of Target Genes

Primers were designed in accordance with the sequences of hGH gene (Goeddel et al. 1979; Goeddel and Heyneker 1982). Restriction enzyme recognition sites were determined by the help of Restriction Mapper web-page of USA Molecular Biology Resources (<http://www.restrictionmapper.org>). The possibility of dimer formation and self-complimentarity of primers and melting temperature, ΔG , ΔH and ΔS values were checked with a computer program (NAR) and they were illustrated in Appendix C. Designed primers were synthesized in Thermo Hybaid GmbH (Germany) laboratories.

Table 3.12 Components of reaction mixture of PCR

10XPCR Buffer (with Mg ⁺⁺)	5µl
dNTPs (1mM)	10µl
Forward Primer (10µM)	1µl
Reverse Primer (10µM)	1µl
Template DNA (0.01-1µg)	1-5 µl
dH ₂ O	up to 49 µl
DNA polymerase	2.5 U

3.7.4 Purification of PCR products

The purification of PCR products were performed by using QIAquick PCR Purification Kit according to manufacturer's recommendations. 1 volume of PCR reaction sample was mixed with 5 volumes of PB buffer and placed to QIAquick spin column. After centrifugation, column was washed with PE twice and DNA molecules were eluted in proper amount of water.

3.7.5 Restriction Enzyme Digestion Reaction

Restriction digestion of the genes of interests were performed by incubating DNA fragments with proper restriction enzymes (REs) and specified buffers, of 20µl final volume at 37°C for overnight. The composition of the restriction digestion reaction mixtures was arranged as given in Tables 3.13, 3.14. After restriction digestion, the reaction was ended by incubating the mixture at 65°C for the enzymes.

Table 3.13 Components of reaction mixture of restriction digestion with *EcoRI* and *Xba1* RE's.

Components	Amounts
DNA fragment	~ 45-200 ng
<i>EcoRI</i> RE (10U/ µl)	1 µl
<i>Xba1</i> RE (10U/ µl)	1 µl
10X Buffer <i>EcoRI</i>	4 µl
dH ₂ O	up to 20 µl

Table 3.14 Components of reaction mixture of restriction digestion with *Pst*I RE.

Components	Amounts
DNA fragment	~ 45-200 ng
<i>Pst</i> I RE (10U/ μ l)	1 μ l
10X Buffer Tango	2 μ l
dH ₂ O	up to 19 μ l

3.7.6 Ligation Reaction

PCR amplified gene was cloned into suitable expression vector from the sticky ends occurred after restriction digestion with altering the gene/vector molar ratio between 3 and 5.

The amount of insert DNA to be added to the reaction mixture was calculated such that insert:vector ratio of 1:3 was achieved, as given in the equation.

$$100 \text{ ng vector (ng)} \times \frac{\text{Size of insert (bp)}}{\text{Size of vector(bp)}} \times \frac{3}{1} = \text{amount of insert}$$

The ligation reactions were performed by incubating the reaction mixture of 10 μ l final volume at 16°C for 16h. The composition of the ligation reaction mixture was arranged as follows:

Table 3.15 Ligation reaction components

10X ligation buffer	: 1 μ l
Insert DNA	:45-75 ng
Double digested vector DNA	: 100 ng
T4 DNA ligase	: 1 μ l
Sterile dH ₂ O	: to 10 μ l

3.7.7 DNA Sequencing

The DNA sequencing is performed by automatic DNA sequencers (Microsynth GmbH, Switzerland) by using the primers designed to control the insertion of target genes. And the primer for AOX1 promoter supplied by Invitrogen (USA).

3.7.8 Transformation of Plasmid DNA by CaCl_2 Method to *E.coli*

1. Incubate *Escherichia coli* overnight in LB-solid medium at 37°C,
2. Pick a single colony from a selective plate and inoculate a starter culture of 5 ml LB medium. Grow for 12h (overnight) at 37°C, with vigorous shaking (~200 rpm)
3. Transfer 1ml sample from the precultivation medium to an 100 ml- LB medium and incubate at 37°C and 250 min⁻¹ for 3.5 hours,
4. Transfer 10 ml of broth into 30 ml sterile polypropylene tubes; and place on ice for 10 minutes,
5. Separate the microorganisms by centrifugation at 4000 min⁻¹, 4°C for 10 minutes,
6. Separate the supernatant; let the cells dry on a paper tissue for 1 minute,
7. Add 1 ml of 0.1 M CaCl_2 solution onto the cells and make a complete solution by vortex, set on ice for 10 minutes,
8. Precipitate the microorganisms by centrifugation at 4000 min⁻¹, 4°C for 10 minutes,
9. Separate the supernatant; let the cells dry on a paper tissue for 1 minute,
10. Add 200 µl of 0.1M CaCl_2 solution onto the cells and make a complete solution by vortex, set on ice for 10 minutes,
11. Transfer 200 µl of solution to an eppendorf tube, and add 0.1 µg of plasmid DNA to this solution. Incubate on ice for 30 minutes,
12. Apply heat-shock to the solution at 42°C for 90 seconds and quickly place the tube on ice for 1 minute,
13. Transfer the cell suspension to sterile culture tubes containing 800 µl of LB medium without antibiotics and incubate at 37°C for 45 minutes with shaking at 140 min⁻¹ to recover cells,

14. Transfer 250 μl of the cultured cells onto the center of LSLB plate containing the desired antibiotic. Immediately spread the cells over the entire surface of the LB plate using a sterile, bent glass rod.
15. Invert the plates and incubate at 37°C overnight. Selected colonies should be visible in 14-24 hours (Sambrook, 2001).

3.7.9 Isolation of Plasmid DNA

1. Pick a single colony from a selective plate and inoculate a starter culture of 30 ml LB medium. Grow for 12h (overnight) at 37°C, with vigorous shaking (~ 200 rpm)
2. Pour 1ml of culture into microfuge tube and centrifuge at 13200 min^{-1} , 4°C, for 30 s,
3. Remove the supernatant and add again 1ml of culture and repeat the centrifugation step,
4. Remove the supernatant and take off all fluid by micropipette; place the tube on ice,
5. Resuspend the bacterial pellet in 100 μl of ice-cold alkaline lysis solution I one by vigorous vortexing. Make sure that the bacterial pellet is completely dispersed in alkaline lysis solution I,
6. Add 200 μl of freshly prepared alkaline lysis solution II to each bacterial suspension. Close the tube tightly, and mix the content by inverting the tube gently 5 times and store at room temperature for 5 minutes,
7. Add 150 μl of ice-cold alkaline lysis solution III. Close the tube and disperse alkaline lysis solution III through the viscous bacterial lysate by inverting the tube 5 times. Store the tube on ice for 10 minutes,
8. Centrifuge the bacterial lysate at 13200 min^{-1} , 4°C, for 10 minutes. Transfer the supernatant to a fresh tube.
9. Add 1/10 volumes of NaAc and 2 volumes of EtOH. Mix the solution by inverting and then allow the mixture to stand for at least 10 minutes at -20°C,
10. Collect the precipitated plasmid DNA by centrifugation at 13200 min^{-1} , 4°C, for 10 minutes.
11. Remove the supernatant gently and stand the tube in an inverted position on a paper towel to allow all of the fluid to drain away.

12. Dissolve the plasmid DNA in suitable amount of dH₂O and store the solution at -20°C (Sambrook, 2001).

3.7.10 Purification of Plasmid DNA

Plasmid purification was carried out by using QIAGEN Minipreps Plasmid Purification Kit according to the procedure provided by manufacturer. Bacterial cells incubated overnight were harvested by centrifugation and resuspended in P1 buffer containing RNase A. After cell lysis in P2 buffer, genomic DNA, proteins, cell debris and SDS were precipitated by adding P3 buffer to the mixture and incubated on ice until lysate become less viscous. Sample was centrifuged to remove the precipitate and supernatant loaded into equilibrated QIAGEN-tip and allowed to enter the resin by gravity. After washing with QC buffer twice, DNA was eluted with QF buffer into clean microcentrifuge tubes. 0.7 volumes isopropanol was added on each sample to precipitate the DNA and centrifuged for 30 min. After washing pellet with 70% ethanol, each pellet was dissolved in proper amount of water.

3.7.11 Transfection of *Pichia pastoris*

Transfection of *P. pastoris* was performed using LiCl method according to manufacturer's instructions (Invitrogen, catalog V195-20).

YPD plate was inoculated with *Pichia pastoris* X-33 and incubated for 48 h in 30°C incubator. 5 ml YPD was inoculated with a single colony and grown overnight to saturation in 30°C shaker. 50 ml culture of YPD was inoculated using preculture, to an initial OD₆₀₀ of approximately 0.1 and incubated at 30°C with shaking to an OD₆₀₀ of 0.8 to 1.0 (approximately 10⁸ cells/ml; 6-7 h). During this period, the plasmid DNA to be integrated into the genome had to be digested at a single site. Therefore, pPICZαA::*baI* plasmid was digested with *Sac* I at 37°C for overnight in Buffer *Sac* I. Full digestion was verified by running 2 µl sample on agarose gel and then purified. The concentration of the plasmid DNA was adjusted to 0.1-0.2 µg/µl and verified by Agarose gel electrophoresis. When the OD₆₀₀ reached 0.8 - 1.0, the cells were harvested at 4000xg for 5 min, washed with 25 ml of sterile water, and centrifuged at 1500xg for 10 min at room temperature. The cell pellet was resuspended in 1 ml of 100 mM LiCl, transferred to a 1.5 ml microcentrifuge tube, centrifuged at

maximum speed for 15 sec. LiCl was removed with a pipet and the cells were resuspended in 400 μ l of 100 mM LiCl. For each transformation, 50 μ l of the cell suspension was dispensed into a 1.5 ml microcentrifuge tube, immediately centrifuged at maximum speed for 15 sec and LiCl was removed with a pipet. To each tube for transformation, 240 μ l of 50% PEG, 36 μ l of 1 M LiCl, 10 μ l of 5 mg/ml single-stranded DNA and 5-10 μ g plasmid DNA in 50 μ l sterile water were added in the order given and vortexed vigorously until the cell pellet is completely mixed. The tube was incubated at 30°C for 30 min without shaking, then heat shocked in a water bath at 42°C for 25 min. The cells were pelleted by centrifugation at 6000 rpm for 15 sec, gently resuspended in 1 ml of YPD and incubated at 30°C with shaking. After 2 h of incubation, 25-100 μ l was spread on YPD + Zeocin plates and incubated for 2-3 days at 30°C.

3.7.12 Isolation of Genomic DNA from Yeast

The isolation of genomic DNA from yeast was performed according to the method described by Burke (2000) with slight modifications.

- 10 ml yeast culture was grown to saturation in YPD at 30° C in 50 ml Falcon tube.
- Cells were collected by centrifugation at 5 000 rpm for 6 min.
- The cells were resuspended in 0.5 ml of dH₂O, transferred to a 1.5 ml microfuge tube and collected by centrifugation at 13200 rpm for 2 min.
- The supernatant was decanted and the pellet was vortexed in residual supernatant.
- 200 μ l yeast lysis solution was added and mixed by inversion to ensure lysis of cells and then 200 μ l phenol:chloroform:isoamyl alcohol (25:24:1) and 0.3 g acid-washed glass beads were added.
- The tube was wrapped with Parafilm and vortexed for 3-4 min.
- 0.2 ml of TE (pH 8.0) was added and centrifuged at 13200 rpm for 5min in a microfuge.
- The aqueous layer was transferred to a fresh Eppendorf tube.
- 1 ml of 100 % EtOH was added and mixed by inversion.
- The tube was centrifuged at 13200 rpm for 2 min and the supernatant was discarded.

- The pellet was resuspended in 0.4 ml of TE and 3 μ l of a 10 mg/ml solution of RNase A.
- The solution was incubated for 10 min at 37 °C and 10 μ l of 4 M ammonium acetate plus 1 ml of 100 % EtOH were added and mixed by inversion.
- The DNA was pelleted by centrifugation at 13200 rpm for 5 min in a microfuge and the supernatant was discarded. The pellet was air-dried and resuspended in 50 μ l of sterile dH₂O.
- 10 μ l was used for each sample to be analyzed by southern blotting. This corresponds to approximately 2-4 μ g of genomic DNA.

3.7.13 DNA Extraction from Agarose Gel

DNA fragments analyzed with gel electrophoresis were extracted from the agarose gel by using Gel Elution Kit (GeneMark). After electrophoresis desired DNA bands were cut and gel slices (up to 350 mg) incubated in 400 μ l Binding Solution at 60°C for 15-30 minutes were loaded into spin columns and centrifuged at maximum speed. Columns washed with Washing Solution twice were transferred into new sterilized microcentrifuge tubes and DNA molecules were eluted in proper amounts of water.

CHAPTER 4

RESULTS AND DISCUSSION

In this study, human growth hormone gene was expressed in *P. pastoris*, in order to produce extracellular protein. In this frame, the gene fused with polyhistidine tag and Factor Xa protease recognition sequence for purification of rhGH was cloned to the expression vector and then transferred into *P. pastoris*. With *dot-blot* analysis, the appropriate two strains producing human growth hormone at high levels and having different methanol utilization phenotype (Mut⁺ and Mut^s) were chosen among other transformants. Then, effects of methanol concentrations on the expression of rhGH and cell growth were analyzed and compared for both phenotypes in defined and complex media in laboratory scale air filtered shake bioreactors. Using the designed defined medium for Mut⁺ phenotype, effects of oxygen transfer on rhGH production, by-product formation, and cell growth, oxygen transfer and fermentation characteristics were investigated by using pilot scale bioreactor. Finally, purification strategy applied was verified with SDS-page, Western-blot and MALDI-TOF mass spectrometry analysis.

4.1 Development of Recombinant *P. pastoris* Carrying hGH gene

The research program for the cloning of *hGH gene* and extracellularly expression of hGH in *Pichia pastoris* was carried out mainly in three parts. Firstly, the gene was fused with a polyhistidine tag and a target site for the Factor Xa protease with primer extension and PCR amplification approaches. Thereafter, the fused gene was cloned into vector pPICZαA, which carries the α-Factor signal peptide, AOX1 promoter and zeocin resistance gene. Finally, the recombinant vector was introduced and expressed in *P. pastoris*. The research plan for the development of the recombinant microorganism producing extracellular hGH is summarized in Figure 4.1.

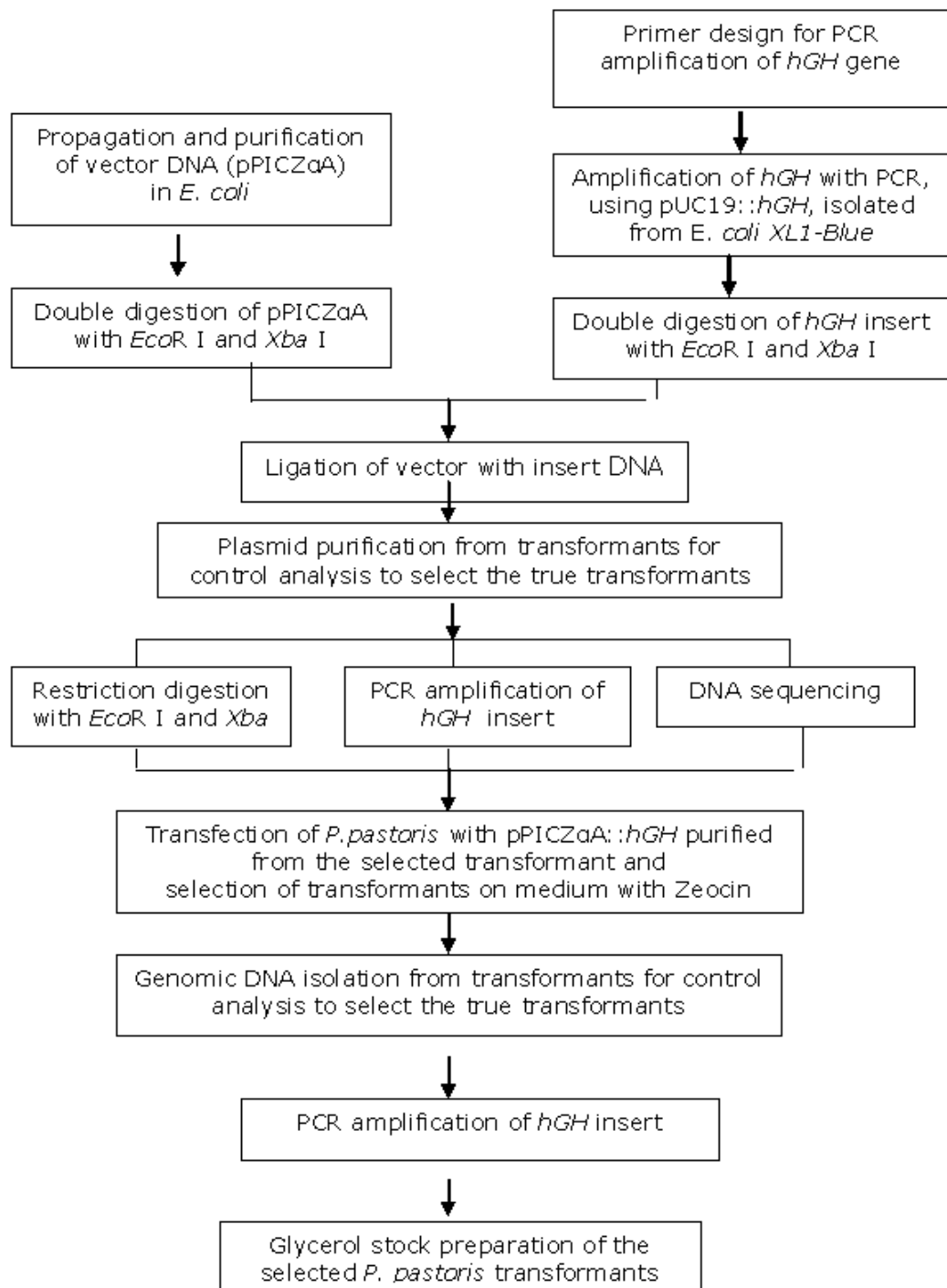


Figure 4.1 Flowchart of the research plan, for the development of the r-*P. pastoris* producing extracellular hGH.

4.1.1 Primer Design for Generation of *hGH* Gene

Recombinant pUC19::*hGH* plasmid (Şentürk, 2006) was used as the template sequence for amplification of *hGH* gene, using the nucleotide sequence defined by Goeddel et al. (1979).

For the amplification of *hGH* gene, two forward and one reverse primers were designed. *EcoR* I restriction site (6 bp), 6xHis-Tag sequence (18 bp) and Factor XA protease recognition sequence (12 bp) were added to add to the 5' end of *hGH* sequence. Since an addition of 36 bases was required at the 5' end of *hGH* sequence, two relatively short forward primers were designed instead of a single long primer. The reverse primer was designed such that, at the 3' end of the *hGH* sequence, stop codon and *Xba* I restriction site (6 bp) are present. Primers used for amplification of *hGH* and control the cloning in this study were given in Table 4.1.

Table 4.1 Primers designed for amplification of desired gene fragments.

Name	Sequence	Target Gene
1 st Forward primer	5'CACCATATTGAAGGGAGATTCCCAACTATACCACTATC'3	<i>hGH</i>
2 nd Forward primer	5'GGAATTCCACCATCACCATCACCATATTGAAGGGAG'3	1 st forward primer
Reverse primer	5'GCTCTAGACTAGAAGCCACAGCTGCCCTCCAC'3	<i>hGH</i>
<i>AOX1</i> Forward primer	5' GACTGGTTCCAATTGACAAGC' 3	<i>AOX1</i>
<i>AOX1</i> Reverse Primer	5' GCAAATGGCATTCTGACATCC' 3	<i>AOX1</i>

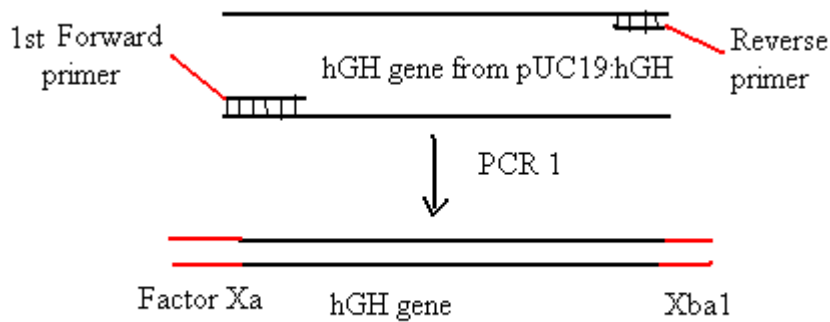
The thermodynamic properties together with melting temperature, T_m , self complimentary and dimer formation affinities were determined by the help of computer program, NAR. These properties were demonstrated in Appendix C. Designed primers were synthesized in Thermo Hybaid GmbH (Germany) laboratories.

4.1.2 Amplification of *hGH* Gene by Polymerase Chain Reaction (PCR)

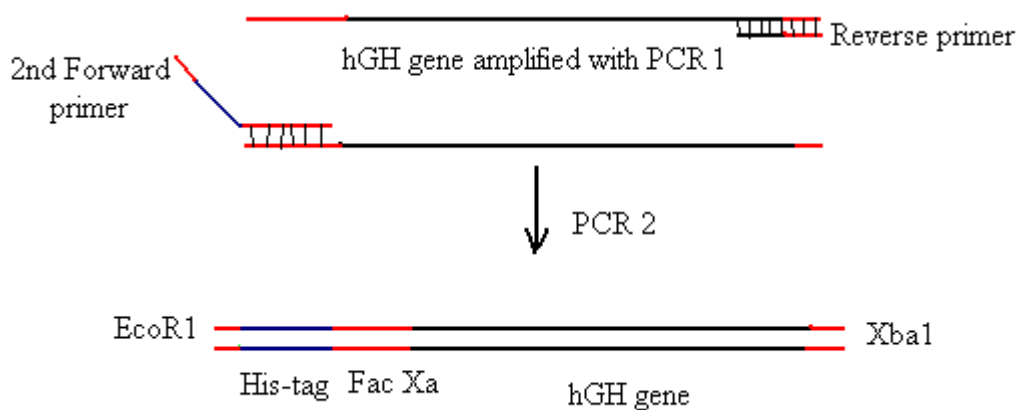
After synthesis of proper single-stranded primers, *hGH* gene with *EcoRI* and *XbaI* restriction enzyme extensions (final length=620 bp) was amplified with polymerase chain reaction (PCR). The PCR involves two oligonucleotide primers, Forward Primer and Reverse Primer, which flank the DNA sequence that is to be amplified. The primers hybridize to opposite strands of the DNA after it has been denatured, and the extension reactions create two double stranded target regions, each of which can again be denatured ready for a second cycle of hybridization and extension. By repeated cycles of heat denaturation, primer hybridization and extension, there follows a rapid exponential accumulation of the specific target fragment of DNA (Primrose et. al., 1994). The denaturation temperature was 94°C, and the extension temperature was 72°C since heat-resistant DNA polymerases were used. The annealing temperature and time are central variables in determining the specificity of a PCR. Hence, temperatures and the length of the reaction vary depending on the sequences to be amplified. Time of amplification of each cycle, which can be calculated from the formula of 1000 bp=1 min, was determined as 1 min to allow enough time for full amplification and the finest annealing temperature was determined as 60°C.

Since two forward primers were designed in order to add his tag and Factor Xa recognition site to the 5' end of *hGH* gene, two PCR processes at the same conditions were applied. The schematic illustration of two different PCR assemblies is shown on figure 4.2 and PCR conditions are given on Table 4.2.

The template DNA of pUC19::*hGH* plasmid was isolated and purified with Plasmid Purification Kit (QIAGEN) before it was utilized as template, to remove RNA, proteins, and chemicals remaining after isolation, since these materials can capture Mg²⁺ ions present in PCR buffer that inhibit the DNA polymerase enzyme and reduce PCR yield. Figure 4.3 (a) illustrates the pUC19::*hGH* plasmid. Figure 4.3 (b) shows the results of PCR1 and PCR2. Since sizes of PCR products are almost the same, difference between those could not be understood properly on agarose gel.



(a)



(b)

Figure 4.2 Schematic illustrations of polymerase chain reactions with primers designed. (a) Illustration of PCR 1; *hGH* gene was amplified from pUC19:*hGH* by using first forward primer and reverse primer. 1st forward primer is complimentary to anti-sense strand of *hGH* gene and includes DNA sequence coding Factor Xa (Fac Xa) recognition site. Reverse primer is complimentary to sense strand of *hGH* gene and associated with Xba1 RE sequence. (b) Illustration of PCR2; EcoR1 RE and polyhistidine tag sequences were further added to the 5' end of *hGH* gene amplified with PCR1. 2nd forward primer is complimentary to 1st forward primer and includes EcoR1 RE and polyhistidine tag sequences.

Table 4.2 PCR process parameters and components of reaction mixture of PCR for amplification of *hGH* gene

Target DNA	PCR conditions	PCR Reaction Mixture Composition:
<i>hGH</i> gene	1 cycle $T_1 = 94^{\circ}\text{C}$, 4 min 30 cycle $\left\{ \begin{array}{l} T_1 = 94^{\circ}\text{C}, 1 \text{ min} \\ T_2 = 60^{\circ}\text{C}, 1 \text{ min} \\ T_3 = 72^{\circ}\text{C}, 1 \text{ min} \end{array} \right.$ 1 cycle $\left\{ \begin{array}{l} T_4 = 72^{\circ}\text{C}, 10 \text{ min} \\ T_5 = 4^{\circ}\text{C}, 5 \text{ min} \end{array} \right.$	10XPCR Buffer 5 μl dNTPs (1mM) 10 μl FP (10 μM) 1 μl RP (10 μM) 1 μl Template DNA 1 μl dH ₂ O 31 μl Tag DNA polymerase 1 μl

4.1.3 Restriction Enzyme Digestion and Ligation

The PCR amplified *hGH* gene purified with PCR Purification Kit (QIAquick), and the pPICZaA vector isolated with Plasmid Purification Kit (QIAGEN), were double digested with *EcoRI* and *XbaI* restriction enzymes, in specified buffers (Tables 4.3) of 20 μl final volume at 37 $^{\circ}\text{C}$ for 6-12h. The reaction mixtures were kept at 65 $^{\circ}\text{C}$ for 20 min for the thermal inactivation of the enzymes used at the end of restriction digestion reaction. After digested with both restriction enzymes DNA fragments were extracted from agarose gels (Section 3.7.13).

The ligation reactions were performed by incubating the reaction mixture of 10 μl final volume at 16 $^{\circ}\text{C}$ for 16h. The reaction components are given on Table 4.4. The amount of DNA was determined according to intensity of the bands on agarose gel. Figure 4.4 illustrates the agarose gel image of *hGH* gene and pPICZaA vector after restriction digestion.

The assembly of the recombinant plasmid, pPICZaA::*hGH*, was schematically illustrated in Figure 4.5.

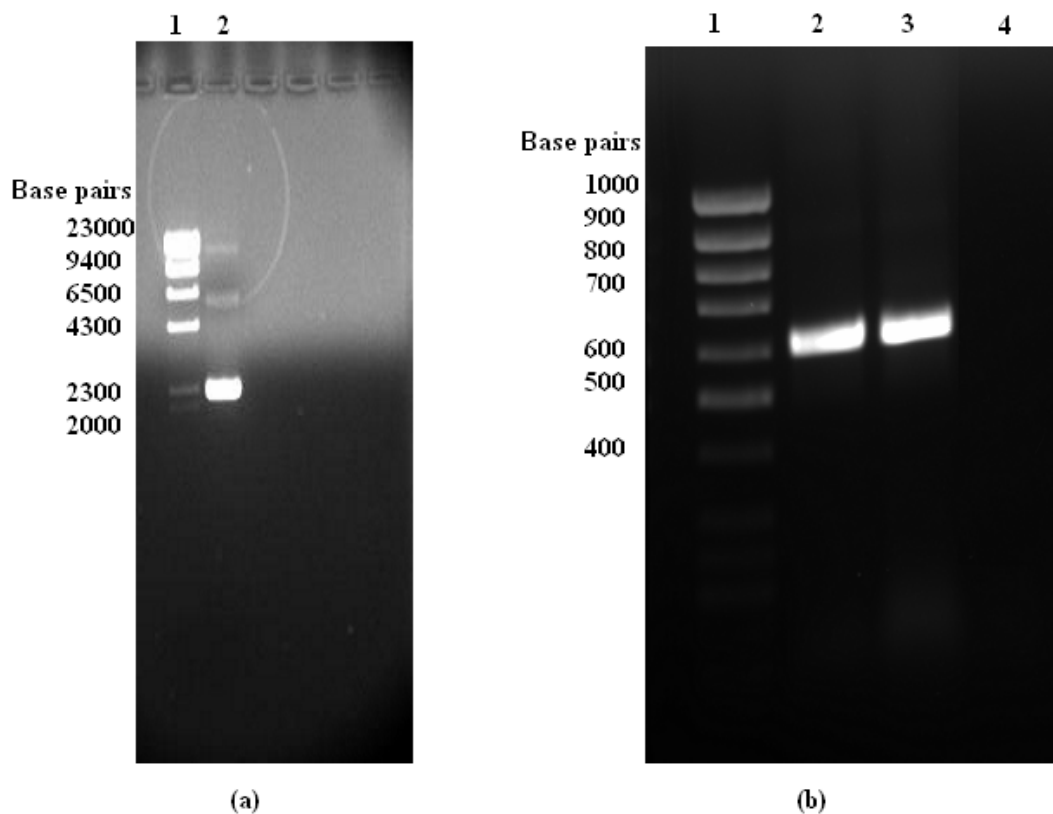


Figure 4.3 (a) Agarose gel electrophoresis image of pUC19::*hGH* plasmid. 1. well: λ DNA/HindIII Marker; 2.well: pUC19::*hGH* plasmid. (b) Agarose gel electrophoresis image of *hGH* gene. 1. well: 50 bp DNA Marker; 2.well: *hGH* gene amplified in PCR1; 3. well: *hGH* gene amplified in PCR2; 4.well: Negative control.

Table 4.3 Components of reaction mixture of restriction digestion of *hGH* gene and pPICZaA vector with *EcoRI* RE and *Xba1* RE.

	<i>hGH</i> gene	pPICZaA
Components	Amounts	Amounts
DNA fragment	~ 150 ng	~ 150 ng
<i>EcoRI</i> RE (10U/ μ l)	1 μ l	1 μ l
<i>Xba1</i> RE (10U/ μ l)	1 μ l	1 μ l
10X Tango buffer	4 μ l	4 μ l
dH ₂ O	up to 20 μ l	up to 20 μ l

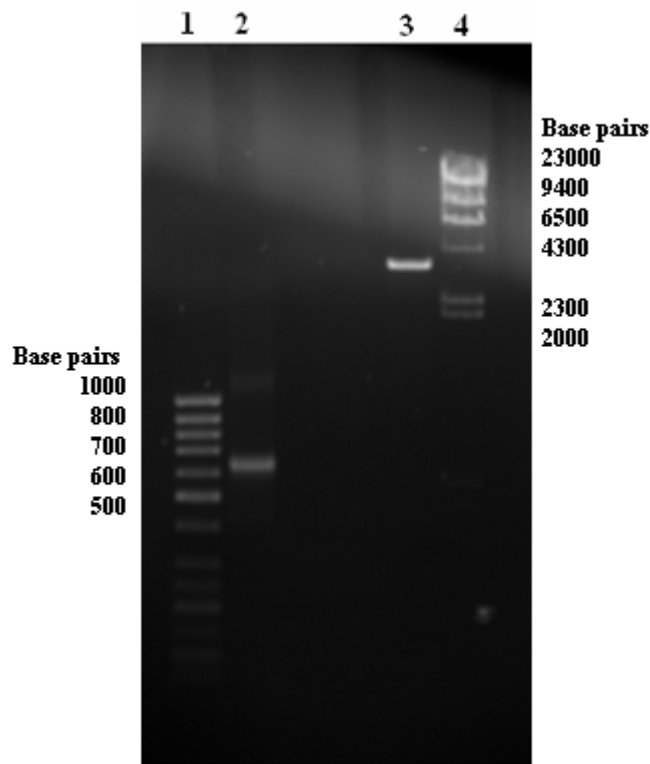


Figure 4.4 Agarose gel electrophoresis image of pPICZaA vector after restriction digestion; 1. well:50 bp DNA ladder; 2.well: *hGH* gene digested with *EcoRI* and *XbaI* and purified 3. well: pPICZaA vector digested with *EcoRI* and *XbaI*; 4. well: λ DNA/HindIII Marker.

Table 4.4 pPICZaA::*hGH* ligation reaction conditions.

10X ligation buffer	1 μ l
Insert DNA (620 bp)	100 ng
Double digested vector DNA (3536 bp)	100 ng
T4 DNA ligase	1 μ l
Sterile dH ₂ O	to 10 μ l

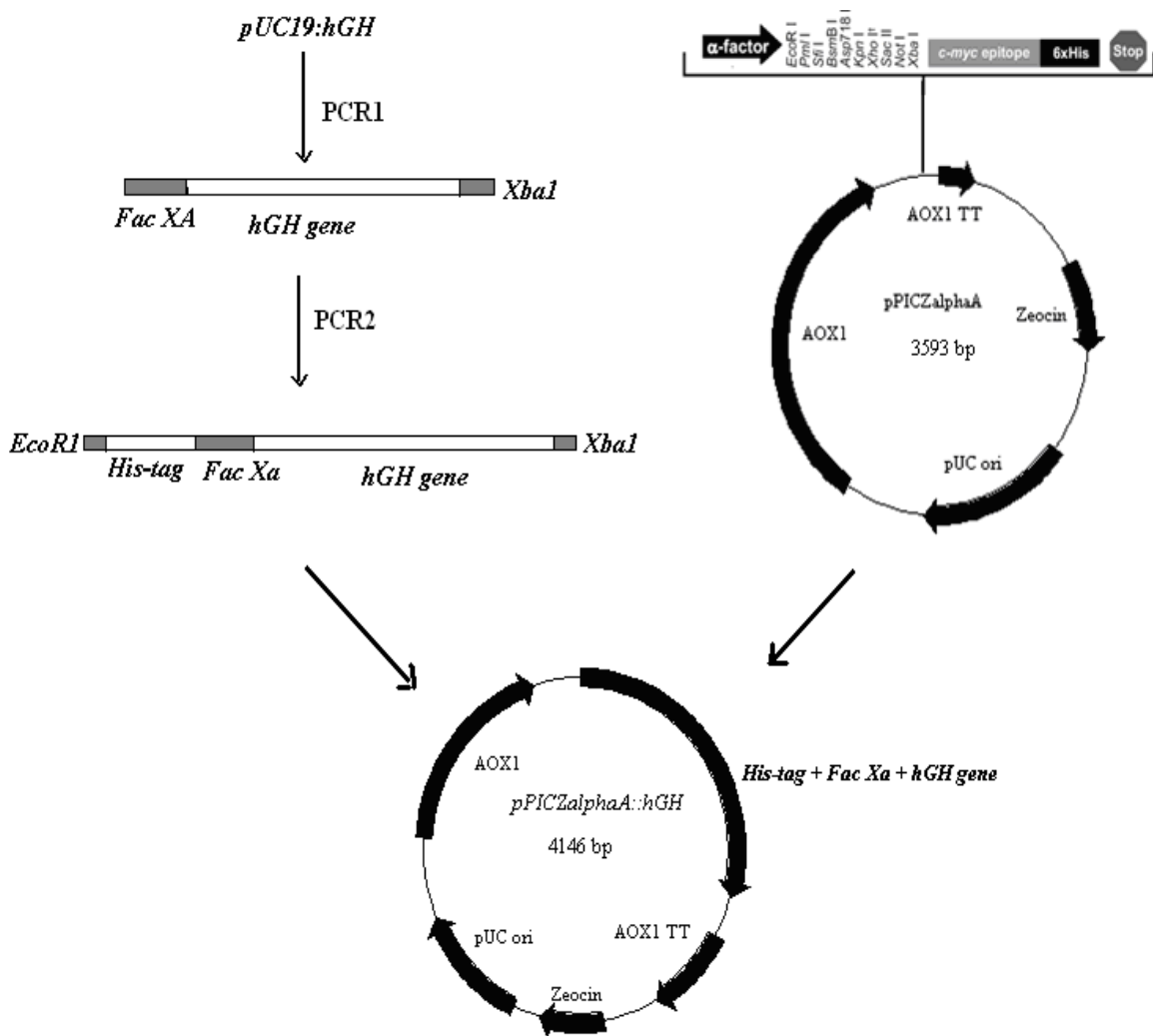


Figure 4.5 Scheme for the construction of the expression system for hGH production in *P. pastoris* strain. 620 bp *hGH* gene fused with DNA sequences coding polyhistidine tag (his-tag) and Factor Xa (Fac Xa) recognition site was cloned into pPICZaA vector from *EcoRI* and *XbaI* restriction sites. The transcription directions were indicated by arrows; TT, transcription termination region; ori, maintenance and replication in *E. coli*.

4.1.4 Transformation of pPICZaA::hGH into *E. coli* cells and Selection of the True Transformants

The ligation products were transformed into *E. coli* JM109 strain by CaCl_2 method described in section 3.7.8 and fresh transformants were grown on LSLB-agar + Zeocin (0.025 kg m^{-3}) for 12-18 h. Three colonies were obtained and these were bigger than pPICZaA vector (Figure 4.6). These plasmids were plated for short term storage and further tests.

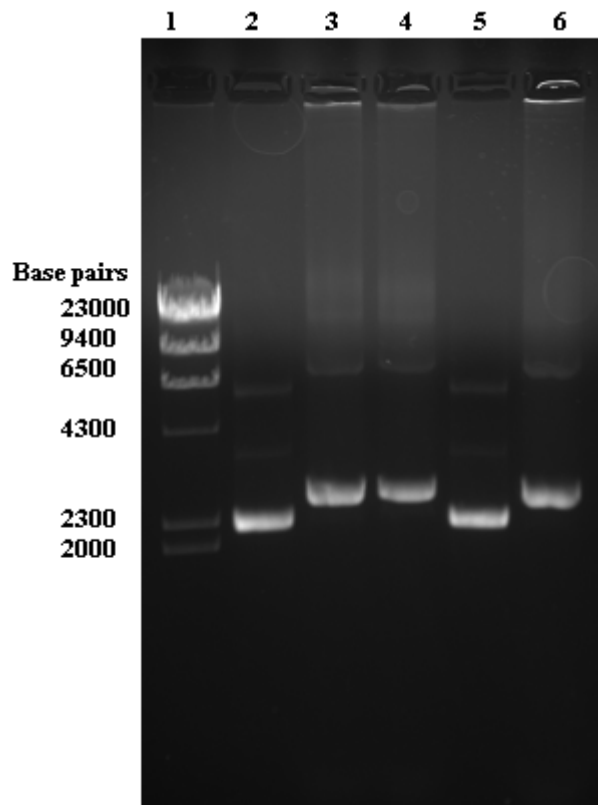


Figure 4.6 Agarose gel electrophoresis image of r-pPICZaA vectors isolated from *E. coli* transformants. 1. well: λ DNA/HindIII Marker; 2. well and 5. well: pPICZaA vectors ; 3. well, 4. well and 6. well : putative recombinant pPICZaA vectors isolated from transformants.

Firstly, putative recombinant plasmids were checked with PCR by being used as template. The primers and expected PCR products listed in Table 4.5. Agarose gel electrophoresis image (Figure 4.7) showed that *hGH* gene is present in these plasmids.

Table 4.5 Primers and expected PCR products length

Forward primer	Reverse primer	Expected length
AOX promoter primer	<i>hGH</i> gene primer	976
<i>hGH</i> gene primer	AOX promoter primer	793
<i>hGH</i> gene primer	<i>hGH</i> gene primer	620

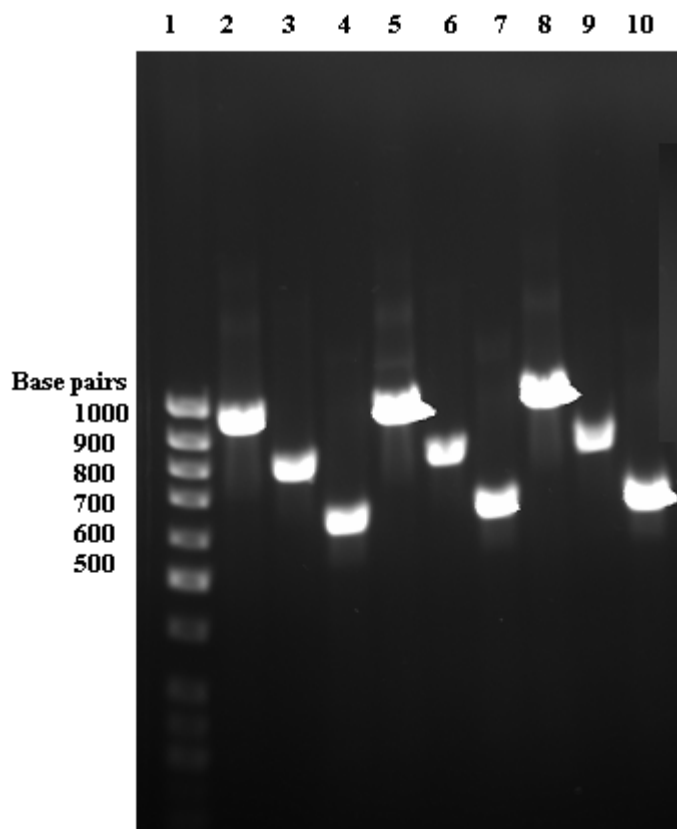


Figure 4.7 Agarose gel electrophoresis image of *PCR products of pPICZαA::hGH* plasmid; 1. well: 50 bp DNA ladder; 2.well: PCR product of *pPICZαA::hGH* plasmid with AOX1 forward primer and *XbaI-hGH* reverse primer; 3.well: PCR product of *pPICZαA::hGH* plasmid with AOX1 reverse primer and *EcoRI-hGH* forward primer 3.well: PCR product of *pPICZαA::hGH* plasmid with *EcoRI-hGH* forward primer and *XbaI-hGH* reverse primer. The other wells shows PCR products for other *pPICZαA::hGH* plasmids isolated from *E. coli* transformants.

The DNA sequence of insert DNA was further controlled by automatic DNA sequencers, (Microsynth GmbH, Switzerland) using *hGH* gene primers. The results proved that cloning was successful. The DNA sequence of *pPICZαA::hGH* is given in Appendix D.

4.1.5 Transfection of *P. pastoris* cells with *pPICZαA::hGH* plasmid

The *pPICZαA::hGH* vector, insert DNA sequence of which was controlled by automatic DNA sequencers (Microsynth GmbH, Switzerland), should be

linearized at its AOX promoter region so that double integration event can occur at AOX locus. *SacI* restriction enzyme was chosen as a single-cutter for linearization of *pPICZαA::hGH* plasmid. *pPICZαA::hGH* plasmid was digested with *SacI* restriction enzyme for overnight and full digestion verified by agarose gel electrophoresis. Then the digestion product was purified by the extraction from agarose gel. The concentration of the digested plasmid solution was kept 0.2 µg/µl for efficient transfection.

Transfection was performed as explained in Section 3.7.11. After 48 h of incubation at 30°C, sixteen single colonies were selected for further controls. The selected colonies were inoculated onto YPD + Zeocin (0.100 kg m⁻³) plates for short term storage and then inoculated into 10 ml YPD + Zeocin medium. Their genomic DNA was isolated to be used in controls by PCR (Figure 4.9). Among sixteen putative recombinant colonies, all of them showed positive results in PCR.

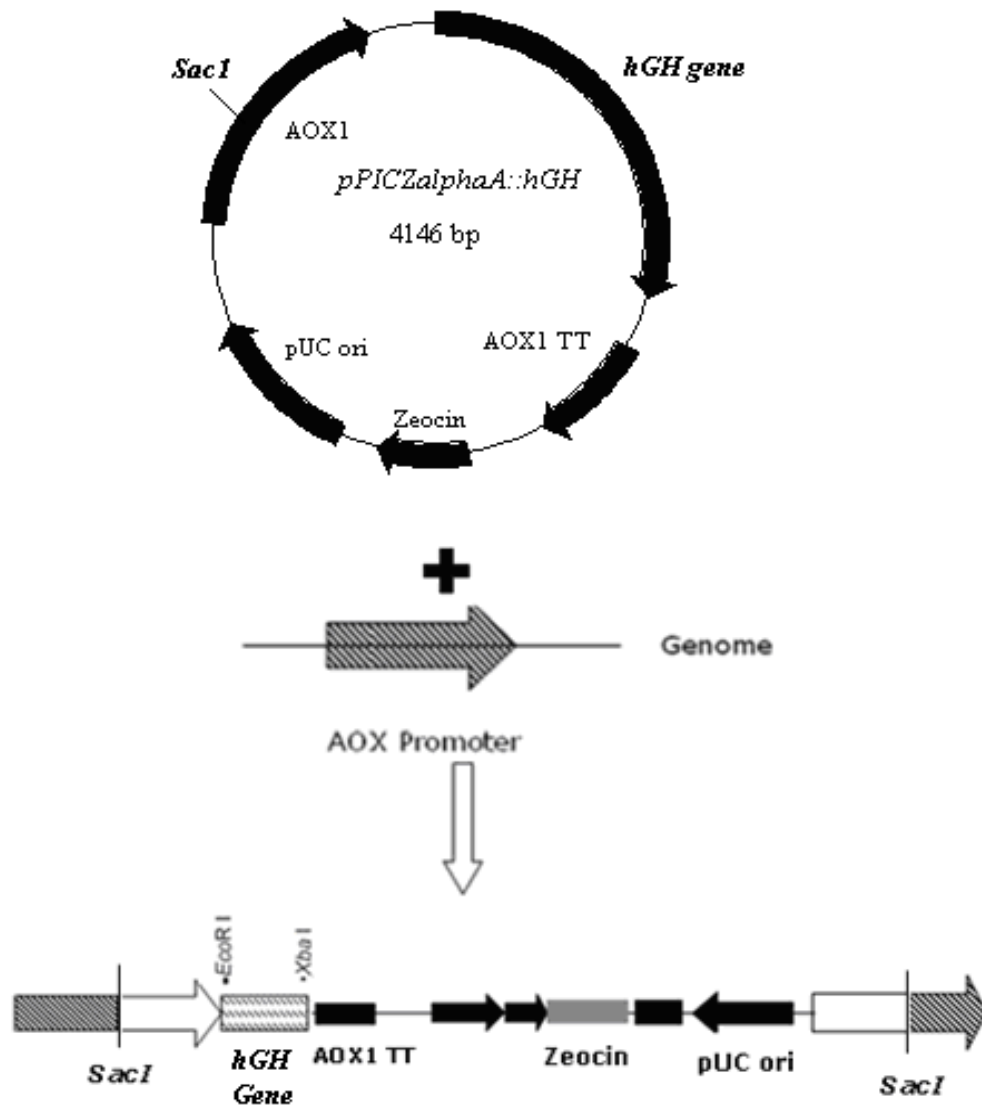


Figure 4.8 Schematic representation of pPICZαA::hGH integration into *P. pastoris* genome. The recombinant plasmid was digested with *SacI* from *AOX* promoter region, yielding a linearized plasmid having homologous regions to the *AOX* promoter in the genome at both ends. After integration of the plasmid to the genome, there are two functional copies of the *AOX* promoter in the genome.

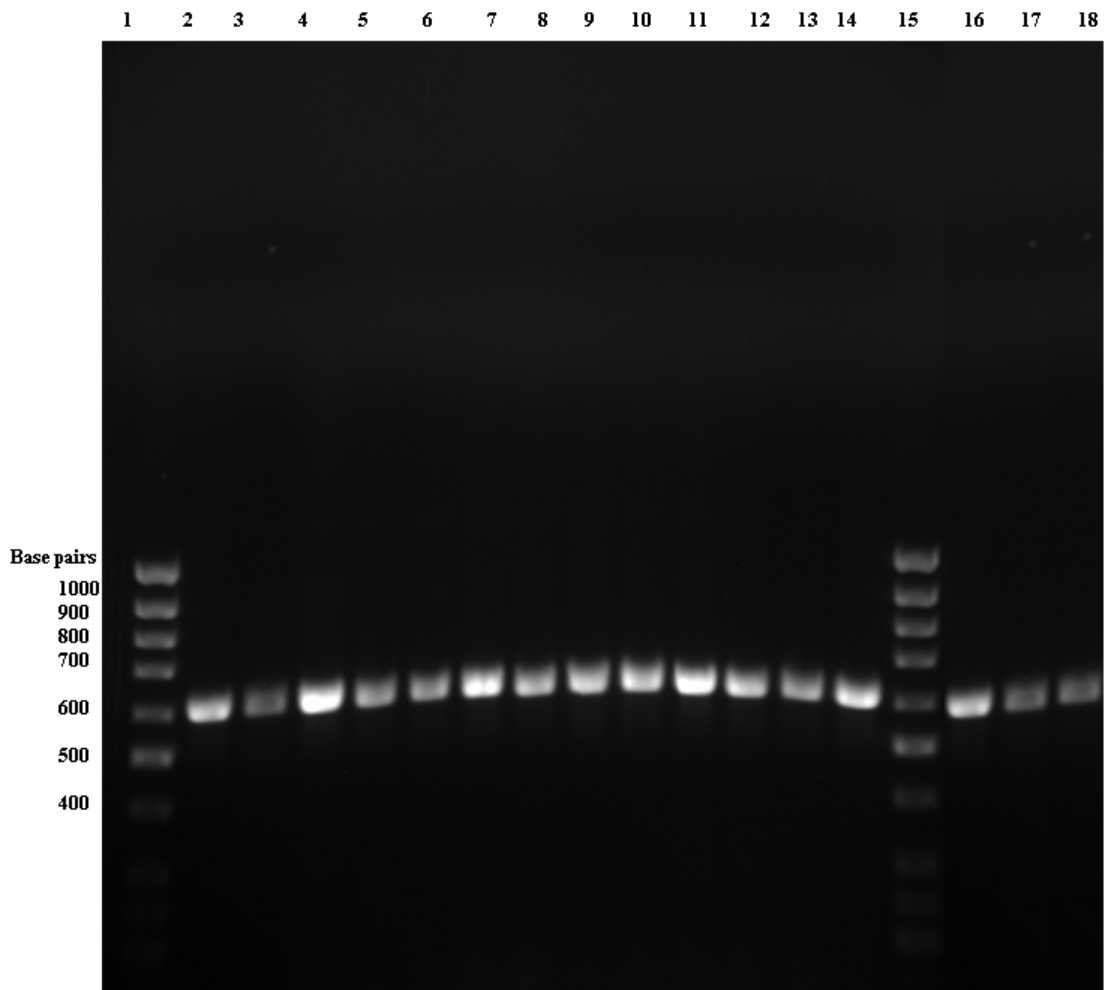


Figure 4.9 Agarose gel electrophoresis image of PCR products of *hGH* gene insert from genomic DNA *P. pastoris* transformants; 1. well and 15. well: 50 bp DNA ladder ; the other wells show the PCR products of sixteen colonies obtained by using forward and reverse primers of *hGH* gene (expected size=620 bp).

4.2 Expression of Human Growth Hormone in Recombinant *P. pastoris* in Laboratory Scale Air Filtered Shake Bioreactors

In this research program, after developing recombinant microorganisms carrying *hGH* gene by genetic engineering techniques, suitable strains producing human growth hormone at high levels were chosen. Thereafter, effects of methanol concentrations on the expression of rhGH and cell growth were analyzed and compared for chosen strains in defined and complex media in laboratory scale air filtered shake bioreactors.

4.2.1 Microorganism Selection

After transfection of *P. pastoris* cells with pPICZαA::*hGH* plasmid, sixteen colonies were selected and tested further with PCR (section 4.1.5). Results showed that all of them were positive colonies including *hGH* gene. In order to choose potential microorganisms producing hGH at high levels, sixteen colonies grown in the solid medium were inoculated into precultivation medium and incubated at 30°C and $N=225 \text{ min}^{-1}$ for 24 h in agitation and heating rate controlled orbital shakers using air-filtered Erlenmeyer flasks 150 ml in size that had working volume capacities of 10 ml. Then, they were harvested by centrifugation at 4000 rpm, 10 min at room temperature and resuspended in BMMY production medium (including 1.0 % (v/v) methanol). The recombinant cells were incubated at 30°C and $N=225 \text{ min}^{-1}$ for 72 h using air-filtered, baffled Erlenmeyer flasks 250 ml in size that had working volume capacities of 50 ml. Every 24 h, 1.0% methanol was added to the production medium and 1 ml of production medium from each flasks was taken for dot-blot analysis.

The appropriate strains producing hGH at high levels were chosen among other transformants with dot-blot analysis. 10 µl production medium for each transformant at $t=24, 48$ and 72 h were transferred to Immobilon-P PVDF nylon membranes (Millipore, Bedford, MA). Dot-blot analysis was achieved by using monoclonal anti-human hGH antibody (R&D Systems, Minneapolis, MN) as primary antibody and antimouse IgG horseradish peroxidase-linked whole antibody (Amersham Biosciences, Uppsala, Sweden) as secondary antibody. The dots were visualized using the Substrate –Chromogen Kit (S10 HRP,

BioMeda, ABD). Detailed information about blotting was explained in section 3.6.4, *western-blotting*.

Figure 4.10 shows the results of dot-blot analysis of sixteen colonies at different time. Dark brown blots on the figure indicate existence of hGH. According to this analysis, 15th colony had the highest capacity of hGH production and the amount of hGH concentration was almost the same during three-day induction. Although 3rd and 9th colonies had also higher capacities when compared with other transformants, rapid degradation of hGH occurred in cultivation medium after t=24 hours.

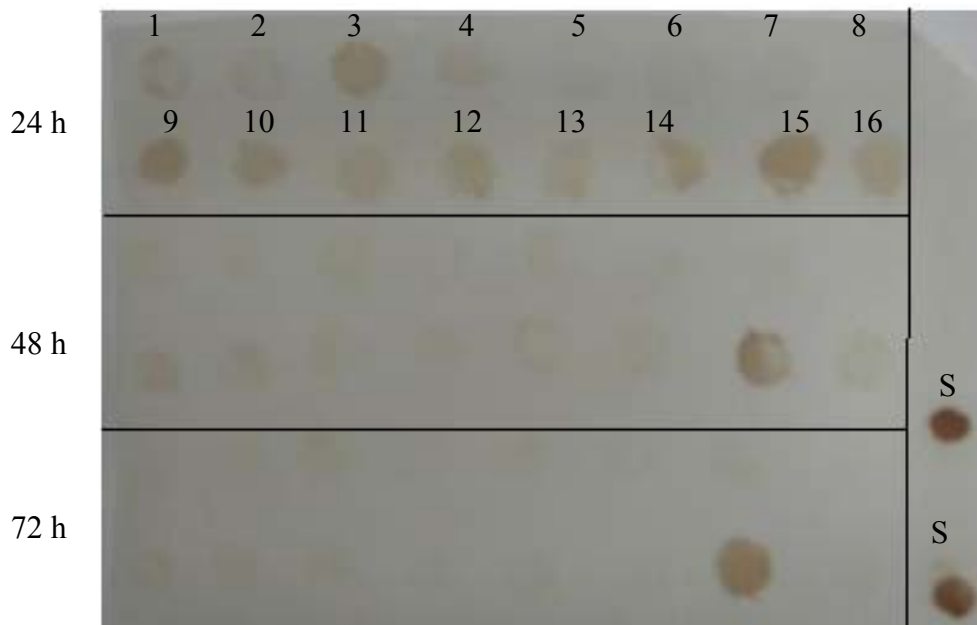


Figure 4.10 Dot-blot analysis. The numbers and the abbreviation; S, represent the supernatants of sixteen colonies and hGH standard.

Cereghino and Cregg (2000) in their review article indicate that approximately 10-20 % of transformation events are the results of a gene replacement event in which the AOX1 gene is deleted and replaced by the expression cassette and marker gene. These strains (Mut^s) are easily identified among transformed colonies from Mut⁺ phenotype by selecting those growing on methanol slowly since specific growth rates of Mut⁺ and Mut^s phenotypes on methanol are respectively 0.14 and 0.04 h⁻¹ (Jungo et al., 2006). When cell

growth and methanol utilization diagram of 15th colony were compared with those of other colonies (since other colonies had the same cell growth and methanol utilization pattern), it was seen that 15th strain had methanol slow utilization phenotype (Mut^s) although all of the other strains showed wild type methanol utilization phenotype (Mut^+). Figure 4.11 compares cell growth and methanol utilization phenotypes of 15th strain (*P. pastoris-hGH-Mut^s*) with the 9th strain (*P. pastoris-hGH-Mut⁺*) which also has high hGH production capacity. It is seen that *P. pastoris-hGH-Mut⁺* strain reaches higher cell density and uses methanol more efficiently.

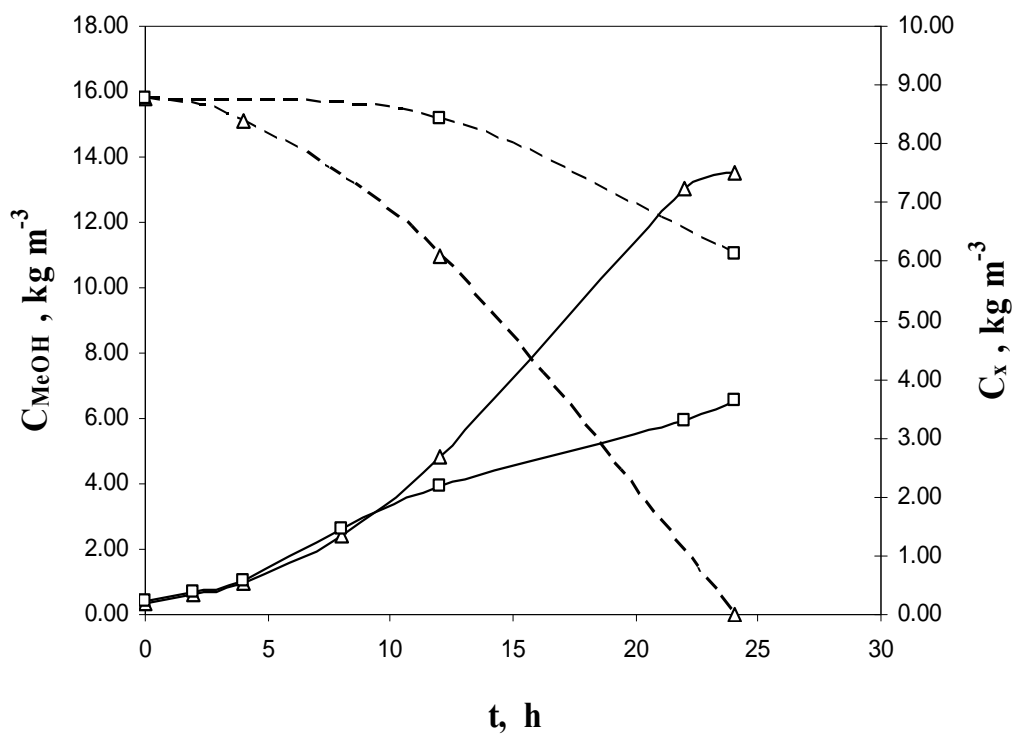


Figure 4.11 Cell growth (solid line) and methanol utilization (dashed line) diagrams for *P. pastoris-hGH-Mut^s* (\square) and *P. pastoris-hGH-Mut⁺* (Δ). Initial methanol concentration in cultivation medium for both phenotypes is %2 (v/v) ($15.8\ kg\ m^{-3}$).

Detailed investigation of Figure 4.10 shows that *P. pastoris-hGH-Mut^s* strain has the highest hGH production capacity. One of the reasons why hGH concentration in supernatant of *P. pastoris-hGH-Mut^s* is higher when compared with other strains is proteolysis. Degradation of hGH in all cultivation media of colonies except the one of 15th colony was most probably due to various yeast proteases present in the culture supernatant (Ohya et al., 2002). Moreover,

the length of induction has an effect on the extent of proteolysis and proteolysis was found to increase over time when the number of viable cells was increased (Dally and Hearn, 2005). Therefore it is possible that colonies with Mut⁺ phenotype produced proteases at high levels due to the number of viable cells which was high. The other reason why Mut^s phenotype produced hGH much may be that it requires lower energy due to the disruption of *AOX1* gene. In wild type phenotype, AOX levels can constitute almost or greater than 30% of soluble protein (Cereghino et al., 2002) which results in stress on the cell since it requires extra energy and resources for production of active AOX1. Deletion of *AOX1* gene may have a positive effect on production of recombinant protein since it may use these extra energy and resources for the production of r-protein.

4.2.2 Effects of Carbon Sources on rhGH Production and Cell Growth for both *P. pastoris-hGH-Mut^s* and *P. pastoris-hGH-Mut⁺*

After selection of two potential strains with Mut^s and Mut⁺ phenotypes, effects of carbon sources (methanol and glycerol) on recombinant protein and cell growth were investigated. Strains were inoculated into precultivation medium and incubated at 30°C and N=225 min⁻¹ for 24 h erlenmeyer flasks 150 ml in size that had working volume capacities of 10 ml. Then, they were harvested by centrifugation at 4000 rpm, 10 min at room temperature and resuspended in sterile dH₂O. Thereafter, some of the resuspended cells were transferred to production medium so that initial cell concentration would become approximately 0.2 kg m⁻³. The recombinant cells were incubated at 30°C and N=225 min⁻¹ using baffled flasks 250 ml in size that had working volume capacities of 50 ml. Besides the cell growth curves, methanol and glycerol utilization curves by using HPLC system were obtained and SDS-page analysis in order to determine the rhGH produced by the cells was done.

4.2.2.1 Effects of Methanol Concentrations in Complex Medium

Two phenotypes, *P. pastoris-hGH-Mut⁺* and *P. pastoris-hGH-Mut^s* were inoculated in BMMY (complex) production medium containing 10 kg m⁻³ yeast extract, 20 kg m⁻³ peptone, 13.4 kg m⁻³ yeast nitrogen base, 4x10⁻⁴ kg m⁻³ biotin and 10% 0.1 M potassium phosphate buffer (pH=6.0) with different methanol concentrations; 0.5 %, 1 %, 2%, 3%, 4% (v/v), in order to analyze

the methanol effects on protein production and cell growth in complex medium. Figure 4.12 and Figure 4.13 exhibit the cell growth characteristics of these two phenotypes. The cell concentration profiles are dependent on the initial methanol concentration. With the increase in methanol concentration cell concentration increased but with a cost of longer cultivation times.

According to analysis of Figure 4.12 and 4.13, it is seen that increasing the methanol concentration has an inhibitory effect on cell growth of both phenotypes. 2% (v/v) methanol concentration and above, cell growth rates decrease considerably at between $t=8$ and 12h. Although substrate inhibition is observed well in both strains, Mut^s strain is not affected by increased methanol concentration as much as Mut^+ strain does. From the Figure 4.14 and Figure 4.15, Mut^+ strain can utilize all methanols and grows more rapidly, but Mut^s strain can not use methanol efficiently and it grows slowly on methanol. These are actually expected results because disruption in AOX1 gene of Mut^s reduced its capacity to assimilate methanol.

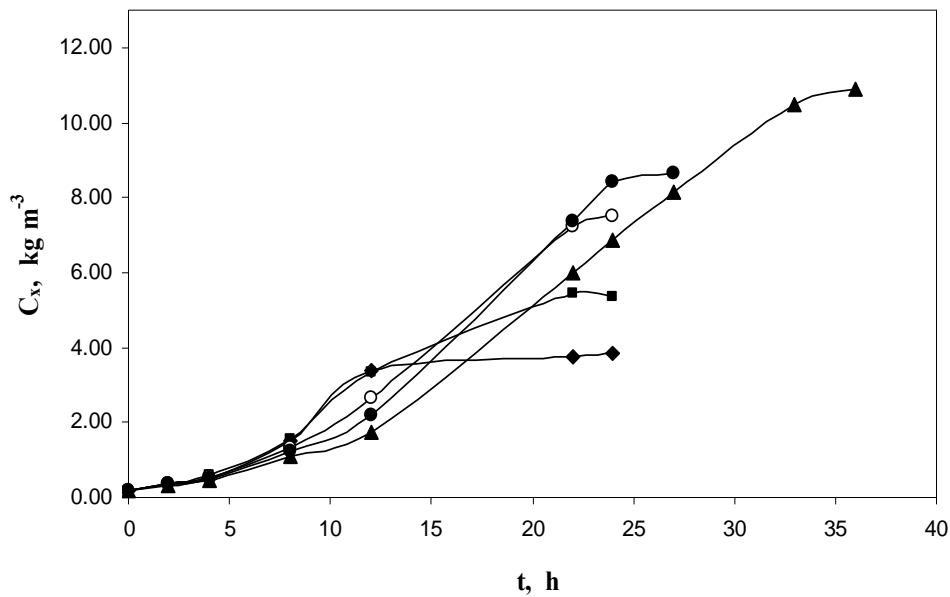


Figure 4.12 Effects of methanol concentrations on cell growth of *P. pastoris-hGH-Mut⁺* strain in complex medium. Methanol concentrations; 0.5% (◆), 1% (■), 2% (○), 3% (●), 4% (▲) (v/v).

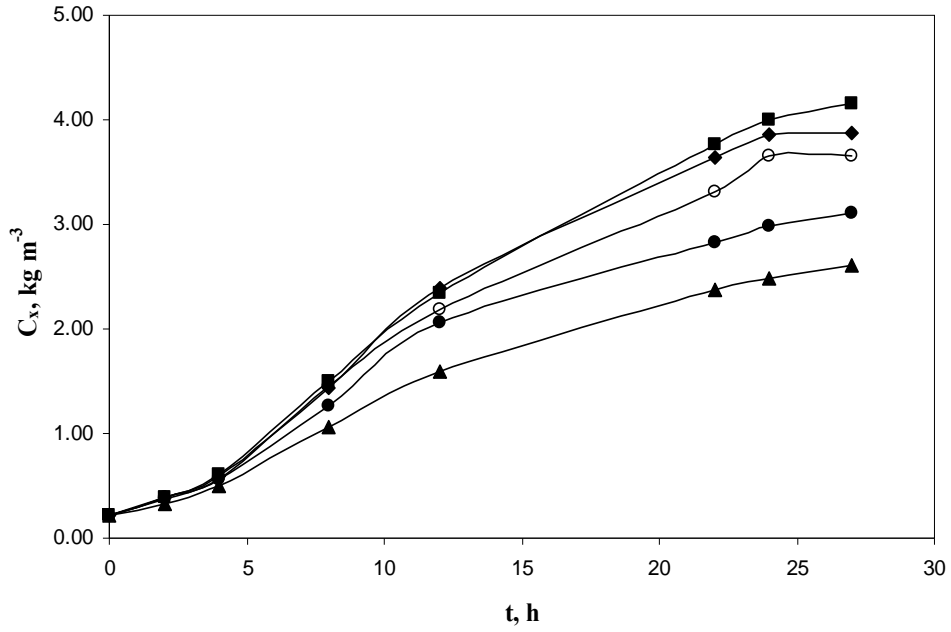


Figure 4.13 Effects of methanol concentrations on cell growth of *P. pastoris-hGH-Mut^S* strain in complex medium. Methanol concentrations; 0.5% (◆), 1% (■), 2% (○), 3% (●), 4% (▲) (v/v).

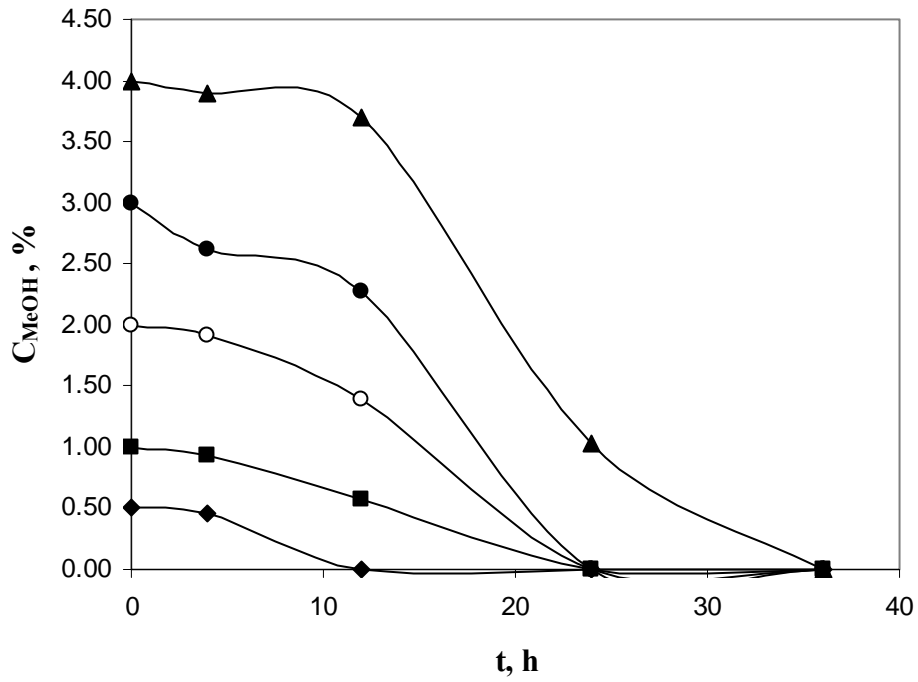


Figure 4.14 Methanol utilization diagram of *P. pastoris-hGH-Mut⁺* strain in complex medium. Methanol concentrations; 0.5% (◆), 1% (■), 2% (○), 3% (●), 4% (▲) (v/v).

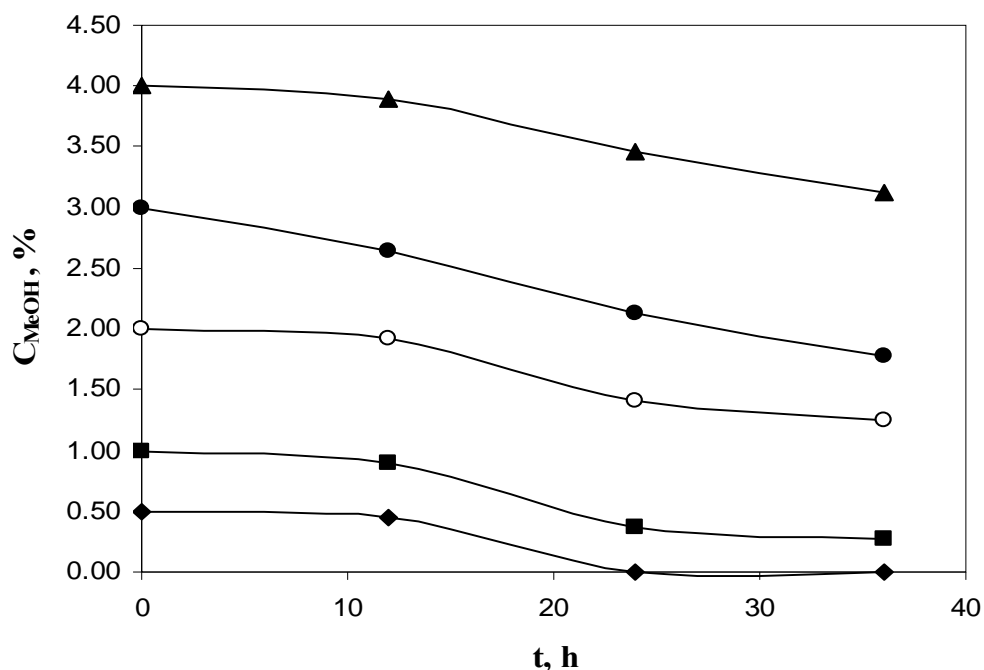


Figure 4.15 Methanol utilization diagram of *P. pastoris-hGH-Mut^s* strain in complex medium. Methanol concentrations; 0.5% (◆), 1% (■), 2% (○), 3% (●), 4% (▲) (v/v).

In this study rhGH production capacity were obtained by using SDS-page analysis. The concentrations were determined according to relative intensity of the bands as explained in section 3.6.4. After full depletion of methanol which was determined by using HPLC analysis system, 15 μ l of supernatant from each culture was loaded to SDS-page running system. Figure 4.16 is the SDS page results of Mut⁺ strain (a) and Mut^s strain (b).

Actually the molecular weight of standard hGH is approximately 22 kDa. Addition of polyhistidine tag and Factor Xa protease recognition sequence increases the molecular weight of rhGH produced by *r-P. pastoris* to 23 kDa. According to Figure 4.15, it is seen that there are two proteins from production culture, which result in two bands in SDS-page gel, having molecular weight of 23 kDa and 22 kDa, respectively. These two bands also appear on Western-blot analysis. It is suggested that cleavage of polyhistidine tag from rhGH produced by the cells occurs, somehow, in cell or across the membrane.

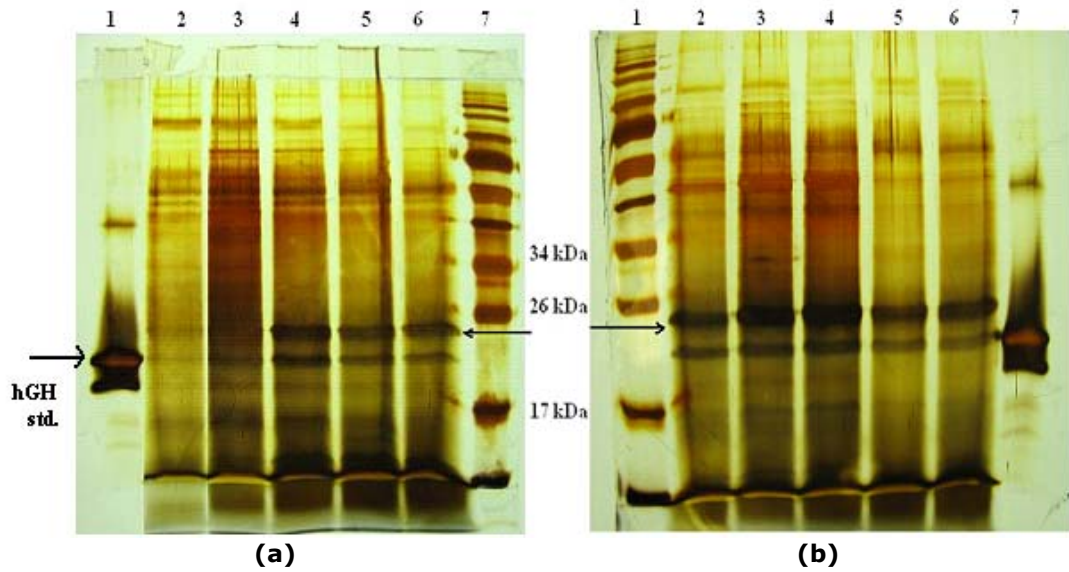


Figure 4.16 SDS-page image of rhGH produced by *P. pastoris-hGH-Mut⁺* **(a)** and *P. pastoris-hGH-Mut^S* **(b)**. Arrows and numbers (wells) indicate the place of rhGH and different production cultures, respectively. **(a)** 1. well: standard hGH, 2. well: 4% (v/v) methanol, 3. well: 3% (v/v) methanol, 4. well: 2% (v/v) methanol, 5. well: 1% (v/v) methanol, 6. well: 0.5% (v/v) methanol, 7. well: protein maker. **(b)** 1. well: protein maker, 2. well: 0.5% (v/v) methanol, 3. well: 1% (v/v) methanol, 4. well: 2% (v/v) methanol, 5. well: 3% (v/v) methanol, 6. well: 4% (v/v) methanol, 7. well: standard hGH.

Eurwilaichitr et al. (2002) investigated the optimal conditions producing high level of secreted rhGH from *P. pastoris Mut⁺* in BMMY complex medium with 100 ml flask. They obtained the highest hGH concentration as 0.190 kg m⁻³ at 3% (v/v) methanol concentration after 3 day induction. In this study no additional induction after inoculation of recombinant cells in complex production medium containing methanol was done. The highest rhGH concentration for both strains; Mut⁺ and Mut^S, was found as 0.52 kg m⁻³ and 0.160 kg m⁻³, respectively, at 2% (v/v) and above this concentration, rhGH production decreased. Table 4.6 and Table 4.7 show the rhGH concentrations, cell densities and yields obtained at the end of the production processes. Human growth hormone concentrations in production media of Mut⁺ strain at methanol concentrations greater than 3% (v/v) were not detectable, most probably due to the substrate inhibition or proteolysis of protein because the length of induction has an effect on the extent of proteolysis and proteolysis increases over time when the number of viable cells is increased (Dally and Hearn, 2005). As seen on Table 4.6, overall biomass and product yields with

respect to substrate consumed and the product yields per unit of cell mass produced decrease when methanol concentration is increased and the highest product yields on substrate and on cell mass were obtained as 0.0094 kg rhGH kg⁻¹ methanol and 0.0096 kg rhGH kg⁻¹ cell, respectively, at 1% (v/v) methanol concentration. On the other hand, these values are much higher in Mut^s strain than those obtained in Mut⁺ and decreasing pattern of yield coefficients with respect to methanol concentration in Mut^s strain is not the same as those found in Mut⁺ strain. It is obvious that Mut^s strain has higher capacity of rhGH production and it reaches lower cell densities when compared with Mut⁺ strain. These result in higher product yield coefficients. At 2% (v/v) methanol concentration, product yield coefficients of Mut^s phenotype are the highest due to the level of rhGH secreted to cultivation medium at this condition; 0.027 kg rhGH kg⁻¹ methanol and 0.044 kg rhGH kg⁻¹ cell. On the other hand, product yield based on substrate consumed was found as approximately 0.0027 kg rhGH kg⁻¹ methanol by Eurwilaichitr et al. (2002) after 3 day of induction. This is much lower than the product yield coefficients found in this study, most probably because they used higher amount of methanol with long cultivation time.

Yields for heterologous protein production depend on factors that influence gene expression and secretion, host strain physiology, growth conditions and cultivation process parameters (Sreekrishna et al., 1997). It is also depends on the characteristics of foreign protein such as cell toxicity, stability and protease sensitivity (Cos et al., 2005). Although many reports defining a successful operational scheme for cultivation of *P. pastoris* Mut⁺ and Mut^s strain point out that productivity yields reached are variable, particularly with regard to specific protein expressed (Cos et al., 2005). It is difficult to make a correlation about level of the recombinant protein with regard to phenotypes of *P. pastoris*, but cells of the Mut^s phenotype tend to produce either similar or higher amounts of protein than Mut⁺ cells in shaken-flask cultures, probably because flasks supply less oxygen (Mut⁺ strains demand more oxygen) or proteolysis of recombinant protein in Mut⁺ strain may be higher due to the long cultivation time and higher cell densities (Daly and Hearn, 2005), or Mut^s strain requires lower energy due to the disruption of *AOX1* gene so that it can utilize these resources for the production of recombinant protein instead of *AOX1* gene.

Table 4.6 Recombinant hGH concentrations, final cell concentrations and overall yield coefficients of *P. pastoris-hGH-Mut⁺* strain

C _{MeOH} (v/v)	Methanol used (kg m ⁻³)	C _{hGH} (kg m ⁻³)	C x (kg m ⁻³)	Y _{x/s} (kg kg ⁻¹)	Y _{p/s} (kg kg ⁻¹)	Y _{p/x} (kg kg ⁻¹)
0.5%	3.95	0.037	3.83	0.969	0.0094	0.0096
1.0%	7.90	0.042	5.34	0.676	0.0053	0.0078
2.0%	15.80	0.052	7.51	0.475	0.0033	0.0069
3.0%	23.70	-	8.67	0.366	-	-
4.0%	31.60	-	10.88	0.344	-	-

Table 4.7 Recombinant hGH concentration, final cell concentrations and overall yield coefficients of *P. pastoris-hGH-Mut^s* strain

C _{MeOH} (v/v)	Methanol used (kg m ⁻³)	C _{hGH} (kg m ⁻³)	C x (kg m ⁻³)	Y _{x/s} (kg kg ⁻¹)	Y _{p/s} (kg kg ⁻¹)	Y _{p/x} (kg kg ⁻¹)
0.5%	3.95	0.080	3.87	0.980	0.020	0.021
1.0%	5.74	0.115	4.16	0.725	0.020	0.028
2.0%	5.89	0.160	3.66	0.621	0.027	0.044
3.0%	6.32	0.121	3.11	0.492	0.019	0.039
4.0%	6.87	0.111	2.61	0.379	0.016	0.042

4.2.2.2 Effects of Methanol Concentrations in Defined Medium

In order to analyze the methanol effects on protein production and cell growth in defined medium, two phenotypes, *P. pastoris-hGH-Mut⁺* and *P. pastoris-hGH-Mut^s* were inoculated in defined production medium at different methanol concentrations; 0.25 %, 0.5 %, 1 %, 1.5 %, 2%, 3%, 4% (v/v).

Defined medium contains basal and trace elements which are 5.62 kg m⁻³ potassium phosphate, 1.1800 kg m⁻³ magnesium sulfate, 0.8300 kg m⁻³ calcium sulfate, 0.0080 kg m⁻³ copper sulfate, 0.0012 kg m⁻³ potassium iodide, 0.0280 kg m⁻³ manganese sulfate, 0.0052 kg m⁻³ sodium molybdate, 0.0080 kg m⁻³ boric acid, 0.0080 kg m⁻³ cobalt chloride, 0.0044 kg m⁻³ zinc sulfate, 0.0750 kg m⁻³ ferric chloride, and 0.00174 kg m⁻³ biotin. The amount of ammonium sulfate used as a nitrogen source varies with respect to methanol concentration on the base of the study of Jungo et al. (2006). 1.86, 3.72,

7.44, 11.6, 14.88, 22.32 and 29.76 kg m⁻³ ammonium sulfate are used respectively, when 0.25 %, 0.5 %, 1 %, 1.5 %, 2%, 3%, 4% (v/v) initial methanol concentrations are used.

Figure 4.17 and Figure 4.18 exhibit the cell growth characteristics of these two phenotypes. Figure 4.19 and Figure 4.20 show the methanol utilization pattern. These configurations resemble the previous ones found in complex medium. But, lower cell densities are obtained due to medium composition. Since complex medium (BMMY) contains rich ingredients such as peptone, yeast extract, it is expected that high cell densities can be obtained. Medium compositions also affect the productivity and yields coefficients.

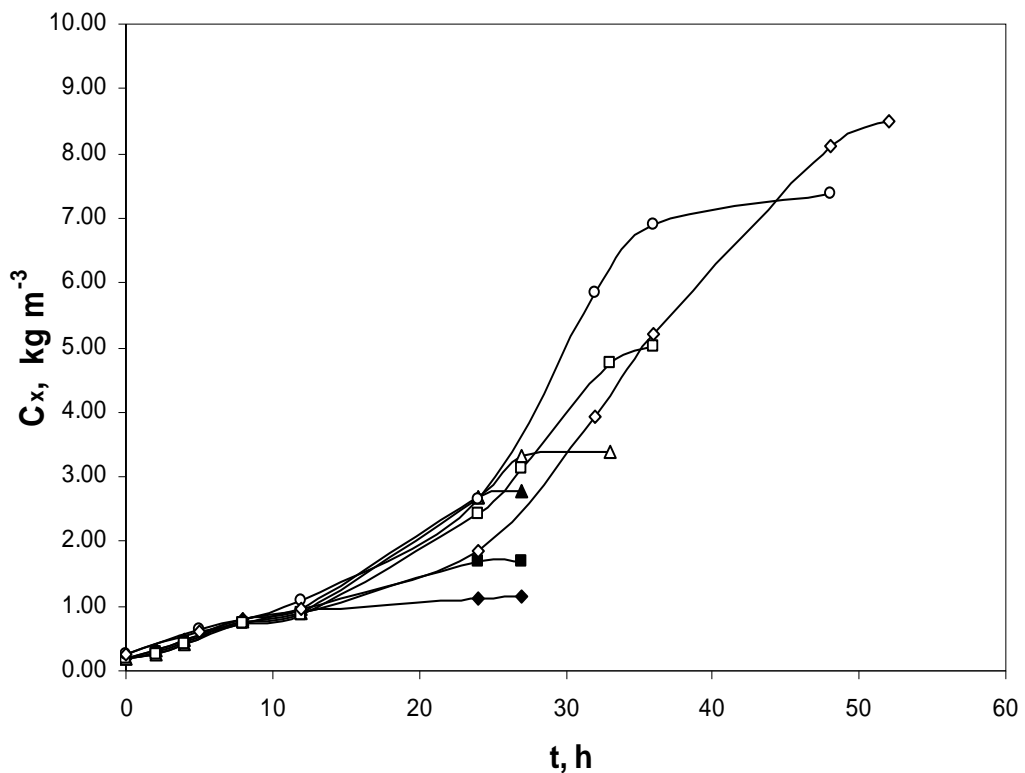


Figure 4.17 Effects of methanol concentrations on cell growth of *P. pastoris-hGH-Mut⁺* strain in defined medium. Methanol concentrations; 0.25% (◆), 0.5 % (■), 1% (▲), 1.5 % (△), 2% (□), 3% (○), 4%(◇) (v/v).

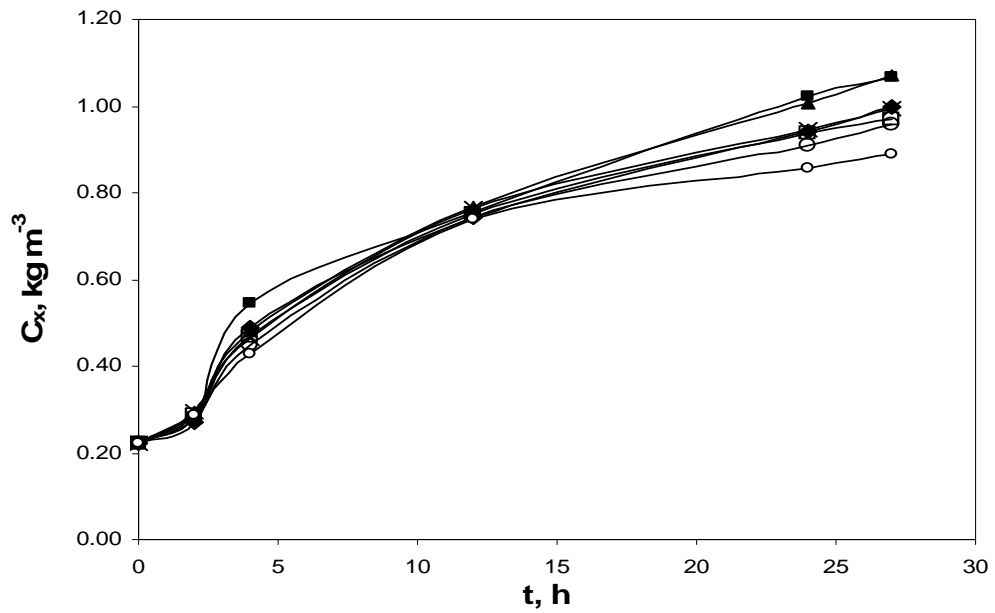


Figure 4.18 Effects of methanol concentrations on cell growth of *P. pastoris-hGH-Mut^s* strain in defined medium. Methanol concentrations; 0.25% (◆), 0.5 % (■), 1% (▲), 1.5 % (△), 2% (□), 3% (○), 4%(◇) (v/v).

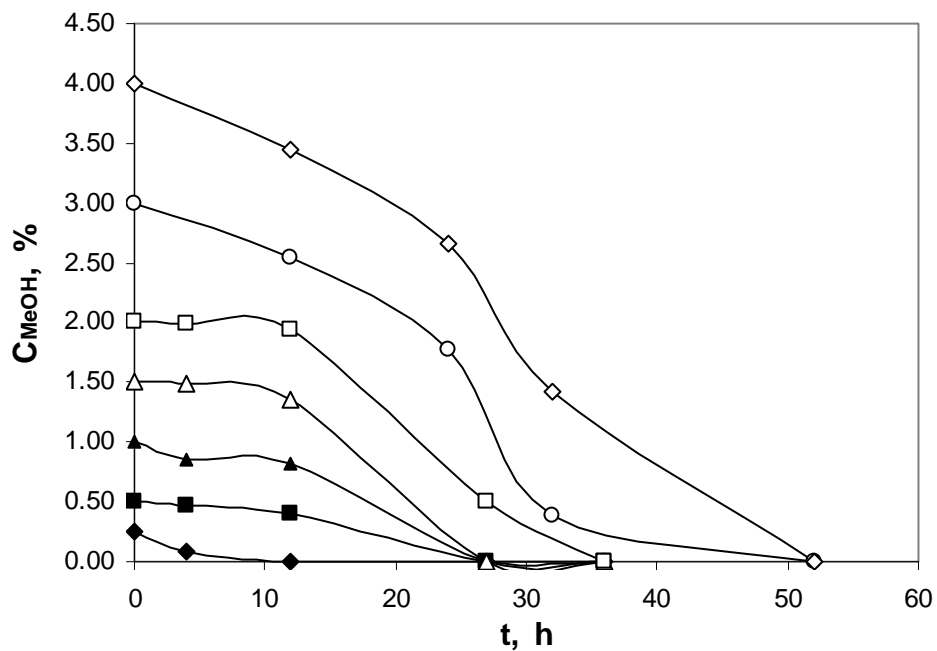


Figure 4.19 Methanol utilization diagram of *P. pastoris-hGH-Mut^t* strain in defined medium. Methanol concentrations; 0.25% (◆), 0.5 % (■), 1% (▲), 1.5 % (△), 2% (□), 3% (○), 4%(◇) (v/v).

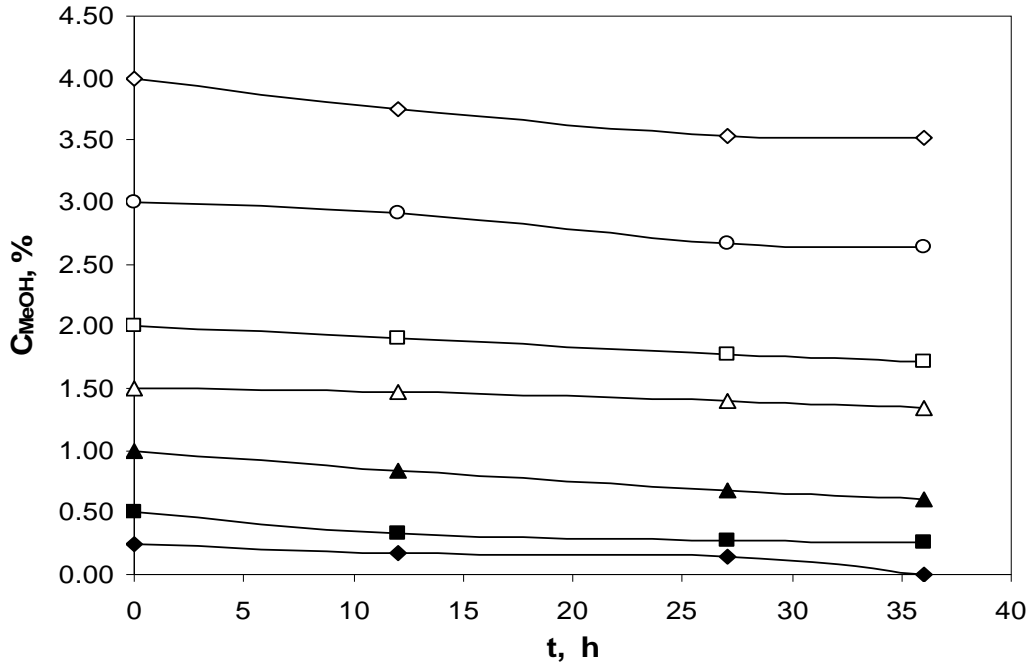


Figure 4.20 Methanol utilization diagram of *P. pastoris-hGH-Mut^S* strain in defined medium. Methanol concentrations; 0.25% (◆), 0.5 % (■), 1% (▲), 1.5 % (△), 2% (□), 3% (○), 4%(◇) (v/v).

Due to the disruption of *AOX1* gene, *Mut^S* phenotype can not use methanol effectively. The result depicted on Figure 18 and Figure 20 is actually evidence of this fact. On the other hand *Mut⁺* strain can grow on methanol well and it can consume all methanol at different time due to substrate inhibition. Figure 4.21 is the SDS-page analysis and Table 4.8 shows the rhGH concentrations and yield coefficients of *P. pastoris-hGH-Mut⁺* strain. Since cell density of *Mut^S* strain could not reach a value for the rhGH production, detectable rhGH was not observed. Therefore any overall biomass and product yield coefficients for *P. pastoris-hGH-Mut^S* could not be obtained. As seen on Table 4.8, overall biomass and product yields with respect to substrate consumed and the product yields per unit of cell mass produced for the *Mut⁺* phenotype decrease when methanol concentration is increased. Optimum rhGH concentrations and product yields were found at 3% methanol concentration. At this condition, 32 kg m⁻³ rhGH was obtained and product yields based on substrate and cell mass were found as 0.00135 kg rhGH kg⁻¹ methanol and 0.00433 kg rhGH kg⁻¹ cell.

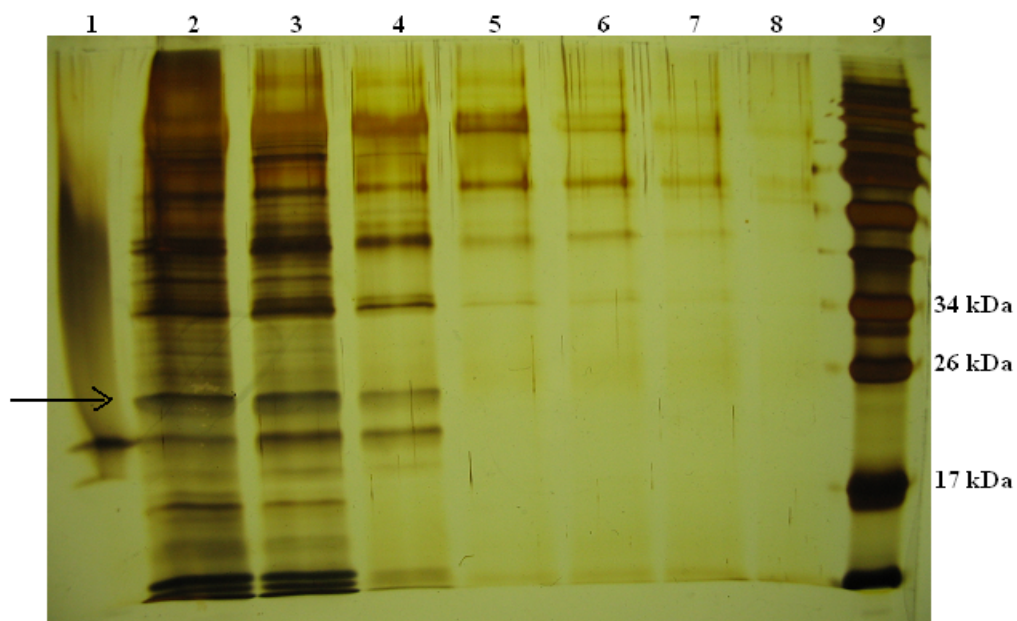


Figure 4.21 SDS-page image of rhGH produced by *P. pastoris-hGH-Mut⁺*. Arrows and numbers (wells) indicate the place of rhGH and different production cultures, respectively. 1. well: standard hGH, 2. well: 4% (v/v) methanol, 3. well: 3% (v/v) methanol, 4. well: 2% (v/v) methanol, 5. well: 1.5% (v/v) methanol, 6. well: 1.0% (v/v) methanol, 7. well: 0.5% (v/v) methanol, 8. well: 0.25% (v/v) methanol, 9. well: protein maker.

There are no detailed studies about the heterologous protein production from *P. pastoris* in defined medium in shaken flask. Cos et al. (2005) carried out a comparative study of the heterologous expression of ROL (*Rhizopus oryzae* lipase) in batch and high cell density fed-batch bioreactor cultivation processes using two different regulated promoters, i.e. *PAOX1* and *PFLD1*. Their investigation of ROL activity in batch bioreactor performed with *Mut⁺* phenotype demonstrates that overall biomass yield coefficient is obtained as 0.27 kg cell kg⁻¹ methanol when approximately 10 kg m⁻³ methanol is consumed, which actually coincide with those found in this study. Due to the use of activity unit in their yield coefficient calculations, overall product yield coefficients could not be compared.

Table 4.8 Recombinant hGH concentration, final cell concentrations and overall yield coefficient of *P. pastoris-hGH-Mut⁺* strain

C _{MeOH} (v/v)	Methanol used (kg m ⁻³)	C _{hGH} (kg m ⁻³)	C _x (kg m ⁻³)	Y _{x/s} (kg kg ⁻¹)	Y _{p/s} (kg kg ⁻¹)	Y _{p/x} (kg kg ⁻¹)
0.25%	1.975	1.15	-	0.58	-	-
0.5%	3.95	1.69	-	0.43	-	-
1.0%	7.90	2.77	-	0.35	-	-
1.5%	11.85	3.37	-	0.28	-	-
2.0%	15.80	5.01	0.019	0.32	0.00120	0.00379
3.0%	23.70	7.39	0.032	0.31	0.00135	0.00433
4.0%	31.60	8.50	0.024	0.27	0.00076	0.00282

4.2.2.3 Effects of Mixed Batch System (Glycerol/Methanol)

In this part, a typical approach; the use of a multicarbon substrate in addition to methanol which was performed experimentally will be explained. Two sets of experiments have been done; first, effects of glycerol concentration on recombinant protein production and cell growth of Mut⁺ and Mut^s strains in defined mixed-batch cultivation medium containing methanol at 3% (v/v) initial concentration, second, the effects of methanol concentration on recombinant protein production and cell growth in defined mixed-batch cultivation medium containing glycerol at 30 kg m⁻³ initial concentration were investigated and reported.

There are actually two reasons of applying this strategy which is the use of multicarbon substrate (methanol/glycerol) in the batch system:

1. to investigate the effects of cell density, increased due to the addition of glycerol, on the recombinant protein production,
2. to reduce induction time.

Mut⁺ phenotypes are more sensitive to methanol concentration; increasing methanol concentration in defined medium results in long lag phase, ~ 20 h (Figure 4.12 and Figure 4.17), and decreases cell growth rate, therefore mixed batch system (glycerol/methanol) may be more appropriate since *P. pastoris* can use glycerol more efficiently and higher cell growth rates can be obtained. In the case of Mut^s strain, defined batch system where methanol is used as a sole carbon source is not suitable because of their

genetically reduced capacity to assimilate methanol, therefore this strategy will be also employed for Mut^s phenotype.

a) Effects of glycerol concentration:

The first part of this approach is to examine r-protein production and cell growth of Mut⁺ and Mut^s strains in defined mixed-batch cultivation medium containing methanol at 3% (v/v) initial concentration with variable glycerol concentrations; 10, 20, 30, 40 kg m⁻³.

The same amount of basal salts and trace elements given in section 4.2.2.2 were used. Based on the C/N ratio in the study of Jungo et al. (2006), 27.0, 31.7, 36.4 and 41.1 kg m⁻³ ammonium sulfate were used respectively, when 10, 20, 30, 40 kg m⁻³ initial glycerol together with 3% (v/v) methanol concentration were used.

Figure 4.22 and Figure 4.23 exhibit the cell growth characteristics obtained at different glycerol concentrations. The solid lines indicate those obtained at mixed batch cultivation, and the dashed lines are growth features of cells grown on glycerol as a sole carbon source at variable concentrations. From these figures, it is obvious that addition of glycerol or increasing glycerol concentration in mixed batch system strongly inhibits the cell growth. This is more apparent at concentrations greater than 30 kg m⁻³ for Mut⁺ strain, and at concentrations greater than 20 kg m⁻³ for Mut^s strain. At lower glycerol concentrations, Mut⁺ strain can utilize methanol better since high cell densities in mixed batch system (solid lines) can be reached when compared the values shown on dashed lines, that is, at the same glycerol concentrations more cell are obtained in mixed-batch system. On the other hand, Mut^s strain can not use methanol as effective as Mut⁺ strain does, as it is expected, and lower cell densities in mixed batch system are obtained. The values on dashed lines are greater than those on solid lines, which indicate strong substrate (glycerol and methanol) inhibition on cell growth in Mut^s strain.

Figure 4.24 and Figure 4.25 show glycerol utilization, Figure 4.26 and Figure 4.27 show methanol utilization diagrams in mixed batch system for Mut⁺ and Mut^s strains, respectively. It is clear that both phenotypes utilize glycerol effectively. Since the same glycerol utilization diagrams are obtained

in the cultivation media containing glycerol as sole carbon source, they were not drawn. As it is expected, all methanols could not be consumed by Mut^s strain, though Mut⁺ strain consumed the entire methanol. According to methanol utilization diagrams, carbon utilization rates are different at different glycerol concentrations in mixed batch system, which demonstrates strong substrate inhibition. From these figures, it is also apparent that methanol consumption begins when glycerol begins to be depleted. When all glycerol is consumed by the cells, methanol utilization rates increase. These results clearly exhibits that glycerol is a repressor of AOX1 promoter, and excess glycerol limits the expression of AOX1 enzyme thus resulting inefficient utilization of methanol.

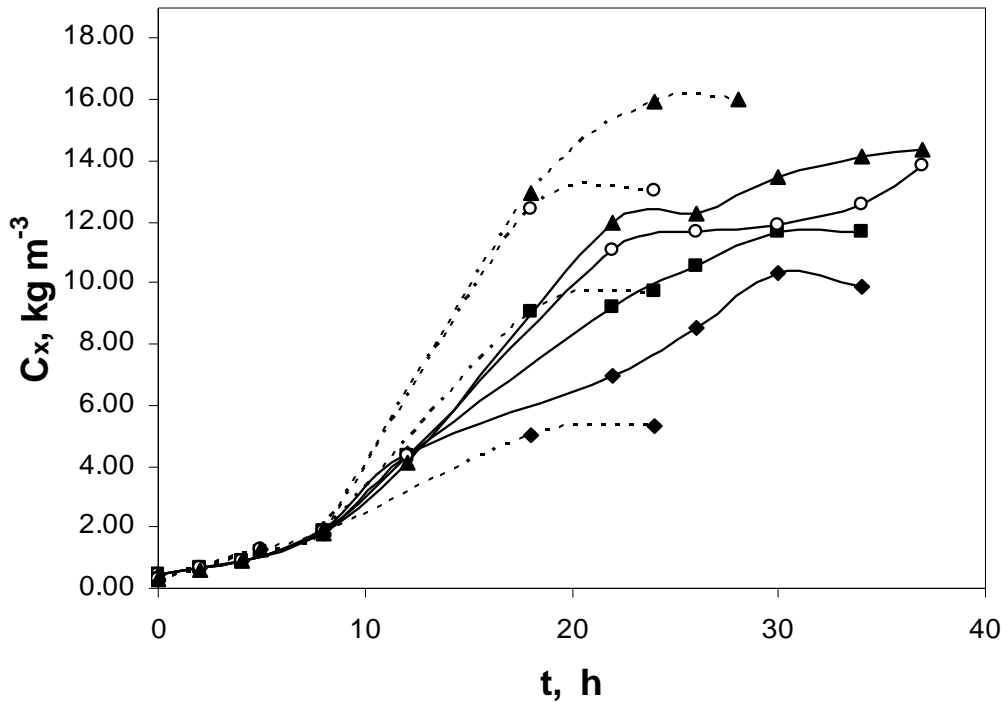


Figure 4.22 Effects of glycerol concentrations on cell growth of *P. pastoris-hGH-Mut⁺* strain in defined mixed-batch medium containing methanol at an initial concentration; 3% v/v (solid lines) or without methanol (dashed lines). Initial Glycerol concentrations; 10 kg m⁻³ (◆), 20 kg m⁻³ (■), 30 kg m⁻³ (○), 40 kg m⁻³ (▲).

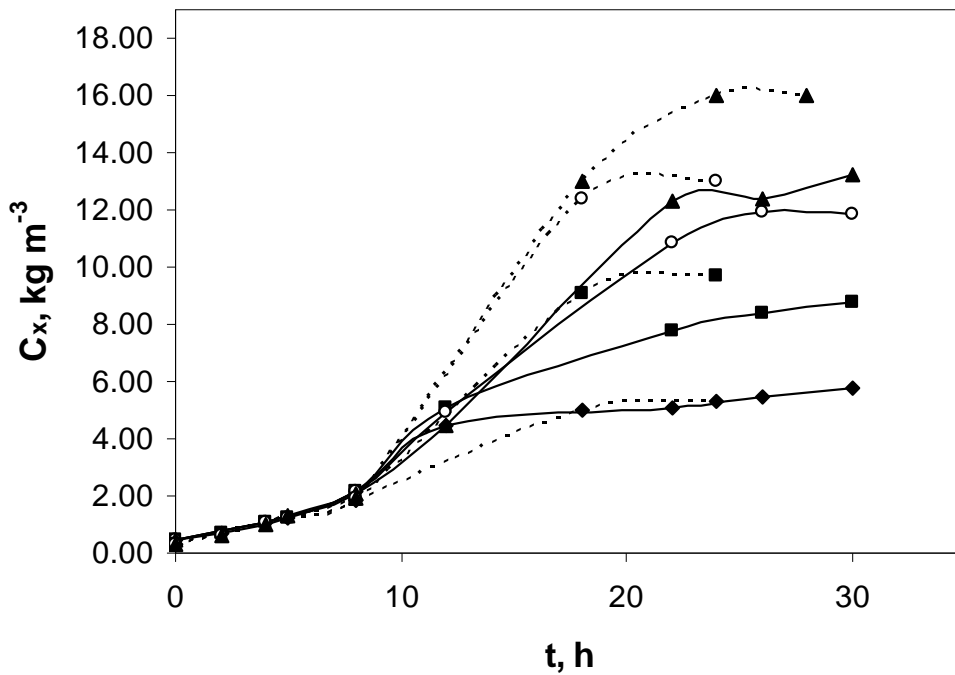


Figure 4.23 Effects of glycerol concentrations on cell growth of *P. pastoris-hGH-Mut⁵* strain in defined mixed-batch medium containing methanol at constant concentration; 3% v/v (solid lines) or without methanol (dashed lines). Initial glycerol concentrations; 10 kg m⁻³ (◆), 20 kg m⁻³ (■), 30 kg m⁻³ (○), 40 kg m⁻³ (▲).

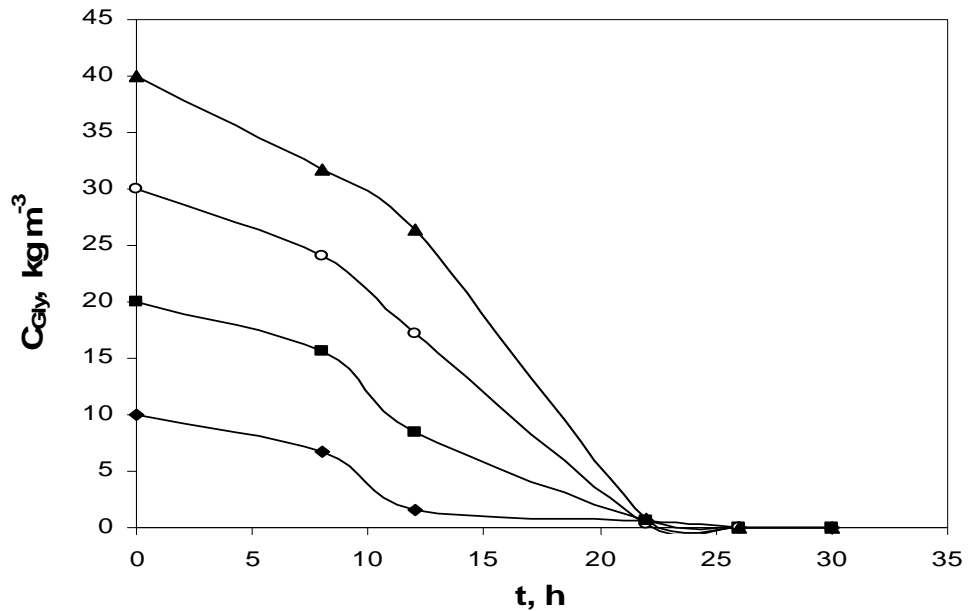


Figure 4.24 Glycerol utilization diagram of *P. pastoris-hGH-Mut⁺* strain in defined mixed-batch medium. Initial glycerol concentrations; 10 kg m⁻³ (◆), 20 kg m⁻³ (■), 30 kg m⁻³ (○), 40 kg m⁻³ (▲).

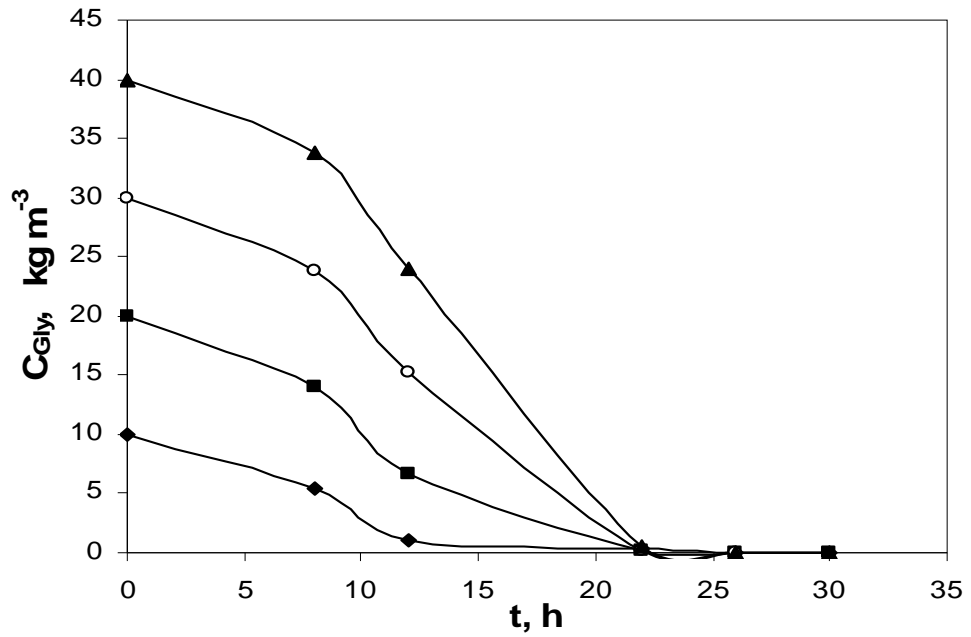


Figure 4.25 Glycerol utilization diagram of *P. pastoris-hGH-Mut^s* strain in defined mixed-batch medium. Initial glycerol concentrations; 10 kg m⁻³ (◆), 20 kg m⁻³ (■), 30 kg m⁻³ (○), 40 kg m⁻³ (▲).

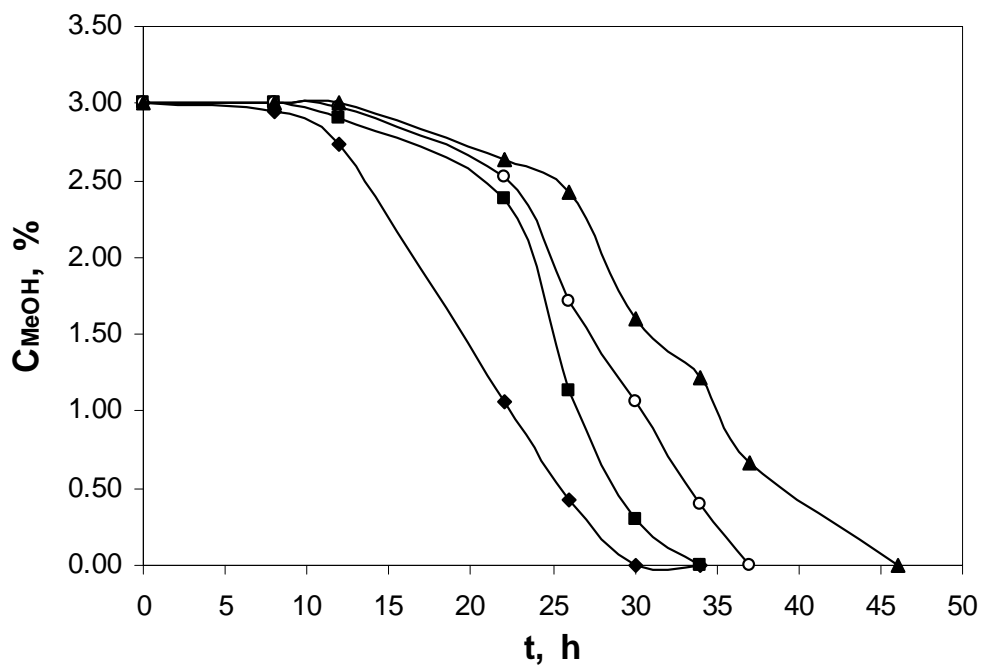


Figure 4.26 Methanol utilization diagram of *P. pastoris-hGH-Mut^t* strain in defined mixed-batch medium. Initial glycerol concentrations; 10 kg m⁻³ (◆), 20 kg m⁻³ (■), 30 kg m⁻³ (○), 40 kg m⁻³ (▲).

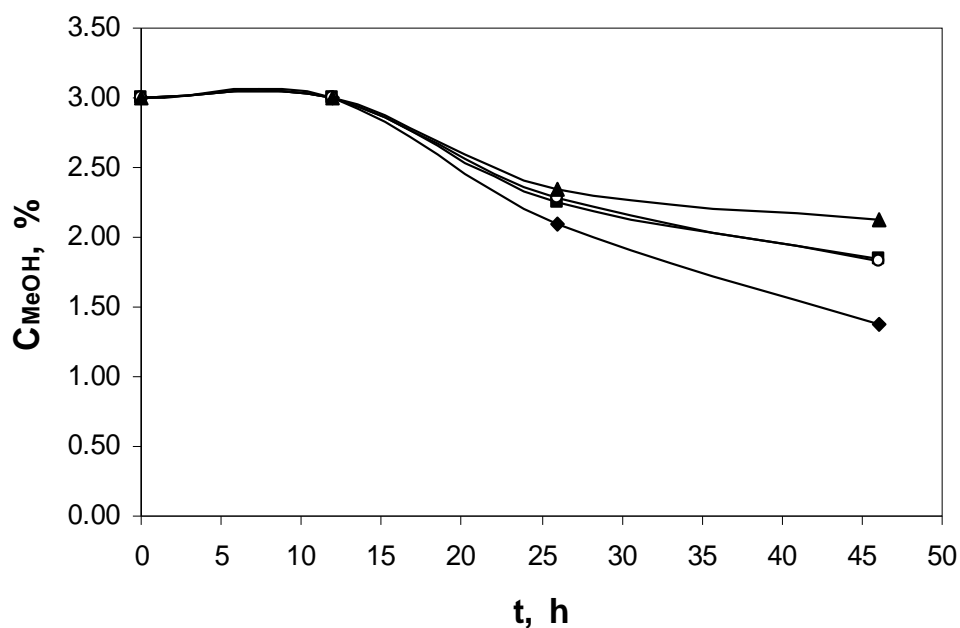


Figure 4.27 Methanol utilization diagram of *P. pastoris-hGH-Mut^s* strain in defined mixed-batch medium. Initial glycerol concentrations; 10 kg m⁻³ (◆), 20 kg m⁻³ (■), 30 kg m⁻³ (○), 40 kg m⁻³ (▲).

Figure 4.28 illustrates SDS-page image of rhGH produced by *P. pastoris-hGH-Mut^s* (a) and *P. pastoris-hGH-Mut⁺* (b). Table 4.9 gives recombinant hGH concentrations and final cell densities of *P. pastoris-hGH-Mut⁺* and *P. pastoris-hGH-Mut^s* strains. According to SDS-page analysis, rhGH concentrations indeed tend to increase with respect to glycerol concentration. This can be explained that at higher glycerol concentration, higher cell densities can be reached, which may increase the secretion of extracellular rhGH. Generally saying, for both phenotypes, optimum rhGH concentration was obtained at 30 kg m⁻³ glycerol, though the rhGH concentrations are closer to each other at glycerol concentrations greater than kg m⁻³. At glycerol concentration greater than 40 kg m⁻³, rhGH production begins to decrease. It is known that glycerol excess represses the *AOX1* promoter and results in lower r-protein production regulated under the control of *AOX1* promoter. According to SDS-page analysis (Appendix E) showing the cultivation media at t=24 h when all glycerol in each mixed-batch cultivation media was depleted, no detectable rhGH was observed. Again SDS-page analysis (Appendix E) indicates that maximum rhGH was obtained when all methanol was consumed by the cells, i.e. at the end of each processes. These results are the evidence

of the fact that rhGH began to be produced after all glycerol was depleted, therefore the amount of rhGH obtained at the end of each processes were not directly affected by the repression characteristics of glycerol over *AOX1* promoter. Instead, it was affected by the cell densities and cultivation times which influence the proteolysis of r-protein.

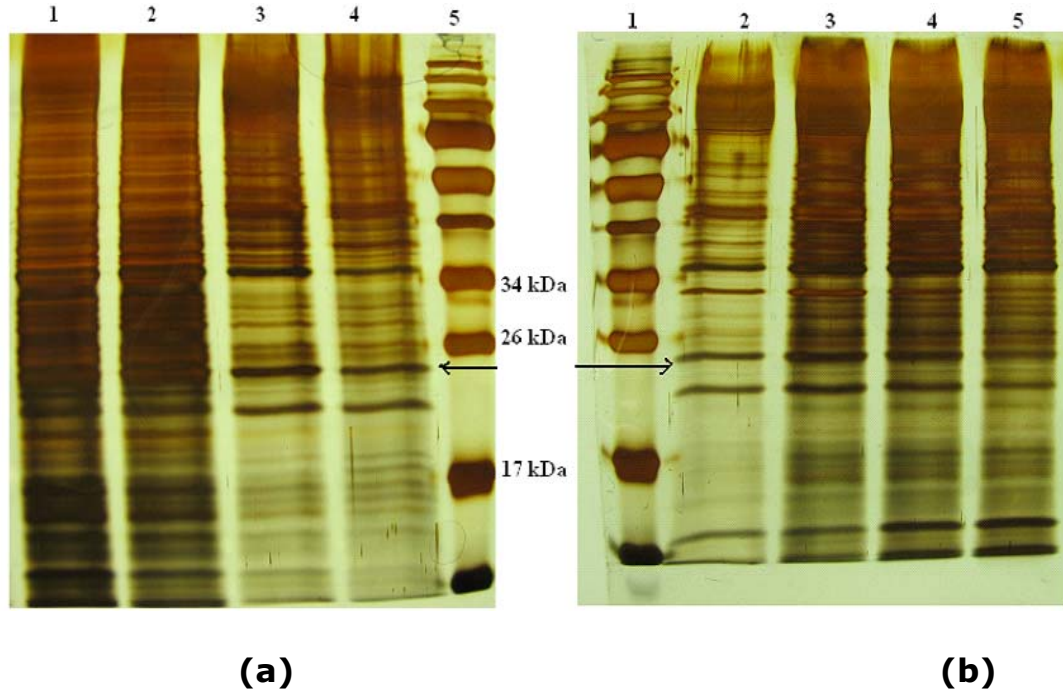


Figure 4.28 SDS-page image of rhGH produced by *P. pastoris-hGH-Mut^s* **(a)** and *P. pastoris-hGH-Mut⁺* **(b)**. Arrows and numbers (wells) indicate the place of rhGH and different production cultures, respectively. **(a)** 1. well: 40 kg m⁻³ glycerol, 2. well: 30 kg m⁻³ glycerol, 3. well: 20 kg m⁻³ glycerol, 4. well: 10 kg m⁻³ glycerol, 5. well: protein maker. **(b)** 1. well: protein maker, 2. well: 10 kg m⁻³ glycerol, 3. well: kg m⁻³ glycerol, 4. well: kg m⁻³ glycerol, 5. well: 40 kg m⁻³ glycerol.

Table 4.9 Recombinant hGH concentrations and final cell concentrations of *P. pastoris-hGH-Mut⁺* and *P. pastoris-hGH-Mut^s* strain

C_{glycerol} (kg m⁻³)	C_{MeOH} (kg m⁻³)	<i>P. pastoris-hGH-Mut⁺</i>		<i>P. pastoris-hGH-Mut^s</i>	
		C_{hGH} (kg m⁻³)	C_x (kg m⁻³)	C_{hGH} (kg m⁻³)	C_x (kg m⁻³)
10	3.0%	0.024	9.90	0.030	5.83
20	3.0%	0.048	11.63	0.040	8.21
30	3.0%	0.050	14.58	0.055	10.96
40	3.0%	0.026	14.34	0.052	13.16

b) Effects of methanol concentration:

In this case, the effects of methanol concentration on r-protein production and cell growth of Mut⁺ and Mut^s strains in defined mixed-batch cultivation medium containing glycerol at 30 kg m⁻³ initial concentration with variable methanol concentrations; 1 %, 2%, 3%, 4% (v/v) were investigated. 21.5, 29.0, 36.4 and 43.9 kg m⁻³ ammonium sulfate were used respectively. The amount of basal salts and trace elements used was the same as one given in section 4.2.2.2.

Figure 4.29 and Figure 4.30 show the cell growth characteristics obtained at different methanol concentrations. The solid lines indicate those obtained at mixed batch cultivation, and the dashed lines indicate cells growth on glycerol as a sole carbon source at an initial concentration 30 g L⁻¹. Detailed investigation of these figures points out that addition of methanol or increasing methanol concentration in mixed batch system inhibits the cell growth. According to HPLC analysis of glycerol consumption of both phenotypes which has been given on Figure 4.31 and Figure 4.32, all glycerol in each culture was depleted at around t=24 h. In spite of the use of all glycerol, biomass concentration in each culture at t=24 h has different values, which indicate that type of substrate and its concentrations affect the metabolism of these strains and yield different biomass concentrations. Moreover it is apparent that increasing methanol concentration in mixed-batch system results in decrease in biomass formation rates. These also coincide with the values given on Figure 4.31 and Figure 4.32, that is, glycerol consumption rates decrease when methanol concentration increases.

It is clear that both phenotypes utilize glycerol effectively. On the other hand, as it is expected, all methanol could not be consumed by Mut^s strain, though Mut⁺ strain consumed the entire methanol except the cells grown on medium containing methanol at a concentration of 4% (v/v) (Figure 4.33 and Figure 4.34). From these figures, it is also clear that methanol consumption begins when glycerol is almost depleted. When all glycerol is consumed by the cells, methanol utilization rates increase. These values on these figures apparently indicate that glycerol is a repressor of *AOX1* promoter, and it limits the expression of *AOX1* enzyme thus resulting inefficient utilization of methanol, as the results shown on the previous diagrams (Figure 4.26 and Figure 4.27).

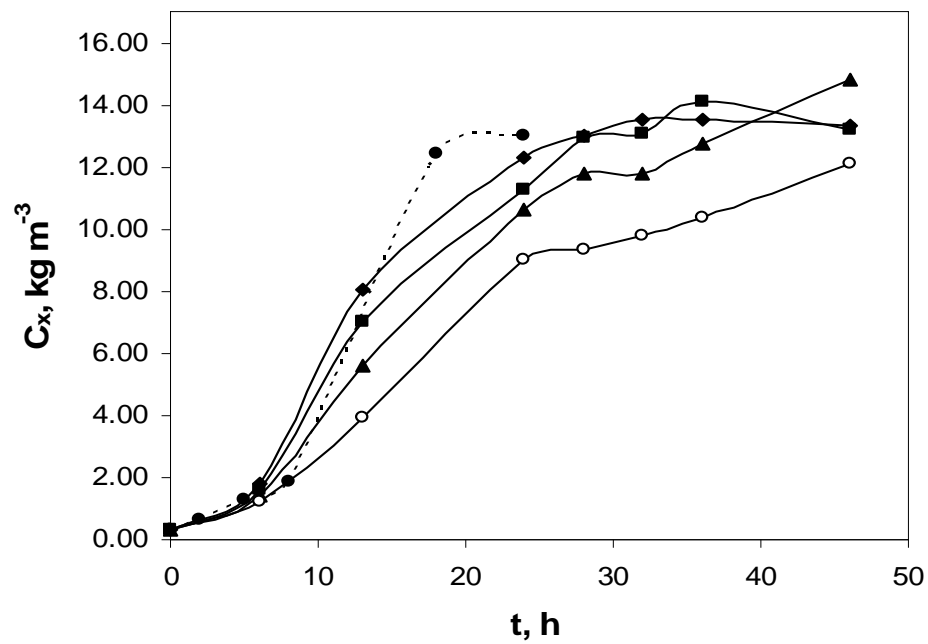


Figure 4.29 Effects of methanol concentrations on cell growth of *P. pastoris-hGH-Mut⁺* strain in defined mixed-batch medium containing glycerol at an initial concentration; 30 kg m⁻³ (solid lines). Dashed line indicates cell growth in media containing only 30 kg m⁻³ glycerol, initially, as sole carbon source. Initial methanol concentrations; 1% (◆), 2% (■), 3% (▲), 4%(○) (v/v) for solid lines.

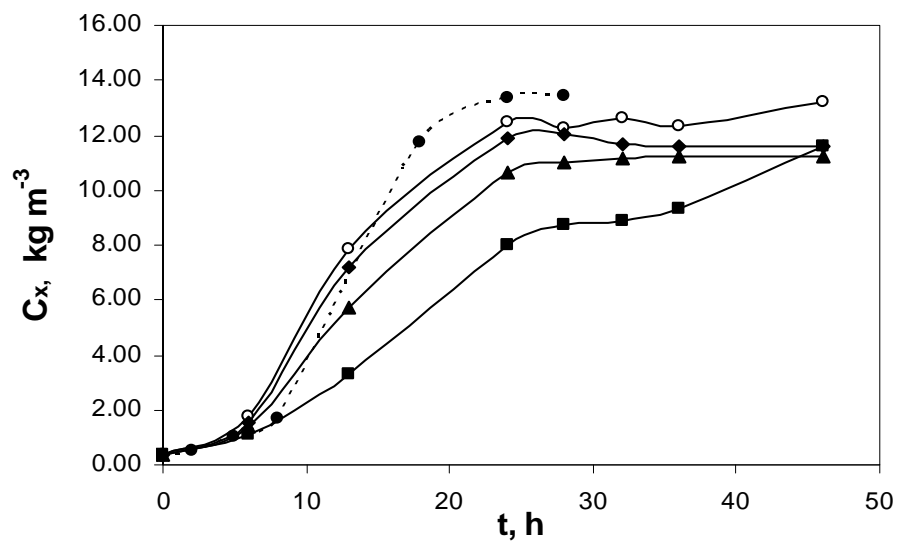


Figure 4.30 Effects of methanol concentrations on cell growth of *P. pastoris-hGH-Mut⁵* strain in defined mixed-batch medium containing glycerol at an initial concentration; 30 kg m⁻³ (solid lines). Dashed line indicates cell growth in media containing only 30 kg m⁻³ glycerol, initially, as sole carbon source. Initial methanol concentrations; 1%(○), 2% (◆), 3% (▲), 4%(■) (v/v) for solid lines.

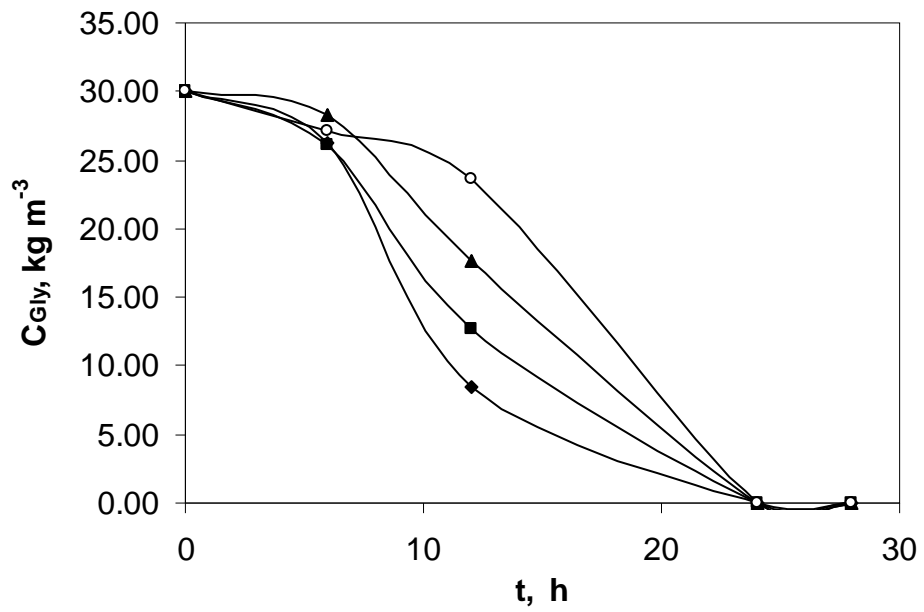


Figure 4.31 Glycerol utilization diagram of *P. pastoris-hGH-Mut⁺* strain in defined mixed-batch medium. Initial methanol concentrations; 1% (◆), 2% (■), 3% (▲), 4%(○) (v/v).

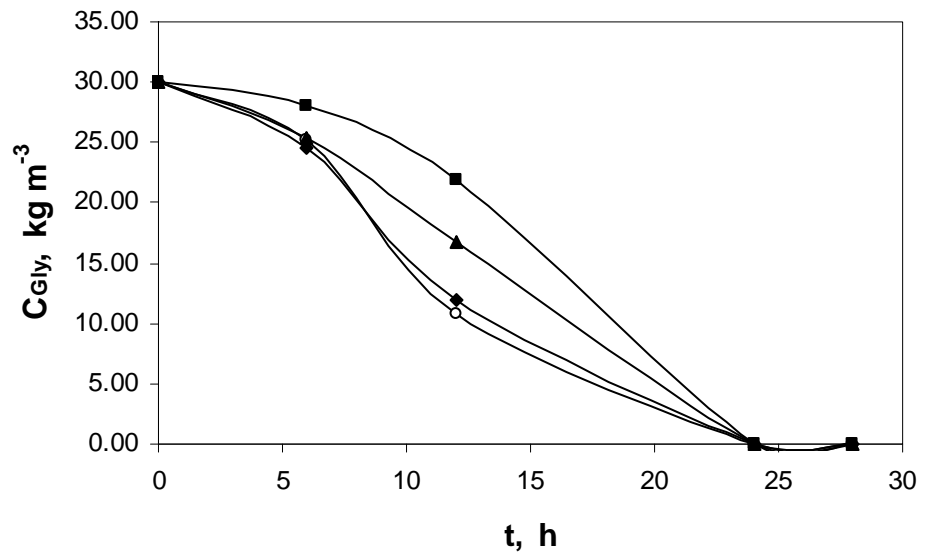


Figure 4.32 Glycerol utilization diagram of *P. pastoris-hGH-Mut^s* strain in defined mixed-batch medium. Initial methanol concentrations; 1 % (○), 2% (◆), 3% (▲), 4%(■) (v/v).

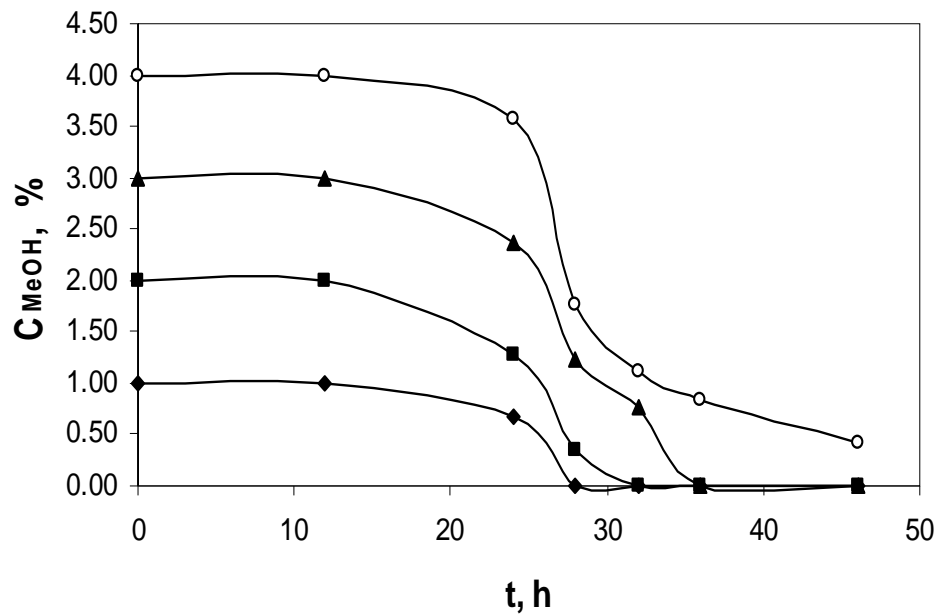


Figure 4.33 Methanol utilization diagram of *P. pastoris-hGH-Mut⁺* strain in defined mixed-batch medium. Initial methanol concentrations; 1% (♦), 2% (■), 3% (▲), 4%(○) (v/v).

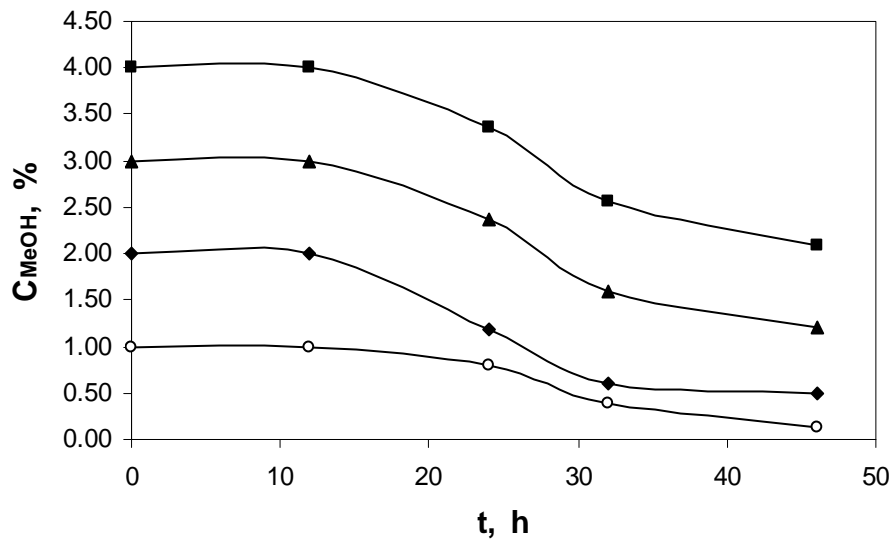


Figure 4.34 Methanol utilization diagram of *P. pastoris-hGH-Mut^S* strain in defined mixed-batch medium. Initial methanol concentrations; 1 % (○), 2% (♦), 3% (▲), 4%(■) (v/v).

The combined effect of glycerol and methanol in shaken flasks (batch system) on productivity and cell growth has not been previously reported. Most of the studies about the mixed substrate; glycerol/ methanol, were performed in fed-batch system (Brierley et al., 1990; Loewen et al., 1997; Jungo et al., 2007). Although, in mixed fed-batch system glycerol co-feeding ensures good cell growth and induction of heterologous protein expression continuous due to the existence of methanol, glycerol excess represses the *AOX1* promoter, which may result in lower specific productivities of recombinant protein (Thorpe et al., 1999 and Xie et al., 2005). Therefore researchers began to turn other carbon sources which do not repress the *AOX1* promoter (Sreekrishna et al., 1997; Thorpe et al., 1999; Inan and Meagher., 2001; Ramon et al., 2007). Ramon et al. (2007) tested the effect of sorbitol/methanol mixed substrates in batch and fed-batch cultures. They observed a different substrate consumption behavior on the host's phenotype (Mut^+ and Mut^s) in batch cultures. According their findings, when Mut^s strain was used, both substrates (sorbitol and methanol) were consumed simultaneously. This effect was not observed in Mut^+ phenotype, where two substrates were consumed sequentially. This is also observed in this study; Figures 4.25, 4.26, 4.33 and 4.34 indicate clearly that two substrates, methanol and glycerol were consumed sequentially.

Figure 4.35 illustrates SDS-page image of rhGH produced by *P. pastoris-hGH-Mut^s* (a) and *P. pastoris-hGH-Mut⁺* (b). Table 4.10 gives recombinant hGH concentrations and final cell densities of *P. pastoris-hGH-Mut⁺* and *P. pastoris-hGH-Mut^s* strains. According to SDS-page analysis, rhGH concentration in Mut^+ strain increases with respect to methanol concentration. On the other hand, Mut^s strain produces rhGH at high level when lower methanol concentration is used. These results are a little bit contradictory, that is, there is no analogy about the rhGH production between these two phenotypes. In defined medium, when methanol is used as a sole carbon source in batch system, it is clear that Mut^+ strain is more sensitive to methanol and production of rhGH increases when methanol concentration is rose, on the other hand, batch system containing only methanol is not appropriate for Mut^s phenotype because it grows on methanol slowly, thus it can not produce rhGH detectable. In the case of mixed-batch system, it is difficult to make a correlation between the methanol concentration and r-

protein production for these two phenotypes due to the complexity of the r-protein production in mixed-batch system. It is clear that glycerol concentration does not affect on rhGH production in mixed-batch system as vigorous as the methanol concentration does. Any change in methanol concentration results in drastic changes in rhGH production (Table 4.10). The different response of these two phenotypes to the methanol may be due to the methanol concentration present in cultivation medium. Mut⁺ strain can consume all methanol (Figure 4.33), which may eliminate the risk caused by undesirable methanol excess which plays important role on recombinant protein production. Furthermore, Mut⁺ strain can consume methanol in a long period when high initial methanol concentration was used as seen on Figure 4.33, which may cause expression of higher rhGH due to the long induction time. On the other hand, Mut^S strain can not use all methanol (Figure 4.34); therefore excess amount of methanol may reduce r-protein production.

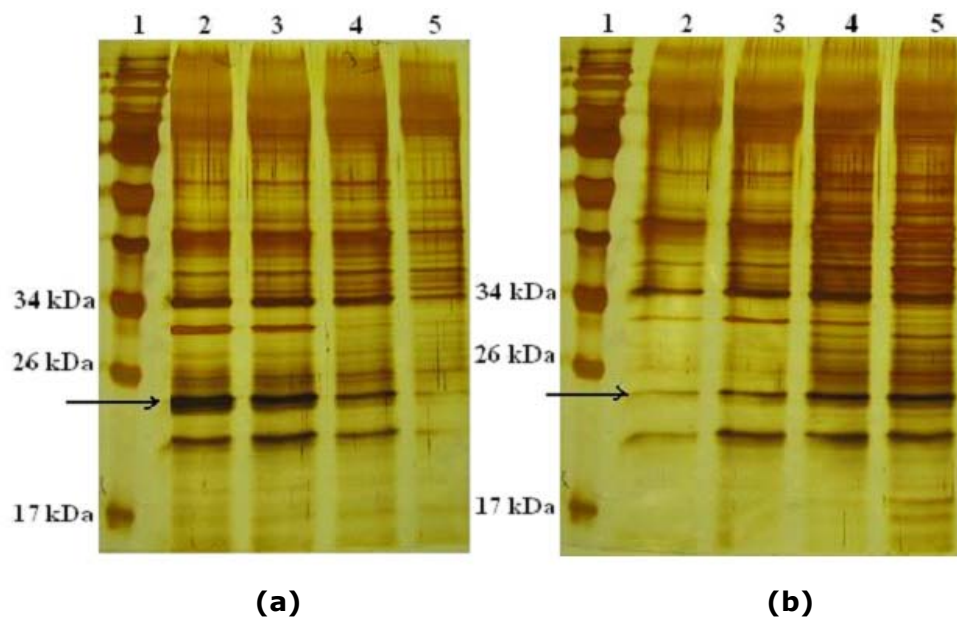


Figure 4.35 SDS-page image of rhGH produced by *P. pastoris-hGH-Mut^S* **(a)** and *P. pastoris-hGH-Mut⁺* **(b)**. Arrows and numbers (wells) indicate the place of rhGH and different production cultures, respectively. **(a)** 1. well: protein maker, 2. well: 1% (v/v) methanol, 3. well: 2% (v/v) methanol, 4. well: 3% (v/v) methanol, 5. well: 4% (v/v) methanol, **(b)** 1. well: protein maker, 2. well: 1% (v/v) methanol, 3. well: 2% (v/v) methanol, 4. well: 3% (v/v) methanol, 5. well: 4% (v/v) methanol (v/v).

Table 4.10 Recombinant hGH concentrations and final cell concentrations of *P. pastoris-hGH-Mut⁺* and *P. pastoris-hGH-Mut^s* strain.

C_{glycerol} (kg m⁻³)	C_{MeOH} (kg m⁻³)	<i>P. pastoris-hGH-Mut⁺</i>		<i>P. pastoris-hGH-Mut^s</i>	
		C_{hGH} (kg m⁻³)	C_x (kg m⁻³)	C_{hGH} (kg m⁻³)	C_x (kg m⁻³)
30	1.0 %	0.016	13.32	0.110	13.21
30	2.0 %	0.035	13.18	0.094	11.63
30	3.0 %	0.050	14.82	0.055	11.25
30	4.0 %	0.060	12.10	0.014	11.56

In conclusion, two main experimental steps were performed in this section 4.2; first most suitable microorganisms having high rhGH production capacity were chosen, and then, by using chosen microorganisms, Mut⁺ and Mut^s, the effects of methanol were investigated and compared in complex medium, in defined medium containing methanol as a sole carbon source and in mixed-carbon source medium containing methanol and glycerol at different ratio.

Due to the its rich components, higher rhGH production were obtained in BMMY complex medium when compared with the defined medium containing methanol as a sole carbon source and mixed-carbon source system. The highest rhGh concentration for both strains; Mut⁺ and Mut^s, was found as 0.052 kg m⁻³ and 0.16 kg m⁻³, respectively, at 2 %(v/v) methanol concentration in complex medium. In defined medium where methanol was used as a sole carbon source, cell density of Mut^s strain could not reach a value for the rhGH production due to the its reduced ability to use methanol, therefore detectable rhGH was not observed, on the other hand, optimum rhGH concentration produced by Mut⁺ strain was found as 0.032 kg m⁻³ at 3% (v/v) methanol concentration and in general, rhGH production increased when higher initial methanol concentration was used. In the case of mixed-batch system (glycerol/methanol) where the highest cell densities were obtained when compared with other media, it is difficult to make a correlation between the methanol concentration and r-protein production for these two phenotypes due to the complicated effect of mixed-carbon sources on the r-protein production. It is clear that glycerol concentration did not affect on rhGH production in mixed-batch system as vigorous as the methanol concentration

did. Any change in methanol concentration resulted in drastic changes in rhGH production. When the optimum glycerol concentration, 30 kg m^{-3} , was used, Mut^s produced the highest rhGH, 0.110 kg m^{-3} , at 1%(v/v) methanol concentration, on the other hand, Mut⁺ strain produced 0.060 kg m^{-3} rhGH at 4%(v/v) methanol concentration. Furthermore, both substrates were consumed sequentially by these two phenotypes and methanol consumption began when glycerol began to be depleted. When all glycerol was consumed by the cells, methanol utilization rates increased. This demonstrates that glycerol is a strong repressor of AOX1 promoter, and excess glycerol limits the expression of AOX1 enzyme thus resulting inefficient utilization of methanol. In addition to this, addition of methanol or increasing glycerol concentration (above 20 kg m^{-3} for Mut^s and 30 kg m^{-3} for Mut⁺) in mixed batch system inhibits the cell growth.

4.3 Expression of Human Growth Hormone in Recombinant *P. pastoris* in Pilot Scale Bioreactor

One of the main objectives of this study is to investigate the effect of oxygen transfer on cell growth and protein production in defined batch culture containing methanol as a sole carbon source and to study the fermentation and oxygen transfer characteristics of the bioprocess, in the pilot scale bioreactor. In this part of the research, the experiments were performed in the batch-bioreactor system consisted of temperature, pH, foam, air inlet and stirring rate controls. Due to the intrinsic characteristics of Mut^s phenotype, i.e. it has very low specific growth rate on methanol; the fermentations were performed only with *P. pastoris-hGH-Mut⁺* phenotype.

In section 4.12 effect of initial methanol concentration at different media (complex, defined containing only methanol and mixed-carbon source) on rhGH production were investigated. Although complex and mixed-carbon source media resulted in higher rhGH production, defined medium containing methanol as a sole carbon source was chosen for the pilot scale bioreactor experiment in order to analyze effects of methanol on metabolism of the cell, oxygen utilization, cell growth and bioreactor characteristics.

The Mut⁺ strain was first inoculated into precultivation medium and incubated at 30°C and $N=225 \text{ min}^{-1}$ for 24 h using baffled flasks 250 ml in size that had working volume capacities of 50 ml. Then, they were harvested by centrifugation at 4000 rpm, 10 min at room temperature and resuspended in sterile dH₂O. Thereafter, some of the resuspended cells were transferred to production medium containing 3% (v/v) (23.7 kg m⁻³) methanol in bioreactor so that initial cell concentration would become approximately 0.2 kg m⁻³. With $V_R = 1000 \text{ cm}^3$ working volume, pH and temperature were kept constant, respectively at pH=6.0 and $T=30 \text{ }^\circ\text{C}$. pH-control was carried out with 12.5% ammonium solution and 10% (v/v) phosphoric acid. Effects of oxygen transfer conditions on product and by-product formations and oxygen transfer characteristics were investigated at five different conditions with the parameters, air inlet rate of $Q_O/V_R = 0.5 \text{ vvm}$, and agitation rates of $N=250, 500, 625, 750 \text{ min}^{-1}$. Dissolved oxygen, pH, cell concentration, hGH volumetric concentrations, methanol concentration, organic acid concentrations, yield values, maintenance coefficients, overall mass transfer coefficients, specific growth rates and oxygen uptake rates were determined throughout the bioprocesses.

In order to determine the effects of cell concentration on oxygen transfer and fermentation characteristics, as well as on rhGH production and by-product formation, an impulse feeding strategy was also performed at the end of the fermentation process, the bioreactor operation conditions which were pH=6.0, $T=30 \text{ }^\circ\text{C}$, $Q_O/V_R = 0.5 \text{ vvm}$ and $N=625 \text{ min}^{-1}$. After consumption of all methanol, initial concentration of which was 3% (v/v) (23.7 kg m⁻³), some amount of methanol was added into production medium.

In aerobic processes, oxygen is a key substrate for cell growth and, therefore, continuous transfer of oxygen from the gas phase to liquid phase is crucial. Methanol is also a substrate with high oxygen demand for anabolic and catabolic purposes, and unlimited methanol supply can lead to sudden oxygen depletion (Katri and Hoffman, 2005). Methanol enters the methanol utilization pathway that is highly compartmentalized in methanol-induced micro-organelles; the peroxisomes, and is oxidized to hydrogen peroxide and formaldehyde by alcohol oxygenase (section 2.3.1.1). Therefore, dissolved oxygen should be maintained at a required level throughout methanol utilization metabolism, because in addition to the oxygen demand associated

with the cellular electron transport, alcohol oxygenase requires molecular oxygen as a substrate (Lee et al., 2003).

It is generally known that oxygen limitation negatively affects the expression of foreign genes (Cereghino and Cregg, 2000), and the dissolved oxygen (DO) concentration is a critical parameter for high cell density cultivation (Cunha et al., 2004) since most of the studies rely on fed batch system. The importance of oxygen affecting the cell growth and productivity makes the cultivation strategies about the oxygen transfer attractive (Katri and Hoffman, 2005).

4.3.1 Oxygen Transfer Effects in Batch Fermentation System

4.3.1.1 Dissolved Oxygen Profiles

The variations in the dissolved oxygen concentration (C_{DO}) with the cultivation time, and the agitation rate applied are illustrated in Figures 4.36. Solubility of oxygen, $C_{O_2}^*$ in cultivation medium at 30°C was determined as 0.22 mol m⁻³.

C_{DO} depends on the extent of the oxygen transfer rate to the media and the oxygen uptake rate of the cells. It varied with the cultivation time depending on the growth status of the cells (Çalık et al., 2000). At all oxygen transfer conditions illustrated on Figure 4.36, between $t \sim 20$ and $t \sim 36$ h a generous decrease due to the rapid uptake of dissolved oxygen by the microorganism was observed in the dissolved oxygen concentration profiles but at different rates depending on the amount of oxygen transferred to the medium and amount of oxygen demanded by the microorganism. The lowest dissolved oxygen concentrations were obtained as 0.10 and 0.08 mol m⁻³ at $N=750$ and 625 min^{-1} conditions, respectively, and almost zero at $N=500 \text{ min}^{-1}$ condition at $t=38-41$ h. Then, dissolved oxygen concentration suddenly increased in general at the end of the bioprocesses of $N= 500, 625$ and 750 min^{-1} conditions. On the other hand it was below 10 % (0.022 mol m⁻³) of the saturation dissolved oxygen at "limited oxygen transfer condition" ($N= 250 \text{ min}^{-1}$) throughout the process.

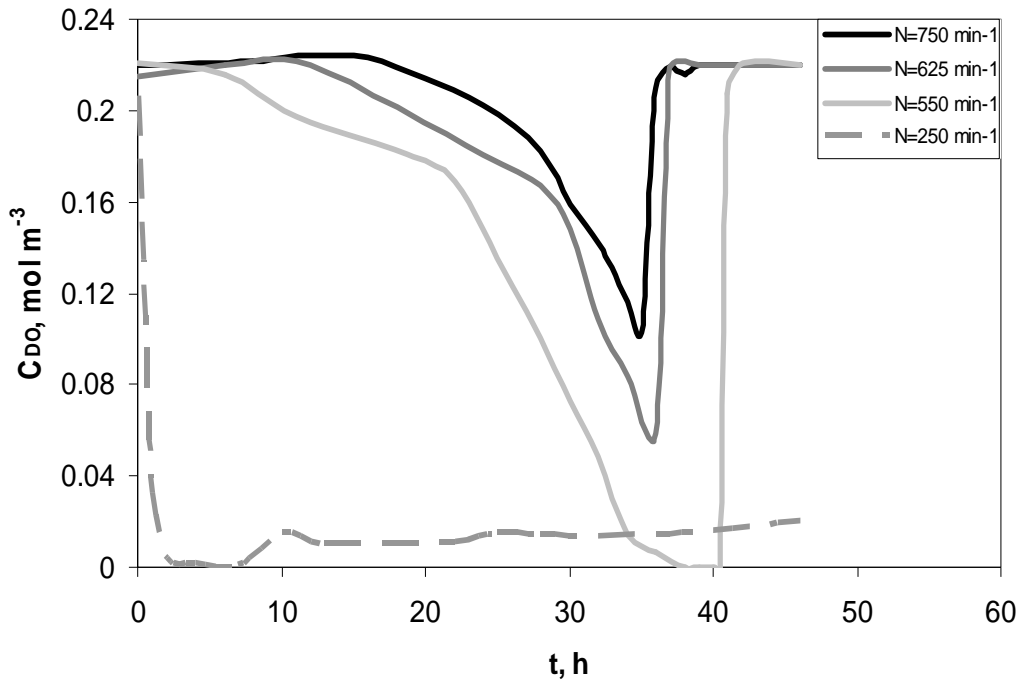


Figure 4.36 The variations in the dissolved oxygen concentration with the cultivation time, and agitation applied. $T=30^{\circ}\text{C}$, $\text{pH}=6.0$, $V_R=1000\text{ cm}^3$: $N=250, 500, 625$ and 750 min^{-1} .

4.3.1.2 Cell Growth Profiles

The variations in the cell concentration with cultivation time and the agitation rate are given in Figure 4.37.

Until $t=20\text{ h}$, the cell formation did not change significantly with respect to the oxygen transfer conditions applied due to the long lag phase. This is most probably due to the low expression level or activity of AOX1 during the lag phase where physicochemical equilibration between the organism and the environment following inoculation occurs with very little growth, and/or higher initial methanol concentration may result in some loss of AOX1 activity (Jahic et al., 2006) until required amount of AOX1 is expressed and methanol concentration begins to decrease. Furthermore, it is also obvious that decrease in agitation rate, i.e. lower oxygen transfer condition, resulted in long lag phase and at lowest agitation rate (250 min^{-1}), it is obvious that oxygen concentration in the fermentation broth was not enough for the catabolic and anabolic reactions taking place in the cells.

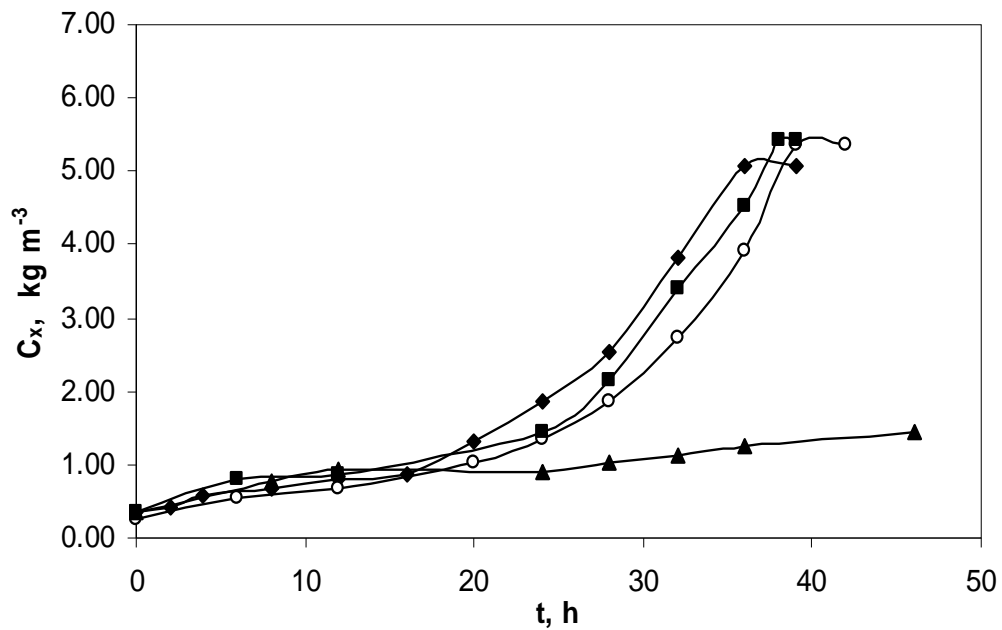


Figure 4.37 The variations in cell concentration with the cultivation time, and agitation applied. $T=37^{\circ}\text{C}$, $\text{pH}= 6.0$, $V_{\text{R}}= 1000 \text{ cm}^3$: $N=250 \text{ min}^{-1}$ (▲), $N=500 \text{ min}^{-1}$ (○), $N=625 \text{ min}^{-1}$ (■), $N=750 \text{ min}^{-1}$ (◆).

After $t=20 \text{ h}$ cell concentration began to increase and cell growth at all conditions reached to stationary phase after $t=39\text{-}40 \text{ h}$ when cell formation rate decreased (Figure 4.37). Although cell concentrations at agitation rate above 500 min^{-1} do not change significantly, the highest cell concentration with a value of $C_{\text{X}}=5.5 \text{ kg m}^{-3}$ was obtained at $N=625 \text{ min}^{-1}$ which is lower than the cell concentration of 7.39 kg m^{-3} obtained at laboratory scale bioreactor with working volume of 50 cm^3 . The lowest cell concentration, $C_{\text{X}}=1.66 \text{ kg m}^{-3}$, was observed at $N=250 \text{ min}^{-1}$ among the investigated oxygen transfer conditions. At this condition, oxygen supply seems to be insufficient for maintenance of oxidative metabolism resulted in a lower cell growth.

The variation of cell concentration with the cultivation time should be related to the dissolved oxygen concentration of the fermentation broth. In a typical batch culture, the dissolved oxygen concentration decreases in the media along with the growth period, until the microorganism reaches the stationary phase and then the dissolved oxygen concentration increases. This decreasing and increasing pattern in dissolved oxygen concentration with respect to cell growth can be seen well on Figures 4.36 and 4.37.

There is no detailed study about the heterologous protein production by *P. pastoris* in defined medium containing methanol as a sole carbon source. Cos et al. (2005b) carried out a comparative study of the heterologous protein expression in batch and high cell density fed-batch bioreactor cultivation. Although they used different bioprocess operation conditions, their investigation about the protein activity in batch bioreactor performed with Mut⁺ phenotype demonstrates that after 49 h of cultivation, overall biomass yield coefficient is obtained as $Y_{x/s}=0.27$ kg cell kg⁻¹ substrate when approximately 10 kg m⁻³ methanol is consumed, which is actually within the same range, $Y_{x/s}=0.23$ kg cell kg⁻¹ substrate, obtained in this study at the same cultivation time. In their study, higher reproducibility than in shake flask cultures has been achieved most probably due to the controlled operational condition; stirring rate 800 min⁻¹, temperature 30 °C, pH controlled at 5.5, dissolved oxygen controlled above 30% with an air flow rate between 1.5 and 20 L min⁻¹.

4.3.1.3 Methanol Concentration Profiles

The variations in the methanol concentration with cultivation time and agitation rate are given in Figure 4.38.

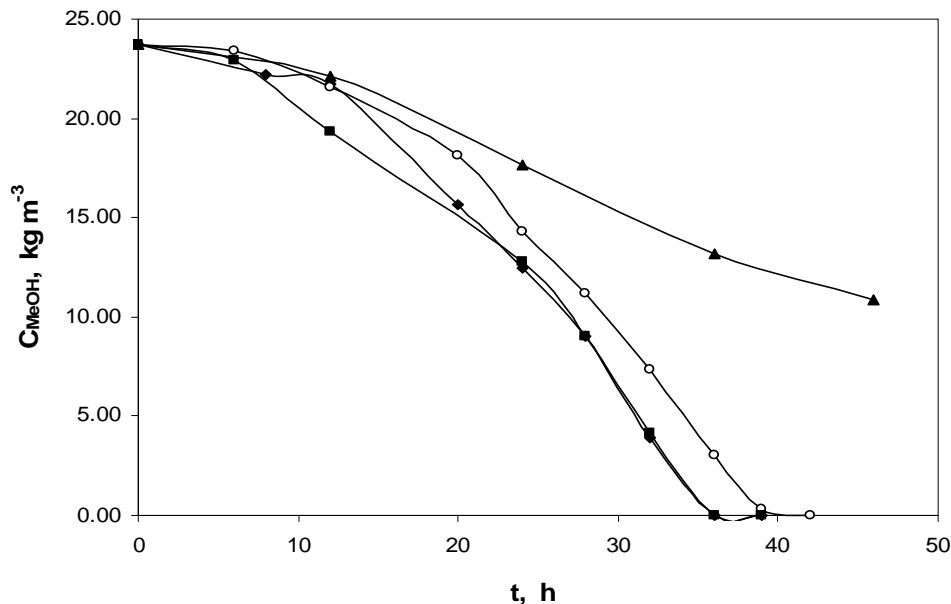


Figure 4.38 The variations in methanol concentration with the cultivation time, agitation and air inlet rates applied. T=37°C, pH= 6.0, V_R= 1000 cm³: N=250 min⁻¹ (▲), N=500 min⁻¹ (○), N=625 min⁻¹ (■), N=750 min⁻¹ (◆).

At $t=0-20$ h of the bioprocess, methanol concentration values were decreased slowly at all the conditions applied due to the lag phase where microbial growth is slow. Thereafter, rapid methanol consumption at all the conditions except, $N=250 \text{ rpm}^{-1}$, was observed in the log phase where the microbial growth rates were higher and all methanol was exhausted at $t= 36-40$ h (Figure 4.38).

Methanol concentration profiles coincide with the cell growth and DO profiles at all the conditions. Due to the long lag phases, $t=0-20$ h, where cells do not consume methanol very much, slow decreases in DO level for all bioprocesses except the one having "limited oxygen transfer condition" ($N=250 \text{ min}^{-1}$) were observed, as it was expected. When methanol utilization rate increased, dissolved oxygen concentration rate decreased rapidly and sudden rise in C_{DO} was observed when the entire methanol was consumed. This indicates that there is a strong relationship between the methanol utilization and dissolved oxygen concentration, i.e. methanol is a substrate with high oxygen demand. Furthermore, at higher methanol utilization rates, higher cell growth rates were obtained. On the other hand, when methanol was totally exhausted, no further cell growth was observed.

4.3.1.4 rhGH Concentration Profiles

Recombinant hGH concentration profiles with cultivation time and agitation rate are illustrated on Figure 4.39. The rhGH concentrations were determined according to relative intensity of the bands on SDS-page (Appendix F) as explained in section 3.6.4.

The highest rhGH volumetric density was obtained as 0.023 kg m^{-3} at $N=500 \text{ min}^{-1}$, and the lowest rhGH volumetric density was obtained at $N=250 \text{ min}^{-1}$ as 0.012 kg m^{-3} among the investigated oxygen transfer conditions at the end of the process (Figure 4.39). The highest rhGH concentration was found when all methanol in fermentation medium was completely consumed by the cells and after the complete depletion of methanol, degradation of rhGH was observed due to the proteolysis taking place in long cultivation.

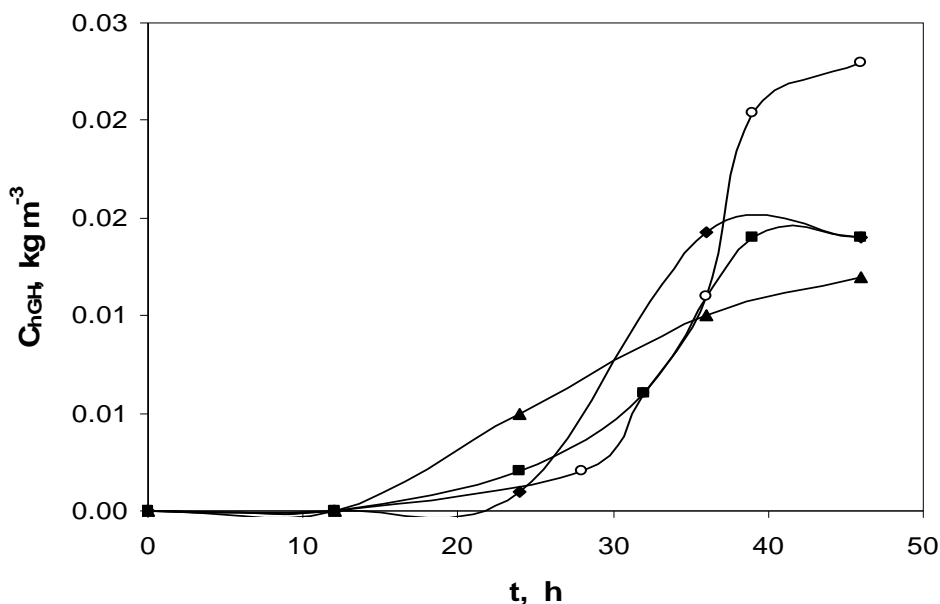


Figure 4.39 The variations in rhGH concentration with the cultivation time, agitation and air inlet rates applied. $T=37^{\circ}\text{C}$, $\text{pH}= 6.0$, $V_{\text{R}}= 1000 \text{ cm}^3$: $N=250 \text{ min}^{-1}$ (▲), $N=500 \text{ min}^{-1}$ (○), $N=625 \text{ min}^{-1}$ (■), $N=750 \text{ min}^{-1}$ (◆).

Agitation rate influences the oxygen transfer rate, and consequently dissolved oxygen concentration, cell growth and methanol utilization profiles. Because in addition to the oxygen demand associated with the cellular electron transport, alcohol oxygenase requires molecular oxygen as a substrate, therefore, dissolved oxygen level plays important role throughout methanol utilization metabolism. Furthermore, dissolved oxygen affects the metabolic pathways taking place in microorganisms and by product and product formations. Although, final cell concentrations do not change very much at three oxygen transfer conditions ($N=500$, 625 and 750 min^{-1}), it is obvious that oxygen transfer conditions affect the methanol utilization pathways, and cell growth rate (Figure 4.37 and Figure 4.38). Among these three conditions, at $N=500 \text{ min}^{-1}$ where methanol utilization rates are lower, the highest production capacity was obtained most probably oxygen condition affects the metabolic pathways, thus increases product formation, and slower methanol utilization rate may raise the induction time.

It was also observed that rhGH production generally began after $t=24 \text{ h}$ when cell densities began to increase. No detailed studies about the recombinant protein expression in defined batch bioreactor are found in literature. Since *P. pastoris* can express r-protein at high level (Cereghino et

al., 2002), it is possible to obtain r-protein in grams per liter of fermentation broth in fed-batch system with long induction time.

Recombinant hGH concentrations, final cell density and overall yield coefficients of bioreactors were given in Table 4.11. The highest product yields on substrate and cell were obtained as 0.00097 kg hGH kg⁻¹ methanol and 0.0072 kg hGH kg⁻¹ cell at N=500 min⁻¹ and N=250 min⁻¹ conditions, respectively. Trevino et al. (2000) was the first group who intended to produce and secrete mature and biologically active rhGH from *P. pastoris* cultivated in laboratory scale bioreactor with fed-batch system. After 48 h induction with methanol, they obtained 73 kg dry weight m⁻³ cell density and 0.049 kg m⁻³ secreted rhGH. The overall product yield with respect to biomass concentration in the study of this group; 0.00067 kg hGH kg⁻¹ cell, was lower than those obtained in this study (Table 4.11).

According to Table 4.11, interestingly high overall product yields were obtained at N=250 min⁻¹; Y_{p/x}= 0.0072 kg hGH kg⁻¹ methanol, Y_{p/s}=0.00093 kg hGH kg⁻¹ biomass, although its cell density reached lower values. According to results obtained, it can be roughly concluded that at lower oxygen limited conditions higher product yields were obtained and decrease in agitation rate increased the production capacity. Oxygen effect on r-protein production causes some contradictory results and no correlation is obtained in literature. While avoiding oxygen limitation has been given priority, successful protein production has also been achieved under oxygen-depleted conditions (Hellwig et al., 2001). Oxygen-limited cultivation can, compared to methanol limitation, reduce product modifications (Trentmann et al., 2004) or increase the specific product purity relative to the amount of total protein released to the medium (Charoenrat et al., 2005).

Table 4.11 Recombinant hGH concentrations, final cell concentrations and overall yield coefficients of bioreactors.

Bioreactor N (min ⁻¹)	Methanol used(kg m ⁻³)	C _x (kg m ⁻³)	C _{hGH} (kg m ⁻³)	Y _{x/s} (kg kg ⁻¹)	Y _{p/x} (kg kg ⁻¹)	Y _{p/s} (kg kg ⁻¹)
750	23.7	5.08	0.014	0.214	0.0027	0.00059
500	23.7	5.37	0.023	0.227	0.0043	0.00097
250	12.8	1.66	0.012	0.130	0.0072	0.00093
625	23.7	5.44	0.014	0.229	0.0026	0.00059

4.3.1.5 Formaldehyde, Organic and Amino Acid Concentration Profiles

The variations in the organic acids and amino acids detected in the fermentation broth with cultivation time and oxygen transfer conditions were demonstrated in Tables 4.12 and 4.13. Most microorganisms have the metabolic machinery to synthesize all essential amino acids from carbon and nitrogen sources for the production of proteins. Formic acid and fumaric acid are the organic acids; aspartic acid, lysine, proline, treonin and leucine are the amino acids that were detected in the medium.

Methanol concentration in fermentation broth plays important role for cell viability. *P. pastoris* strains can not tolerate high methanol concentration due to the accumulation of formaldehyde and hydrogen peroxide inside the cells, both of which are the oxidized products of methanol by AOX and are toxic to the cell (Zhang et al., 2000). Both oxygen and methanol concentrations in *Pichia* processes affecting the cell growth and product formation may theoretically result in elevated formaldehyde concentrations in the cell if they generate an imbalance between the initial oxidation of methanol and the formaldehyde consuming reactions in anabolism and catabolism (Charoenrat et al., 2006). Figure 4.40 depicts formaldehyde concentration profiles of all cultivation media. Theoretically, oxygen limitation in *Pichia* processes may result in elevated formaldehyde concentrations in the cell (Charoenrat et al., 2006). As seen on figure 4.43 lowest formaldehyde concentration was obtained at $N=750 \text{ min}^{-1}$, although, accumulation of formaldehyde generally increases when agitation rate decreases, which causes oxygen limitation in fermentation processes. Since formaldehyde is the product of AOX and used as a substrate for energy and biomass formation, consumption of formaldehyde was observed in cultivation conditions at $N=500, 625$ and 750 min^{-1} . On the other hand, continuous accumulation of formaldehyde in fermentation medium at $N=250 \text{ min}^{-1}$ was seen, as it was expected. The highest formaldehyde concentrations were obtained at approximately $t=30$ and 45 h , where methanol utilization rates were higher. This figure clearly explains that at exponential growth phase, AOX1 enzyme production level was so high that formation rate of formaldehyde was greater than consumption rate of this substrate, thus accumulation of formaldehyde began to rise. Towards the end of the processes, cells started to use formaldehyde as substrate.

Table 4.12 The variations in organic acid concentrations with cultivation time and oxygen transfer conditions.

BIOREACTOR 1, N=750 rpm						
Time (h)	0	12	24	28	32	36 39
Formic acid (kg m ⁻³)	-	-	0.0091	0.0064	0.0032	- -
Fumaric acid(kg m ⁻³)	-	-	0.0017	0.0046	0.0050	0.0079 0.0064
BIOREACTOR 2, N=500 rpm						
Time (h)	0	12	24	28	32	36 39
Formic acid (kg m ⁻³)	-	0.0030	0.0144	0.0108	0.0063	0.0044 -
Fumaric acid(kg m ⁻³)	-	-	0.0013	0.0023	0.0041	0.0060 0.0046
BIOREACTOR 3, N=250 rpm						
Time (h)	0	12	24	36	46	
Formic acid (kg m ⁻³)	-	0.0020	0.0025	0.0022	0.0054	
Fumaric acid(kg m ⁻³)	-	-	-	-	0.0070	
BIOREACTOR 4, N=625 rpm						
Time (h)	0	12	24	28	32	36 39
Formic acid (kg m ⁻³)	-	0.0186	0.0128	0.0088	0.0052	0.0021 -
Fumaric acid(kg m ⁻³)	-	0.0097	0.0186	0.0251	0.0328	0.0405 0.0428

Table 4.13 The variations in amino acid concentrations with cultivation time and oxygen transfer conditions.

BIOREACTOR 1, N= 750 rpm					
Time (h)	0	12	24	32	36
Aspartic acid(kg m ⁻³)	-	-	0.109	0.057	0.121
Lysine (kg m ⁻³)	-	-	0.011	0.046	0.078
BIOREACTOR 2, N=500 rpm					
Time (h)	0	12	24	32	39
Aspartic acid(kg m ⁻³)	-	0.057	0.049	0.101	0.108
Lysine (kg m ⁻³)	-	-	0.007	0.045	0.071
BIOREACTOR 3, N=250 rpm					
Time (h)	0	12	24	46	
Aspartic acid(kg m ⁻³)	-	0.023	0.055	0.042	
BIOREACTOR 4, N=625 rpm					
Time (h)	0	12	24	32	39
Aspartic acid(kg m ⁻³)	-	0.040	0.007	0.118	0.124
Lysine (kg m ⁻³)	-	0.0071	0.013	0.053	0.100
Leucine (kg m ⁻³)	-	-	0.013	-	-

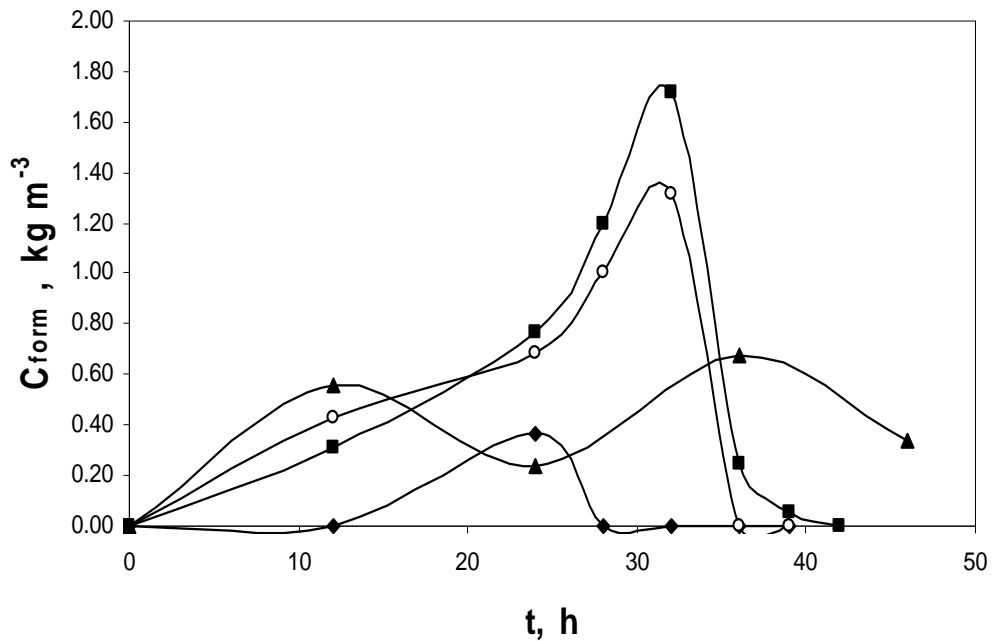


Figure 4.40 The variations in formaldehyde concentration with the cultivation time, agitation and air inlet rates applied. $T=37^{\circ}\text{C}$, $\text{pH}=6.0$, $V_R=1000\text{ cm}^3$: $N=250\text{ min}^{-1}$ (▲), $N=500\text{ min}^{-1}$ (○), $N=625\text{ min}^{-1}$ (■), $N=750\text{ min}^{-1}$ (◆).

The enzyme alcohol oxidase (AOX) catalyzes the first step in the methanol utilization pathway, converts the methanol to formaldehyde and hydrogen peroxide. Some portion of formaldehyde is converted to cell materials and some leaves peroxisome and is further oxidized to formate (formic acid) and carbon dioxide, which is a source of energy. On Table 4.12 it is clear that formic acid was generally produced and secreted to the medium until $t=24\text{ h}$ and then most probably entered the carbon metabolism and began to be consumed by the cell towards the end of the processes at $N=500, 625$ and 750 min^{-1} conditions. One of the reasons why higher formate concentration was obtained throughout the lag phase may be most of the formaldehyde was converted to formate and carbon dioxide for energy. Since slow growth was observed in this phase, inconsiderable amount of formate was used. On the other hand, in growth phase (log phase) cell began to use formate and in this phase formation of formate rate was slower than the consumption rate. In the case of limited oxygen condition ($N=250\text{ min}^{-1}$), a continuous formate production was observed since most of the formaldehyde may be converted to formate instead of cell materials, which may also resulted

in slow cell growth rate. Mutually, slow cell growth also affects the consumption of fumaric acid.

4.3.1.6 Oxygen Transfer Characteristics

The Dynamic Method was applied to find the oxygen transfer parameters which are oxygen uptake rate (OUR), r_0 , and oxygen transfer coefficient, K_La . At $t < 0$ h, the physical oxygen transfer coefficient K_{La_0} was measured in the medium in the absence of the microorganism. The variations in K_La , oxygen uptake rate, the enhancement factor $E (=K_{La}/K_{La_0})$, oxygen uptake rate (OUR), oxygen transfer rate (OTR), maximum oxygen utilization rate (OD), Damköhler number (Da) and effectiveness factor (η) throughout the bioprocesses are given in Table 4.14.

All calculations were performed according to data obtained in log phase ($t=20-42$ h) where maximum growth rate was observed. Since very low cell growth in lag phase ($t=0-20$ h) and no cell growth at the end of the bioprocesses, maximum oxygen utilization rates, Damköhler numbers (Da) and effectiveness factors could not be calculated.

Volumetric mass transfer coefficient, K_La , a physical parameter, depends on operational conditions such as geometrical parameters of the bioreactor, medium properties, and the presence of microorganism. The K_La coefficients were obtained almost the same throughout out the lag phase ($t=0-20$ h) because very slow cell growth and small change in medium were obtained at all conditions (Table 4.14). The calculated K_La values at $t=0-20$ h are 0.048, 0.022 and 0.015 h^{-1} at $N=750$, 625 and 500 min^{-1} conditions, respectively. With an increase in cell concentration with respect to time, K_La values, first, tend to increase and then decrease (Figure 4.41). Any increase in cell concentration actually results in resistance to mass transfer, on the other hand higher cell concentration causes higher oxygen uptake rate, which affects the volumetric mass transfer coefficient positively. Mutual effect of these two parameters (mass transfer resistance and OUR) determines the inclination of K_La properties throughout the fermentation process.

Table 4.14 The variations in oxygen transfer parameters with oxygen transfer conditions.

N min ⁻¹	t (h)	k _L a (s ⁻¹)	E k _L a/k _L a ₀	OTR×10 ³ (molm ⁻³ s ⁻¹)	OTR _{max} ×10 ³ (molm ⁻³ s ⁻¹)	OUR×10 ³ (molm ⁻³ s ⁻¹)	OD×10 ³ (molm ⁻³ s ⁻¹)	Da OD/OTR _{mx}	η OUR/OD
750	<0	0.018	-	-	-	-	-	-	-
	≥0	0.048	2.87	0.60	10.5	0.60	-	-	-
	20	0.048	2.87	0.29	10.5	1.70	1.68	0.16	1.00
	24	0.050	3.00	0.88	11.0	1.80	2.42	0.22	0.75
	28	0.050	3.00	1.91	11.0	2.10	2.40	0.22	0.87
	32	0.051	3.04	3.95	11.2	2.30	2.62	0.23	0.87
	36	0.040	2.40	0.70	8.8	0.70	2.20	0.25	0.32
	39	0.038	2.28	0.40	8.4	0.40	-	-	-
625	<0	0.016	-	-	-	-	-	-	-
	≥0	0.022	1.42	0.60	4.87	0.60	-	-	-
	20	0.022	1.43	0.25	4.93	1.50	1.48	0.30	1.00
	24	0.023	1.44	0.73	4.95	1.60	1.71	0.34	0.94
	28	0.026	1.64	1.12	5.65	1.80	2.00	0.35	0.89
	32	0.035	2.27	3.53	7.78	1.70	1.98	0.25	0.85
	36	0.030	1.95	4.51	6.68	1.30	1.87	0.28	0.69
	39	0.021	1.31	0.50	4.51	0.5	-	-	-
500	<0	0.013	-	-	-	-	-	-	-
	≥0	0.015	1.17	0.60	3.27	0.60	-	-	-
	20	0.015	1.17	0.63	3.27	1.60	1.59	0.48	1.00
	24	0.033	2.65	2.4	7.42	1.60	1.94	0.26	0.82
	28	0.023	1.85	2.8	5.17	1.50	1.95	0.37	0.76
	32	0.021	1.65	3.6	4.62	1.10	1.53	0.33	0.72
	42	0.017	1.34	0.40	3.76	0.40	-	-	-

As mentioned above, very small change in cell growth and medium did not affect the K_{La} values. Since K_{La} properties were calculated by using dynamic method which is explained in section 2.3.4 with details, it was difficult to find these properties at $t > 0$ h at $N = 250 \text{ min}^{-1}$ oxygen transfer condition due to the rapid decline in oxygen concentration after $t = 0$ h. But, it is reasonable to assume that throughout out the process the K_{La} values were not changing and equaled to 0.003 h^{-1} found at $t = 0$ h because of no drastic change in operational conditions such as medium properties, and the presence of microorganism.

Furthermore, from the figure 4.41 it can be easily seen that agitation rate affects the K_{La} properties. K_{La} values increased with the increase in agitation rate and the time of maximum K_{La} values obtained had a tendency of declining when agitation rate decreased. This effect attributed to the rapid breakage of the bubbles into smaller size with an increase in the impeller speed and enhancement in the gas-liquid interfacial area available for mass transfer. As a result, stirring rate can be considered as one of the major parameter altering K_{La} .

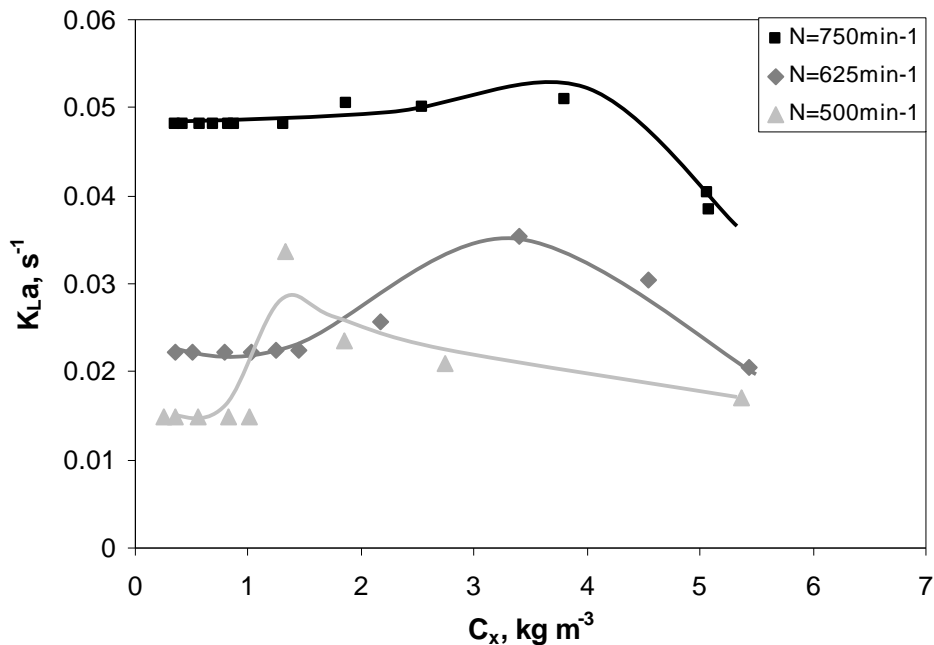


Figure 4.41 The trend of K_{La} profiles with cell concentration and stirring rate, $T = 30^\circ\text{C}$, $V_R = 1000 \text{ cm}^3$, $Q_0/V_R = 0.5 \text{ vvm}$, $N = 500, 625 \text{ and } 750 \text{ min}^{-1}$, $\text{pH}_c = 6.0$.

At $t < 0$ h, the physical oxygen transfer coefficient K_{La_0} was measured in the medium in the absence of the microorganism, and the enhancement factors $E = K_{La}/K_{La_0}$ were calculated throughout the bioprocess at different oxygen transfer conditions. K_{La_0} values increased with oxygen transfer conditions as expected. They were found as 0.017, 0.016, 0.013 and 0.0026 h^{-1} at $N=750, 625, 500,$ and 250 min^{-1} , respectively. Since the enhancement factors were obtained from the ratio between K_{La} and K_{La_0} , the same increasing and decreasing trend as K_{La} values was observed. Enhancement factor changes between 1.17-3.04 (Table 4.14). The low E values obtained shows that slow reaction is accompanied with mass transfer, as expected in most of the fermentation processes accomplished in stirred bioreactors. Since it was assumed that K_{La} values did not change throughout the process at $N=250 \text{ min}^{-1}$ oxygen transfer condition, E factor was assumed to be constant consequently during the fermentation process and it was obtained as 1.134.

Table 4.14 and Figure 4.42 show the change of OUR with cultivation time and cell concentration, respectively. OUR actually depends on the growth phases of the microorganisms. Firstly, increases during the lag phase and exponential phases of the microbial growth and takes a maximum at the exponential phase as it is the case in this analysis. OUR takes its maximum value at between $t=20 \text{ h}$ and $t=32 \text{ h}$ of the bioprocess. The highest OUR values were obtained as 0.0023, 0.0018, and 0.0016 $\text{mol m}^{-3}\text{s}^{-1}$ at $N=750, 625$ and 500 min^{-1} oxygen transfer conditions. From the cell growth profiles (Figure 4.37), it is clear that growth rates are decreasing proportionally with respect to agitation rates at exponential phase although final cell concentration is not directly proportional to agitation rate. Higher cell growth rate at $N=750 \text{ min}^{-1}$ resulted in higher OUR. The lowest OUR values were obtained at the beginning and at the end of the bioprocesses changing between 0.0004 and 0.0006 $\text{mol m}^{-3}\text{s}^{-1}$ where lower cell growth was observed. In the case of $N=250 \text{ min}^{-1}$ oxygen transfer conditions, it is difficult to obtain OUR values by using dynamic method due to the rapid decrease in dissolved oxygen concentration at the very beginning of the processes. The calculated OUR at $t=0 \text{ h}$ at this condition is 0.0005 $\text{mol m}^{-3}\text{s}^{-1}$ and again assumed to be constant throughout the bioprocess because no drastic change in cultivation medium and conditions was occurred.

Besides the OUR, the variation of OTR with cell concentration is given in Figure 4.53 and its variation with cultivation time is shown on Table 4.14. Oxygen transfer rates were calculated from the volumetric mass transfer coefficients obtained from experimental data and difference between the saturated oxygen concentration and dissolved oxygen concentration in fermentation medium. According to Figure 4.36, it is clear that at the beginning of the fermentation process, i.e. throughout the lag phase, and at the end of fermentation where no cell growth was observed, dissolved oxygen concentration was at its saturated level (0.22 mol m^{-3}), i.e. there was almost no change in oxygen concentration with respect to time, therefore OTR was equal to OUR. With an increase in cell growth, OTR began to increase and then decreased sharply, which is expected because OTR is directly proportional to K_{La} and $(C_{DO}^* - C_{DO})$ and these values increased firstly and then decreased with respect to time and cell concentration at $N=500$, 625 and 750 min^{-1} conditions. The highest OTR values are 0.0036 , 0.00451 and $0.00395 \text{ mol m}^{-3} \text{ s}^{-1}$ at $N=500$, 625 and 750 min^{-1} conditions, respectively. Among the three different agitation rates, the highest OTR was obtained at $N=625 \text{ min}^{-1}$ oxygen transfer condition, although volumetric mass transfer coefficients at $N=750 \text{ min}^{-1}$ were higher than those found at other conditions. On the other hand, driving force, i.e. difference between the saturated and dissolved oxygen concentrations, increased reversely with agitation rate. The interaction of these inverse values (K_{La} and $[C_{DO}^* - C_{DO}]$) resulted in highest OTR at $N=625 \text{ min}^{-1}$ condition. Since K_{La} values were assumed to be constant throughout the fermentation process at $N=250 \text{ min}^{-1}$, OTR values were also calculated. At this fermentation process, DO level was below 10% of saturated DO and almost constant. This resulted in nearly constant OTR which was approximately $0.0006 \text{ mol m}^{-3} \text{ s}^{-1}$.

To express the oxygen limitation in an aerobic process, Damköhler (Da) number is defined. Da is a dimensionless number, which relates maximum oxygen uptake and maximum transfer rates. It is clear that Da is less than 1 and does not change very much through the bioprocess (Table 4.14 and Figure 4.44), which means that biochemical reaction limitations are effective. From the Figure 4.36, it is clear that oxygen utilization rates began to increase when methanol utilization rates increased, which indicates high oxygen demand in methanol utilization pathways; but, this does not mean that maximum possible oxygen utilization rate by the cells should be high. Biomass yields on

oxygen consumed and specific growth rates (Section 4.3.1.7) obtained show that oxygen demand (OD), i.e. maximum possible oxygen utilization rate by the cells, is low and does not change very much with respect to cultivation time and microbial growth (Table 4.4). Since Da is a function of OD, Da values obtained throughout the processes are very low and vary between 0.16-0.48. In the case of limited oxygen transfer condition, $N=250 \text{ min}^{-1}$, Da numbers on the base of assumption where K_La values were constant throughout the process were found between 5.0 and 6.0. Since it is greater than one, mass transfer resistance became more effective, i.e. OD values were higher than OTR_{max} values as it was expected.

The change of effectiveness factor along the bioprocess is also shown with respect to time and cell concentration (Table 4.14 and 4.45). It can be observed that the effectiveness factor, η , took values which were close to 1 at the beginning of log phase ($t=20 \text{ h}$) where cell growth rate increased, indicating that the cells are consuming oxygen with a high rate and generally, they decreased with respect to time and cell concentration.

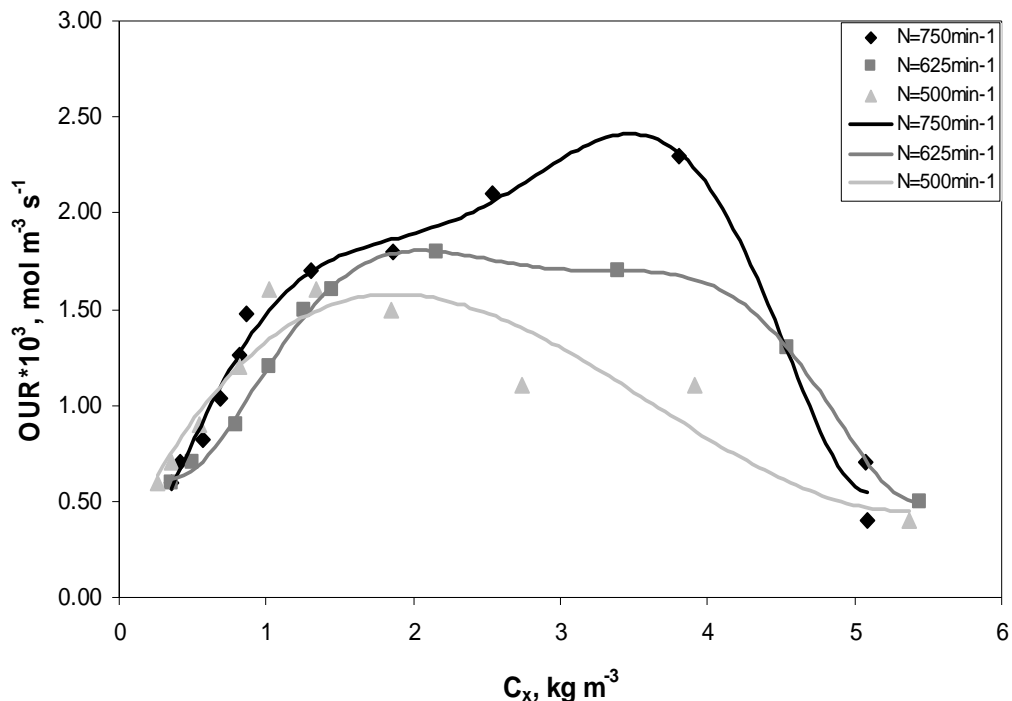


Figure 4.42 The variation of OUR with cell concentration and stirring, $T=30^\circ\text{C}$, $V_R=1000 \text{ cm}^{-3}$, $Q_o/V_R=0.5 \text{ vvm}$, $N=500, 625 \text{ and } 750 \text{ min}^{-1}$, $\text{pH}_c=6.0$.

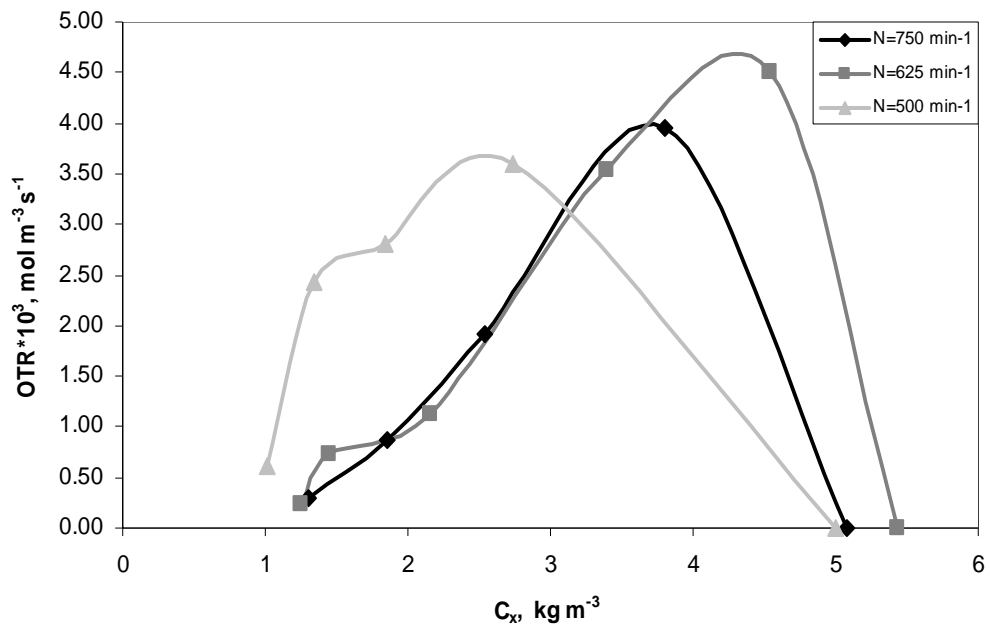


Figure 4.43 The variation of OTR with cell concentration and stirring rate, $T=30^{\circ}\text{C}$, $V_R= 1000 \text{ cm}^{-3}$, $Q_0/V_R=0.5 \text{ vvm}$, $N= 500, 625 \text{ and } 750 \text{ min}^{-1}$, $\text{pH}_C=6.0$.

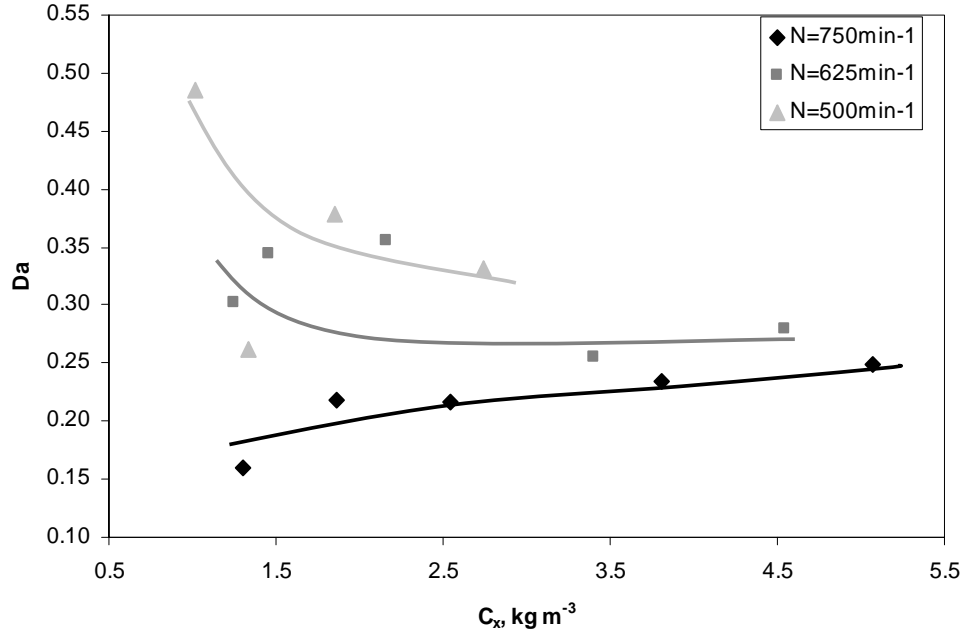


Figure 4.44 The variation of Da numbers with cell concentration and stirring rate, $T=30^{\circ}\text{C}$, $V_R= 1000 \text{ cm}^{-3}$, $Q_0/V_R=0.5 \text{ vvm}$, $N= 500, 625 \text{ and } 750 \text{ min}^{-1}$, $\text{pH}_C=6.0$.

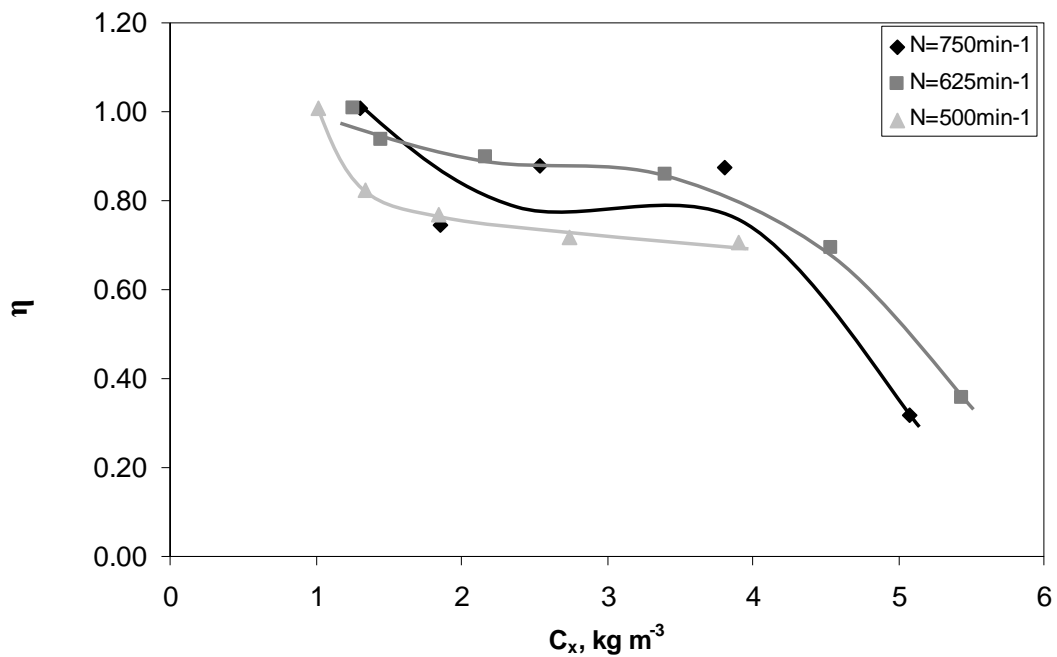


Figure 4.45 The variation of η with cell concentration and stirring rate, $T=30^{\circ}\text{C}$, $V_R=1000\text{ cm}^{-3}$, $Q_0/V_R=0.5\text{ vvm}$, $N=500, 625\text{ and }750\text{ min}^{-1}$, $\text{pH}_c=6.0$.

4.3.1.7 Specific Growth Rate, Yield and Maintenance Coefficients

The variations in the specific growth rate, μ ; the specific oxygen uptake rate, q_0 ; specific product formation rate, q_p ; maintenance coefficients for oxygen and substrate m_0 , m_s and m_0' , m_s' and the yield coefficients with the cultivation time are given in Table 4.15.

As mentioned before, all calculations were performed according to data obtained in log phase ($t=20-42\text{ h}$). Since lag phase at all conditions was very long, data obtained at this phase was not applicable for the formulation of the system explained in section 2.3.4.

At all oxygen transfer conditions, the specific growth rate (μ) decreased with cultivation time as seen in Figure 4.45. The maximum μ values are obtained as $0.10, 0.10, 0.13$ and 0.03 h^{-1} at $N=750, 625, 500$ and 250 min^{-1} conditions, respectively. At the beginning of exponential phase of the bioprocesses, a general decrease in μ is observed with some fluctuations. After

a while a sharp decrease in specific growth rates at $N=750, 625, 500 \text{ min}^{-1}$ conditions is seen and at the end of the bioprocesses specific growth rates become almost zero since no cell growth occurred. At limited oxygen transfer condition, specific growth rates are much smaller than those found at other conditions (Figure 4.46). Because of insufficient oxygen level at this condition, lower cell growth rates were observed (Figure 4.36) which also resulted in lower specific growth rates.

Table 4.15 The variations in specific growth rate and yield coefficients.

N	t	μ	q_o	$q_p * 10^{-3}$	q_s	$Y_{x/s}$	$Y_{p/s} * 10^{-3}$	$Y_{x/o}$
min^{-1}	h	h^{-1}	$\text{kg kg}^{-1} \text{h}^{-1}$	$\text{kg kg}^{-1} \text{h}$	$\text{kg kg}^{-1} \text{h}^{-1}$	kg kg^{-1}	kg kg^{-1}	kg kg^{-1}
750	20	0.10	0.15	0.01	0.59	0.17	0.16	0.68
	24	0.08	0.11	0.36	0.44	0.17	0.82	0.68
	28	0.08	0.09	0.42	0.42	0.21	1.02	0.93
	32	0.08	0.07	0.29	0.29	0.30	1.00	1.27
	36	0.03	0.02	0.12	0.11	0.30	1.13	2.01
	39	0.00	0.01	0.00	0.00	-	-	-
625	20	0.10	0.14	0.20	0.43	0.24	0.46	0.75
	24	0.10	0.13	0.34	0.50	0.19	0.68	0.76
	28	0.09	0.10	0.35	0.50	0.19	0.69	0.96
	32	0.09	0.06	0.22	0.33	0.27	0.67	1.53
	36	0.07	0.03	0.22	0.15	0.46	1.43	2.17
	39	0.03	0.01	0.00	0.00	-	-	3.47
500	20	0.13	0.18	0.12	0.68	0.19	0.18	0.70
	24	0.10	0.14	0.18	0.65	0.16	0.30	0.75
	28	0.10	0.09	0.34	0.47	0.21	0.73	1.04
	32	0.09	0.05	0.41	0.37	0.24	1.10	1.97
	36	0.09	0.03	0.52	0.26	0.35	2.03	2.76
	39	0.04	-	0.37	0.09	0.4	4.00	-
	42	0.00	0.01	0.16	0.00	-	-	-
250	12	0.03	0.06	0.24	0.28	0.10	0.86	0.45
	24	0.01	0.06	0.41	0.36	0.04	1.11	0.25
	36	0.01	0.05	0.25	0.24	0.07	1.05	0.35
	46	0.01	0.04	0.13	0.15	0.09	0.91	0.34

The variations in oxygen uptake rates which were found by using dynamic method and the variations in substrate utilization rates are shown on Figure 4.47 and Figure 4.48. Specific oxygen uptake rate and substrate utilization rate were observed to decrease with the cultivation time at all conditions. At the beginning of the exponential phase, consumption rate of methanol (carbon source) and oxygen by the cells is higher than the cell formation rates, therefore decreasing feature of q_s and q_o with cultivation time was reasonable.

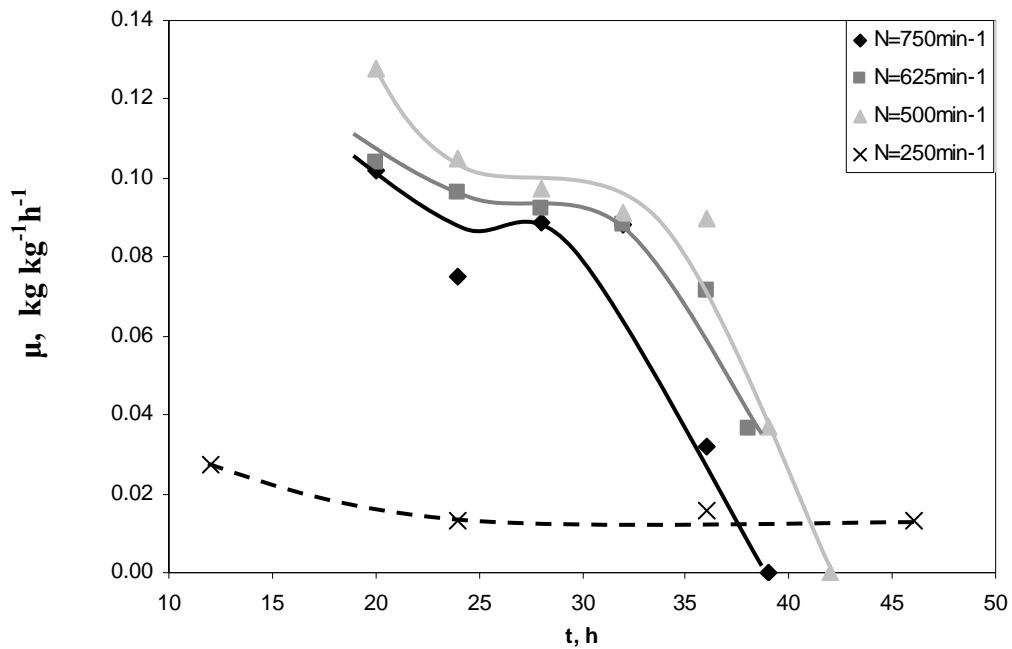


Figure 4.46 The variations in the specific growth rates with the cultivation time, and agitation rate. $T=30^{\circ}\text{C}$, $V_R=1000\text{ cm}^3$, $Q_o/V_R=0.5\text{ vvm}$, $N=250, 500, 625$ and 750 min^{-1} , $\text{pH}_c=6$.

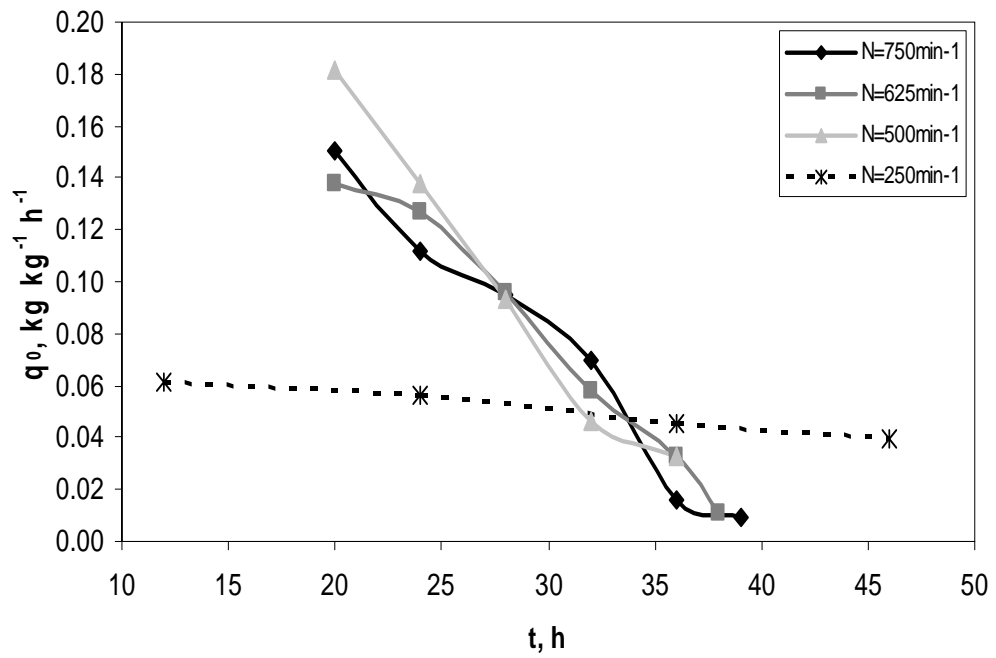


Figure 4.47 The variations in the specific oxygen uptake rates with the cultivation time, and agitation rate. $T=30^{\circ}\text{C}$, $V_R=1000\text{ cm}^3$, $Q_o/V_R=0.5\text{ vvm}$, $N=250, 500, 625$ and 750 min^{-1} , $\text{pH}_c=6.0$.

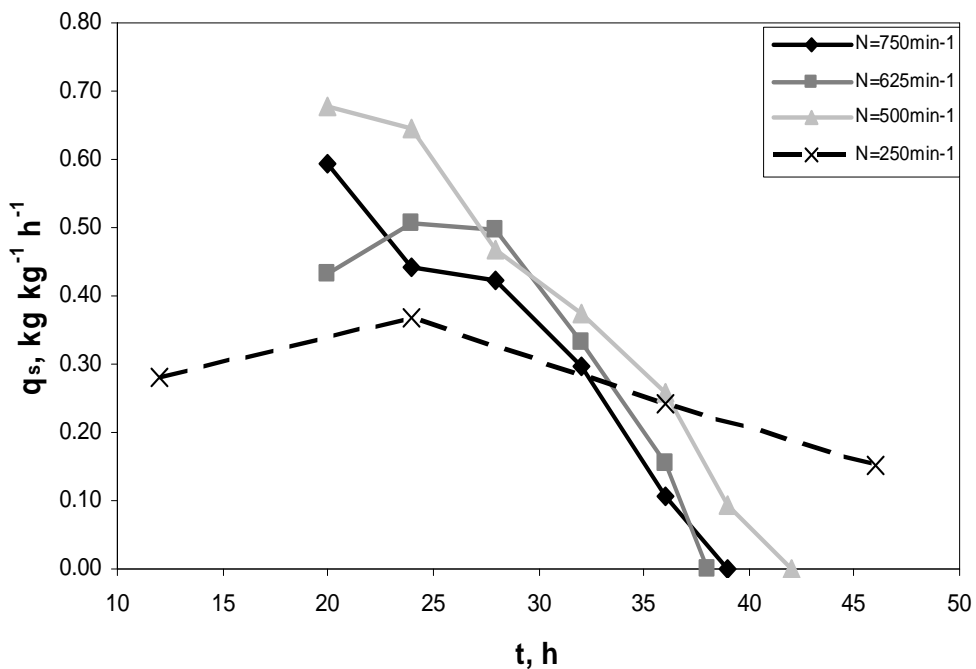


Figure 4.48 The variations in the specific substrate consumption rate with the cultivation time, and agitation rate. $T=30^{\circ}\text{C}$, $V_R=1000\text{ cm}^3$, $Q_o/V_R=0.5\text{ vvm}$, $N=250, 500, 625$ and 750 min^{-1} , $\text{pH}_c=6.0$.

In the case of specific product formation rates with respect to time and agitation rates (Figure 4.49), it is seen that these profiles had different trend when compared with the others in Figures 4.46- 4.48. At the beginning of log phase, $t > 20$ h, it is clear that cell growth rates are smaller thus increasing pattern in specific product formation rate was observed. After a while, explosion in cell growth rate resulted in higher biomass concentration, which lessened q_p values. From the Figure 4.549, the highest specific product formation rate was obtained as $0.00052 \text{ kg kg}^{-1} \text{ m}^{-3}$ at $N= 500 \text{ min}^{-1}$ condition.

Besides the specific growth rates, yield coefficients were also calculated. Biomass yields based on substrate and oxygen, $Y_{x/s}$ and $Y_{x/o}$, and product yield based on biomass, $Y_{p/x}$, increased with cultivation time at all conditions, (Table 4.15). Among the calculated results higher biomass yields were obtained at $N=625 \text{ min}^{-1}$, $Y_{x/s} = 0.46 \text{ kg kg}^{-1} \text{ m}^{-3}$ and $Y_{x/o} = 3.47 \text{ kg kg}^{-1} \text{ m}^{-3}$ and higher product yield was found as, $Y_{p/x} = 4.0 \text{ kg kg}^{-1} \text{ m}^{-3}$ at $N= 500 \text{ min}^{-1}$, though these yield coefficients are closer to each other at $N= 500, 625$ and 750 min^{-1} oxygen transfer conditions.

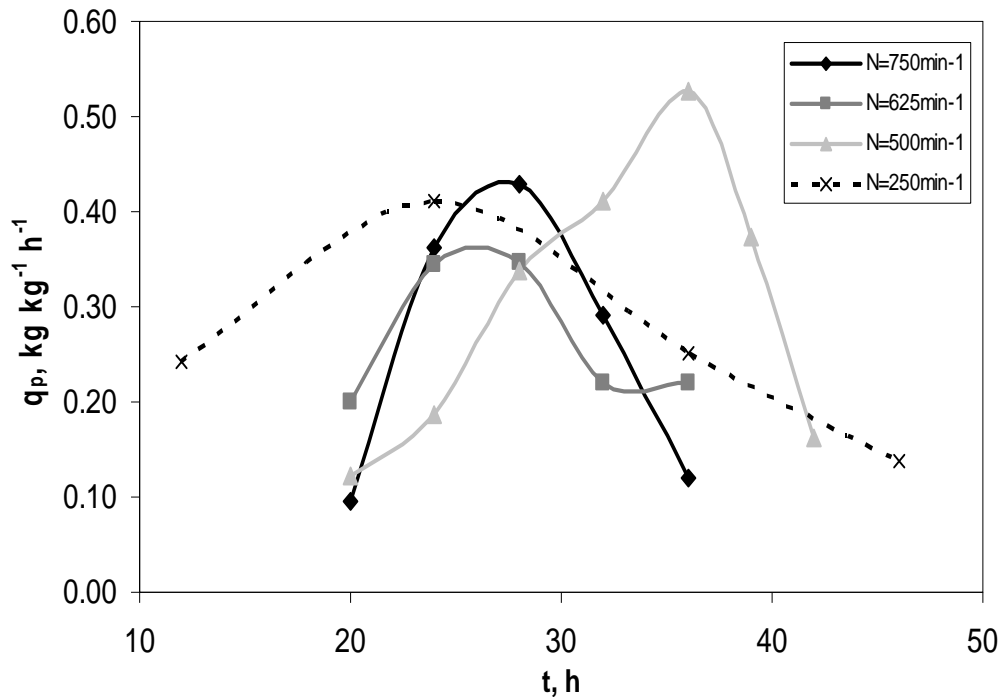


Figure 4.49 The variations in the specific production formation rate with the cultivation time, and agitation rate. $T=30^{\circ}\text{C}$, $V_R= 1000 \text{ cm}^{-3}$, $Q_o/V_R=0.5 \text{ vvm}$, $N= 250, 500, 625$ and 750 min^{-1} , $\text{pH}_c=6.0$.

From the slope of the plot of $1/Y_{X/O}$ versus $1/\mu$, the rate of oxygen consumption for maintenance and from the slope of the plot $1/Y_{X/S}$ versus $1/\mu$, the rate of methanol consumption for maintenance were obtained. The variation of m_0 vs. m_0' and m_s vs. m_s' with oxygen transfer strategy and the Leudeking-Piret constants calculated for the bioprocesses are given in Table 4.16. Since by-product formation occurred generally between $t=20$ h and $t=30$ h, maintenance coefficients were calculated within this period. Maintenance energy, denoted by m_0 and m_s that represents the energy expenditures to repair damaged cellular components, to transfer some nutrients and products in and out of the cell, for motility, and to adjust the osmolarity of the cells' interior volume were obtained higher than m_0' and m_s' , approximately two-folds, since in the calculation of m_0 and m_s by product formation was neglected. Maintenance coefficient profiles decreased generally when agitation rate decreased, indicating that at high stirring rate cells use more energy to repair the damaged cellular components and to stabilize themselves with the environment. The lowest maintenance coefficients were obtained at $N=500$ min^{-1} condition; $m_s' = 0.254$ and $m_0' = 0.064$. This may be expected result since among the other oxygen transfer conditions, this agitation rate was the optimum value in this defined-batch fermentation system and resulted in less stress on cell that was caused by extreme oxygen conditions, therefore cells require less energy for maintenance.

Table 4.16 The variations in Leudeking-Piret constants and maintenance coefficients

N min^{-1}	β	a	m_0 $\text{kg kg}^{-1} \text{h}^{-1}$	m_0' $\text{kg kg}^{-1} \text{h}^{-1}$	m_s $\text{kg kg}^{-1} \text{h}^{-1}$	m_s' $\text{kg kg}^{-1} \text{h}^{-1}$
750	0.034	0.046	0.280	0.148	0.620	0.488
625	0.026	0.034	0.260	0.149	0.530	0.419
500	0.030	0.045	0.180	0.064	0.370	0.254
250	0.013	0.031	0.120	0.079	0.330	0.289

4.3.2 Effects of Cell Density in Impulse Feeding Fermentation

In order to determine the effects of cell concentration on oxygen transfer and fermentation characteristics, as well as on rhGH production and by-product formation, and to understand the effects of methanol addition to the cultivation medium during the process, an impulse feeding strategy was also performed at the end of the fermentation process, the bioreactor operation conditions which were $\text{pH}=6.0$, $T=30^\circ\text{C}$, $Q_0/V_R = 0.5 \text{ vvm}$ and $N=625 \text{ min}^{-1}$. After consumption of all methanol, initial concentration of which was 3% (v/v) (23.7 kg m^{-3}), some amount of methanol was added into production medium.

The variations in the dissolved oxygen, methanol concentration and cell concentration with cultivation time are given in Figure 4.50.

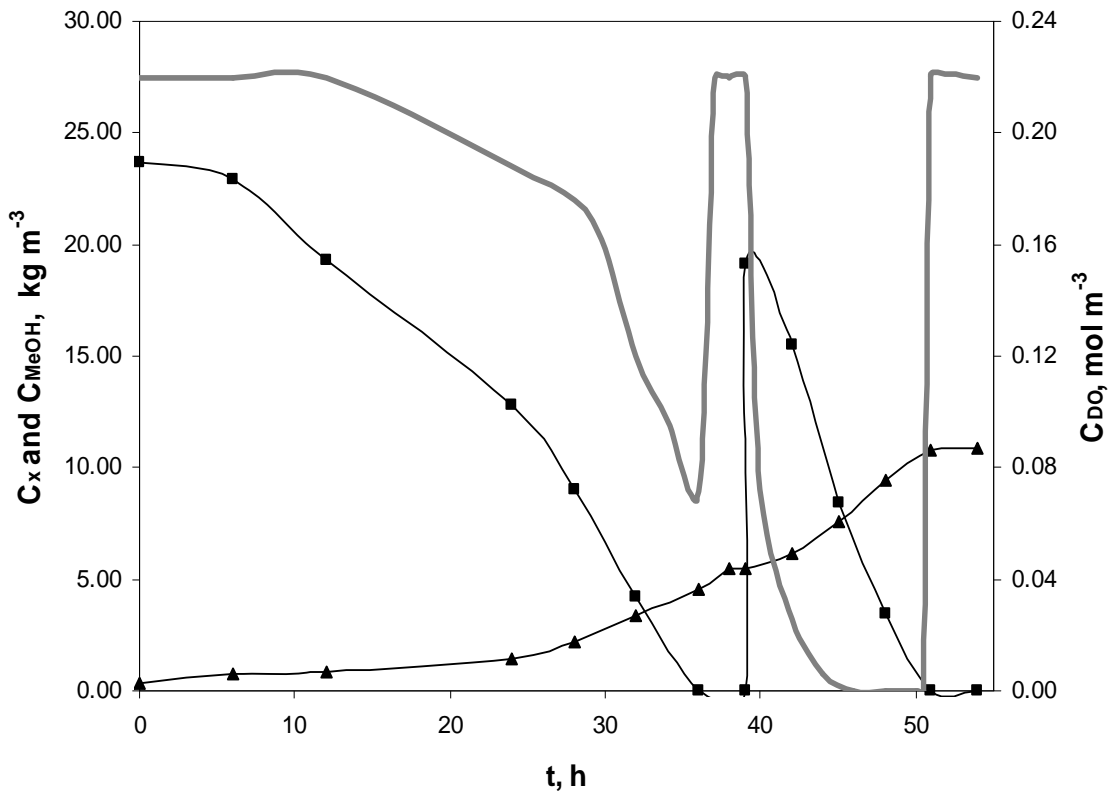


Figure 4.50 The variations in the dissolved oxygen, methanol and cell concentration with the cultivation time. $T=30^\circ\text{C}$, $\text{pH}=6.0$, $V_R= 1000 \text{ cm}^3$: $N=625 \text{ min}^{-1}$. Cell concentration profile (\blacktriangle), methanol concentration profile (\blacklozenge), dissolved oxygen concentration profile (grey line).

The same C_{DO} profile was obtained in impulse feeding fermentation process until the end of the consumption of initial methanol when compared the oxygen profiles shown in Figure 4.36 (between $t=0$ and $t=40$ h). From the Figure 4.50, it is obvious that oxygen concentration began to decrease when methanol utilization rate increased. At $t=39$ when all methanol was exhausted, a sharp rise in C_{DO} level was observed. This is actually evidence of strong relation between the methanol and oxygen. After the addition of methanol for the second time a sudden decrease in C_{DO} was observed, and this time its level is much lower than previous one though the same bioprocess conditions were applied. This actually shows that the C_{DO} is a critical parameter for high cell density cultivation (Cunha et al., 2004) and unlimited methanol supply can lead to sudden oxygen depletion (Katri and Hoffman, 2005). Since low cell densities are obtained in batch fermentation processes, C_{DO} in this case may not be as critical as the one in fed-batch system. Since the feeding procedures commonly employed rely on restricted methanol addition in fed-batch system, C_{DO} plays important role, therefore alternative approaches are sought to maintain both oxygen and methanol sufficient conditions, for example, reducing the metabolic activity by cultivation at low temperature (Jahic et al., 2003b) or at low cell density in continuous culture (Curvers et al., 2001). Charoenrat et al. (2006) increased the driving force for the diffusion from the air bubbles to the medium by elevating the air pressure in order to increase the oxygen transfer rate (OTR) in the process by simple means.

Until $t \sim 20$ h, cell formation did not change significantly with respect to the oxygen transfer conditions applied and due to the long lag phase. After all initial methanol was consumed by the cell at $t \sim 36-38$ h and addition of methanol for the second time was performed, it is seen on the Figure 4.50 that long lag phase was not observed.

Higher cell density was obtained at impulse feeding fermentation broth, as twice as that one obtained in batch system at the same bioprocess operation conditions, since a sudden methanol addition was performed at $t=39$ h. Until the end of the process where all initial methanol utilization was depleted, cell density reached a value; 5.43 kg m^{-3} . Addition of methanol for the second time increased cell concentration to 10.88 kg m^{-3} . The overall biomass yield coefficients based on substrate were found as 0.229 and 0.254 kg cell kg^{-1} substrate, respectively.

Methanol concentration profile (Figure 4.50) in impulse feeding fermentation broth coincides with the cell growth and DO profiles of this system. After addition of methanol for the second time, without any long lag phase, rapid decrease in methanol concentration was observed, meanwhile, higher cell growth rate and sudden decrease in DO level were obtained.

The variation in rhGH concentration profile of the impulse feeding fermentation broth is shown on Figure 4.51. The rhGH concentration after the addition of methanol at $t \sim 30$ h was obtained as twice as the one obtained before addition of methanol, which were 0.014 and 0.030 kg m^{-3} , respectively. Addition of methanol increased not only the biomass concentration but also volumetric rhGH concentration due to the induction of AOX1 promoter by methanol. It can be also concluded that enhancement of biomass density resulted in higher recombinant hGH production. Overall product yield coefficients were also calculated for both conditions. Slightly higher overall yields were obtained when methanol was added for the second time; these were $Y_{p/x}=0.0028 \text{ kg hGH kg}^{-1} \text{ cell}$ and $Y_{p/s}=0.0007 \text{ kg hGH kg}^{-1} \text{ methanol}$. On the other hand, the overall product yields obtained before the addition of methanol were $Y_{p/x}=0.0026 \text{ kg hGH kg}^{-1} \text{ cell}$ and $Y_{p/s}=0.0006 \text{ kg hGH kg}^{-1} \text{ methanol}$.

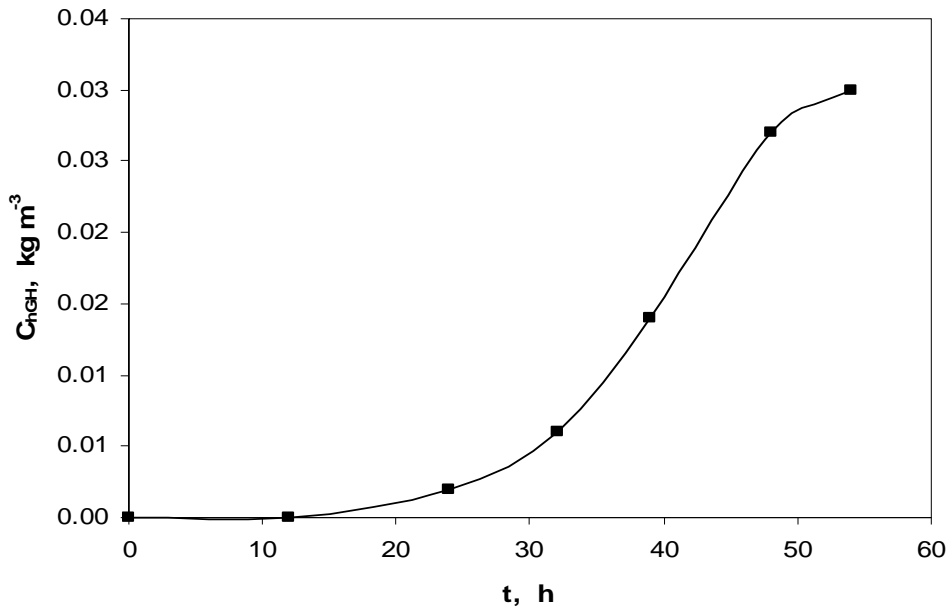


Figure 4.51 The variations in rhGH concentration of impulse feeding fermentation with the cultivation time. $T=30^{\circ}\text{C}$, $\text{pH}=6.0$, $V_R=1000 \text{ cm}^3$; $N=625 \text{ min}^{-1}$.

Formic acid and fumaric acid are some organic acids; aspartic acid, lysine, proline, treonin and leucine are some amino acids that were detected in the impulse feeding medium. The variations in the organic acids and amino acids detected in the fermentation broth with cultivation time and oxygen transfer conditions were demonstrated in Tables 4.15 and 4.16. Higher amount of organic acids and amino acids were detected in impulse feeding fermentation broth when compared with the others shown on Table 4.13 and Table 4.12 most probably due to higher cell density obtained

P. pastoris strains can not tolerate high methanol concentration due to the accumulation of formaldehyde and hydrogen peroxide inside the cells, both of which are the oxidized products of methanol by AOX and are toxic to the cell (Zhang et al., 2000), therefore analyzing formaldehyde production throughout the fermentation process is important. Figures 4.52 shows the formaldehyde concentration profiles with cultivation time. Since formaldehyde is the product of AOX and used as a substrate for energy and biomass formation, consumption of formaldehyde was also observed.

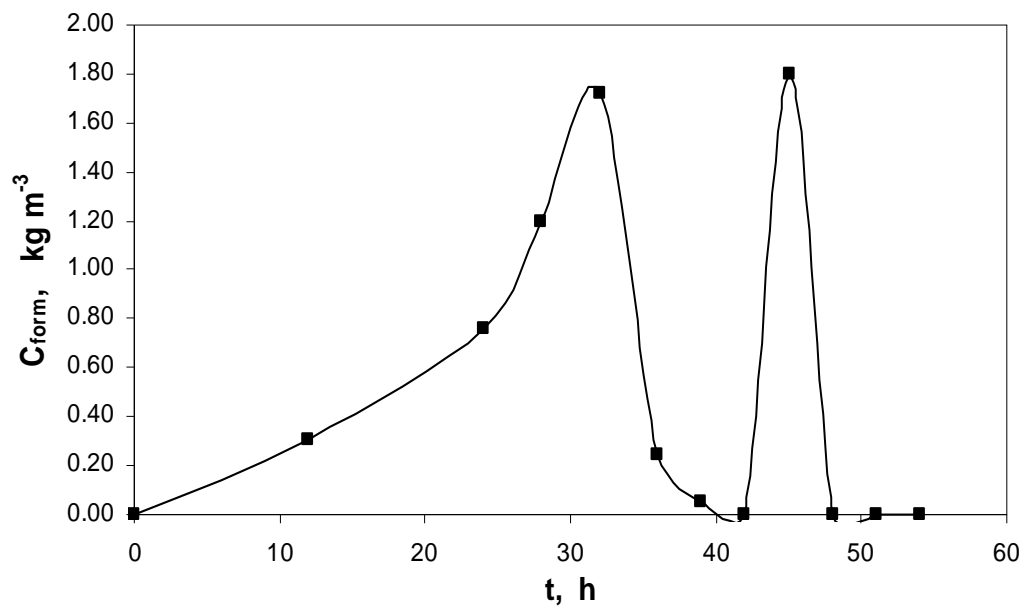


Figure 4.52 The variations in formaldehyde concentration of impulse feeding fermentation with the cultivation time. T=30°C, pH= 6.0, V_R= 1000 cm³: N=625 min⁻¹.

From the figure 4.52, the highest formaldehyde concentrations were obtained at approximately $t=30$ and 45 h, where methanol utilization rates were higher. Since formaldehyde is the product of alcohol oxidase enzyme, this figure clearly explains that at exponential growth phase, AOX1 enzyme production level was so high that formation rate of formaldehyde was greater than consumption rate of this substrate, thus accumulation of formaldehyde began to rise. Towards the end of the processes, i.e. when all methanol was consumed, cells started to use formaldehyde as substrate. As mentioned before, some portion of formaldehyde is converted to cell materials and some leaves peroxisome and is further oxidized to formate (formic acid). On Table 4.17 it is clear that formic acid was generally produced and secreted to the medium until $t=24$ h and then began to be consumed by entering the carbon metabolism. Throughout the lag phase higher formate concentration was obtained due to the conversion of formaldehyde to formate and inconsiderable amount of formate was consumed by the cell. At $t=48$, some amount of formate was secreted to the medium and consumed immediately at $t=51$ h when methanol added for the second time was totally depleted. As a result, It can be concluded that small amount of formaldehyde formation occurs in lag phase because AOX1 level is low and most of the formaldehyde produced in this phase is converted to formate, on the other hand with the increase in AOX1 level in growth phase (log phase), formaldehyde accumulation was observed and cells growing rapidly used formate.

Oxygen transfer characteristics of impulse feeding strategy could not be analyzed properly since overall mass transfer coefficient and oxygen uptake rate values could not be obtained by dynamic method. After addition of methanol, rapid decrease in dissolved oxygen level occurred. This prevented the use of dynamic method. At $t=51$ h, K_La value was obtained since dissolved oxygen level increased to its saturated level since all methanol added was completely consumed. Around the end of the impulse feeding process, i.e. $t=51$ h, K_La value was found as 0.027 h^{-1} , on the other hand these value varied between 0.021 and 0.035 before addition of methanol for the second time. It is clear that addition of methanol and enhancement of cell concentration did not affect the K_La value very much in this process. From the figure 4.42 and Table 4.14, OUR changed between 0.0005 and $0.0018\text{ mol m}^{-3}\text{s}^{-1}$ at $N=625\text{ min}^{-1}$ and it increased, first, and then decreased with cultivation time. At the end of consumption of initial methanol, $t=39$ h, OUR was obtained

as $0.0005 \text{ mol m}^{-3}\text{s}^{-1}$, on the other hand around the end of consumption of second methanol, $t=51 \text{ h}$, OUR was $0.0017 \text{ mol m}^{-3}\text{s}^{-1}$. This high value most probably was due to the rise in the cell concentration which increased the oxygen utilization. Again from the Table 4.14, before the addition of methanol for the second time, Da was less than 1 and did not change very much through the bioprocess (between 0.20 and 0.35). On the other hand, after impulse feeding Da number increased and $t=51 \text{ h}$, it was found as 0.91, though it was still less than one, meaning that biochemical reaction limitations were effective. But, rise in Da number was resulted from maximum possible oxygen utilization rate by the cells which increased also.

Table 4.17 The variations in organic acid concentrations with cultivation time

		N=625 rpm (impulse feeding)									
Time (h)	0	12	24	28	32	36	39	45	48	51	
Formic acid (g L ⁻¹)	-	0.0186	0.0128	0.0088	0.0052	0.0021	-	-	0.005	-	
Fumaric acid(g L ⁻¹)	-	0.0097	0.0186	0.0251	0.0328	0.0405	0.0428	0.029	0.028	0.032	

Table 4.18 The variations in amino acid concentrations with cultivation time

		N=625 rpm (impulse feeding)									
Time (h)	0	12	24	32	39	45	48	51			
Aspartic acid(g L ⁻¹)	-	0.040	0.007	0.118	0.124	0.084	-	0.175			
Lysine (g L ⁻¹)	-	0.007	0.013	0.053	0.100	0.083	0.056	0.310			
Leucine (g L ⁻¹)	-	-	0.013	-	-	-	-	0.124			
Treonin (g L ⁻¹)	-	-	-	-	-	-	-	0.215			
Prolin (g L ⁻¹)	-	-	-	-	-	-	-	0.247			

4.4 Purification of rhGH Produced by *Pichia Pastoris*

In this study, a strategy for the purification of human growth hormone produced by *P. pastoris* was applied using recombinant DNA technology. The cDNA of hGH was fused with a polyhistidine tag and a target site for the Factor Xa protease by using primer extension and PCR amplification approaches. Therefore, expression of this gene by the r- *P. pastoris* results in hGH protein with polyhistidine tag for rapid purification using immobilized metal affinity chromatography (IMAC) purification and Factor Xa protease target site, in which cleavage produces a mature form of rhGH, having N- and C- termini.

In order to produce rhGH *P. pastoris-hGH-Mut^s* strain, having higher rhGH production capacity, was inoculated into BMMG precultivation medium and incubated at 30°C and N=225 min⁻¹ for 24 h using air-filtered Erlenmeyer flasks 150 ml in size that had working volume capacities of 10 ml. Then, they were harvested by centrifugation at 4000 rpm, 10 min at room temperature and resuspended in BMMY production medium, including 1.0% (v/v) methanol. The recombinant cells were incubated at 30°C and N=225 min⁻¹ for 24 h using air-filtered, baffled Erlenmeyer flasks 250 ml in size that had working volume capacities of 50 ml. Cells were harvested by centrifugation at 8000 rpm, 10 min at +4 °C and supernatant was taken used for the purification process.

Figure 4.53 is the SDS-page and Western analysis which shows the purification steps. All steps used for purification are explained with details in Section 3.6.4.

The first step of purification process after production was concentrating and desalting of the supernatant of *P. pastoris* production medium, which was achieved by ultrafiltration and by using 10 kDa ultrafiltration polyethersulfone membranes giving the highest possible retention with the lowest possible adsorption of the protein. During ultrafiltration and the following processes, the temperature of solution containing protein was kept at 2-8°C to prevent microbial and proteolytic degradation. Ultrafiltration was carried until about 10 fold concentration is achieved. The cultivation supernatant and concentrated supernatant are shown in Lane 1 and Lane 2, respectively, on Figure 4.53. The

rhGH shown on these lanes has a molecular weight of 23 kDa approximately since it includes Fac Xa protease recognition site and His-tag.

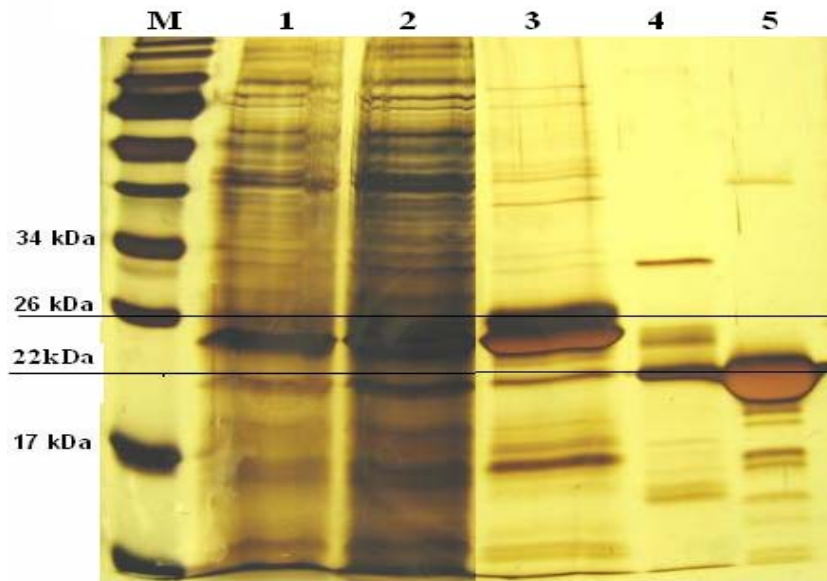
Cobalt-based metal affinity resins were added to the concentrated sample, for His-tag purification as explained in 3.6.4. The amount of resin used was approximately 20% of concentrated sample. The binding step was carried out overnight in order to increase efficiency. Then, the resin was transfer to a 2-ml gravity-flow column and eluted with imidazole solution. The protein was observed in the first two 0.5 ml eluates (Lane 3- Figure 4.53).

Finally, the polyhistidine tag was removed by Factor Xa. Factor Xa protease digestion site is just after its recognition site, so there will not be any extra amino acids left following digestion. Since Factor Xa protease is sensitive to imidazole used in elution of His-Tag purification, and in order to obtain a concentration of 0.25 μg of protein/ μl of reaction buffer for the protease digestion, ultrafiltration spin columns with 10 kDa cut-off (Sartorius) were used. After digestion of the His-tag by Factor Xa (Lane 4- Figure 4.53), the protease was removed by Xa removal resins provided with the enzyme, according to manufacturer's instructions. The resulted protein was the mature rhGH having a molecular weight of 22 kDa (Lane 4- Figure 4.53).

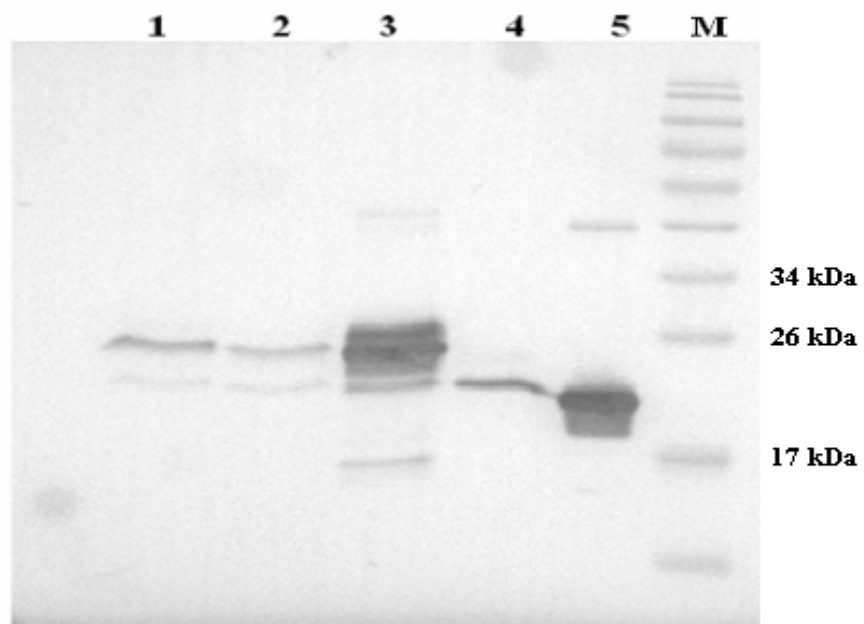
Moreover, Automated Edman degradation was performed by PROCISE 494 gas-phase/liquid-pulse sequencer (Applied Biosystems, Foster City, CA) for N terminal analysis. The result showed that seven amino acid residues at the N termini of rhGH treated with Factor Xa were the same as original ones.

The molecular weights of the affinity purified rhGH and Factor Xa digested rhGH were determined by MALDI-TOF MS, to further verify the structure of the secreted and the digested forms of the recombinant hormone. The commercial rhGH analyzed first, showed a spectral peak at m/z 22126 (Figure 4.54 a). The stated molecular weight of the commercial hormone is 22125 Da, thus the ion detected was $[M+H]^+$, with the exact molecular mass of 22126 Da, where $z=1$. RhGH purified by polyhistidine-tag affinity purification from the supernatant of production, gave a spectral peak centered at m/z 23699 (Figure 4.54 b), which again is possibly of the $[M+H]^+$ form. Thus the molecular weight difference, $23698 - 22125 = 1573$ Da, corresponds well with the undigested 12 amino acids in the N-terminal region of rhGH, with

a calculated average mass of 1572.7 Da. After digestion of the purified hormone with Factor Xa protease, the native length of the protein was obtained, as the peak at m/z 22133 (Figure 4.54 c) corresponds to the $[M+H]^+$ ion of rhGH detected with 0.03 % error. The Factor Xa protease (42.5 kDa) unpurified from the digestion reaction medium to serve as the internal mass calibration control reagent showed peaks in two ionic forms; $[M+H]^+$ ion detected at m/z 42634 and $[M+2H]^{2+}$ ion detected at m/z 21341 (Figure 4.54 c).



(a)



(b)

Figure 4.53. SDS-page (a) and Western blot (b) of rhGH, produced by *P. pastoris* and purified. For both of the figures (a) and (b); M: Protein marker, Lane 1: Supernatant from wild type *P. pastoris* production medium, Lane 2: Ultrafiltered medium containing hGH. Lane 3: Purified and concentrated rhGH by his-tag method. Lane 4: Factor Xa digested rhGH. Lane 5: standard hGH.

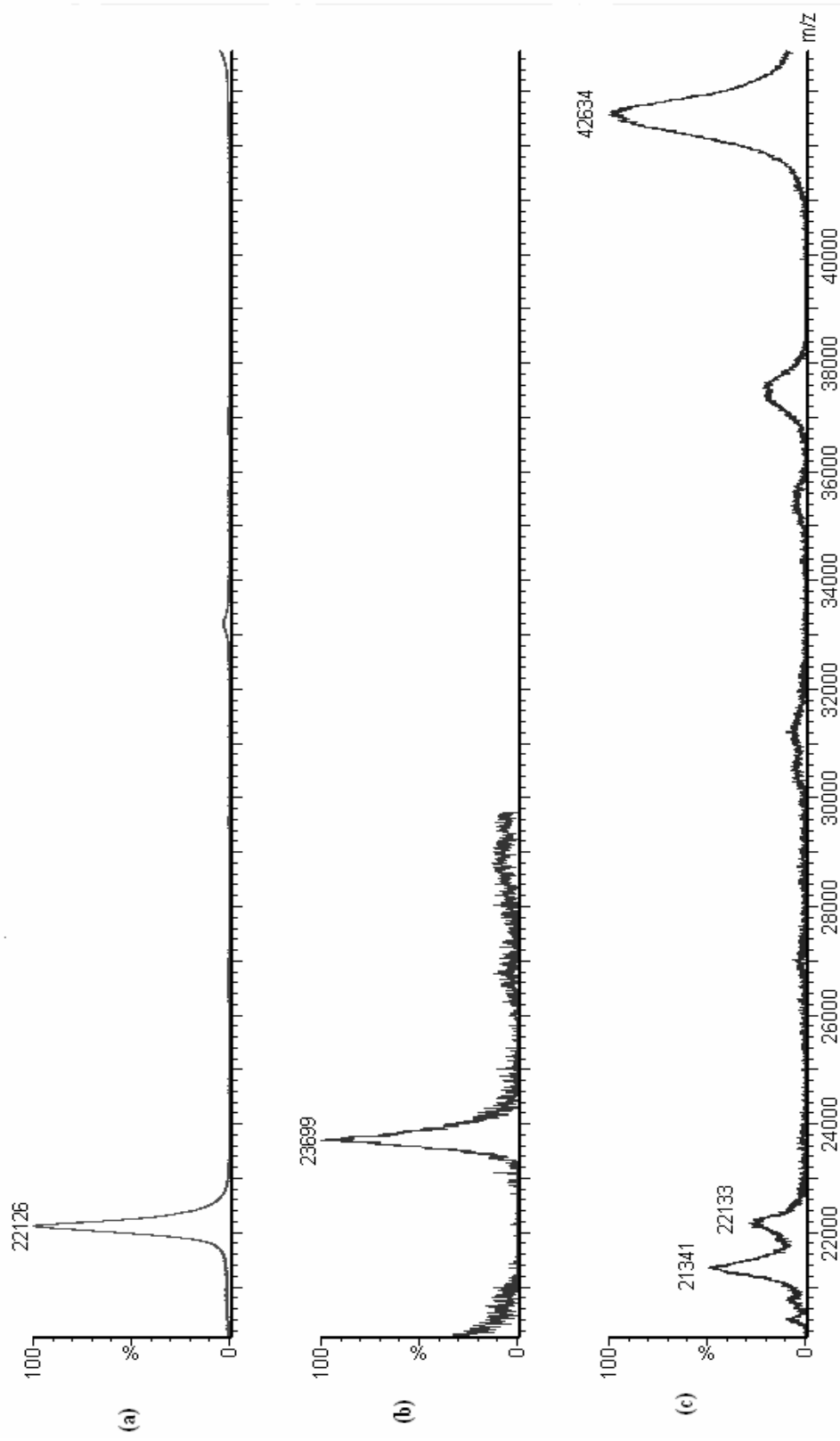


Figure 4.54 MALDI-TOF MS analysis. (a) Commercial rhGH (standard), (b) produced rhGH purified with Factor Xa, (c) rhGH digested with Factor Xa.

CHAPTER 5

CONCLUSION

In this study for the extracellular expression and purification of human growth hormone by recombinant *P.pastoris* the cDNA of hGH, fused with a polyhistidine tag and also fused with a target site for the Factor Xa protease in which cleavage produces a mature form of rhGH, was cloned into pPICZaA plasmid and the constructed system within the plasmid, *pPICZaA::hGH*, was integrated to AOX1 locus of *P. pastoris* and expressed under alcohol oxidase promoter. With *dot-blot* analysis, the appropriate two strains producing human growth hormone at high levels and having different methanol utilization phenotype (Mut⁺ and Mut^s) were chosen among the other transformants. Thereafter, the effects of carbon sources, glycerol and methanol, on rhGH production by the strains selected (*P. pastoris-hGH-Mut⁺* and *P. pastoris-hGH-Mut^s*) were investigated in small scale air filtered shake bioreactors and using the designed defined medium finally effects of oxygen transfer on rhGH production, by-product formation, and cell growth, oxygen transfer and fermentation characteristics were investigated by using laboratory scale bioreactor.

For extracellular expression and purification of hGH in *Pichia pastoris*, *hGH* forward and *hGH* reverse primers for amplification of *hGH* gene were designed. Since an addition of 36 bases (*EcoR* I restriction site , 6xHis-Tag sequence and Factor XA recognition sequence) was required at the 5' end of hGH sequence, two relatively short forward primers were designed instead of a single long primer. The PCR product obtained by using these designed primers cloned into pPICZaA vector, *E. coli/ Pichia pastoris* shuttle vector after restriction digestion with proper restriction enzymes. Recombinant pPICZaA:*hGH* plasmid was transfected into *Pichia pastoris* for extracellular expression and two potential phenotypes (Mut⁺ and Mut^s) were chosen for further studies.

Due to its rich components, higher rhGH production were obtained in BMMY complex medium (10 kg m⁻³ yeast extract, 20 kg m⁻³ peptone, 13.4 kg m⁻³ yeast nitrogen base, 4x10⁻⁴ kg m⁻³ biotin and 10% 0.1 M potassium phosphate buffer, pH=6.0) when compared with the defined medium containing methanol as a sole carbon source and mixed carbon source (glycerol/methanol) The highest rhGH concentration for both strains; Mut⁺ and Mut^S, was found as 0.052 kg m³ and 0.16 kg m³, respectively, at 2 % (v/v) methanol concentration in complex medium.

In defined medium (5.62 kg m⁻³ potassium phosphate, 1.1800 kg m⁻³ magnesium sulfate, 0.8300 kg m⁻³ calcium sulfate, 0.0080 kg m⁻³ copper sulfate, 0.0012 kg m⁻³ potassium iodide, 0.0280 kg m⁻³ manganese sulfate, 0.0052 kg m⁻³ sodium molybdate, 0.0080 kg m⁻³ boric acid, 0.0080 kg m⁻³ cobalt chloride, 0.0044 kg m⁻³ zinc sulfate, 0.0750 kg m⁻³ ferric chloride, and 0.00174 kg m⁻³ biotin with varying methanol and ammonium sulfate) where methanol was used as a sole carbon source, Mut^S strain could not grow properly due to its reduced ability to use methanol, therefore detectable rhGH was not observed, on the other hand, optimum rhGH concentration produced by Mut⁺ strain was found as 0.032 kg m³ at 3% (v/v) methanol concentration.

In the case of defined mixed-batch system (glycerol/methanol) containing the same basal salts and trace elements given above with varying methanol, glycerol and ammonium sulfate concentrations, it is difficult to make a correlation between the methanol concentration and r-protein production for these two phenotypes due to the complexity of the r-protein production in mixed-batch system. However, it is found that glycerol concentration did not have an effect on rhGH production in mixed-batch system as vigorous as the methanol concentration did. Any change in methanol concentration resulted in drastic changes in rhGH production. Although rhGH production capacity of Mut⁺ phenotype increased when initial methanol concentration was increased, this was not valid in the case of Mut^S phenotype. When the optimum glycerol concentration, 30 kg m³, was used, Mut^S produced the highest rhGH, 0.110 kg m³, at 1% (v/v) methanol concentration, on the other hand, Mut⁺ strain produced 0.060 kg m³ rhGH at 4% (v/v) methanol concentration. Furthermore, both substrates were

consumed sequentially by these two phenotypes and methanol consumption began when glycerol was depleted. When glycerol was totally consumed by the cells, methanol utilization rates increased, demonstrating that glycerol is a repressor of *AOX1* promoter, and excess glycerol limits the expression of *AOX1* enzyme thus resulting inefficient utilization of methanol. In addition to this, addition of methanol or increasing glycerol concentration (above 20 kg m⁻³ glycerol for Mut^s and 30 kg m⁻³ glycerol for Mut⁺) in mixed batch system inhibits the cell growth.

Using the designed defined medium for Mut⁺ phenotype where methanol was used as a sole carbon source and its optimum concentration was obtained as 3% (v/v), (22.30 kg m⁻³ ammonium sulfate, 5.62 kg m⁻³ potassium phosphate, 1.1800 kg m⁻³ magnesium sulfate, 0.8300 kg m⁻³ calcium sulfate, 0.0080 kg m⁻³ copper sulfate, 0.0012 kg m⁻³ potassium iodide, 0.0280 kg m⁻³ manganese sulfate, 0.0052 kg m⁻³ sodium molybdate, 0.0080 kg m⁻³ boric acid, 0.0080 kg m⁻³ cobalt chloride, 0.0044 kg m⁻³ zinc sulfate, 0.0750 kg m⁻³ ferric chloride, and 0.00174 kg m⁻³ biotin) oxygen transfer effects on rhGH production and cell growth were investigated at $Q_O/V_R=0.5$ vvm; pH=6.0, T=30 °C, N=250, 500, 625, 750 min⁻¹ conditions. The highest rhGH concentration was obtained at 0.5 vvm, 500 min⁻¹ condition as 0.023 kg m⁻³ with 5.37 kg m⁻³ cell density. In laboratory scale bioreactor, methanol concentration profiles coincide with the cell growth and DO profiles at all the conditions. At higher methanol utilization rates, rapid decrease in DO levels and higher cell growth rates were obtained. On the other hand, when all methanol was exhausted, no cell growth and a sudden increase in dissolved oxygen concentration were observed. This indicates that there is a strong relationship between the methanol utilization and dissolved oxygen concentration, i.e. methanol is a substrate with high oxygen demand.

Formic acid and fumaric acid, aspartic acid, lysine, proline, treonine and leucine are the organic and amino acids that were detected in the fermentation broths. Formaldehyde which is a product of alcohol oxidize enzyme was also secreted to the fermentation broth. The highest formaldehyde concentrations were obtained at growth phase, where methanol utilization rates were higher. Formate which was also detected in cultivation medium is the product of oxidized formaldehyde. Formate (formic acid) was generally produced and secreted to the medium in lag phase and then consumed by the cells in growth

phase most probably entering the carbon metabolism. It can be concluded that small amount of formaldehyde formation occurs in lag phase because AOX1 level is low and most of the formaldehyde produced in this phase is converted to formate, on the other hand with the increase in AOX1 level in growth phase, formaldehyde accumulation was observed and cells growing rapidly used formate.

In bioreactor experiments, oxygen transfer parameters which are oxygen uptake rate (OUR), r_o , and oxygen transfer coefficient, K_{La} , the physical oxygen transfer coefficient K_{La_0} , Da and η were also obtained. It was seen that agitation rate affected the K_{La} . K_{La} values increased with the increase in agitation rate and the cultivation time. The time when maximum K_{La} values were found decreased when agitation rate decreased. Furthermore, the K_{La} values obtained were almost the same throughout out the lag phase ($t=0-20$ h) because of slow cell growth.

OUR and OTR had the same trend through the fermentation processes. With an increase in cell growth, these values began to increase and then decreased. OUR was also affected by the agitation rate, i.e. increase in agitation rate resulted in increase in OUR.

Da , a dimensionless number, which relates maximum oxygen uptake and maximum transfer rates was less than 1 and did not change very much through the bioprocesses. Oxygen demand (OD), i.e. maximum possible oxygen utilization rate by the cells, was low and did not change significantly with respect to cultivation time and microbial growth. Since Da is a function of OD, Da values obtained throughout the processes were very low and varied between 0.16-0.48, which means that biochemical reaction limitations were effective.

The effectiveness factor, η , took values which were close to 1 at the beginning of log phase ($t=20$ h) where cell growth rate increased, indicating that the cells are consuming oxygen with a high rate and they generally decreased with respect to time and cell concentration.

The variations in the specific growth rate, μ ; the specific oxygen uptake rate, q_o ; specific product formation rate, q_p ; maintenance coefficients for

oxygen and substrate m_o , m_s and m_o' , m_s' and the yield coefficients with the cultivation time were investigated. At all oxygen transfer conditions, the specific growth rate (μ), specific oxygen uptake rate and substrate utilization rate were observed to decrease with the cultivation time at all conditions. In the case of specific product formation rates with respect to cultivation time and agitation rates, it is seen that these profiles had different trend. At the beginning of log phase, $t > 20$ h, it is clear that cell growth rates are smaller thus increasing pattern in specific product formation rate was observed. After a while, explosion in cell growth rate resulted in higher biomass concentration, which lessened q_p values.

Maintenance energy, denoted by m_o and m_s obtained were higher than m_o' and m_s' , approximately as twice as, since in the case of m_o and m_s by product formation was neglected. Maintenance coefficient profiles decreased generally when agitation rate decreased, indicating that at high stirring rate cells use more energy to repair the damaged cellular components and to stabilize themselves with the environment. The lowest maintenance coefficients were obtained at $N=500 \text{ min}^{-1}$ condition. This may be expected result since among the other oxygen transfer conditions, this agitation rate was the optimum value in this defined-batch fermentation system and resulted in less stress on cell that was caused by extreme oxygen conditions, therefore cells require less energy for maintenance.

In addition to batch bioreactors which were used for investigation of oxygen effects on rhGH production and bioreactor characteristics, an impulse feeding strategy was also applied to understand the effects of methanol addition to the cultivation medium during the process. Addition of methanol for the second time after the initially supplied methanol was consumed completely, increased the cell concentration from $C_x=5.43 \text{ kg m}^{-3}$ to $C_x=10.88 \text{ kg m}^{-3}$ and and rhGH concentration from 0.014 kg m^{-3} to 0.030 kg m^{-3} rhGH. Slightly higher overall yields were obtained when methanol was added for the second time; these were $Y_{p/x}=0.0028 \text{ kg hGH kg}^{-1} \text{ cell}$ and $Y_{p/s}=0.0007 \text{ kg hGH kg}^{-1} \text{ methanol}$. On the other hand, the overall product yields obtained before the addition of methanol were $Y_{p/x}=0.0026 \text{ kg hGH kg}^{-1} \text{ cell}$ and $Y_{p/s}=0.0006 \text{ kg hGH kg}^{-1} \text{ methanol}$. Moreover, after addition of methanol for the second time, almost no lag phase was observed due to the present of AOX1 enzyme and a rapid decrease in oxygen concentration level occurred. In addition to

this, the same organic acids, amino acids and formaldehyde profiles were determined but higher amount of these substances were detected in impulse feeding fermentation broth when compared with the others, most probably due to higher cell density obtained. Since oxygen transfer characteristics of impulse feeding strategy could not be analyzed properly, overall mass transfer coefficient and oxygen uptake rate values could not be obtained by dynamic method and other coefficients could not be compared adequately. After addition of methanol, rapid decrease in dissolved oxygen level occurred. This prevented the use of dynamic method. At $t=51$ h, K_La value, OUR and Da were obtained since dissolved oxygen level increased to its saturated level since all methanol added was completely consumed. These are 0.027 h^{-1} , $0.0017 \text{ mol m}^{-3}\text{s}^{-1}$, 0.91, respectively. Although Da was still less than one, meaning that biochemical reaction limitations were effective, a rise in Da number was resulted after addition of methanol for the second time, which indicates that maximum possible oxygen utilization rate by the cells increased also.

Finally, purification strategy applied was verified with SDS-page, Western-blot and MALDI-TOF mass spectrometry analysis and automated Edman degradation was performed by PROCISE 494 gas-phase/liquid-pulse sequencer (Applied Biosystems, Foster City, CA) for N terminal analysis, which showed that six amino acid residues at the N termini of rhGH treated with Factor Xa were the same as the mature hGH.

REFERENCES

- Atkinson, B., Mavituna, F., 1991. Biochemical Engineering and Biotechnology Handbook, 2nd ed., Macmillan Publishers Ltd., England.
- Bailey, E. J., Ollis, F. D., 1986. Biochemical Engineering Fundamentals, 2nd ed., McGraw-Hill, Inc., Singapore.
- Baulieu, E., and Kelly, P. A., 1990. "HORMONES from molecules to disease", Herman Press, New York
- Becker, G.W. and Hsiung, H.M., 1986. Expression, secretion and folding of human growth hormone in *Escherichia coli*. FEBS Letters, 204 (1) :145-150.
- Binkley, S. A., 1994. Endocrinology, Harper Collins College Publishers, New York.
- Brierley, R.A., Bussineau, C., Kosson, R., Melton, A., Siegel, R.S., 1990. Fermentation development of recombinant *Pichia pastoris* expressing the heterologous gene: bovine lysozyme, Ann. N.Y. Acad. Sci. 589: 350-362.
- Bryan, P. N., 2002. Prodomains and protein folding catalysis, Chem. Rev.,102: 4805-4815.
- Boze, H., Laborde, C., Chemardin, P., *et al.* 2001. High-level secretory production of recombinant porcine follicle-stimulating hormone by *Pichia pastoris*. *Process Biochem* 36: 907–913.
- Bylund, F., Castan,a., Mikkola,R.,Andide,A. and Larsson,G.,2000. Influence of scale-up on the quality of recombinant human growth hormone. *Biotechnology and Bioengineering*, 69 (2) : 119-128.
- Castan, A.,Narsman, A. and Enfors, S.D., 2002. Oxygen enriched air supply in *Escherichia coli* processes: production of biomass and recombinant human growth hormone. *Enzyme and Microbial Technology*, 30:847-854.
- Cereghino, J. L., Cregg, J. M., Heterologous, 2000. Protein Expression in the Methylotropic Yeast *Pichia Pastoris*, *FEMS Microbiology Reviews* 24; 45-66
- Cereghino, G. P. L., Cereghino, J. L., Ilgen, C., Cregg, J. M., 2002. Production of recombinant proteins in fermenter cultures of the *Pichia Pastoris*, *Biotechnology*, 13:329–332
- Chang, C.N.,Rey, M.,Bachner, B.,Heyneker,H.L., and Gray, G.,1987. High-level secretion of human growth hormone by *Escherichia coli*. *Gene*, 55:189-196.

- Charoenrat, T., Ketudat-Cairns, M., Jahic, M., Veide, A., Enfors, S. O., 2005. Oxygen-limited fed-batch process: an alternative control for *Pichia pastoris* recombinant protein processes, *Bioprocess Biosyst. Eng.*, 27: 399–406.
- Charoenrat, T., Ketudat-Cairns, M., Jahic, M., Veide, A., Enfors, S.O., 2006. Increased total air pressure versus oxygen limitation for enhanced oxygen transfer and product formation in a *Pichia pastoris* recombinant protein process, *Biochemical Engineering Journal*, 30;205–211.
- Clare, J.J., Rayment, F.B., Ballantyne, S.P., Sreerkrishna, K., Romanos, M.A., 1991. High-level expression of tetanus toxin fragment C in *Pichia pastoris* strains containing multiple tandem integrations of the gene. *BioTechnology* 9: 455–460.
- Cos, O., Resina, D., Ferrer, P., Montesinos, J.L., Valero, F., 2005a. Heterologous protein production of *Rhizopus oryzae* lipasa in *Pichia pastoris* using the alcohol oxidase and formaldehyde dehydrogenase promoters in batch and fed-batch cultures. *Biochem. Eng. J.* 26, 86–94.
- Cos, O., Serrano, A., Montesinos, J.L., Ferrer, P., Cregg, J.M., Valero, F., 2005b. Combined effect of the methanol utilization (Mut) phenotype and gene dosage on recombinant protein production in *Pichia pastoris* fed-batch cultures. *J. Biotechnol.* 116, 321–335.
- Cregg, J.M., Vedvick, T.S., Raschke W.C., 1993. Recent advances in the expression of foreign genes in *Pichia pastoris*. *Biotechnology*, 11: 905–909.
- Cregg, J.M., 1999. Gene expression systems, Edited by Joseph M. Fernandez and James P. Hoeffler, Academic Press, San Diego, California.
- Cunha, A.E., Clemente, J.J., Gomes, R., Pinto, F., Thomaz, M., Miranda, S., Pinto, R., Moosmayer, D., Donner, P., Carrondo, M.J.T., 2004. Methanol induction optimization for scFv antibody fragment production in *Pichia pastoris*, *Biotechnol Bioeng* 86:458–467.
- Curvers S., Brixius P., Klauser T., Thommes J., Weuster-Botz D., Takors R., Wandrey C. 2001. Human chymotrypsinogen B production with *Pichia pastoris* by integrated development of fermentation and downstream processing. Part 1. Fermentation. *Biotechnol Prog* 17:495– 502
- Çalık, P., Çalık, G., and Özdamar, T.H., 1998. Oxygen transfer effects in serine alkaline protease fermentation by *Bacillus licheniformis*: Use of citric acid as the carbon source. *Enzyme and Microbial Technology.* 23, 451-461.

- Çalık, P., Çalık, G., Takaç, S., Özdamar, T.H., 1999. Metabolic Flux Analysis for Serine Alkaline Protease Fermentation by *Bacillus licheniformis* in a Defined Medium: Effects of the Oxygen Transfer Rate, *Biotechnology and Bioengineering*, 64, 151-167.
- Çalık P., Çalık G., Özdamar T.H., 2000. Oxygen-Transfer Strategy and Its Regulation Effects in Serine Alkaline Protease Production by *Bacillus licheniformis*, *Biotechnology And Bioengineering*, 69, 301-311.
- Çalık P, Yılgor P, Ayhan P, Demir A, 2004. Oxygen Transfer effects on recombinant benzaldehyde lyase production, *Chemical Engineering Science*, 59, 5075-5083.
- Çalık P, Yılgor P, Demir A, 2006. Influence of controlled-pH and uncontrolled-pH operations on recombinant benzaldehyde lyase production by *Escherichia coli*, *Enzyme and Microbial Technology*, 38, 617-627.
- Daly, R. and Hearn, M. T. W., 2005, Expression of heterologous proteins in *Pichia Pastoris*: a useful experimental tool in protein engineering and production, *J. Mol. Recognit.*, 18: 119–138
- Ellis, S.B., Brust, P. F., Koutz, P.J., Waters, A.F., Harpold, M.M., and Gingeras, T. R., 1985. Isolation of alcohol oxidase and two other methanol regulatable genes from the yeast *Pichia Pastoris*. *Mol. Cell Biol.* 5:1111-1121.
- Eurwilaichitr, L., Roytroku, R., Suprosongsin, C., Manitchotpisit, P. and Panyim, S., 2002. Glutamic acid and alanine spacer is not necessary for removal of MF α -1 signal sequence fused to the human growth hormone produced from *Pichia pastoris*. *World Journal of Microbiology and Biotechnology*, 18 : 493-495.
- Franchi, E., Maisano, F., Testori, S.A., Galli, G., Toma, S., Parente, L., Ferra, F. and Grandi, G., 1991. A new human growth hormone production process using a recombinant *Bacillus subtilis* strain. *Journal of Biotechnology*, 18: 41-54.
- Glazer, A. N., Nikaido, H., 1995. *Microbial Biotechnology: Fundamentals of Applied Biotechnology*, W.H. Freeman and Company, USA
- Goeddel, D.V., Heyneker, H.L., Hozumi, T., Arentzen, R., Itakura, K., Yansura, D.G., Ross, M.J., Miozzari, G., Crea, R. and Seeburg, P.H., 1979. Direct expression in *Escherichia coli* of a DNA sequence coding for human growth hormone. *Nature*, 281:544-548.
- Gray, G.L., Bladridge, J.S., McKeown, K.S., Heyneker, H.L. and Chang, C.N., 1985. Periplasmic production of correctly processed human growth

- hormone in *Escherichia coli* : natural and bacterial signal sequences are interchangeable. *Gene*, 39:247-25.
- Hellwig, S., Emde, F., Raven, N.P.G., Henke, M., van der Logt, P., Fischer, R.. 2001. Analysis of single-chain antibody production in *Pichia pastoris* using on-line methanol control in fed-batch and mixed-feed fermentations, *Biotechnol Bioeng* 74:344–352.
- Higgins, D.R., Cregg, J.M.,1998. *Pichia* protocols. *Methods in Molecular Biology*. Totowa, NJ: Humana Press, Inc.
- Hsiung, H.M., Mayne, N.G. and Becker, G.W.,1986. High-level expression, efficient secretion and folding of human growth hormone in *Escherichia coli*. *Bio/technology*, 4:991-995.
- Ikehara, M.,Ohtsuka ,E.,Tokunaga, T.,Taniyama,Y., Iwai, S.,Kitano, K.,Miyamoto, S.,Oghi,T.,Sakuragawa,Y.,Fujiyama,K.,Ikari, T.,Kobayashi, M.,Miyake, T.,Shibahar,,S.,Ono, A.,Ueda, T.,Tanaka, T.,Baba, H.,Miki, T.,Sakurai, A.,Oishi, T.,Chisaka, O. and Metsubara, K., 1984. Synthesis of a gene for human growth hormone and its expression in *Escherichia coli*. *The Proceedings of the National Academy of Sciences USA*, 81: 5956-5960.
- Inan, M., Meagher M. M., 2001. The effect of ethanol and acetate on protein expression in *Pichia Pastoris*, *journal of Bioscience and Bioengineering* , Vol.92, No.4, 337-341.
- Jacobs, M.,Eliasson, M.,Uhlen, M. and Flock, J., 1985. Cloning, sequencing and expression of subtilisin Carlsberg from *Bacillus licheniformis*. *Nucleic Acids Research*, 13: 8913-8927.
- Jahic M., Wallberg F., Bollok M., Garcia P., Enfors S-O. 2003b. Temperature limited fed-batch technique for control of proteolysis in *Pichia pastoris* bioreactor cultures. *Microbial Cell Factories* 2:6.
- Janic, M., Veide, A., Charoenrat, T., Teeri, T., and Enfors, S.O., 2006. Process technology for production and recovery of heterologous proteins with *Pichia pastoris*, *Biotechnol. Prog.*, 22:1465-1473.
- Jensen, E.B. and Carlsen, S.,1990. Production of recombinant human growth hormone in *Escherichia coli* : Expression of different precursors and physiological effects of glucose, acetate, and salts. *Biotechnology and Bioengineering*, 36: 1-11.
- Jungo, C., Rerat, C., Marison, I.W., von Stockar, U., 2006. Quantitative characterization of the regulation of the synthesis of alcohol oxidase and

- of the expression of recombinant avidin in a *Pichia pastoris* Mut⁺ strain. *Enzyme Microb. Technol.* 39 (4), 936–944.
- Jungo, C., Marison, I., von Stockar, U., 2007. Regulation of alcohol oxidase of a recombinant *Pichia pastoris* Mut⁺ strain in transient continuous cultures *Journal of Biotechnology* 130; 236–246
- Kajino, T., Saito, Y., Asami, O., Yamada, Y., Hirai, M. and Umeta, S., 1997. Extracellular production of an intact and biologically active human growth hormone by the *Bacillus Brevis* system. *Journal of Industrial Microbiology & Biotechnology*, 19: 227-231.
- Kane, J.F., and Hartley, D.L., 1988. Formation of recombinant protein inclusion bodies in *Escherichia Coli*. *Trends in Biotechnology*, 6: 95-101.
- Katakura, Y., Zhang, W.H., Zhuang, G.Q., Omasa, T., Kishimoto, M., Goto, W., Suga, K.I., 1998. Effect of methanol concentration on the production of human beta(2)-glycoprotein I domain V by a recombinant *Pichia pastoris*: a simple system for the control of methanol concentration using a semiconductor gas sensor. *J. Ferm. Bioeng.* 86, 482–487.
- Kato, C., Kobayashi, T., Kudo, T., Frusetto, T., Murakami, Y., Tanaka, T., Baba, H., Oishi, T., Ohtsuka, E., Ikehera, M., Yanagida, T., Keto, H., Moriyama, S. and Horikoshi, K., 1987. Construction of an excretion vector and extracellular production of human growth hormone from *Escherichia coli*. *Gene*, 54: 197-202.
- Katri, K.N., Hoffmann, F., 2006, Impact of methanol concentration on secreted protein production in oxygen-limited cultures of recombinant *Pichia pastoris*. *Biotechnol. Bioeng.* 93, 871- 879.
- Kirk, R. E., Othmer, D. F., 1994. *Encyclopedia of Chemical Technology*, 4th Ed., the Interscience Encyclopedia Inc., New York.
- Klug, W. S., Cummings, M. R., Spencer, C. A., 2006. *Concepts of genetics*, Eight Edition, Pearson Prentice Hall, New Jersey.
- Lee, C.Y., Lee, S.J., Jung, K.H., Katoh, S., Lee, E.K., 2003. High dissolved oxygen tension enhances heterologous protein expression by recombinant *Pichia pastoris*, *Process Biochem.*, 38; 1147–1154.
- Lehninger, A.L., 1979. *Biochemistry*, Second edition, Worth Publishers Inc., New York.
- Li, Z., Xiong F, Lin, Q., et al. 2001. Low temperature increases the yield of biologically active herring antifreeze protein in *Pichia pastoris*. *Prot Exp Pur* 21(3): 438–445.

- Lodish, H., Berk, A., Zipursky, S. L., Matsudaira, P., Baltimore, D., Darnell, J., 2004. *Molecular Cell Biology*, 5th Ed., W.H. Freeman Co., New York.
- Loewen, M.C., Liu, X., Davies, P.L., Daugulis, A.J., 1997. Biosynthetic production of type II fish antifreeze protein fermentation by *Pichia pastoris*. *Appl. Microbiol. Biotechnol.* 48, 480–486.
- Nakayama, A., Ando, K., Kawamura, K., Mita, I., Fukazawa, K., Hori, M., Honjo, M. and Furutani, Y., 1988. Efficient secretion of the authentic mature human growth hormone by *Bacillus subtilis*. *Journal of Biotechnology*, 8: 123-134.
- Nielsen, J., Villadsen, J., 1994. *Bioreaction Engineering Principles*, Plenum Press, New York.
- Nielsen, J., Villadsen, J., Liden, G., 2003. *Bioreaction Engineering Principles*, Second Edition, Plenum Press, New York.
- Macauley-Patrick, S., Fazenda, M. L., McNeil, B., and Harvey, L. M., 2005. Heterologous protein production using the *Pichia Pastoris* expression system, *Yeast*; 22: 249–270.
- Middleton, R. and Hofmeister, A., 2004. New shuttle vectors for ectopic insertion of genes into *Bacillus Subtilis*, *Plasmid*, 51: 238- 245.
- Moses, V., Cape, R. E., 1991. *Biotechnology: The Science and the Business*, Harwood Academic Publishers, Switzerland.
- Ohya, T., Morita, M., Miura, M., Kuwae, S., and Kabayashi, K., 2002. High level production of Preurokinase-Annexin V Chimeras in the methylotropic yeast *Pichia pastoris*, *Journal of Bioscience and Bioengineering*, Vol.94, No:5, 467-473.
- Patra, A.K., Mukhopadhyay, R., Mukhija, R., Krishnan, A., Garg, L.C. and Panda, A.K., 2000. Optimization of inclusion body solubilization and renaturation of recombinant human growth hormone from *Escherichia coli*. *Protein Expression and Purification*, 18: 182-192.
- Primrose, S.B., Twyman, R.M. and Old, R.W., 2001. *Principles of gene manipulation*, 6th edition. Blackwell Publishing, USA.
- Rainer, B., W., 1990. Determination Methods of the Volumetric Oxygen Transfer $K_L a$ in Bioreactors, *Chem. Biochem. Eng. Q.*, 4(4), 185-186.
- Rena, H.T., Yuan, J.Q., Bellgardt, H., 2006. Macrokinetic model for methylotrophic *Pichia pastoris* based on stoichiometric balance, *Journal of Biotechnology* 106, 53-68.

- Roman, R, Ferrer, P., Valero, F., 2007. Sorbitol co-feeding reduces metabolic burden caused by the overexpression of a *Rhizopus oryzae* lipase in *Pichia pastoris*, *Journal of Biotechnology*, 130: 39-46.
- Romanos, M., 1995. Advances in the use of *Pichia pastoris* for high level gene expression. *Curr.Opin.Biotechnol.*, 6: 527-533.
- Sambrook, J., Russell, D. W., 2001. *Molecular Cloning: A Laboratory Manual* Vol. 1, 2, 3, 3rd ed., Cold Spring Harbor, USA.
- Sarramegna, V., Talmont, F., de Roch, M.S., Milon, A., Demange, P., 2002. Green fluorescent protein as a reporter of human μ -opioid receptor over expression and localization in the methylotrophic yeast *Pichia pastoris*. *J Biotechnol* 99: 23-39.
- Scragg, A. H., 1988. *Biotechnology for Engineers: Biological Systems in Technological Processes*, Ellis Horwood Ltd., ENGLAND.
- Shin, C.S., Hong, M.S., Kim, D.Y., Shin, H.C., and Lee, J., 1998. Growth-associated synthesis of recombinant human glucagon and human growth hormone in high-cell density cultures of *Escherichia coli*. *Applied Microbial Biotechnology*, 49: 364-370.
- Shin, N.K., Kim, D.Y., Shin, C.S., Hong, M.S., Lee, J., Shin, H.C., 1998. High-level production of human growth hormone in *Escheriichia coli* by a simple recombinant process. *Journal of biotechnology*, 62: 143-151.
- Shuler, M. L., Kargi, F., 2002. *Bioprocess Engineering: Basic Concepts*, 2nd Ed., Prentice Hall Inc., USA.
- Soares, C.R.J., Gomide, F.I.C., Ueda, E.K.M, Bartolini, P., 2003. Periplasmic expression of human growth hormone via plasmid vectors containing the λP_L promoter: use of HPLC for product quantification. *Protein Engineering*, 16: 1131-1138.
- Sreekrishna, K., Brankamp, R.G., Kroop, K.E., Blankenship, D.T., Tsay, J.T., Smith, P.L., Wierschke, J.D., Subramaniam, A., Birkenberger, L.A., 1997. Strategies for optimal synthesis and secretion of heterologous proteins in the methylotrophic yeast *Pichia pastoris*. *Gene*, 190: 55-62.
- Sunga A.J., Cregg J.M., 2004, The *Pichia Pastoris* formaldehyde dehydrogenase gene (PNO1) as marker for selection of multicopy expression strains of *P. Pastoris*. *Gene* 330: 39-47
- Şentürk, B., 2006. Reaksiyon mühendisliği prensipleriyle rekombinant insan büyüme hormonu üretimi için bioproses geliştirilmesi. Y.Lisans tezi, Ankara Üniversitesi, Ankara.

- Tabandeh, F., Shojaosadeti A.A., Zomorodipour, A., Khodabandeh, M., Saneti, M.H., Yakhchali, B., 2004. Heat-induced production of human growth hormone by high cell density cultivation of recombinant *Escherichia coli*. *Biotechnology Letters*, 26: 245-250.
- Trentmann, O., Khatri, N. K., Hoffmann, F., 2004 Reduced oxygen supply increases process stability and product yield with recombinant *Pichia pastoris*. *Biotechnol. Prog.*, 20, 1766-1775.
- Trevino, L. L., Viader-Salvado, J.M., Barrera-Saldana, H.A., Guerrero-Olazarán, M., 2000. Biosynthesis and secretion of recombinant human growth hormone in *Pichia pastoris*. *Biotechnology Letters*, 22: 109-114.
- Trinh, L. B.; Phue, J. N.; Shiloach, J., 2003 Effect of methanol feeding strategies on production and yield of recombinant mouse endostatin from *Pichia pastoris*. *Biotechnol. Bioeng.*, 82, 438-444.
- Thorpe, E.D., d'Anjou, M.C., Daugulis, A.J., 1999. Sorbitol as a non-repressing carbon source for fed-batch fermentation of recombinant *Pichia pastoris*. *Biotechnol. Lett.* 21, 669-672.
- Tschop J. F., Brust, P. F., Cregg, J.M., Stillman, C.A., and Gingeras, J. R., 1987. Expression of the *lacZ* gene from two methanol-regulated promoters in *Pichia Pastoris*. *Nucleic Acids Res.* 15:3859-3879.
- Uchida, H., Naito, N., Asada, N., Wada, M., Ikeda, M., Kobayashi, H., Asanagi, M., Mori, K., Fujita, Y., Konda, K., Kusuhara, N., Kamioka, T., Nakashima, K., Honjo, M., 1997. Secretion of authentic 20-kDa human growth hormone in *Escherichia coli* and properties of the purified product. *Journal of Biotechnology*, 55: 101-112.
- Wang, J.J., Rojanatavorn, K., Shih, J.C.H., 2004. Increased production of Bacillus Keratinase by chromosomal integration of multiple copies of the *kerA* gene, *Biotechnology & Bioengineering*, Vol. 87, No.4
- Xie, J., Zhang, L., Ye, Q., *et al.* 2003. Angiostatin production in cultivation of *Pichia pastoris* fed with mixed carbon sources. *Biotechnol Letts* 25: 173-177.
- Xie, J.L., Zhou, Q.W., Pen, D., Gan, R.B., Qin, Y., 2005. Use of different carbon sources in cultivation of recombinant *Pichia pastoris* for angiostatin production. *Enzyme Microb. Technol.* 36, 210-216.
- Zhang, X.W., Sun, T., Lui, X., Gu, D., Huang, X.N., 1998. Human growth hormone production by high cell density fermentation of recombinant *Escherichia coli*. *Process Biochemistry*, 33: 683-686.

- Zhang, W., Inan, M., Meagher, M.M., 2000a. Fermentation strategies for recombinant protein expression in the methylotrophic yeast *Pichia pastoris*. *Biotechnol. Bioproc. Eng.* 5, 275–287.
- Zhou, X.-S., Zhang, Y.-X., 2002. Decrease of proteolytic degradation of recombinant hirudin produced by *Pichia pastoris* by controlling the specific growth rate. *Biotechnol. Lett.* 24, 1449–1453.

APPENDIX A

Preparation of Buffers and Solutions Used in Experiments

LB

Soytryptone	10 kg m ⁻³
Yeast extract	5 kg m ⁻³
NaCl	10 kg m ⁻³

LBA

Soytryptone	10 kg m ⁻³
Yeast extract	5 kg m ⁻³
NaCl	10 kg m ⁻³
Agar	15 kg m ⁻³

ALKALINE LYSIS SOLUTION I

Glucose	50 mM
Tris-HCl (pH=8.0)	25 mM
EDTA	10 mM

ALKALINE LYSIS SOLUTION II

NaOH	0.2 N
SDS	% 1

ALKALINE LYSIS SOLUTION III

Potassium Acetate	5 M
Acetic Acid	11.5 (v/v)

SET

NaCl	75 mM
EDTA	25 mM

10X TBE

Tris	108 kg m ⁻³
Boric Acid	55 kg m ⁻³
EDTA	9.3 kg m ⁻³

TSE

Tris HCl, pH= 8.0	10 mM
NaCl	300 mM
EDTA	10 mM

SOLUTION A

Tris HCl, pH= 8.1	10 mM
EDTA	10 mM
NaCl	50 mM
Saccharose	8% (w/v)

SOLUTION B

SDS	1% (w/v)
NaOH	0.2 M

SOLUTION C

Potassium Acetate	5 M
Acetate Acid	60 ml
dH ₂ O	Up to 100 ml

Antibiotics	Stock Solutions	
	Concentration	Storage
Zeocin	100 mg/ml in dH ₂ O	-20°C
Chloramphenicol	35 mg/ml in ethanol	-20°C
Ampicillin	100 mg/ml in dH ₂ O	-20 °C

Lysis buffer (1 liter)

50 mM NaH ₂ PO ₄	6.90 g NaH ₂ PO ₄ ·H ₂ O (MW 137.99 g/mol)
300 mM NaCl	17.54 g NaCl (MW 58.44 g/mol)
10 mM imidazole	0.68 g imidazole (MW 68.08 g/mol)

Adjust pH to 8.0 using NaOH

Wash buffer (1 liter)

50 mM NaH ₂ PO ₄	6.90 g NaH ₂ PO ₄ ·H ₂ O (MW 137.99 g/mol)
300 mM NaCl	17.54 g NaCl (MW 58.44 g/mol)
20 mM imidazole	1.36 g imidazole (MW 68.08 g/mol)

Adjust pH to 8.0 using NaOH

Elution buffer (1 liter)

50 mM NaH ₂ PO ₄	6.90 g NaH ₂ PO ₄ ·H ₂ O (MW 137.99 g/mol)
300 mM NaCl	17.54 g NaCl (MW 58.44 g/mol)
250 mM imidazole	17.00 g imidazole (MW 68.08 g/mol)

Adjust pH to 8.0 using NaOH

1x Equilibration / wash buffer for His-Tag purification

50 mM sodium phosphate buffer, pH 7.0; 300 mM NaCl.

**1x Elution buffer for His-Tag purification
PBS buffer**

50 mM sodium phosphate buffer, pH 7.0; 300 mM NaCl; 150 mM Imidazole.

8.0 g NaCl, 0.2 g KCl, 1.44 g NaHPO₄, 0.24 g K₂HPO₄ were dissolved in dH₂O and the volume made up to 1000 ml. The pH was adjusted at pH:7.0

1 M potassium phosphate, pH 6.0

56.48 g KH₂PO₄, 14.8 g K₂HPO₄ was dissolved in dH₂O

and the volume made upto 500 ml. The pH was controlled. The buffer was autoclaved and stored at room temperature.

**10x YNB
Stock solution**

17 g Yeast Nitrogen Base without amino acids, 50 g $(\text{NH}_4)_2\text{SO}_4$ was dissolved in dH_2O and the volume made upto 500 ml. The solution was autoclaved, aliquoted into 50 ml Falcon[®] tubes and stored at room temperature in dark.

**3 M Sodium
acetate, pH 5.2**

24.6 g sodium acetate was dissolved in 80 ml dH_2O and the pH was adjusted to 5.2 with 3M acetic acid. The buffer was filter sterilized and stored at 2-8°C.

**Yeast Lysis
Solution**

2 % Triton X-100, 1% SDS, 100 mM NaCl, 10 mM Tris-Cl-pH8.0, 1mM Na_2EDTA . The solution was autoclaved and stored at room temperature.

**50 mM potassium
acetate, pH 5.5**

0.049 g potassium acetate, dissolved in 8.5 ml dH_2O , titrated with 10N glacial acetic acid to pH 5.5 and make up to 10 ml with dH_2O . Autoclaved and store at room temperature.

TE Buffer, pH 8.0

1 ml of 1M Tris-Cl (pH 8.0), 200 μl of 0.5 M EDTA (pH 8.0) was added to dH_2O and the volume was made up to 100 ml. The buffer was autoclaved and stored at room temperature.

**0.125 M (or 0.5 M)
EDTA, pH 8.0**

4.65 g (or 18.61 g) Ethylenediaminetetra acetic acid disodium salt dihydrate was dissolved in 80 ml dH_2O . NaOH was added until EDTA was dissolved. The final pH was further adjusted to pH 8.0 and the final volume was adjusted to 100 ml. The buffer was autoclaved and stored at room temperature.

APPENDIX B

Preparation of SDS-Polyacrylamide Gel and Staining

Preparation of Separation and Stacking Gel for SDS-Polyacrylamide Gel

Electrophoresis:

	Stacking Gel	Seperating Gel		
	5%	7.5%	10%	12%
30% acrylamide mix	1.67 ml	2.5 ml	3.33 ml	4 ml
dH ₂ O	5.68 ml	4.85 ml	4.05 ml	3.35 ml
1.5 M Tris-HCl, pH 8.8	-	2.5 ml	2.5 ml	2.5 ml
0.5 M Tris-HCl, pH 6.8	2.5 ml	-	-	-
10% (w/v) SDS	100 µl	100 µl	100 µl	100 µl
10% (w/v) ammonium persulfate	60 µl	50 µl	50 µl	50 µl
TEMED	15 µl	10 µl	10 µl	10 µl

Preparation of Materials Used for Staining of SDS-Polyacrylamide Gels with Coomassie Brilliant Blue:

A. Staining Solution:

Dissolve 0.25g Coomassie Brilliant Blue in 100 ml methanol: acetic acid solution.

B. Methanol: Acetic Acid Solution:

Combine 900 ml of methanol:H₂O (500 ml of methanol and 400 ml of H₂O) and 100 ml of glacial acetic acid.

Preparation of Materials Used for Staining of SDS-Polyacrylamide Gels with Silver Salts:

A. Fixer

Mix 150 ml methanol + 36 ml acetic acid + 150 μ l 37% formaldehyde and complete to 300 ml with distilled water. This solution can be used several times.

B. 50% Ethanol

Mix 600 ml pure ethanol + 600 ml distilled water. This solution should always be prepared freshly.

C. Pretreatment Solution

Dissolve 0.08 g sodium thiosulphate ($\text{Na}_2\text{S}_2\text{O}_3 \cdot 5\text{H}_2\text{O}$) in 400 ml distilled water by mixing with a glass rod. Take 8 ml and set aside for further use in developing solution preparation.

D. Silver Nitrate Solution

Dissolve 0.8 g silver nitrate in 400 ml distilled water and add 300 μ l 37% formaldehyde.

E. Developing Solution

Dissolve 9 g potassium carbonate in 400 ml distilled water. Add 8 ml from pretreatment solution and 300 μ l 37% formaldehyde.

F. Stop Solution

Mix 200 ml methanol + 48 ml acetic acid and complete to 400 ml with distilled water.

APPENDIX C

Thermodynamic properties of designed primers together with dimer and self-complimentary formation affinities

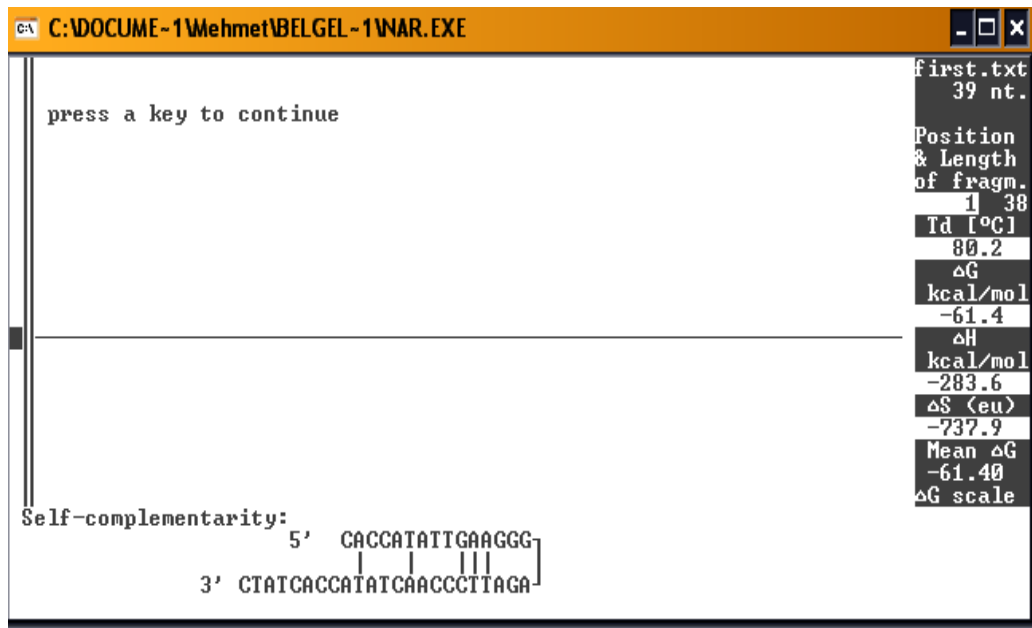


Figure A.1 First forward primer.

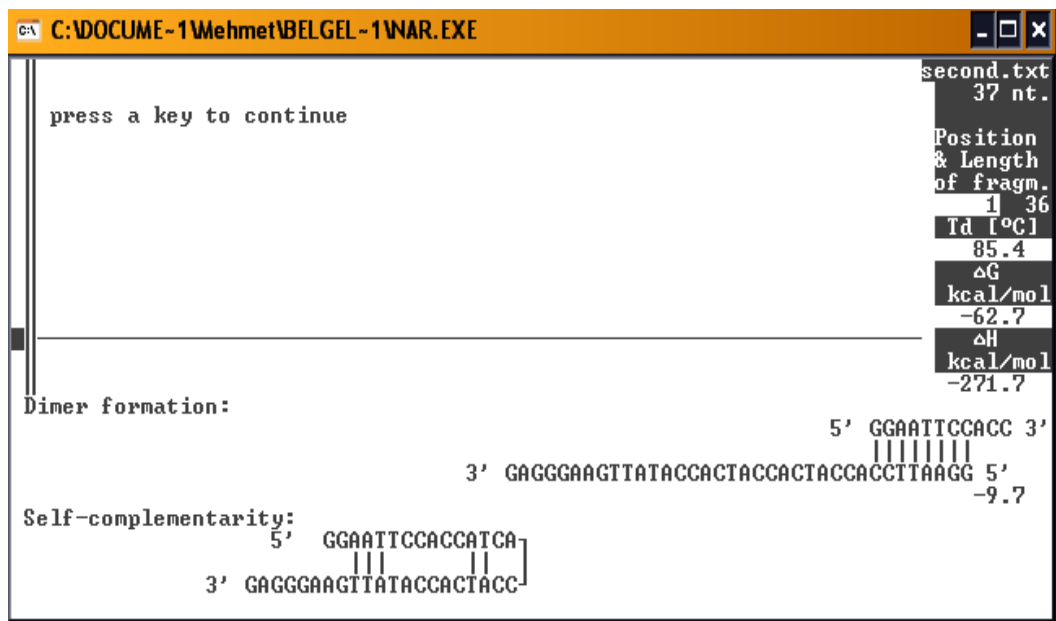


Figure A.2 Second forward primer.

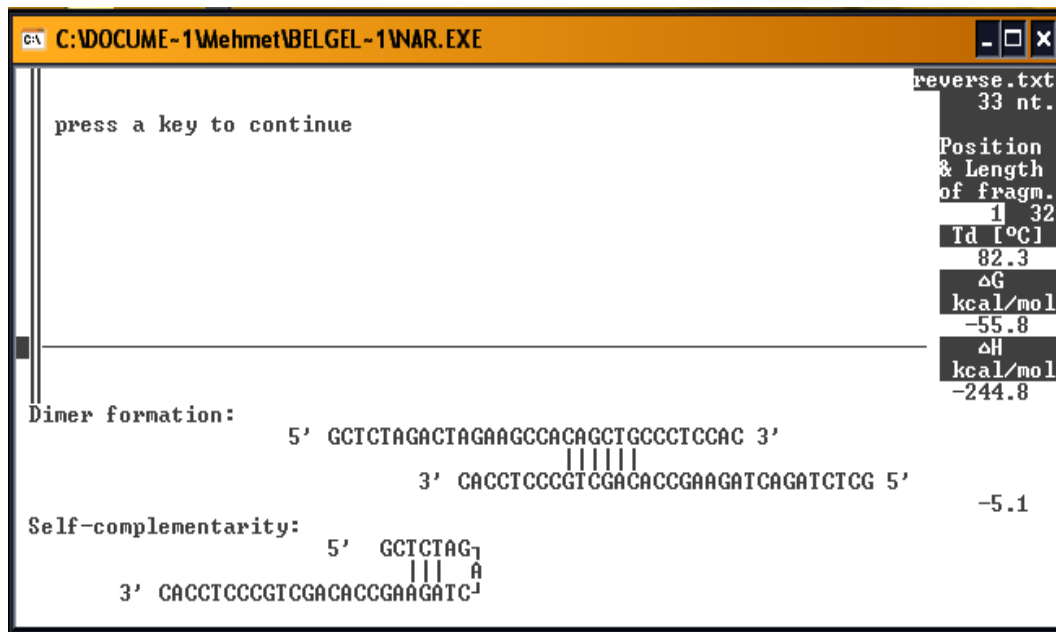


Figure A.3 Reverse primer.

APPENDIX D

Sequence of pPICZaA::hGH plasmid

agatctaacatccaaagacgaaaggttgaatgaaaccttttggccatccgacatccacaggtccat
tctcacacataagtgcacaaacgcaacaggaggggatacactagcagcagaccgttgcaaacgcagg
acctccactcctcttctcctcaacaccacttttggccatcgaaaaaccagcccagttattgggctt
gattggagctcgctcattccaattccttctattaggctactaacaccatgactttattagcctgtc
tatcctggccccctggcgagggtcatgtttgtttatttccgaatgcaacaagctccgcattacac
ccgaacatcactccagatgagggctttctgagtggtgggtcaaatagtttcatgttccccaaatgg
cccaaaactgacagtttaaacgctgtcttggaaacctaatatgacaaaaagcgtgatctcatccaaga
tgaactaagtttgggttcggttgaatgctaaccggccagttgggtcaaaaagaaacttccaaaagtcgg
cataccgtttgtcttgggtattgattgacgaatgctcaaaaataatctcattaatgcttagcg
cagtcctctctatcgcttctgaacccccggtgcacctgtgcccgaacgcaaatggggaaacaccccgt
tttggatgattatgcattgtctccacattgtatgcttccaagattctgggtgggaatactgctgat
agcctaacgttcatgatcaaaatttaactgttctaaccctacttgacagcaatataataaacagaa
ggaagctgccctgtcttaaaccttttttttatcatcattattagcttactttcataattgcgact
ggttccaattgacaagcttttgattttaacgacttttaacgacaacttgagaagatcaaaaaacaa
ctaattattcgaacgatgagatttccttcaatttttactgctgttttattcgcagcatcctccgc
attagctgctccagtcacactacaacagaagatgaaacggcacaatcccggtgaagctgtcat
cggttactcagattagaaggggatttcgatgttgcgtgttttggccattttccaacagcacaaaataa
cgggttattgtttataaatactactattgcccagcattgctgctaaagaagaaggggtatctctcga
gaaaagagaggctgaagctgaattcaccatcaccatcaccatattgaagggagattcccaactat
accactatctcgtctattcgataacgctatgcttcggtgctcatcgtcttcatcagctggccttga
cacctaccaggagtttgaagaagcctatatcccaaagggaacagaagtattcattcctgcagaacc
ccagacctccctctgtttctcagagctatcccgacacctccaacagggaggaaacacaaacagaa
atccaacctagagctgctccgcctctccctgctgctcatccagtcgtggctggagcccgtgcagtt
cctcaggagtgcttcgccaacagcctagtgtagcggcctctgacagcaacgtctatgacctcct
aaaggacctagaggaaggcatccaacgctgatggggaggctggaagatggcagccccggactgg
gcagatcttcaagcagacctacagcaagttcgacacaaactcacacaacgatgacgcaactactcaa
gaactacgggctgctctactgcttcaggaaggacatggacaaggctcgagacattcctgcgcatcgt
gcagtgccgctctgtggagggcagctgtggcttctagcttagaacaaaaactcatctcagaagagg
atctgaatagcgcgctcgacctatcatcatcatcattgagtttgtagccttagacatgactgtt
cctcagttcaagttgggcacttacgagaagaccggtcttgctagatttcaatcaagaggatgtcag
aatgccatttgctgagagatgcaggcttcatTTTTGATACTTTTTATTGTAACCTATATAGTA
taggatttttttgtcattttgtttcttctcgtacgagcttgctcctgatcagcctatctcgcagc
tgatgaatatcttgggtaggggtttgggaaaatcattcgagtttgatgttttcttggatattcc
cactcctcttcagagtacagaagattaagtgagaccttcgtttgtgaggatccccacacaccata
gcttcaaaatgtttctactcctttttactcctccagattttctcggactccgcgcatcgccgtac
cacttcaaacacccaagcagcactaactaaatTTTCCCTCTTCTCCTCTAGGGTGTCTTAAT
TACCCGTACTAAAGGTTTGGAAAAGAAAAAGAGACCGCTCGTTTCTTTTCTTCTCGTAAAAAG
GCAATAAAAAATTTTATCACGTTTCTTTTCTTGAATTTTTTTTTTAGTTTTTTCTCTTTCAG
TGACCTCATTGATATTTAAGTTAATAAACGGTCTTCAATTTCTCAAGTTTCAGTTTCATTTTTCT
TGTTCTATTACAACTTTTTTACTTCTTGTTCATTAGAAAAGAAAGCATAGCAATCTAATCTAAGGG
GCGGTGTGACAATTAATCATCGGCATAGTATATCGGCATAGTATAATACGACAAGGTGAGGAAC
AAACCATGGCCAAGTTGACCAGTGCCGTTCCGGTGTCCACCGCGCGGACGTCGCCGGAGCGGTCTG

agttctggaccgaccggctcgggttctcccgggacttcgtggaggacgacttcgccggtgtggtcc
gggacgacgtgaccctgttcatcagcgcggtccaggaccaggtggtgccggacaacaccctggcct
gggtgtgggtgcgcggtcctggacgagctgtacgccgagtggtcggagggtcgtgtccacgaacttcc
gggacgcctccggggcggccatgaccgagatcggcgagcagccgtggggcgaggagttcgccctgc
gcgacccggccggcaactgcggtgcaacttcgtggccgaggagcaggactgacacgtccgacggcggc
ccacgggtcccaggcctcggagatccgtcccccttttccctttgtcgatatcatgtaattagttatg
tcacgcttacattcacgcctccccccacatccgctctaaccgaaaaggaaggagttagacaacct
gaagtctaggtccctatttatTTTTTTTatagttatgtagtattaagaacgttatTTTatTTTcaa
atTTTTTctTTTTTTTctgtacagacgcggtgtacgcatgtaacattatactgaaaaccttgcttgag
aaggTTTTTgggacgctcgaaggctTTAatTTTgcaagctggagaccaacatgtgagcaaaaaggccag
caaaaaggccaggaaccgtaaaaaaggccgcggttgctggcgTTTTTccataggtccgccccctgac
gagcatcacaAAAatcgacgctcaagtcagaggtggcgaaacccgacaggactataaagataccag
gcgTTTTccccctggaagctccctcgtgcgctctcctgTTccgaccctgccgcttaccggatacctg
tccgcctTTTctccctcgggaagcgtggcgctTTTctcaatgctcacgctgtaggtatctcagttcg
gtgtaggtcgTTcgctccaagctgggctgtgtgcaacgaacccccgTTcagcccgaccgctgcgcc
ttatccggtaactatcgtcttgagttccaacccggtaagacacgacttatcgccactggcagcagcc
actggtaacaggattagcagagcaggtatgtaggcggtgctacagagttccttgaagtgggtggcct
aactacggctacactagaaggacagtatTTTggatctgcgctctgctgaagccagttaccttcgga
aaaagagttggtagctcttgatccggcaaaacaaaccaccgctggtagcggtggTTTTTTTgtttgc
aagcagcagattacgcgcagaaaaaaaggatctcaagaagatcctttgatctTTTctacggggtct
gacgctcagtggaacgaaaactcacgttaagggtTTTTTggatcatgagatc

Note:

Underlined sequences are restricted enzyme recognition sites (EcoR1 and Xba1).
Highlighted sequences are complementary parts of primers on *hGH* gene.
Sequence denoted by thick characters is His-tag and Factor Xa recognition site.

APPENDIX E

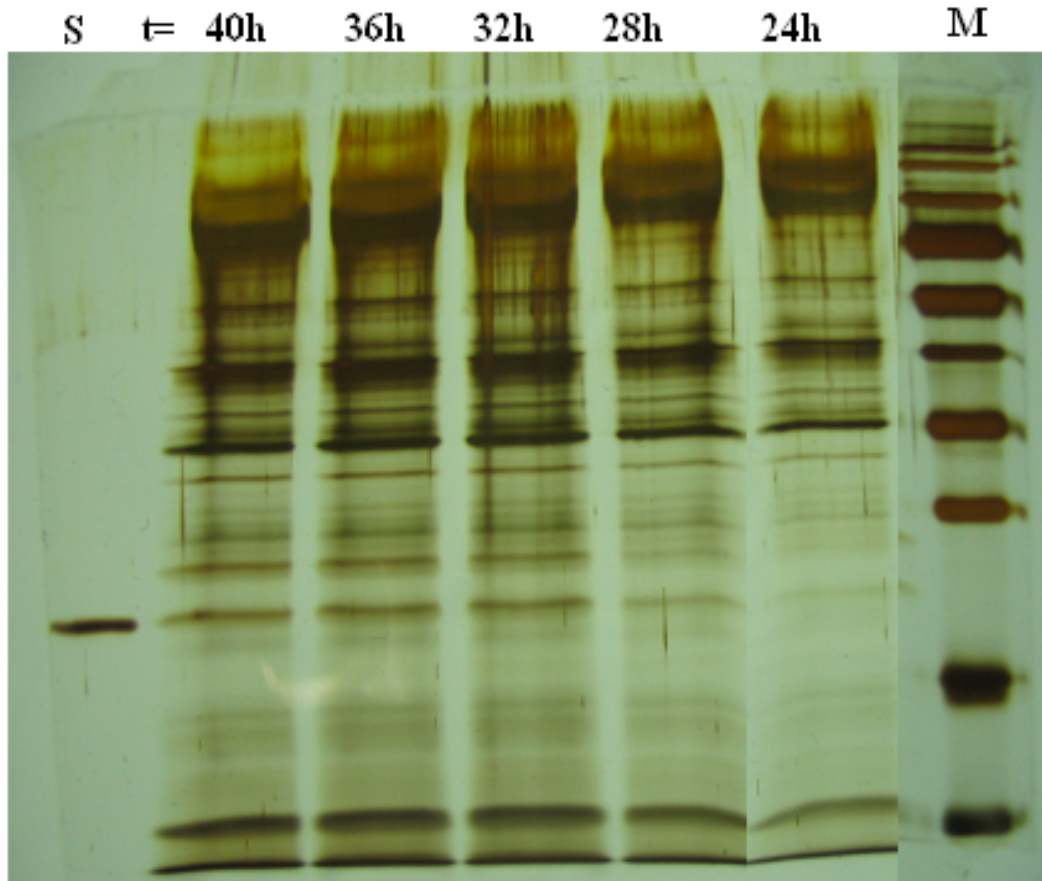


Figure A.4 SDS-page analysis showing the cultivation media at different time when mixed carbon sources (glycerol/methanol) were used. M and S are protein marker and standard hGH, respectively.

APPENDIX F

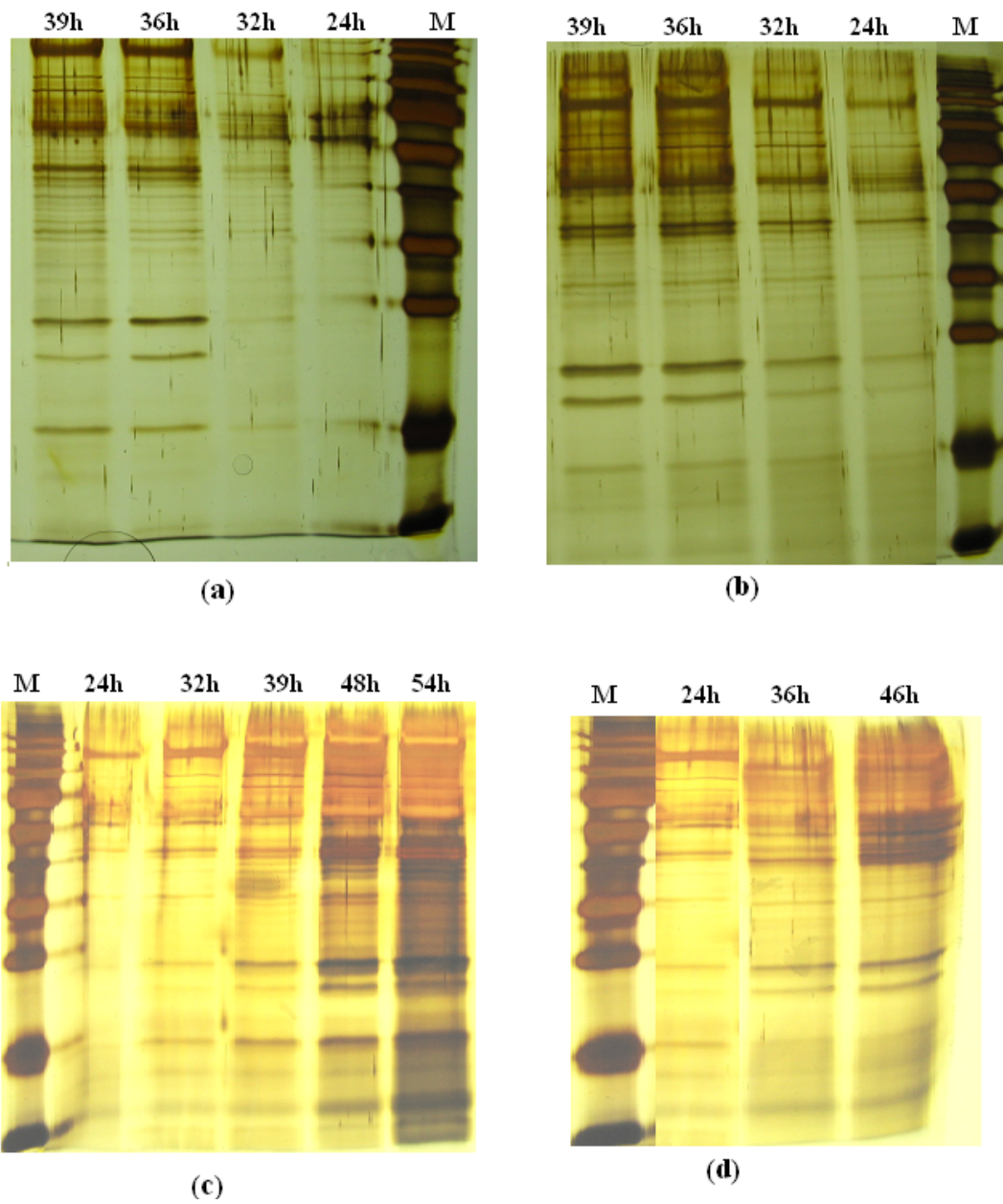


Figure A.5 SDS page analysis of bioreactors at different time. M: protein marker, (a) $N=750 \text{ min}^{-1}$, (b) $N=500 \text{ min}^{-1}$, (c) $N=625 \text{ min}^{-1}$, (d) $N=250 \text{ min}^{-1}$.